Spring 5-15-2015

The Role of Myc and AP-1 Transcription Factors in the Development and Function of the Dendritic Cell Lineage

Wumesh K.C.
Washington University in St. Louis

WASHINGTON UNIVERSITY IN ST. LOUIS

Division of Biology and Biomedical Sciences
Immunology

Dissertation Examination Committee:
Kenneth M. Murphy, Chair
Deepta Bhattacharya
Marco Colonna
Brian T. Edelson
Robert Schreiber
Thaddeus S. Stappenbeck

The Role of Myc and AP-1 Transcription Factors in the Development and Function of the Dendritic Cell Lineage

by
Wumesh K.C.

A dissertation presented to the
Graduate School of Arts & Sciences
of Washington University in
partial fulfillment of the
requirements for the degree
of Doctor of Philosophy

May 2015
St. Louis, Missouri

Table of Contents

List of Figures

List of Supplementary Figures

List of Tables

List of Abbreviations

cDC	classical dendritic cell
pDC	plasmacytoid dendritic cell
BTB	broad complex, tramtrack, bric-à-brac
bZIP	basic leucine zipper
HSC	hematopoietic stem cell
CMP	common myeloid progenitor
CDP	common dendritic cell progenitor
MDP	Monocyte/Macrophage dendritic cell progenitor
Pre-cDC	Precursor to classical dendritic cells
GMP	granulocyte macrophage progenitor
GM-CSF	granulocyte macrophage colony-stimulating factor
Flt3L	fms-like tyrosine kinase 3 ligand
MLN	mesenteric lymph node
SLN	skin draining lymph node
LCMV	lymphocytic choriomeningitis virus
LM-OVA	*Listeria monocytogenes* expressing ovalbumin
LM-EGD	*Listeria monocytogenes* (EGD strain)
ChIP-Seq	chromatin immunoprecipitation with parallel DNA sequencing
MACS	model-based analysis of ChIP-Seq
IRF	interferon regulatory factor
AP-1	activator protein 1
VSV	vesicular stomatitis virus
FACS	Fluorescence activated cell sorting

Acknowledgements

The completion of this dissertation was made possible by the constant support of family, friends, and scientific colleagues. First, I would like to thank my thesis mentor, Ken Murphy, for welcoming me into his lab despite my having no background in immunology. From the very first days in lab, Ken has provided tremendous resources for my work and created a highly collaborative research environment, and he has tirelessly challenged me to do science at the highest level possible. He has shown me incredible latitude with my projects and encouraged me to take risks in my science. His singular ability to distill the essence of complicated experiments and data is something I have come to admire throughout my training. I would also like to thank Theresa Murphy who has been a second mentor and a fantastic collaborator on multiple projects. She has always been generous with her time and resources for which I am grateful. I would also like to thank my thesis committee members, Deepta Bhattacharya, Marco Colonna, Brian Edelson, Bob Schreiber, and Thaddeus Stappenbeck for their constructive advice and guidance.

I owe many thanks to past and present members of the Murphy lab, who have always offered their time and expertise at a moment's notice. My colleagues have made lab a fun place to be, no matter the hour or situation. I owe special thanks to Ansuman Satpathy, Jorn Albring, Malay Haldar, Xiaodi Wu, Carlos Briseno, and Nicole Kretzer with whom I have enjoyed talking endlessly about science. I am also grateful to my collaborators from the Colonna lab, namely Aaron Rapaport and Melissa Swiecki, and the Allen lab, specifically Steve Persaud. Lastly, I am forever appreciative of the financial support provided by the Washington University in St. Louis Medical Scientist Training Program's internal funding source, the Howard Hughes Medical Institute, and the American Heart Association's predoctoral fellowship program.

I want to thank my brother, Bhusan, my mother, Sarita, my father, Ramesh, and the Graseck and Sorensen families for their love and endless encouragement throughout this long process.

Lastly, I want to thank my son, Owen, who greets me every morning with an ecstatic smile, and my wife, Anna, whose enduring support and advice have been a tremendous help throughout my training. I am forever indebted to her.

Wumesh K.C.

Washington University in St. Louis

May 2015

ABSTRACT OF THE DISSERTATION

The Role of Myc and AP-1 Transcription Factors in the Development and Function of the Dendritic Cell Lineage

by
Wumesh K.C.
Doctor of Philosophy in Biology and Biomedical Sciences
(Immunology)
Washington University in St. Louis, 2015
Professor Kenneth M. Murphy, Chair

Dendritic cells (DCs) orchestrate immune responses to foreign and self proteins by capturing, processing and presenting antigens to naïve $CD4^+$ and $CD8^+$ T cells in specialized regions of lymphoid organs. Consequently, DCs function in many disparate infectious settings, during which their activation can result in both pathogenic and protective responses. The diverse properties of DCs manifest through the actions of a limited set of lineage-specifying DNA-binding proteins called transcription factors (TFs). The precise molecular program controlled by these developmentally important TFs (such as *Irf8* and *Batf3*) is largely unknown because most studies to date have been largely descriptive. We have identified *bona fide* targets of BATF3 and IRF8 by comparative microarray analysis and chromatin immunoprecipitation followed by sequencing (ChIP-Seq). These targets provided insights into the specialized processes carried out by DCs and may also represent future pathways for manipulation during the development of vaccines.

We characterized the stage-specific actions of BATF3 in the development of $CD8a^+$ DCs, a critical initiator of cellular immunity to intracellular pathogens and tumors. *Batf3* induction occurs after the expression of *Irf8* in the precursor to classical DCs (pre-cDC), in which BATF3 acts subsequent to an Irf8-dependent lineage commitment step to induce the terminal maturation

and survival of $CD8a^+$ DCs. Genomic regions bound by IRF8 and BATF3 were identified by ChIP-Seq, and notably, the proximal promoters of $CD8a^+$ DC-specific genes showed IRF8 and BATF3 co-occupancy. Furthermore, we evaluated IRF8 binding in BATF3-deficient cells to identify BATF3-independent targets. One such candidate was the Myc homolog *Mycl1* (L-Myc). Analysis by quantitative real-time PCR (qPCR) of the hematopoietic compartment revealed that *Mycl1* expression is restricted to pDCs and cDCs.

To evaluate the significance of L-Myc activity in dendritic cells, we generated a new knock-in mouse model of the *Mycl1* locus by replacing the first coding exon with an in-frame GFP cassette. Analysis of heterozygous mice ($Mycl1^{+/gfp}$) revealed that *Mycl1* expression is restricted to dendritic cells. Interestingly, induction of *Mycl1* occurs at the CDP to pre-cDC transition concurrent with the loss of *Myc* (c-Myc) from DCs. Although dispensable for the development of DCs, L-Myc supports the growth and survival of dendritic cells. Moreover, following activation of DCs with pathogen associated molecular patterns (PAMPs) or activating cytokines, L-Myc protein levels either remained constant or increased, suggesting that growth-promoting circumstances are intricately linked to levels of L-Myc. Lastly, L-Myc deficient DCs primed antigen-specific responses poorly and were incapable of supporting the intracellular growth of *Listeria monocytogenes*.

Collectively, these findings suggest that the switch from *Myc* to *L-Myc* expression represents a strategy of growth in the face of disparate inflammatory signals experienced during infections. *L-Myc* may therefore represent a therapeutic target for selective inhibition or augmentation of immune responses driven by dendritic cell

Chapter 1 Introduction to dendritic cells

Contents of this chapter have been previously published in *Seminars in Immunology*.
Satpathy AT, Murphy KM, KC W**.** Transcription factor networks in dendritic cell development. *Semin Imm*. 2011 Oct; 23(5):388-97. Epub 2011 Sep 15

1.1 Abstract

The immune system comprises a broadly distributed collection of functionally specialized cells that must constantly recognize and remove infectious threats. Considerable progress has been made in our understanding of immunological recognition by intensively studying lymphocytes and their clonally distributed antigen-specific receptors. By comparison, the "accessory" cell type(s) responsible for initiating and directing immune responses has received less attention in several important ways despite being identified by Ralph Steinman and colleagues as a unique cell type with "stellate" or dendritic morphology nearly 40 years ago. The relative paucity and similarity to other myeloid lineages – such as macrophage and monocytes – has been a major barrier to characterizing DCs at the molecular level. Though the recent identification of lineage-restricted progenitors and cytokines and transcription factors necessary for DC homeostasis represent major breakthroughs in the field, further insight into the molecular mechanisms underlying DC diversity and function is needed.

In this dissertation, we have characterized and compared the stage-specific actions of the transcription factors *Irf8* and *Batf3*, which act in concert to regulate the terminal differentiation and survival of $CD8a^{+}$ DCs. Moreover, gene expression profiles combined with ChIP-Seq analysis of IRF8 and BATF3 occupancy led to the identification of unstudied candidate gene targets. We then investigated the role of one such target called *Mycl1*, a putative oncogene that belongs to the Myc family of basic helix-loop-helix transcription factors. By targeting exon 1 of the endogenous *Mycl1* locus, we generated a new knock-out mouse model that also serves as a reporter for *Mycl1* promoter activity. Analysis of lymphoid and peripheral tissues revealed that *Mycl1* is exclusively expressed by immature and mature cells of the DC lineage. Interestingly,

neither c-Myc nor N-Myc was expressed in DC progenitors or any of the mature DC populations surveyed. Subsequent characterization of L-Myc-deficient DCs revealed deficits in local proliferation and survival, which magnified in response to DC activation by pathogen associated molecular patterns (PAMPs) or live pathogens. The net consequence of L-Myc deficiency was poorer priming of antigen-specific $CD4^+$ and $CD8^+$ T cells in response to challenges with *Listeria monocytogenes* and vesicular stomatitis virus. Lastly, L-Myc-deficient $CD8a^+$ DCs captured bacteria normally but failed to support the initial burst of *L. monocytogenes*, thereby making L-Myc-deficient mice highly resistant to lethal challenge. This last observation revealed an unappreciated cell-intrinsic role for $CD8a^+$ DCs in the dissemination of bacteria during the initial phase of infection. In summary, our studies have clarified a critical circuit of three transcriptional regulators that function to maintain DCs and therefore support functional responses to intracellular pathogens.

1.2 Isolation and functional characterization of dendritic cells

DCs were discovered nearly 40 years ago by Steinman and Cohn, who identified a "large stellate cell" population among adherent splenocytes on particular glass and plastic surfaces [1]. Beginning with a strictly descriptive analysis, these cells were defined as a distinct lineage, separate from B and T cells as well as granulocytes and macrophages, on the basis of several criteria. Initially, their "dendritic" morphology and clear phagocytic capacity set them apart from lymphocytes. However, it was their profound capacity for stimulating T cells in a allogeneic and syngeneic mixed lymphocyte reaction (MLR) that prompted the notion that these cells could play a unique role in directing adaptive immunity [2]. Subsequently, the demonstration that DCs could support the in vitro generation of anti-trinitrophenol (TNP) cytotoxic T lymphocytes (CTL)

suggested that DCs represented the critical accessory cell for the in vivo development of immune responses [3,4]. Additional hallmarks emerged from flow cytometric analyses that identified a distinct set of cell-surface markers separating DCs from macrophages and other myeloid lineages [5,6]. Subsequent studies have demonstrated that, in addition to stimulating the immune response, DCs also possess a capacity to impose a tolerogenic state on T cells under appropriate conditions [7,8].

The first two decades of work on DCs largely considered this cell a homogenous population. In 1992, the first clear-cut example of subset differentiation within DCs was put forth, based upon the expression of the murine CD8-alpha marker. Clearly distinct from developing or re-circulating thymic T cells, this subset represented a relatively small population within the thymus, and was thought to derive from an intrathymic lymphoid-restricted precursor rather than from bone marrow precursors [6,9]. As a byproduct of differences in identification and separation methods, the demarcation of various subsets has since been somewhat inconsistent [10]. Currently, the field considers four major subsets of lymphoid-resident DCs. In addition to the CD8-alpha positive DC, two other populations of conventional DCs (cDC) are defined by the presence or absence of the cell-surface molecule CD4 [11]. These two populations show a high degree of similarity with respect to function, development, and gene expression, and for simplicity will be grouped together and further referred to as $CD4^+$ cDCs in this review [12]. A fourth population of plasmacytoid DCs (pDC) is defined by the expression of several distinguishing markers including B220, Siglec-H, and Bst2 [13-15]. Human counterparts for each of these DC subtypes have been identified, underscoring the conservation of DC lineage diversification across species, presumably owing to their important functional specialization [16-18]. As discussed briefly below, monocyte-derived cells sharing many features with DCs arise under

inflammatory rather than steady-state conditions, although little is currently known regarding the transcriptional and molecular basis of their differentiation [19,20].

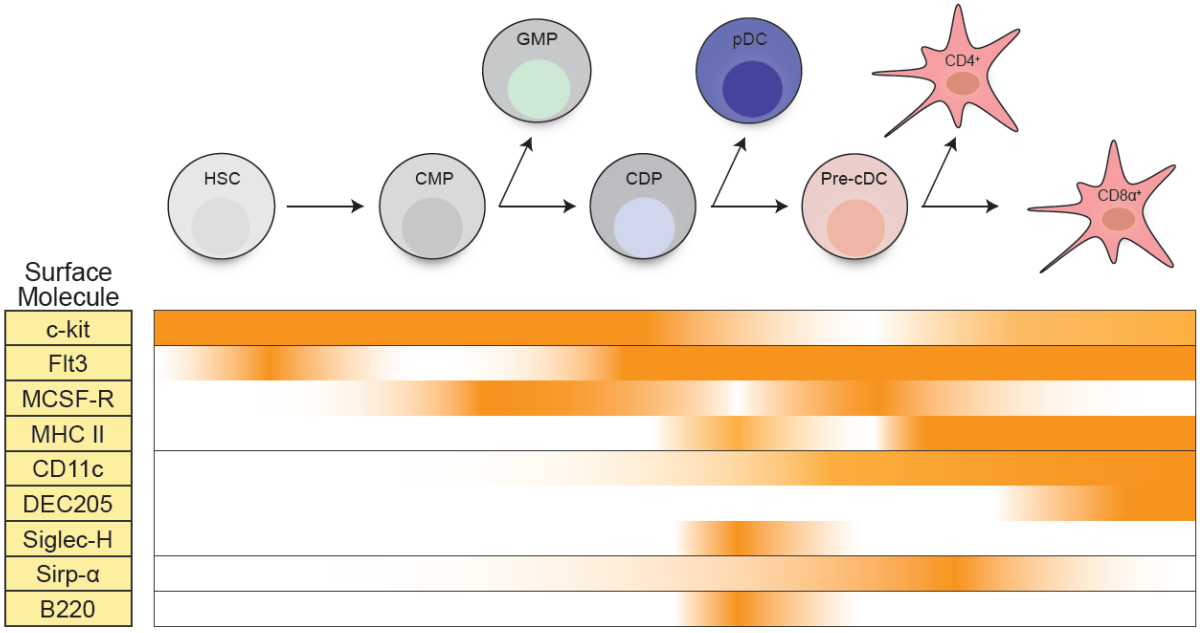

Figure 1.1: Temporal expression of genes in DCs and progenitors

The expression of key surface markers used for the identification of mature dendritic cells (DCs) and their bone marrow precursors is depicted. In addition, the expression of important growth factors required for the development of DC subsets is shown.

All subsets express high levels of the complement receptor CD11c, and also display a variety of surface receptors endowing them with the properties of growth factor responsiveness, efficient phagocytosis, and antigen presentation. Figure 1.1 outlines the expression of some of these key surface proteins as DC subsets differentiate from hematopoietic precursors (discussed further below). While they are convenient markers in the murine system, there is no known function of the CD4 and CD8-alpha molecules in the execution of specific functional processes.

In addition, these two markers are among the few that do not show conservation with subsets of DCs in the human system.

Beyond differences in cell-surface receptors as the basis for defining distinct subsets, non-overlapping functions for these populations are beginning to emerge. For example, pDCs appear to be a major source of type I interferon during viral infections. Recent models in which pDCs are selectively eliminated highlight their contributions in some, but not all, settings of infections by pathogens [21-23]. The cDC subsets appear to be primarily concerned with priming adaptive immune responses, particularly those of T cells, although important interactions with other immune cells, such as B cells and NK cells, have also been described [24-26].

1.2.1 The role of $CD8a^+$ and $CD103^+$ dendritic cells in immune responses

The immune system has evolved distinct effector modules to combat pathogens that may reside in the intracellular or extracellular microenvironment. Consequently, the DC lineage, like other hematopoietic lineages, comprises multiple subsets, each apparently dedicated to the elimination of particular pathogens. The initial proposal for DC heterogeneity was in fact based on the differential expression of CD8a on thymic and splenic DCs [6]. Early observations that self-tolerance to peripheral tissue antigens could be mediated by the $CD8a^+$ DC led to the idea that this DC subset surveyed the peripheral tissues for cellular antigens to present to naïve $CD4^+$ and $CD8^+$ T cells. Furthermore, a study by den Haan and colleagues indicated that one potentially unique function of the $CD8a^+$ DC is its capacity to cross-present exogenous antigens on MHC class I [27]. As a result, it was hypothesized that these cells are uniquely capable of cross-priming $CD8^+$ T cells, a process first described in 1976 and now implicated as a critical response in viral and anti-tumor immunity [28-30]. A developmentally related DC subset (called the $CD103^+$ DC)

exists in all peripheral tissues and is also a critical player in initiating T cell responses to mucosal pathogens[31,32]. By virtue of this unique function, these cells could provide an efficient mechanism to induce $CD8^+$ T cells against pathogens that fail to infect DCs directly, and therefore evade classical mechanisms of inducing CTL (cytotoxic T lymphocyte) responses. In support of this role, $CD8^+$ DCs are now recognized to reside in the T cell zones of the spleen, and are thought to traffic from areas of pathogen trapping into areas of T cell presentation [33,34]. Other studies have also proposed that these cells may provide functions independent of cross-presentation, such as the production of essential cytokines in response to various pathogens [35,36]. A definite example of an indispensable innate effector function of the $CD8a^+$ DC was elucidated with *Batf3* deficient mice, which lack the $CD8a^+$ DCs and thus cannot generate adequate amounts of IL-12 necessary for defense against *Toxoplasma gondii*[37].

1.2.2 The role of $CD11b^+$ dendritic cells in immune responses

$CD4^+$ cDCs for the most part have been considered poor cross-presenters in comparison to their $CD8^+$ counterparts. These cells are largely considered to activate $CD4^+$ T cells, rather than having any specialized role in the induction of CTLs [38]. However, the classical paradigm of functionally segregating cDC subsets based on the efficiency and quality of MHC class I and II presentation is not without controversy. For example, a recent study suggests that the distinction between $CD8^+$ and $CD4^+$ DCs may instead lie in the inability of the former to process antigens for MHC class II efficiently; and when controlled for antigen dose and delivery, both subsets are capable of efficient cross-presentation [39]. In fact, under certain inflammatory conditions, the monocyte-derived DC can present exogenous antigens more efficiently than either of the lymphoid-tissue resident cDCs [40,41]. Collectively, these seemingly conflicting observations may

be explained by the type of antigen and the context in which it is being studied. Recently, an innate effector function has also been ascribed to the Notch2-dependent CD11b$^+$ DCs. In response to attaching-and-effacing intestinal pathogens such as *Citrobacter rodentium*, intestinal CD11b$^+$ DCs are the obligate source of IL-23[42,43]. However, an alternative strategy for ablating this lineage concluded that these cells were not necessary for resistance to *C. rodentium*[44]. Additional studies comparing these two methods will be necessary to determine the reasons for this discrepancy.

1.2.3 The role of plasmacytoid dendritic cells in immune responses

pDCs secrete large amounts of type I interferon in response to viral infection[45-47]. Naturally, it was believed that these cells were critically important for controlling viral replication and even priming antigen-specific responses. For example, a recent study using an LCMV strain that leads to chronic infection concluded that pDCs play some role in the accumulation of antigen-specific T cells[23]. Another approach to conditionally deplete pDCs with DTR under the control of *SiglecH* concluded that pDCs mount responses to *Listeria monocytogenes* and control tumor rejection[48]. However, new genetic tools have cast some doubt on the importance of pDCs during the early phase of viral infection[21]. More specific genetic tools for the proper characterization and ablation of pDCs is required to settle these controversies.

1.3 Accurately defining the DC lineage

As discussed above, the criteria to mark the DC lineage has relied on a constantly evolving rubric, beginning with the purely descriptive analyses of Steinman and colleagues in the

1970's to a more functional and phenotypic characterization at present. Yet such seeming clarity has not resolved the topic of the exact contribution of DCs during an immune response, in part because of the shared expression of many surface markers between DCs and other myeloid cells. In fact, some of the seminal studies over the last decade that relied on genetic or antibody-based depletion of specific myeloid populations also affected several other cell types [49]. For instance, two independent reports have claimed that basophils, and not DCs, are critical for mediating T helper type 2 responses (Th2) [50,51]. However, these reports were disputed by another group who demonstrated that the antibody-based depletion of basophils in the previous studies also removed a key DC population, which actually appears to be necessary for initiating Th2 immunity [52]. More recently, a report claiming the importance of beta-catenin signaling in intestinal DCs to gut tolerance was based upon the selective deletion of this molecule in only DCs, a specious claim given there was also complete deletion in a sizeable fraction of macrophages [53]. These ambiguous results are the byproduct of a strict reliance on cell-surface markers to segregate myeloid populations. Instead, when considering any lineage, especially one as heterogeneous and plastic as DCs, more rigorous criteria need to be applied for its functional characterization in various contexts. Some authors have suggested defining DCs based on their anatomical location, origin from dedicated precursors, and antigen presenting properties in addition to phenotypic markers [54]. However, all of these measures can be inconsistent depending on the physiological context or method of measurement. Therefore, we suggest that the most succinct and reliable definition of the DC lineage is based on the expression of key lineage-specifying transcription factors which are unequivocally required for their development in all settings. Parsing these transcriptional networks will help resolve developmental and functional controversies that currently exist within the field.

1.4 The developmental origin of DCs

An issue with particular relevance to the transcriptional basis of DC development is their derivation from bone marrow progenitors. It is now clearly established that DCs are short lived and are continuously repopulated in the periphery, both within lymphoid and non-lymphoid tissues, from progenitors that arise in the bone marrow [55,56]. For some period of time, there was confusion about the origin of DCs, based primarily on the initial classification of immune lineages as broadly derived either from a common lymphoid-restricted progenitor (CLP), or from a common myeloid-restricted progenitor (CMP) [57,58]. Whereas other cells of the immune system, such as T cells, B cells or neutrophils, are derived strictly from the CLP or from the CMP, it is now clear that all DC subsets can be derived from either population [59-61]. This unexpected finding overturned the existing paradigm that $CD8^+$ DCs were of lymphoid while $CD4^+$ DCs were of myeloid origin [6,62]. Despite the ability of CLPs to generate DCs upon adoptive transfer into irradiated hosts, the mechanisms and cell intermediates through which this occurs is unclear. Moreover, recent lineage tracing studies by Schlenner *et al.* indicate that the contribution of this pathway to the steady-state DC compartment is minimal [63]. Therefore, our focus will be on the CMP-derived pathway of DC development.

Fogg and colleagues identified the first precursor downstream of the CMP that still retained DC potential, termed the macrophage-dendritic cell precursor (MDP) [64]. As its name would indicate, the MDP strictly has the potential to generate macrophages and DCs whereas alternate myeloid lineages proceed through the granulocyte-macrophage precursor (GMP) [58]. Soon thereafter, two groups reported the identification of a purely DC-restricted bone marrow progenitor called the common dendritic cell progenitor (CDP), which is efficiently able to generate all DC subsets at a clonal level [65,66]. The CDP was shown to originate from the MDP

following the loss of monocyte lineage potential [67]. Similar to the MDP, the CDP expresses relatively high levels of macrophage colony-stimulating factor 1 receptor (M-CSFR) and FMS-like tyrosine kinase 3-ligand receptor (Flt3), but lower levels of the stem cell factor receptor (c-Kit). Presently it is thought that both the MDP and the CDP derive exclusively from the CMP *in vivo*, strengthening the argument that DCs are minimally derived from lymphoid precursors. Finally, the terminal steps in diversification of DC subsets appear to begin at the CDP stage. As outlined in Figure 1.2, CDPs seem to be the immediate precursor of both pre-pDCs and pre-cDCs, which are cells restricted to their respective lineages but not yet fully mature [68,69]. pDCs complete their maturation in the bone marrow and circulate through the blood to secondary lymphoid organs. In contrast, pre-cDCs seed lymphoid and non-lymphoid tissues via the blood where-upon they complete their differentiation into either the $CD8^+$ or $CD4^+$ cDC subsets.

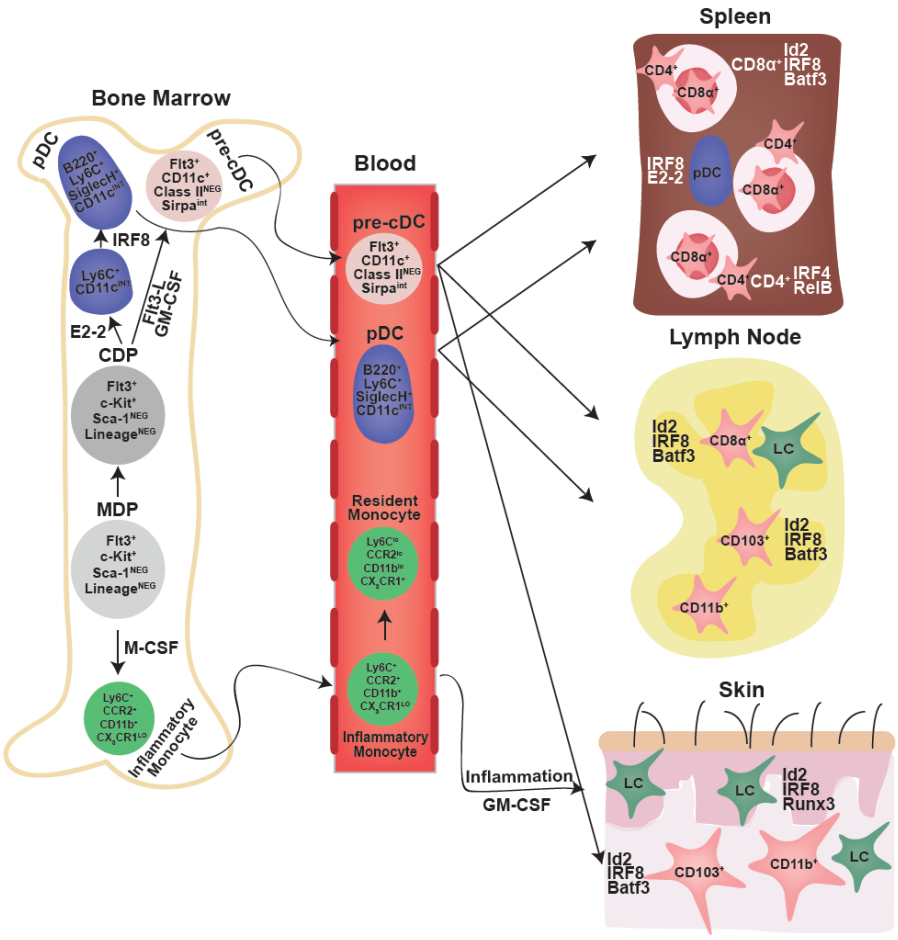

Figure 1.2: Stages of DC development

DCs derive from BM–resident hematopoietic progenitors.

1.5 Extracellular cues supporting DC development

A number of extracellular cues induce the progression through the progenitor stages described above, mainly by activating several cytokine receptors. The major cytokine receptors influencing DC development are M-CSFR, granulocyte-macrophage colony-stimulating factor receptor (GM-CSFR) and Flt3, which are all expressed variably on early hematopoietic precursors but remain highly expressed on committed DC progenitors (Figure 1.1).

The importance of these cytokines in the differentiation of DCs was first established by early studies demonstrating the ability of GM-CSF, either alone or in combination with IL-4, to drive the formation of DCs from mouse bone marrow or human peripheral monocytes [62,70]. The unique potency of these cells for antigen presentation, combined with their expression of CD11c and MHC class II, confirmed their identity as *bona fide* DCs and provided a widely used model system for *in vitro* studies. Therefore, it was surprising when both GM-CSF- and GM-CSFR-deficient mice showed a largely unperturbed DC compartment, leading to the conclusions that GM-CSF is dispensable or redundant in steady-state DC development [71,72]. The recent identification of TNF-alpha- and iNOS-producing DCs under inflammatory conditions, and their dependence on GM-CSF, points to the relevance of this cytokine in infectious settings and likely explains its ability to induce DC development *in vitro* [39,73,74].

Nonetheless, these early results suggested that other cytokines were likely responsible for the steady-state development of DCs *in vivo*. In 1996, McKenna and colleagues reported that the administration of exogenous Flt3-ligand (Flt3L) potently induces the expansion of all DC subsets *in vivo* [75]. This cytokine was then also shown to support the development of all subsets *in vitro* [76]. Moreover, forced expression of Flt3 (receptor for Flt3L), or its downstream effector molecule STAT3, in progenitors committed to alternative lineages can re-direct their development into DCs [77]. The requirement for Flt3L *in vivo* was confirmed by the greatly reduced numbers of DCs in Flt3L-deficient mice and Flt3-deficient mice [78,79]. Interestingly, the absence of Ftl3L presented with a stronger DC phenotype than the absence of Flt3, suggesting that the ligand may interact with a hitherto undefined receptor. These findings have been reinforced by subsequent studies on STAT3-null mice, which appear to phenocopy Flt3L deficiency [80]. Recent evidence suggests that the activation of STAT3 is mediated by mTOR (mammalian target of rapamycin)

signaling, and accordingly, chemical inhibition of mTOR with rapamycin perturbs the development of DCs *in vitro* [81].

While Flt3L appears to be the dominant cytokine controlling steady state DC development, GM-CSF may contribute, as mice deficient in both Flt3L and GM-CSF have lower numbers of DCs than either single cytokine deficiency alone [71]. The precise degree of redundancy is still a matter of ongoing work. Much in the same manner as differential localization within the bone marrow has been proposed to regulate B cell development through various stages by distinct actions of cytokines and cell-surface proteins on stroma, a similar combinatorial regulation of DCs has recently been proposed [82,83]. First, as noted above, there is a compound defect in mice deficient in both Flt3L and GM-CSF, suggesting contributions of both cytokines to DC development. In addition, different cytokines appear to have varying effects on the development of specific DC subsets. For instance, GM-CSF favors the development of cDCs while inhibiting the development of pDCs, through a mechanism dependent upon activation of STAT5 [84]. In contrast, culturing bone marrow cells in M-CSF in combination with Flt3L has the opposite effect, favoring pDC development [65]. It is conceivable that specific stromal niches within the bone marrow could support distinct DC developmental outcomes through differential cytokine production. Indirect evidence supporting this model comes from clonal studies of the CDP, which noted that some cells within the population already appear to be biased toward either pDCs or cDCs [66]. The generation of unique, non-overlapping reporter systems for each of the abovementioned cytokines will greatly aid in the resolution of this outstanding question of niche-dependent effects.

1.6 Transcription factors control DC commitment and specification

Generally, cell fate specification occurs through the actions of transcription factors which may be induced or inhibited by initiating extracellular cues. Recently, a number of transcription factors have been identified that control commitment, specification, and survival of DCs. In this review, we will group these factors into two major categories. The first category consists of transcription factors that are required for the development of early DC progenitors, which for the most part influence all DC subsets. As one might expect with factors influencing such early decisions, the loss of these genes often affects a number of additional immune lineages besides DCs. The second category is comprised of more lineage-restricted transcription factors, which regulate later stages of DC fate decisions. Deficiency of these factors usually results in more specific defects within the DC lineage. It is worth keeping in mind that the expression of some factors from the first category is not extinguished as the steps of commitment and specification unfold, and therefore may influence both progenitors and mature cell types in distinct ways. Importantly, unique developmental outcomes may emerge from transcriptional programs initiated by broadly expressed factors of the first category through the induction and then interaction with factors from the second.

1.6.1 Factors regulating early DC progenitor development

The landmark discovery of the indispensable role of the zinc finger transcription factor Ikaros in the development of all lymphoid lineages also represents the initial identification of a factor necessary for DC development. Specifically, Ikaros-null mice lack pDCs and $CD4^+$ cDCs, and mice harboring a dominant-negative form exhibit a complete absence of all DC subsets [85,86]. Unexpectedly, Ikaros-null mice retain a residual population of $CD8^+$ cDCs, although the function

or origin of these cells has not been examined. The apparent mechanism by which Ikaros controls DC development is through its regulation of a large panel of receptors and transcription factors. Although classically considered to be required only for the priming of lymphoid lineages, gene expression analysis of the earliest cell stages of hematopoietic development revealed that the loss of Ikaros affects the expression of large gene sets associated with both lymphoid and myeloid lineages [87]. For example, the expression of Flt3, IL-7 receptor, Notch1, and the transcription factor Mef2c are all controlled by Ikaros, suggesting that it acts globally on many aspects of lineage specification [88].

Another well-known transcription factor influencing the early development of DCs is the ETS factor PU.1. Recently, PU.1 was unequivocally shown to be necessary for DC development, resolving earlier studies that resulted in conflicting conclusions [89,90]. Mice with a conditional deletion of PU.1 within the hematopoietic compartment fail to develop all DC subsets, but also show defects in other myeloid lineages including but not limited to macrophages and neutrophils [91]. Similar to Ikaros, PU.1 appears to control the induction of a broad range of genes necessary for development of many hematopoietic lineages. In particular, PU.1 controls the early expression of Flt3, GM-CSFR, and M-CSFR on progenitors, although only the absence of Flt3 was confirmed on DC precursors [92,93]. Notably, forced expression of Flt3 in PU.1-deficient progenitor cells did not rescue DC development, reinforcing the notion that PU.1 regulates other important programs aside from the signaling downstream of Flt3.

Finally, Gfi1, a known transcriptional repressor, appears to play a role in the development of all DC subsets. Gfi1-null mice have a global reduction in lymphoid-organ DC compartments, albeit not as severe as either Ikaros- or PU.1-deficient mice [94]. Analysis of $Flt3^+$ DC progenitors revealed a cell-autonomous role for Gfi1 in the activation of STAT3, suggesting that it may act

downstream of Ikaros or PU.1. One proposed mechanism is through its ability to inhibit PIAS3 (protein inhibitor of activated STAT3), a specific inhibitor of STAT3 [95]. In this model, loss of Gfi1 leads to the maintenance of PIAS3 activity and thus a reduction in transcriptional events mediated by STAT3. Additionally, studies in human monocytes have shown that Gfi1 can bind to a large number of myeloid gene loci such as JAK3, IL-8, and the CEBP family of transcription factors, indicating a potential role beyond its effect on STAT3 [96]. Interestingly, surviving Gfi1-deficient DCs closely resemble their counterparts from mice deficient in members of the NF-kappaB signaling cascade, suggesting that these two factors may converge on a common developmental pathway (see below) [97]. The dependence of DC development on both PU.1 and Gfi1 is in stark contrast to B cell ontogeny, during which these two factors act in opposition [98]. Whether Ikaros, PU.1, and Gfi1 act in concert or independently in DC development remains to be determined.

1.6.2 Factors regulating late DC progenitor development

Whereas the factors discussed above appear to be necessary during the HSC to CDP transition, particularly for the proper expression of key cytokine receptors, several transcription factors exert control over developmental options after commitment to the DC lineage has already occurred. These factors are expressed beginning in the CDP stage, and thus specify commitment into subsets or act on survival or proliferation programs in immediate precursors. For the most part, the factors acting in this realm of DC development have been evaluated for their actions on lymphoid resident DCs. However, it is clear that they likely affect the development of corresponding non-lymphoid DCs as well by mediating similar genetic programs in both compartments (Figure 1.2) [32,99].

The first transcription factor identified to affect a particular subset was RelB, a member of the NF-kappaB family of transcription factors, which also consists of RelA (p65), c-Rel, p50 and p52. In contrast to RelA and c-Rel, RelB selectively forms a heterodimer with p52 or the precursor form, p100 [100]. Expression of RelB is induced in the pre-cDC and then preferentially maintained in $CD4^+$ DCs. Consequently, mice deficient in RelB show a significant decrease in the $CD4^+$ population of cDCs, a defect determined to be cell intrinsic, while $CD8^+$ cDCs and pDCs appear to be unaffected [101,102], 1995 1 /id}.

Although studies investigating the mechanism by which RelB controls DC differentiation are lacking, one gene suggested to be a target of RelB is interferon regulatory factor 4 (IRF4), whose deletion also results in a large reduction in the number of $CD4^+$ DCs [103]. IRF4, one of nine IRF family members, contains an N-terminal DNA-binding domain (DBD) and a C-terminal IRF-associated domain (IAD). IRF4 is known to interact with a number of other transcription factors, including ETS factors and AP1 family members. In different settings, these interactions are critical in determining the DNA-binding specificity and functional nature of the IAD, either as an activator or repressor of transcription [104-106]. However, whether these interactions occur within the context of DCs remain to be defined, although PU.1 (ETS) and Batf3 (AP1) are attractive candidates.

Of the IRF family members, the member most functionally related to IRF4 is IRF8. IRF8 has also been demonstrated to play a critical role in DC differentiation. IRF8 deficiency leads to a complete loss of both $CD8^+$ cDCs and pDCs, and mice lacking both IRF4 and IRF8 exhibit essentially a compound phenotype, with a severe reduction in the total number of DCs and an absence of all but a few $CD4^+$ and double negative cDCs [107,108]. This result suggests that these factors may provide an overlapping function in certain subsets, but for most DCs, these two

factors display essentially non-overlapping patterns of expression. It is not yet known what signals are controlled by the IRF proteins, or what signals or transcription factors lead to the induction of IRF4 or IRF8 in their respective subsets.

In contrast to the selective expression of IRFs within DC subsets, Batf3 is expressed in both $CD8^+$ and $CD4^+$ cDCs, but loss of Batf3 leads to an abrogation in the development of only one of these subsets, the $CD8^+$ DC [109]. Batf3 is a member of the AP1 family of transcription factors that forms an obligate heterodimer with cJun or other Jun paralogs. However, unlike other AP1 members, Batf3 lacks a C-terminal extension that would provide a transcriptional activation domain, and instead consists only of a basic DNA-binding motif followed by a dimer-forming leucine zipper region [110,111]. Batf3 is most similar to a related factor Batf, which was recently found to be necessary for Th17 and Tfh differentiation as well as for isotype-switching in B cells [112,113]. These recent findings reverse the earlier notion that these minimal AP1 family members, Batf3 and Batf, were simply dominant-negative analogs of Fos, and instead suggest that these factors form unique heterodimers with Jun that posses distinct transcriptional activities. In the case of Batf3, this activity presumably includes the activation of genes selectively expressed by $CD8^+$ DCs.

Mice deficient in Batf3 have normal numbers of precursors, including CDPs and pre-cDCs [32], and appear deficient in only the most terminal stage of $CD8^+$ DC maturation. This final step is defined by the induction of genes important for the function of this DC subset, including Langerin and CD103. However, at present the immediate transcriptional targets of Batf3 are unknown.

The factors discussed above appear to regulate terminal steps of commitment to particular DC lineages. In contrast, two additional transcription factors appear to regulate the survival of

terminally committed precursors or mature cell types. The transcription factor Rbp-j, a critical mediator of the Notch signaling pathway, was recently found to be required for the survival of $CD4^+$ DCs *in vivo* [114]. Mice deficient in Rbp-j lack more than 50% of their $CD4^+$ DCs. Detailed analysis revealed that commitment to this lineage appears to be unaffected since the population of splenic pre-cDCs in these mice is normal. Rather, higher levels of Annexin-V staining and BrdU incorporation in surviving $CD4^+$ DCs suggest increased apoptosis of the terminal cell stage.

Similarly, the zinc finger transcription factor Bcl6 appears to regulate the survival of cDC precursors [115]. Bcl6 is a BTB (bric-a-brac, tramtrack, broad) -domain containing repressor that also has important actions in Tfh differentiation and exerts a repressive action on plasma cell genes within germinal center B cells [116-118]. In DCs, Bcl6 deficiency causes a severe reduction in both types of cDCs. While *in vitro* Flt3L experiments suggest a more pronounced effect on $CD8^+$ DC equivalents, the *in vivo* results indicate a larger effect on $CD4^+$ DC frequency. In contrast to Rbp-j deficiency, Bcl6-null mice do appear to exhibit increased Annexin V staining in cDC precursors and accordingly, express markers of apoptosis such as p53.

1.7 The balance between E2-2 and Id2 determines the choice between cDC and pDC fates.

A family of transcription factors known as class I basic helix loop helix (bHLH) factors plays an important role in the differentiation and survival of a number of lymphocyte populations [119]. Class I bHLH proteins, also referred to as E proteins, comprise a family of four members: E12, E47, E2-2, and HEB. These proteins function either as homodimers or heterodimers between family members, and bind to a conserved DNA motif referred to as an E-box. The

DNA-binding activity of these heterodimers can be interrupted by formation of a complex between E proteins and members of the inhibitor of differentiation (Id) HLH protein family, which lack the necessary DNA-binding motif of the basic region. Of the four members of the Id protein family, Id2 and Id3 appear to be the major inhibitors of E2 protein activity during lymphocyte development.

The first indication of the importance of E proteins in DC development arose from the observation that over-expression of Id2 or Id3 inhibits the development of pDCs *in vitro* [120]. This was extended by the finding that Id2 expression is induced *in vitro* in response to GM-CSF, and that Id2 is required for *in vivo* development of $CD8^+$ DCs, but not other subsets [121]. Surprisingly, the frequency of pDCs is increased in these mice suggesting that Id2 may function to divert cDC precursors away from the pDC fate. This hypothesis is supported by the finding that DCs developing in Id2-deficient mice also show de-repression of many genes normally associated with B cells as well as pDCs, as they share a large common gene signature [122].

A major breakthrough in the understanding of DC subset development resulted from the discovery that E2-2 is required for the development of pDCs *in vivo* [68]. These findings also helped to establish the identity of a pDC-restricted precursor: a $CD11c^+$ $Ly6C^+$ $SiglecH^-$ cell termed the pre-pDC. Mechanistically, E2-2 regulates a large pDC gene program including the direct regulation of other key transcription factors associated with pDC development, including IRF8, Bcl11a, and Spi-B. Interestingly, E2-2 also appears to repress genes associated with cDC subsets [123]. This was shown using an inducible Cre-deletion system whereby E2-2 was deleted in mature pDCs. Terminal deletion of E2-2 results in the induction of a number of cDC-associated genes including the re-expression of Id2. However, only a small subset of cDC genes appears to be affected. Therefore, it is not clear whether the emergence of these genes represents

a conversion of pDCs into *bona fide* cDCs, or instead into the recently reported alternative $CD8^+$ $CX3CR1^+$ DC lineage that appears to be more closely related to pDCs [124]. In any event, de-repression of Id2 caused by the loss of E2-2 expression now highlights an important regulatory circuit that controls the switch between pDCs and cDCs. In this circuit, induction of Id2 decreases E2-2 expression, and E2-2 activity suppresses Id2 expression. This arrangement represents a classical "flip-flop" circuit based upon mutual antagonism of alternately expressed factors. Presently, it is unknown what signals might control the induction of alternate states of this circuit.

1.8 Gene expression analysis of the CDP points to "pDC-priming"

Elaborating the transcriptional mechanism of T cell development was greatly aided by the identification of distinct cellular stages through which T cells progress. For example, the fate choice between T and NK cell lineages in the thymus was known to take place during the CLP to pro-T cell transition and to be dependent on Notch1 [125]. Careful gene expression analysis of intermediate cell stages allowed three groups to identify the downstream factor Bcl11b as a key mediator of this specification process [126-128], 2010 4712 /id} .

In contrast to T cell development, the specific intermediate stages of DC development have only recently been identified, as discussed above. In addition, the difficulty in identifying and isolating these progenitors, as well as their relative paucity in the bone marrow, has made them difficult to study. As a result, the relationships between the transcription factors that regulate DC development and the progenitor stages at which they act are still unclear. One plausible arrangement of the transcription factor network with respect to cellular differentiation

is shown in Figure 1.3. In this scheme, we have diagrammed the potential relationships between key transcription factors, some of which were suggested in the original reports.

We propose that the CDP represents the key stage at which the choice between the pDC and cDC lineage is made. The CDP is the natural candidate for this choice, since it has extinguished its ability to form alternate lineages, but still retains the ability to generate all DC subsets. Recent studies, as well as unpublished studies from our lab, have provided expression profile data for each sequential stage of DC differentiation *in vivo* including the CDP [129]. Strikingly, analysis of transcription factors expressed in CDPs reveals that a number of pDC factors, including E2-2, Bcl11a, and Runx2, are already expressed at moderate levels (Figure 1.4). In contrast, factors associated with the cDC lineage, such as Id2, Batf3, and Bcl6, are expressed either at very low levels or not at all. One interpretation of this data is that CDPs may be set to "default" into the pDC lineage unless a trigger is received to induce Id2. Id2 becomes highly expressed at the pre-cDC stage where-upon pDC-associated genes are lost. Such a default pathway could be likened to the strong skewing of naïve T cells towards the Th2 phenotype, which is mediated by an auto-activation of Gata-3 [130].

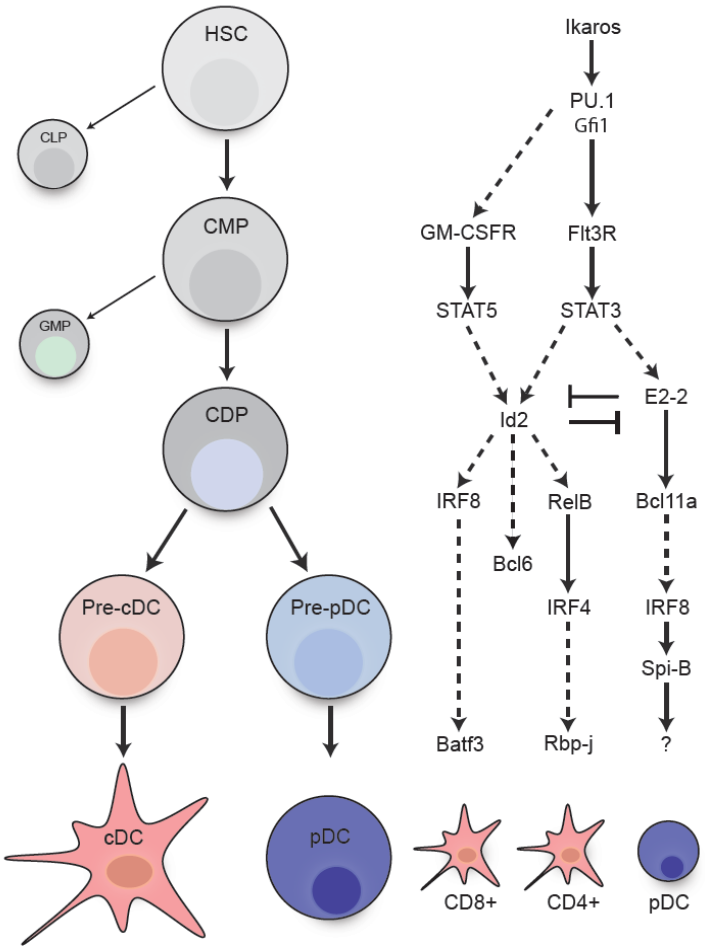

Figure 1.3: Transcription factor networks control DC development

A number of transcription factors regulate the commitment and survival of dendritic cells at various stages of development. However, the coordinated action of these factors with respect to one another as well as to relevant progenitor stages has not been well defined. One plausible network of these factors is depicted alongside the cellular stage in which they likely exert their functions. Solid arrows indicate connections that have been proven or suggested within original reports. Dotted arrows indicate hypothesized relationships.

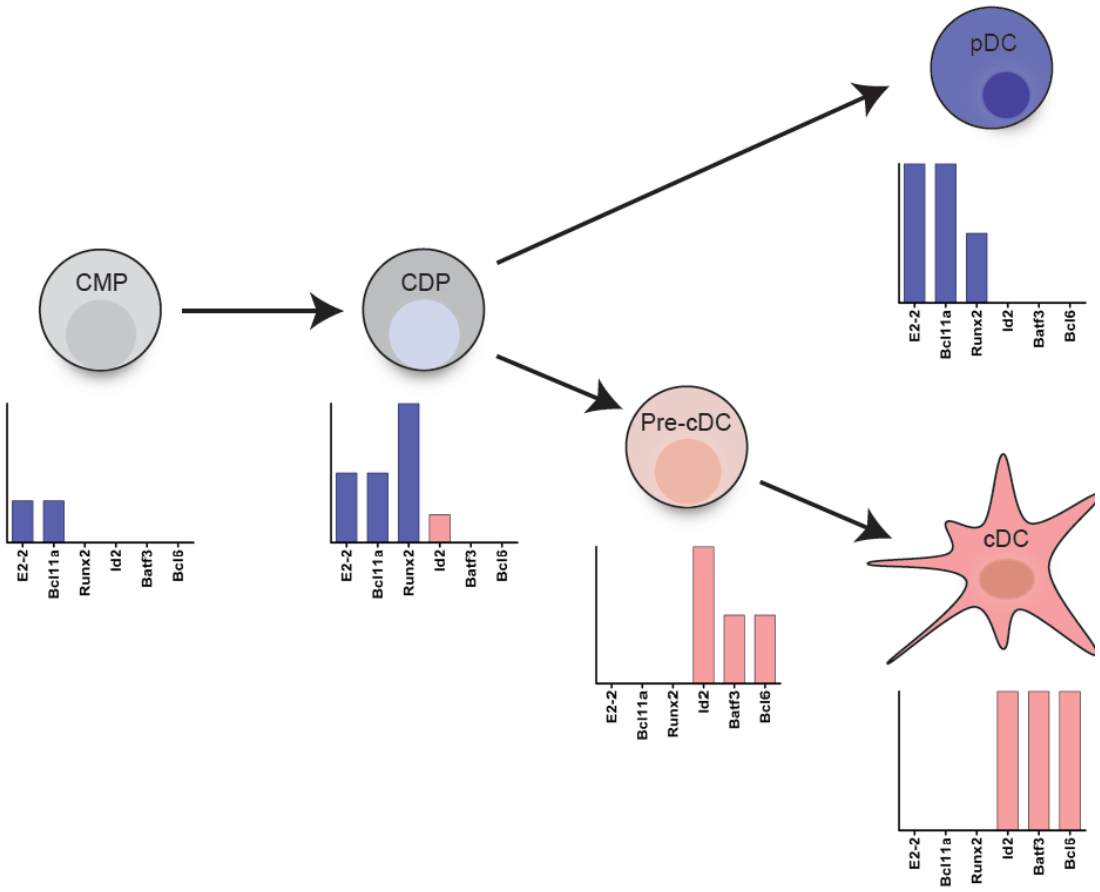

Figure 1.4: CDPs are "pDC-primed"

CDPs represent the last common precursor for both cDCs and pDCs, and thus a likely stage of specification into either lineage. This decision is dependent on a mutually antagonist balance between the transcription factors E2-2 and Id2. Gene expression analysis of progenitor populations reveals that CDPs express a number of pDC-specific transcription factors. Shown is the expression of pDC factors (E2-2, Bcl11a, and Runx2) in comparison to cDC factors (Id2, Batf3, and Bcl6). Expression of pDC factors and the lack of expression of cDC factors in the CDP points to a "default" pDC pathway during DC differentiation. Re-direction into the cDC lineage requires the induction of Id2 and repression of pDC factors in the pre-cDC.

1.9 Conclusions

The transcriptional networks regulating the diversification of myeloid lineages are currently being elucidated. Arguably, DCs remain the most enigmatic and developmentally

uncharacterized cell type within this system. However, recent studies have defined key steps in the DC differentiation pathway by identifying restricted bone marrow precursors. We hope that these advances will encourage the current transition of the field from a relatively descriptive state to one in which molecular mechanisms are emphasized. This shift in approach is needed to clarify confusion regarding the precise role of the DC lineage, and particularly specific DC subsets, in settings of infection and tolerance. For example, our understanding of the functional differences between pDCs and cDC subsets has greatly improved since the identification of transcription factors which are required for their development, such as E2-2 and Batf3, respectively. The deletion of either gene leads to a model in which the exact function of the relevant cell can be interrogated.

Clearly, many questions regarding the transcriptional regulation of DC fate decisions still remain unanswered. The basis for the initial commitment to the DC lineage or its split from the monocyte pathway downstream of the MDP is unknown. Similarly, the mechanisms regulating the transition from the cDC precursor into either the $CD4^+$ or $CD8^+$ subset are also unclear. Another key issue is whether the combinatorial action of cytokines within distinct stromal niches plays any role in influencing these fate choices. Answers to these outstanding questions will allow for the arrangement of the current transcription factor network into a resolvable structure that can be used for manipulation of DCs in clinical settings.

1.10 References

1. Steinman,R.M. & Cohn,Z.A. Identification of a novel cell type in peripheral lymphoid organs of mice. I. Morphology, quantitation, tissue distribution. *J Exp. Med.* 137, 1142-1162 (1973).

2. Steinman,R.M. & Witmer,M.D. Lymphoid dendritic cells are potent stimulators of the primary mixed leukocyte reaction in mice. *Proc. Natl. Acad. Sci U. S A* 75, 5132-5136 (1978).

3. Nussenzweig,M.C., Steinman,R.M., Gutchinov,B. & Cohn,Z.A. Dendritic cells are accessory cells for the development of anti-trinitrophenyl cytotoxic T lymphocytes. *J. Exp. Med.* 152, 1070-1084 (1980).

4. Banchereau,J. & Steinman,R.M. Dendritic cells and the control of immunity. *Nature* 392, 245-252 (1998).

5. Crowley,M., Inaba,K., Witmer-Pack,M. & Steinman,R.M. The cell surface of mouse dendritic cells: FACS analyses of dendritic cells from different tissues including thymus. *Cell Immunol.* 118, 108-125 (1989).

6. Vremec,D. *et al.* The surface phenotype of dendritic cells purified from mouse thymus and spleen: investigation of the CD8 expression by a subpopulation of dendritic cells. *J. Exp. Med.* 176, 47-58 (1992).

7. Ohnmacht,C. *et al.* Constitutive ablation of dendritic cells breaks self-tolerance of CD4 T cells and results in spontaneous fatal autoimmunity. *J Exp. Med.* 206, 549-559 (2009).

8. Birnberg,T. *et al.* Lack of conventional dendritic cells is compatible with normal development and T cell homeostasis, but causes myeloid proliferative syndrome *Immunity* 29, 986-997 (2008).

9. Wu,L., Li,C.L. & Shortman,K. Thymic dendritic cell precursors: relationship to the T lymphocyte lineage and phenotype of the dendritic cell progeny. *J. Exp. Med.* 184, 903-911 (1996).

10. Naik,S.H. Demystifying the development of dendritic cell subtypes, a little. *Immunology and Cell Biology* 86, 439-452 (2008).

11. Vremec,D. *et al.* CD4 and CD8 expression by dendritic cell subtypes in mouse thymus and spleen. *J. Immunol.* 164, 2978-2986 (2000).

12. Edwards,A.D. *et al.* Relationships among murine CD11c(high) dendritic cell subsets as revealed by baseline gene expression patterns. *J. Immunol.* 171, 47-60 (2003).

13. Blasius,A.L. *et al.* Bone marrow stromal cell antigen 2 is a specific marker of type I IFN-producing cells in the naive mouse, but a promiscuous cell surface antigen following IFN stimulation. *J Immunol* 177, 3260-3265 (2006).

14. Zhang,J. *et al.* Characterization of Siglec-H as a novel endocytic receptor expressed on murine plasmacytoid dendritic cell precursors. *Blood* 107, 3600-3608 (2006).

15. Grouard,G. *et al.* The enigmatic plasmacytoid T cells develop into dendritic cells with interleukin (IL)-3 and CD40-ligand. *J. Exp. Med.* 185, 1101-1111 (1997).

16. Crozat,K. *et al.* The XC chemokine receptor 1 is a conserved selective marker of mammalian cells homologous to mouse CD8alpha+ dendritic cells. *J Exp. Med.* 207, 1283-1292 (2010).

17. Poulin,L.F. *et al.* Characterization of human DNGR-1+ BDCA3+ leukocytes as putative equivalents of mouse CD8alpha+ dendritic cells. *J. Exp. Med.* 207, 1261-1271 (2010).

18. Bachem,A. *et al.* Superior antigen cross-presentation and XCR1 expression define human CD11c+CD141+ cells as homologues of mouse CD8+ dendritic cells. *J Exp. Med.* 207, 1273-1281 (2010).

19. Randolph,G.J., Inaba,K., Robbiani,D.F., Steinman,R.M. & Muller,W.A. Differentiation of phagocytic monocytes into lymph node dendritic cells in vivo. *Immunity.* 11, 753-761 (1999).

20. Randolph,G.J., Beaulieu,S., Lebecque,S., Steinman,R.M. & Muller,W.A. Differentiation of monocytes into dendritic cells in a model of transendothelial trafficking. *Science* 282, 480-483 (1998).

21. Swiecki,M., Gilfillan,S., Vermi,W., Wang,Y. & Colonna,M. Plasmacytoid dendritic cell ablation impacts early interferon responses and antiviral NK and CD8(+) T cell accrual. *Immunity* 33, 955-966 (2010).

22. Swiecki,M. & Colonna,M. Unraveling the functions of plasmacytoid dendritic cells during viral infections, autoimmunity, and tolerance. *Immunol Rev* 234, 142-162 (2010).

23. Cervantes-Barragan,L. *et al.* Plasmacytoid dendritic cells control T-cell response to chronic viral infection. *Proc. Natl. Acad. Sci. U. S A* 109, 3012-3017 (2012).

24. Sapoznikov,A. *et al.* Perivascular clusters of dendritic cells provide critical survival signals to B cells in bone marrow niches. *Nat Immunol* 9, 388-395 (2008).

25. McCartney,S. *et al.* Distinct and complementary functions of MDA5 and TLR3 in poly(I:C)-mediated activation of mouse NK cells. *J Exp. Med.* 206, 2967-2976 (2009).

26. Miyake,T. *et al.* Poly I:C-induced activation of NK cells by CD8 alpha+ dendritic cells via the IPS-1 and TRIF-dependent pathways. *J Immunol* 183, 2522-2528 (2009).

27. den Haan,J.M., Lehar,S.M. & Bevan,M.J. CD8(+) but not CD8(-) dendritic cells cross-prime cytotoxic T cells in vivo. *J Exp. Med.* 192, 1685-1696 (2000).

28. Bevan,M.J. Cross-priming for a secondary cytotoxic response to minor H antigens with H-2 congenic cells which do not cross-react in the cytotoxic assay. *J Exp. Med.* 143, 1283-1288 (1976).

29. Sigal,L.J., Crotty,S., Andino,R. & Rock,K.L. Cytotoxic T-cell immunity to virus-infected non-haematopoietic cells requires presentation of exogenous antigen. *Nature* 398, 77-80 (1999).

30. Ochsenbein,A.F. *et al.* Roles of tumour localization, second signals and cross priming in cytotoxic T-cell induction. *Nature* 411, 1058-1064 (2001).

31. Bedoui,S. *et al.* Cross-presentation of viral and self antigens by skin-derived CD103(+) dendritic cells. *Nat.* 10, 488-495 (2009).

32. Edelson,B.T. *et al.* Peripheral CD103+ dendritic cells form a unified subset developmentally related to CD8alpha+ conventional dendritic cells. *J. Exp. Med.* 207, 823-836 (2010).

33. Idoyaga,J., Suda,N., Suda,K., Park,C.G. & Steinman,R.M. Antibody to Langerin/CD207 localizes large numbers of CD8alpha+ dendritic cells to the marginal zone of mouse spleen. *Proc. Natl. Acad. Sci U. S A* 106, 1524-1529 (2009).

34. Qiu,C.H. *et al.* Novel Subset of CD8 alpha(+) Dendritic Cells Localized in the Marginal Zone Is Responsible for Tolerance to Cell-Associated Antigens. *J. Immunol.* 182, 4127-4136 (2009).

35. Reis e Sousa,C. *et al.* In vivo microbial stimulation induces rapid CD40 ligand-independent production of interleukin 12 by dendritic cells and their redistribution to T cell areas [see comments]. *J. Exp. Med.* 186, 1819-1829 (1997).

36. Hochrein,H. *et al.* Differential production of IL-12, IFN-alpha, and IFN-gamma by mouse dendritic cell subsets. *J Immunol* 166, 5448-5455 (2001).

37. Mashayekhi,M. *et al.* CD8a+ Dendritic Cells Are the Critical Source of Interleukin-12 that Controls Acute Infection by Toxoplasma gondii Tachyzoites. *Immunity* 35, 249-259 (2011).

38. Dudziak,D. *et al.* Differential antigen processing by dendritic cell subsets in vivo. *Science* 315, 107-111 (2007).

39. Kamphorst,A.O., Guermonprez,P., Dudziak,D. & Nussenzweig,M.C. Route of antigen uptake differentially impacts presentation by dendritic cells and activated monocytes. *J Immunol* 185, 3426-3435 (2010).

40. Cheong,C. *et al.* Microbial stimulation fully differentiates monocytes to DC-SIGN/CD209(+) dendritic cells for immune T cell areas. *Cell* 143, 416-429 (2010).

41. Nakano,H. *et al.* Blood-derived inflammatory dendritic cells in lymph nodes stimulate acute T helper type 1 immune responses. *Nat.* 10, 394-402 (2009).

42. Satpathy,A.T. *et al.* Notch2-dependent classical dendritic cells orchestrate intestinal immunity to attaching-and-effacing bacterial pathogens. *Nat. Immunol.* (2013).

43. Kinnebrew,M.A. *et al.* Interleukin 23 production by intestinal CD103(+)CD11b(+) dendritic cells in response to bacterial flagellin enhances mucosal innate immune defense. *Immunity* 36, 276-287 (2012).

44. Welty,N.E. *et al.* Intestinal lamina propria dendritic cells maintain T cell homeostasis but do not affect commensalism. *J. Exp. Med.* (2013).

45. Perussia,B., Fanning,V. & Trinchieri,G. A leukocyte subset bearing HLA-DR antigens is responsible for in vitro alpha interferon production in response to viruses. *Nat. Immun. Cell Growth Regul.* 4, 120-137 (1985).

46. Cella,M. *et al.* Plasmacytoid monocytes migrate to inflamed lymph nodes and produce large amounts of type I interferon [see comments]. *Nature Medicine* 5, 919-923 (1999).

47. Siegal,F.P. *et al.* The nature of the principal type 1 interferon-producing cells in human blood. *Science* 284, 1835-1837 (1999).

48. Takagi,H. *et al.* Plasmacytoid dendritic cells are crucial for the initiation of inflammation and T cell immunity in vivo. *Immunity.* 35, 958-971 (2011).

49. Hume,D.A. Macrophages as APC and the dendritic cell myth. *J Immunol* 181, 5829-5835 (2008).

50. Yoshimoto,T. *et al.* Basophils contribute to T(H)2-IgE responses in vivo via IL-4 production and presentation of peptide-MHC class II complexes to CD4+ T cells. *Nat Immunol* 10, 706-712 (2009).

51. Sokol,C.L. *et al.* Basophils function as antigen-presenting cells for an allergen-induced T helper type 2 response. *Nat Immunol* 10, 713-720 (2009).

52. Hammad,H. *et al.* Inflammatory dendritic cells--not basophils--are necessary and sufficient for induction of Th2 immunity to inhaled house dust mite allergen. *J Exp. Med.* 207, 2097-2111 (2010).

53. Manicassamy,S. *et al.* Activation of beta-catenin in dendritic cells regulates immunity versus tolerance in the intestine. *Science* 329, 849-853 (2010).

54. Geissmann,F., Gordon,S., Hume,D.A., Mowat,A.M. & Randolph,G.J. Unravelling mononuclear phagocyte heterogeneity. *Nat Rev Immunol* 10, 453-460 (2010).

55. Liu,K. *et al.* Origin of dendritic cells in peripheral lymphoid organs of mice. *Nat Immunol* 8, 578-583 (2007).

56. Kamath,A.T. *et al.* The development, maturation, and turnover rate of mouse spleen dendritic cell populations. *J. Immunol.* 165, 6762-6770 (2000).

57. Kondo,M., Weissman,I.L. & Akashi,K. Identification of clonogenic common lymphoid progenitors in mouse bone marrow. *Cell* 91, 661-672 (1997).

58. Akashi,K., Traver,D., Miyamoto,T. & Weissman,I.L. A clonogenic common myeloid progenitor that gives rise to all myeloid lineages. *Nature* 404, 193-197 (2000).

59. Manz,M.G., Traver,D., Miyamoto,T., Weissman,I.L. & Akashi,K. Dendritic cell potentials of early lymphoid and myeloid progenitors. *Blood* 97, 3333-3341 (2001).

60. Manz,M.G. *et al.* Dendritic cell development from common myeloid progenitors. *Ann. N. Y. Acad. Sci* 938, 167-173 (2001).

61. Traver,D. *et al.* Development of CD8alpha-positive dendritic cells from a common myeloid progenitor. *Science* 290, 2152-2154 (2000).

62. Inaba,K. *et al.* Generation of large numbers of dendritic cells from mouse bone marrow cultures supplemented with granulocyte/macrophage colony-stimulating factor. *J Exp. Med.* 176, 1693-1702 (1992).

63. Schlenner,S.M. *et al.* Fate mapping reveals separate origins of T cells and myeloid lineages in the thymus. *Immunity* 32, 426-436 (2010).

64. Fogg,D.K. *et al.* A clonogenic bone marrow progenitor specific for macrophages and dendritic cells. *Science* 311, 83-87 (2006).

65. Onai,N. *et al.* Identification of clonogenic common Flt3(+) M-CSFR+ plasmacytoid and conventional dendritic cell progenitors in mouse bone marrow. *Nat.* 8, 1207-1216 (2007).

66. Naik,S.H. *et al.* Development of plasmacytoid and conventional dendritic cell subtypes from single precursor cells derived in vitro and in vivo. *Nat Immunol* 8, 1217-1226 (2007).

67. Liu,K. *et al.* In vivo analysis of dendritic cell development and homeostasis. *Science* 324, 392-397 (2009).

68. Cisse,B. *et al.* Transcription factor E2-2 is an essential and specific regulator of plasmacytoid dendritic cell development. *Cell* 135, 37-48 (2008).

69. Naik,S.H. *et al.* Intrasplenic steady-state dendritic cell precursors that are distinct from monocytes. *Nat Immunol* 7, 663-671 (2006).

70. Sallusto,F. & Lanzavecchia,A. Efficient presentation of soluble antigen by cultured human dendritic cells is maintained by granulocyte/macrophage colony-stimulating factor plus interleukin 4 and downregulated by tumor necrosis factor alpha. *J Exp. Med.* 179, 1109-1118 (1994).

71. Kingston,D. *et al.* The concerted action of GM-CSF and Flt3-ligand on in vivo dendritic cell homeostasis. *Blood* 114, 835-843 (2009).

72. Vremec,D. *et al.* The influence of granulocyte/macrophage colony-stimulating factor on dendritic cell levels in mouse lymphoid organs. *Eur. J Immunol* 27, 40-44 (1997).

73. Serbina,N.V., Salazar-Mather,T.P., Biron,C.A., Kuziel,W.A. & Pamer,E.G. TNF/iNOS-producing dendritic cells mediate innate immune defense against bacterial infection. *Immunity* 19, 59-70 (2003).

74. Xu,Y., Zhan,Y., Lew,A.M., Naik,S.H. & Kershaw,M.H. Differential development of murine dendritic cells by GM-CSF versus Flt3 ligand has implications for inflammation and trafficking. *J Immunol* 179, 7577-7584 (2007).

75. Maraskovsky,E. *et al.* Dramatic numerical increase of functionally mature dendritic cells in FLT3 ligand-treated mice. *Adv. Exp. Med. Biol* 417, 33-40 (1997).

76. Brasel,K., De Smedt,T., Smith,J.L. & Maliszewski,C.R. Generation of murine dendritic cells from flt3-ligand-supplemented bone marrow cultures. *Blood* 96, 3029-3039 (2000).

77. Onai,N., Obata-Onai,A., Tussiwand,R., Lanzavecchia,A. & Manz,M.G. Activation of the Flt3 signal transduction cascade rescues and enhances type I interferon-producing and dendritic cell development. *J Exp. Med.* 203, 227-238 (2006).

78. McKenna,H.J. *et al.* Mice lacking flt3 ligand have deficient hematopoiesis affecting hematopoietic progenitor cells, dendritic cells, and natural killer cells. *Blood* 95, 3489-3497 (2000).

79. Waskow,C. *et al.* The receptor tyrosine kinase Flt3 is required for dendritic cell development in peripheral lymphoid tissues. *Nat Immunol* 9, 676-683 (2008).

80. Laouar,Y., Welte,T., Fu,X.Y. & Flavell,R.A. STAT3 is required for Flt3L-dependent dendritic cell differentiation. *Immunity* 19, 903-912 (2003).

81. Sathaliyawala,T. *et al.* Mammalian target of rapamycin controls dendritic cell development downstream of Flt3 ligand signaling. *Immunity* 33, 597-606 (2010).

82. Tokoyoda,K., Egawa,T., Sugiyama,T., Choi,B.I. & Nagasawa,T. Cellular niches controlling B lymphocyte behavior within bone marrow during development. *Immunity* 20, 707-718 (2004).

83. Schmid,M.A., Kingston,D., Boddupalli,S. & Manz,M.G. Instructive cytokine signals in dendritic cell lineage commitment. *Immunol Rev* 234, 32-44 (2010).

84. Esashi,E. *et al.* The signal transducer STAT5 inhibits plasmacytoid dendritic cell development by suppressing transcription factor IRF8. *Immunity* 28, 509-520 (2008).

85. Wu,L., Nichogiannopoulou,A., Shortman,K. & Georgopoulos,K. Cell-autonomous defects in dendritic cell populations of Ikaros mutant mice point to a developmental relationship with the lymphoid lineage. *Immunity* 7, 483-492 (1997).

86. Allman,D. *et al.* Ikaros is required for plasmacytoid dendritic cell differentiation. *Blood* 108, 4025-4034 (2006).

87. Ng,S.Y., Yoshida,T., Zhang,J. & Georgopoulos,K. Genome-wide lineage-specific transcriptional networks underscore Ikaros-dependent lymphoid priming in hematopoietic stem cells. *Immunity* 30, 493-507 (2009).

88. Yoshida,T., Ng,S.Y. & Georgopoulos,K. Awakening lineage potential by Ikaros-mediated transcriptional priming. *Curr. Opin. Immunol* 22, 154-160 (2010).

89. Guerriero,A., Langmuir,P.B., Spain,L.M. & Scott,E.W. PU.1 is required for myeloid-derived but not lymphoid-derived dendritic cells. *Blood* 95, 879-885 (2000).

90. Anderson,K.L. *et al.* Transcription factor PU.1 is necessary for development of thymic and myeloid progenitor-derived dendritic cells. *J Immunol* 164, 1855-1861 (2000).

91. Carotta,S. *et al.* The transcription factor PU.1 controls dendritic cell development and Flt3 cytokine receptor expression in a dose-dependent manner. *Immunity* 32, 628-641 (2010).

92. Zhang,D.E., Hetherington,C.J., Chen,H.M. & Tenen,D.G. The macrophage transcription factor PU.1 directs tissue-specific expression of the macrophage colony-stimulating factor receptor. *Mol Cell Biol* 14, 373-381 (1994).

93. Hohaus,S. *et al.* PU.1 (Spi-1) and C/EBP alpha regulate expression of the granulocyte-macrophage colony-stimulating factor receptor alpha gene. *Mol Cell Biol* 15, 5830-5845 (1995).

94. Rathinam,C. *et al.* The transcriptional repressor Gfi1 controls STAT3-dependent dendritic cell development and function. *Immunity* 22, 717-728 (2005).

95. Rodel,B. *et al.* The zinc finger protein Gfi-1 can enhance STAT3 signaling by interacting with the STAT3 inhibitor PIAS3. *EMBO J* 19, 5845-5855 (2000).

96. Duan,Z. & Horwitz,M. Targets of the transcriptional repressor oncoprotein Gfi-1. *Proc. Natl. Acad. Sci U. S A* 100, 5932-5937 (2003).

97. Kobayashi,T. *et al.* TRAF6 is a critical factor for dendritic cell maturation and development. *Immunity* 19, 353-363 (2003).

98. Spooner,C.J., Cheng,J.X., Pujadas,E., Laslo,P. & Singh,H. A recurrent network involving the transcription factors PU.1 and Gfi1 orchestrates innate and adaptive immune cell fates. *Immunity* 31, 576-586 (2009).

99. Ginhoux,F. *et al.* The origin and development of nonlymphoid tissue CD103+ DCs. *J Exp. Med.* 206, 3115-3130 (2009).

100. Vallabhapurapu,S. & Karin,M. Regulation and function of NF-kappaB transcription factors in the immune system. *Annu. Rev Immunol* 27, 693-733 (2009).

101. Wu,L. *et al.* RelB is essential for the development of myeloid-related CD8alpha- dendritic cells but not of lymphoid-related CD8alpha+ dendritic cells. *Immunity.* 9, 839-847 (1998).

102. Burkly,L. *et al.* Expression of relB is required for the development of thymic medulla and dendritic cells. *Nature* 373, 531-536 (1995).

103. Suzuki,S. *et al.* Critical roles of interferon regulatory factor 4 in CD11bhighCD8alpha- dendritic cell development. *Proc. Natl. Acad. Sci U. S. A* 101, 8981-8986 (2004).

104. Eisenbeis,C.F., Singh,H. & Storb,U. Pip, a novel IRF family member, is a lymphoid-specific, PU.1-dependent transcriptional activator. *Genes Dev.* 9, 1377-1387 (1995).

105. Brass,A.L., Kehrli,E., Eisenbeis,C.F., Storb,U. & Singh,H. Pip, a lymphoid-restricted IRF, contains a regulatory domain that is important for autoinhibition and ternary complex formation with the Ets factor PU.1. *Genes Dev.* 10, 2335-2347 (1996).

106. Biswas,P.S., Bhagat,G. & Pernis,A.B. IRF4 and its regulators: evolving insights into the pathogenesis of inflammatory arthritis? *Immunol Rev* 233, 79-96 (2010).

107. Tamura,T. *et al.* IFN regulatory factor-4 and -8 govern dendritic cell subset development and their functional diversity. *J Immunol* 174, 2573-2581 (2005).

108. Schiavoni,G. *et al.* ICSBP is essential for the development of mouse type I interferon-producing cells and for the generation and activation of CD8alpha(+) dendritic cells. *J Exp. Med.* 196, 1415-1425 (2002).

109. Hildner,K. *et al.* Batf3 deficiency reveals a critical role for CD8alpha+ dendritic cells in cytotoxic T cell immunity. *Science* 322, 1097-1100 (2008).

110. Iacobelli,M., Wachsman,W. & McGuire,K.L. Repression of IL-2 promoter activity by the novel basic leucine zipper p21(SNFT) protein. *J. Immunol.* 165, 860-868 (2000).

111. Bower,K.E., Fritz,J.M. & McGuire,K.L. Transcriptional repression of MMP-1 by p21SNFT and reduced in vitro invasiveness of hepatocarcinoma cells. *Oncogene* 23, 8805-8814 (2004).

112. Schraml,B.U. *et al.* The AP-1 transcription factor Batf controls T(H)17 differentiation. *Nature* 460, 405-409 (2009).

113. Betz,B.C. *et al.* Batf coordinates multiple aspects of B and T cell function required for normal antibody responses. *J. Exp. Med.* 207, 933-942 (2010).

114. Caton,M.L., Smith-Raska,M.R. & Reizis,B. Notch-RBP-J signaling controls the homeostasis of CD8- dendritic cells in the spleen. *J Exp. Med.* 204, 1653-1664 (2007).

115. Ohtsuka,H. *et al.* Bcl6 is required for the development of mouse CD4+ and CD8alpha+ dendritic cells. *J Immunol* 186, 255-263 (2011).

116. Johnston,R.J. *et al.* Bcl6 and Blimp-1 Are Reciprocal and Antagonistic Regulators of T Follicular Helper Cell Differentiation. *Science* 325, 1006-1010 (2009).

117. Niu,H., Cattoretti,G. & Dalla-Favera,R. BCL6 Controls the Expression of the B7-1/CD80 Costimulatory Receptor in Germinal Center B Cells. *J. Exp. Med.* 198, 211-221 (2003).

118. Nurieva,R.I. *et al.* Bcl6 Mediates the Development of T Follicular Helper Cells. *Science* 325, 1001-1005 (2009).

119. Kee,B.L. E and ID proteins branch out. *Nat Rev Immunol* 9, 175-184 (2009).

120. Spits,H., Couwenberg,F., Bakker,A.Q., Weijer,K. & Uittenbogaart,C.H. Id2 and Id3 inhibit development of CD34(+) stem cells into predendritic cell (pre-DC)2 but not into pre-DC1. Evidence for a lymphoid origin of pre-DC2. *J Exp. Med.* 192, 1775-1784 (2000).

121. Hacker,C. *et al.* Transcriptional profiling identifies Id2 function in dendritic cell development. *Nat Immunol* 4, 380-386 (2003).

122. Robbins,S.H. *et al.* Novel insights into the relationships between dendritic cell subsets in human and mouse revealed by genome-wide expression profiling. *Genome Biol* 9, R17 (2008).

123. Ghosh,H.S., Cisse,B., Bunin,A., Lewis,K.L. & Reizis,B. Continuous expression of the transcription factor e2-2 maintains the cell fate of mature plasmacytoid dendritic cells. *Immunity* 33, 905-916 (2010).

124. Bar-On,L. *et al.* CX3CR1+ CD8alpha+ dendritic cells are a steady-state population related to plasmacytoid dendritic cells. *Proc. Natl. Acad. Sci. U. S A* 107, 14745-14750 (2010).

125. Pui,J.C. *et al.* Notch1 expression in early lymphopoiesis influences B versus T lineage determination. *Immunity* 11, 299-308 (1999).

126. Li,L., Leid,M. & Rothenberg,E.V. An early T cell lineage commitment checkpoint dependent on the transcription factor Bcl11b. *Science* 329, 89-93 (2010).

127. Li,P. *et al.* Reprogramming of T cells to natural killer-like cells upon Bcl11b deletion. *Science* 329, 85-89 (2010).

128. Ikawa,T. *et al.* An essential developmental checkpoint for production of the T cell lineage. *Science* 329, 93-96 (2010).

129. Felker,P. *et al.* TGF-beta1 accelerates dendritic cell differentiation from common dendritic cell progenitors and directs subset specification toward conventional dendritic cells. *J Immunol* 185, 5326-5335 (2010).

130. Ouyang,W. *et al.* Stat6-independent GATA-3 autoactivation directs IL-4-independent Th2 development and commitment. *Immunity* 12, 27-37 (2000).

Chapter 2 *Batf3* regulates survival and maturation subsequent to an *Irf8*-dependent lineage commitment step in the development of CD8α^{+} dendritic cells

2.1 Abstract

Classical dendritic cells (cDCs) in lymphoid tissues are composed of two major subtypes distinguished by differential expression of CD8α. CD8α$^+$ cDCs are important for responses to many viruses based on their *in vivo* capacity for cross-presentation and priming of CD8$^+$ T cells. While CD8α$^+$ cDCs require *Batf3* and *Irf8* for development, the cellular basis of these actions remains unclear. Here, we analyzed the developmental stage and cellular processes controlled by *Batf3* and *Irf8* in ontogeny of CD8α$^+$ cDCs. *Irf8* is highly expressed in CD8α$^+$ cDCs and in progenitors of mature cDCs and pDCs. In contrast, *Batf3* is not expressed in early cDC progenitors, and is induced only in the terminal stages of cDC maturation. We find that *Irf8*$^{-/-}$ mice exhibit reduced numbers of common dendritic cell progenitors (CDPs) and committed cDC precursors (pre-cDCs). Furthermore, *Irf8*$^{-/-}$ mice show a complete absence of CD24$^+$ Sirp-α$^-$ cDCs, which represent the committed progenitors of mature CD8α$^+$ cDCs. In contrast, *Batf3*$^{-/-}$ mice have normal numbers of CDPs and pre-cDCs and retain a reduced population of CD24$^+$ Sirp-α$^-$ cDCs that express high levels of *Irf8*. However, *Batf3*$^{-/-}$ CD24$^+$ Sirp-α$^-$ cDCs exhibit decreased lifespan and reduced competitive fitness *in vivo* and fail to express genes characteristic of functionally mature CD8α$^+$ cDCs such as *Xcr1*, *Clec9a* and *Tlr3*. These results indicate that *Irf8* and *Batf3* act at distinct stages of CD8α$^+$ cDC development, with Irf8 initiating CD8α-lineage commitment and Batf3 acting in survival and maturation of these committed progenitors.

2.2 Introduction

Murine dendritic cells (DCs) comprise classical DCs (cDCs) involved in T cell activation and plasmacytoid DCs (pDCs) involved in viral sensing and interferon production [1,2]. cDCs in lymphoid tissues segregate into two major subsets based on expression of the CD8α marker [3,4]. Although lacking expression of CD8α in non-lymphoid tissues, peripheral DCs segregate into two functionally related subsets distinguished by the expression of CD103 and CD11b [2,5]. Lymphoid-resident $CD8\alpha^+$ cDCs and tissue-resident $CD103^+$ cDCs are related by shared expression of several markers, such as XCR1 and Clec9a, and by providing antigen cross-presentation in the activation of $CD8^+$ T cells against viruses [6-9].

Adoptive transfer studies [10-12] suggest both the common lymphoid progenitor (CLP) [13] and common myeloid progenitor (CMP) [14] can generate all DC subsets. However, lineage tracing indicates that steady-state DCs *in vivo* are predominantly CMP-derived [15]. The CMP generates a macrophage/dendritic cell-restricted precursor (MDP) [16,17] which then gives rise to a common dendritic cell progenitor (CDP) [18,19]. The CDP appears to be the immediate precursor of pre-pDCs [20] and pre-cDCs [16,21], both of which are lineage- restricted but immature. While pDCs mature in the bone marrow (BM) and circulate through the blood to secondary lymphoid organs, pre-cDCs migrate via the blood to populate both lymphoid- and non-lymphoid tissues where upon development into either $CD8\alpha^+$ cDC or $CD8\alpha^-$ cDC is completed [16]. While the precursor-product relationship for murine dendritic cells is mostly resolved, the molecular mechanism and stage of action for key transcription factors important in DC development is still poorly understood.

Some transcription factors regulate broad aspects of DC development [22,23]. Ikaros (*Ikzf1*) is required for the development of all lymphoid lineages [24] and for some DCs subsets. *Ikzf1*$^{-/-}$ mice lack pDCs and CD8α^{-} cDCs, and a dominant negative form of Ikaros eliminates all DCs [24,25]. Deletion of PU.1 (*Sfpi1*) from hematopoietic cells eliminates all DC subsets and causes defects in macrophages, neutrophils and other myeloid lineages [26]. This may relate to the regulation by PU.1 of FMS-like tyrosine kinase 3-ligand receptor (Flt3) [27,28], a key receptor for DC homeostasis *in vivo*[29]. Similarly, loss of Gfi1 broadly reduces the size of DC populations, albeit not as severely as in *Ikzf1*$^{-/-}$ or *Sfpi1*$^{-/-}$ mice [30]. In addition to DCs, many other myeloid and lymphoid lineages are broadly affected by defects in Ikaros, PU.1 or Gfi1, consistent with their relatively high expression in early hematopoietic progenitors.

In contrast, other transcription factors are expressed late in DC development and regulate subsets of DCs. Within cDCs, *Irf4* and *Irf8* are expressed in CD8α^{+} or CD8α^{-} DCs, respectively [31]. *Irf4*$^{-/-}$ mice reportedly have reduced numbers of CD8α^{-} DCs [32] and also have defects in T and B cells [33,34]. *Irf8*$^{-/-}$ mice lack CD8α^{+} cDCs and pDCs , but also display defects in macrophages and B cells [35-40]. Despite being recognized for nearly a decade as a requirement in CD8α^{+} cDC development, the cellular and molecular basis for the actions of *Irf8* are not yet understood.

Finally, the AP-1 family member *Batf3* is selectively required for CD8α^{+} [7] and peripheral CD103^{+} cDC development[8]. In contrast to the expression of *Irf4* and *Irf8*, *Batf3* is expressed in both DC subsets. The cellular basis for the requirement of *Batf3* in CD8α^{+} cDC development is currently unclear. In the present study, we characterize the cellular basis for *Batf3* and *Irf8* in the development of CD8α^{+} cDCs.

2.3 Results

2.3.1 *Batf3* induction occurs subsequent to the expression of *Irf8* in DC progenitors

The AP-1 family member basic leucine zipper transcription factor, ATF-like 3 (Batf3; also known as JDP1 and $p21^{SNFT}$) is critically required for the proper development of $CD8\alpha^+$ DCs in lymphoid organs and the related $CD103^+$ DCs in peripheral tissues despite being expressed in both subsets of DCs [7,8]. Additionally, interferon regulatory factor 8 (Irf8; also known as ICSBP) is required for the development of $CD8\alpha^+$ cDCs and pDCs[41-43]; and in the setting of competitive bone marrow reconstitution, it is also required for the reconstitution of $CD11b^+$ DCs. Moreover, IRF8-deficient mice show profound changes in both lymphoid and myeloid progenitors in the bone marrow[44]. Lastly, several reports have recently demonstrated a functional interaction between AP-1 and IRF proteins on AP1-IRF composite elements (AICE). To characterize the stage-specific actions of *Batf3* and *Irf8*, we quantitated the relative expression of both genes in early myeloid progenitors and mature DC populations. *Irf8* is expressed highly in DC progenitors (CDP and pre-cDC) and $CD8\alpha^+$ DCs, but largely absent from $CD4^+$ DCs. In contrast, *Batf3* is induced at the progenitor stage and then highly upregulated mature DC subsets (Figure 2.1 **A-C**).

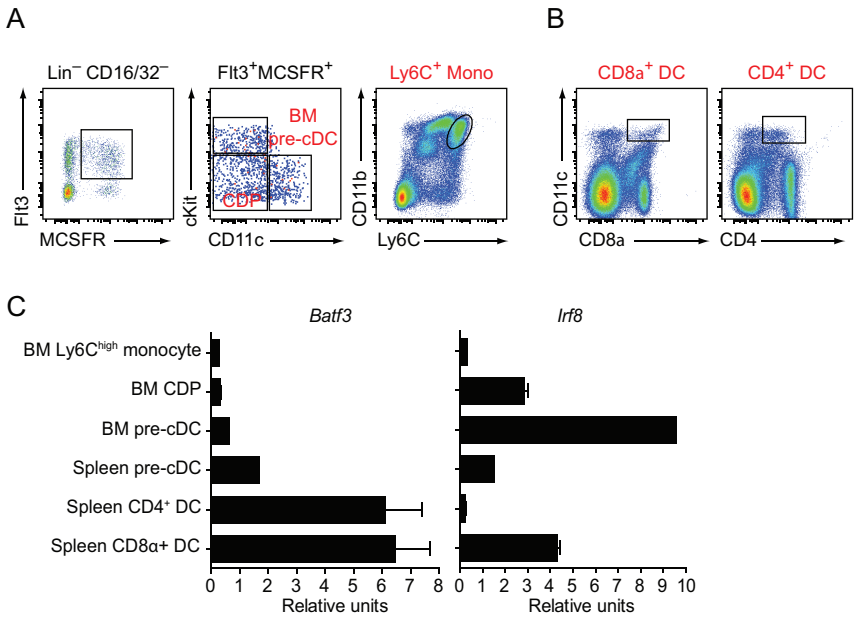

Figure 2.1: Batf3 induction occurs subsequent to the expression of Irf8 in DC progenitors

(A) Bone marrow cells from C57BL/6 wild-type mice were stained for the indicated markers and the gated populations were isolated by cell sorting. (B) Splenocytes were stained with the indicated markers and the DC populations were purified by cell sorting. (C) Quantitative real-time PCR (qPCR) for Batf3 and Irf8 in the indicated cell populations. The assay was performed on two independently purified sets of each cell type, except for BM and spleen pre-cDCs, which were only sorted a single time. Bars represent the mean and standard deviation.

2.3.2 Neither *Irf8* nor *Id2* rescue *Batf3* deficiency in dendritic cell development

Although *Irf8* expression precedes the induction of *Batf3* in BM DC progenitors, we determined whether BATF3 was necessary for the subsequent maintenance of *Irf8* downstream of the CDP and pre-cDC stages of development. Similarly, we evaluated whether the transcription factor inhibitor of DNA binding 2 (*Id2*), which is also necessary for CD8α$^+$ DC development, is downstream of *Batf3*. To directly test these two hypotheses, we adapted a previously reported *in vitro* system for the generation and retroviral transduction of DCs[37,45];

Ozato and colleagues have successfully used this system to rescue Irf8-deficient DCs. Therefore, we generated retroviral constructs harboring the cDNA of either murine *Irf8* or *Id2* (cloned from splenic cDNA library) upstream of an internal ribosome entry site (IRES) and green fluorescent protein (GFP). We then confirmed efficient transduction of DC precursors generated with the cytokine FMS-like tyrosine kinase ligand (Flt3L) [46]. However, neither IRF8 nor ID2 transduction rescued Batf3-deficiency *in vitro* (Figure 2.2 **A)**. We obtained similarly negative results *in vivo* with radiation bone marrow chimeras[47] that were transplanted with transduced hematopoietic stem cells (HSCs) (Figure 2.2 **B**). These data suggest that BATF3 activity is non-redundant with respect to other known transcriptional regulators of DC development.

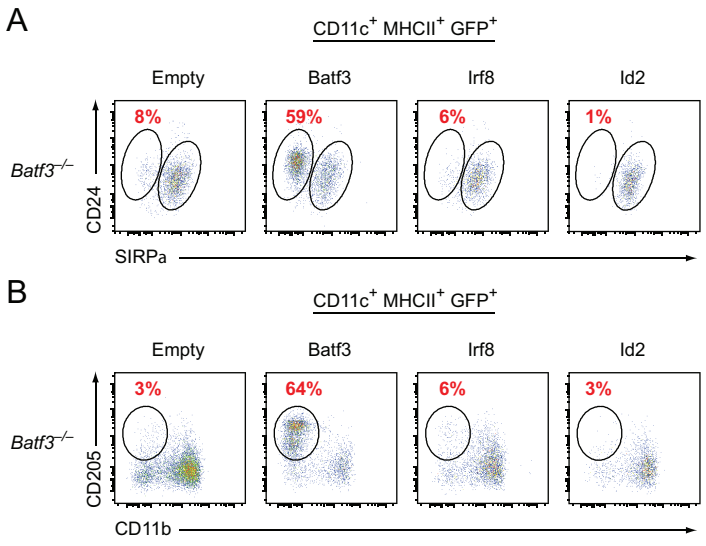

Figure 2.2: Irf8 and Id2 fail to rescue Batf3 deficiency

Transduction of bone marrow DC cultures (A) or cKit enriched cells was carried out as described in Methods. Shown are two-color histograms for the indicated markers. Numbers represent percent of cells in the gate. cKit enriched BM cells were cultured in the presence of stem cell factor (SCF) and thrombopoietin for 12 hours and then transplanted into conditioned mice.

2.3.3 AP-1 complexes consisting of BATF3 are non-redundant and play a unique role in the context of DC development

The inability of IRF8 and ID2 to restore BATF3-deficient CD8α^+ DCs suggests a unique role for BATF3-containing AP-1 complexes. Interestingly, the two components of the canonical AP-1 complex, FOS and JUN (and their related paralogs), are thought to be widely expressed in both hematopoietic and non-hematopoietic tissues, in which AP-1 is known to regulate gene expression broadly [48-50]. *Batf3* is a member of the ATF family, which is a subgroup of a larger family of DNA binding proteins collectively called basic leucine zipper (bZIP) transcription factors[51]. These factors minimally contain a α-helical basic DNA-binding region and regularly spaced leucine zipper motif[52-54]. The function of bZIP proteins as transcription factors was described through extensive studies on two of the earliest identified family members, FOS and JUN, which together constitute the heterodimeric transcription factor complex called activator protein 1 (AP-1)[49]. AP-1 complex is thought to regulate gene expression through its *trans*-activating domains (TAD), which mediate recruitment of chromatin remodeling complexes. Alternatively, the AP-1 complex can directly interact with nearby transcription factors, such as nuclear factor of activated T cells (NFAT), to modulate gene expression.

Unlike the canonical members of the AP-1 family, BATF3 contains no TAD and thus has been proposed to inhibit gene expression through a dominant-negative mechanism. And yet the numerous functional and developmental defects observed in *Batf3*$^{-/-}$ and *Batf*$^{-/-}$ mice suggest a positive transcriptional activity for BATF(3)-containing AP-1 complexes [7,55]. To clarify this matter, we performed multiple sequence alignment of FOS, JUN, and ATF family members, paying particular attention to the basic region and leucine zipper (Figure 2.3 **A**). The relevant

basic residues that contact the major groove of DNA are highly conserved among all members, agreeing with previous studies showing that BATF3 binds to the AP-1 consensus site[56]. Although the dimerization-promoting leucine residues (which face inward on the heterodimer complex) are also highly conserved, the outward facing residues show poor conservation, especially for BATF and BATF3. Next, we tested each AP-1 member for its functional similarity to BATF3 in DC development (Figure 2.3 **B**). We found that neither FOS nor JUN family members promoted the *in vitro* generation of $CD8\alpha^+$ DCs. Given FOS and JUN contain TAD, which might account for the observed difference, we used a naturally occurring splice variant of *Fosb* that lacks the TAD (ΔFosb) and functions effectively as a dominant negative [57]. ΔFosb showed the greatest inhibitory activity during the generation of *in vitro* derived $CD8\alpha^+$ DC equivalents. This result suggests that the determinant for AP-1 activity during DC development is either in the basic region or the leucine zipper. We also evaluated the more closely related ATF family members, activating transcription factor 3 (ATF3) and JUN dimerization protein 2 (JDP2), which also associate with JUN proteins to form a functional AP-1 complex. Neither ATF3 nor JDP2 were able to rescue BATF3-deficient cells, again suggesting a unique function of BATF3-containing AP-1 complexes. The molecular basis of this differential activity must lie within either the DNA binding domain (DBD) or the leucine zipper motif. Two possibilities exist, then – the DBD binds to the consensus AP-1 motif but also recognizes degenerate sequences which are distinct from those recognized by FOS-containing complexes; or the leucine zipper mediates distinct interactions with different partner proteins[58]. Recently, several reports concluded that BATFs can interact with IRF family members through the leucine zipper region[59-61]. While the interaction analysis was performed on *bona fide* target genes for

lymphocytes, the studies minimally evaluated DC targets under the dual control of IRFs and BATFs.

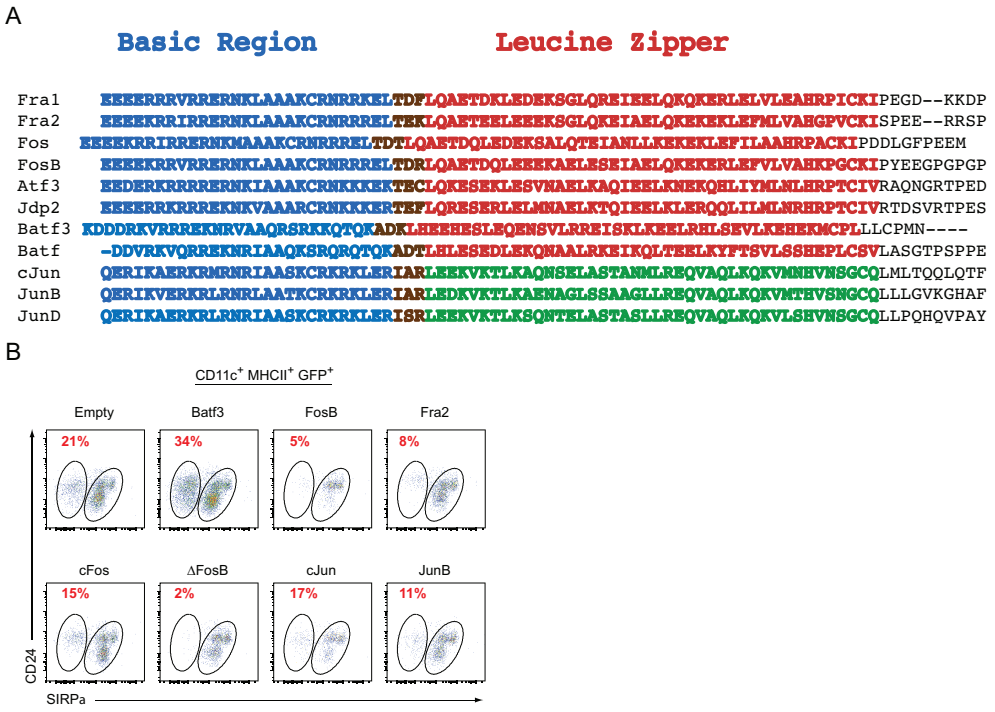

Figure 2.3: BATF3 containing AP1 complexes are uniquely required for DC development

(A) Protein sequences of the indicated AP-1 factors were compared with ClustalW2 (EMBL-EBI). Single-letter amino acid sequence is shown, with the basic region and leucine zipper indicated. Within each segment, sequences that contact the DNA (basic region) or play a role in protein dimerization (leucine zipper) are raised. (B) BM cells were cultured for 10 days in the presence of recombinant Flt3L. Retroviral transduction of DC cultures was carried out on day 2 and cells were stained for analysis on day 10. Shown are two-color histograms for the indicated markers. Numbers represent percent of cells in the gate. Data are representative of 2 independent experiments.

2.3.4 *Batf3* induction primes progenitors toward CD8α$^+$ DC commitment

The overexpression of BATF3 in progenitors actively promoted the generation of *in vitro* derived CD8α$^+$ DCs. Yet *Batf3* levels are rather low in BM DC progenitors. It has also been

noted that the CDP is a pDC-primed state, in which pDC-related transcription factors (such as *Tcf4*, *Bcl11a*, *Runx2*) are moderately expressed but cDC-related factors are poorly expressed[23]. Thus, we hypothesized that *Batf3* induction promotes the active commitment of early DC progenitors away from pDC or CD11b$^+$ DCs and toward CD8α$^+$ DCs. One potential inducer of *Batf3* is Flt3L, as it has long been recognized for its propensity to increase CD8α$^+$ DC numbers dramatically after exogenous administration [29]. We tested this by administering Flt3L by intraperitoneal route and isolating pre-cDCs from the bone marrow and performed microarray analysis on the purified RNA.

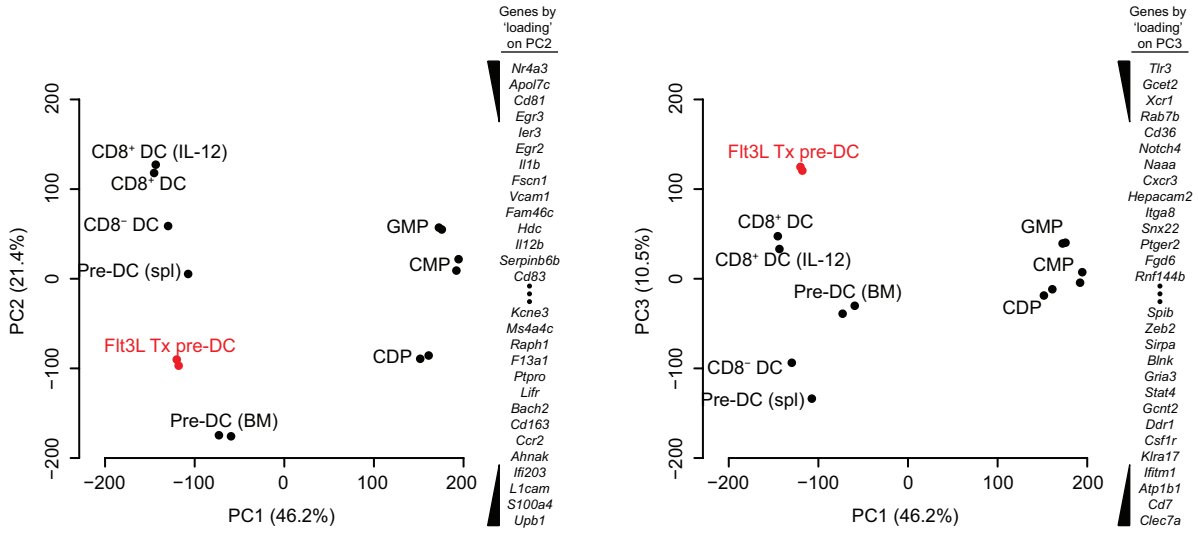

Figure 2.4: *Batf3* induction primes DC progenitors toward CD8α$^+$ DCs

(A) WT C57BL/6 mice were treated with a single dose of 10 mg per mouse recombinant Flt3L. Bone marrow cells were isolated two days later and DC progenitors were sorted as lineage-negative, CD11c+ cKit+. Purified RNA was converted to labeled product and microarray analysis performed. PCA analysis was carried out in R. Top 14 genes with the highest positive and negative loading scores are shown for PC2 and PC3.

Next, an unbiased assessment of the treated progenitor was carried out through the use of principal-component analysis (PCA). In PCA of multiple myeloid progenitor populations and mature DCs, most of the variation in gene expression is captured in three principal components (Figure 2.4). PC1 segregates cell types as either myeloid progenitors (CDP, CMP, GMP) or immature and mature DC subsets (the most negative loadings include *H2-A/E*, *Zbtb46*, *Batf3* which are all known cDC genes). When genes are ordered by their relative weights in PC3, the most positive loadings correspond to well characterized CD8α$^+$ DC genes such as *Tlr3*, *Xcr1*, and *CD36*[62,63]; the most negative loadings correspond to genes such as *Spib*, *Zeb2*, *Sirpa* and *Csf1r*, which are associated with functions in CD11b$^+$ DCs or monocytes [64-67]. This analysis suggests that early BM DC progenitors can be induced to express *Batf3*, which then partly initiates the CD8α$^+$ DC commitment program.

2.3.5 Commitment by pre-cDCs to the CD8α$^+$ cDC subset requires Irf8 but not Batf3

Since mature CD8α$^+$ DCs arise from pre-cDCs through a CD24^{High}Sirp-α^{Low} intermediate population [16,21], we asked whether the expression of these two markers could identify an earlier stage of CD8α$^+$ DC development (Figure 2.5 **A**). *Batf3*$^{-/-}$ mice on the 129SvEv background have a significant reduction in spleen-resident CD8α$^+$Dec205$^+$ DCs, comprising 0.1% of total cDCs, as compared to wild type (WT) mice, which have 6.3% of total cDCs (Figure 2.5 **A, upper panels**). However, 129SvEv *Batf3*$^{-/-}$ mice retain a residual 2-3% population of CD24$^+$Sirp-α$^-$ cDCs, representing a 4-fold reduction relative to WT 129SvEv mice (Figure 2.5 **A, lower panels**). Interestingly, *Batf3*$^{-/-}$ mice on the C57BL/6 background show a less complete loss of CD8α$^+$Dec205$^+$ DCs as compared to 129SvEv mice (Figure 2.5 **B, upper panels**), as we previously reported [68], but still exhibit defective CD8α$^+$ cDC function *in vivo* [69,70]. Notably,

C57BL/6 *Batf3*$^{-/-}$ mice also retain a CD24^{+}Sirp-α^{-} cDC population that is again slightly larger than the CD8α^{+}Dec205^{+} cDC population (Figure 2.5 **B, lower panels**). These results suggest that CD24^{+}Sirp-α^{-} cDCs are only partially dependent on Batf3.

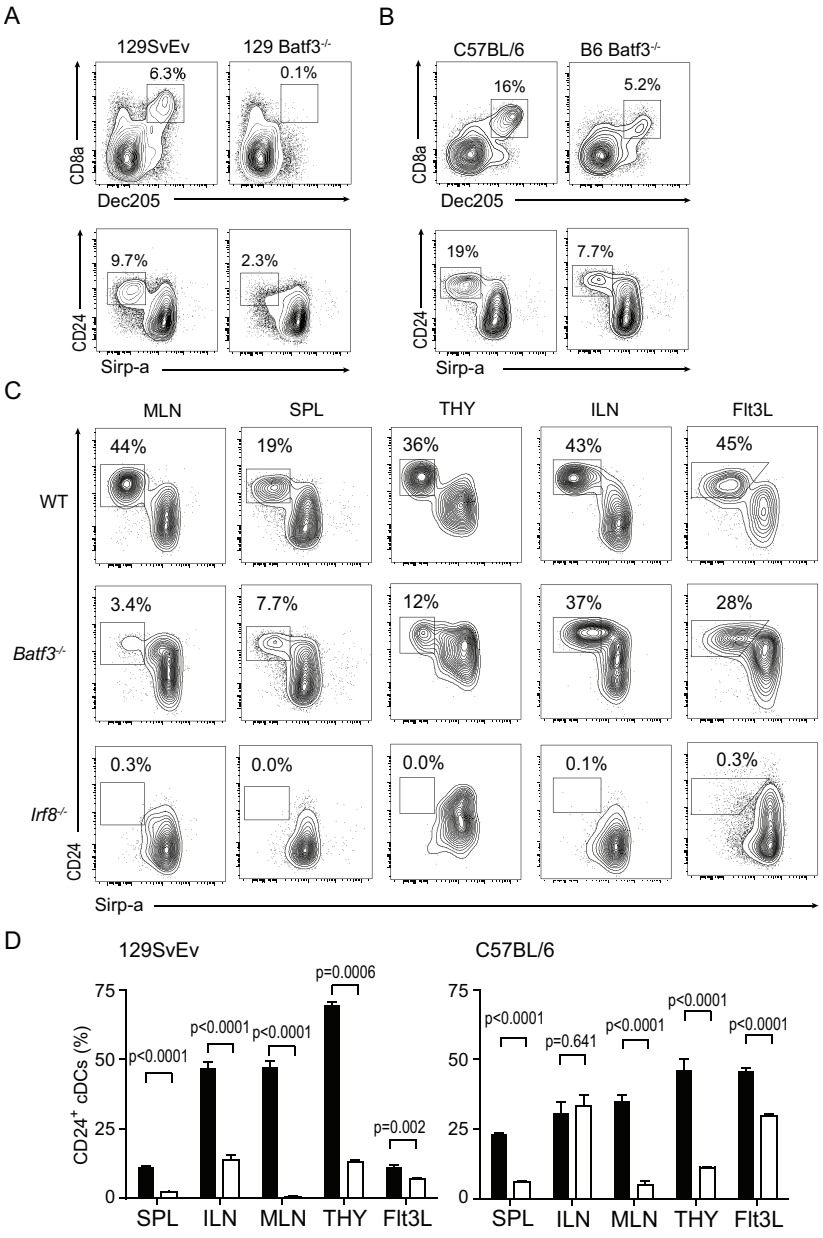

Figure 2.5: Development of CD24$^+$SIRPα$^-$ DC requires Irf8 but not Batf3

(A) FACS analysis of splenocytes from indicated genotypes. Histograms of cells previously gated as CD11c$^+$MHCII$^+$B220$^-$. Numbers represent the percentage of cells in the indicated gate. (B) WT or Batf3$^{-/-}$ mice (B6 Batf3-/-) and analyzed as in (A). (C) spleen (SPL), inguinal lymph nodes (ILN), mesenteric lymph nodes (MLN), and thymus (THY) or bone marrow (BM) of WT, Batf3$^{-/-}$ or Irf8$^{-/-}$ mice on the C57BL/6 genetic background. BM DCs (Flt3L) were generated with Flt3 ligand *in vitro* as described in Methods. (D) The percentage of cells present within the CD24$^+$SIRPα$^-$ gate from (C) are presented for WT (black bars) and Batf3$^{-/-}$ mice (open bars) on either the 129SvEv (left) or C57BL/6 (right) genetic backgrounds. At least 5 mice were analyzed per group. Numbers represent the p value for an unpaired Student's t test.

Since *Irf8*$^{-/-}$ mice also lack CD8α^{+} cDCs, we analyzed resident DCs from spleen, lymph nodes, thymus and Flt3L-treated bone marrow (BM) cultures between C57BL/6 *Irf8*$^{-/-}$ and *Batf3*$^{-/-}$ mice (Figure 2.5 **C, D,** Supplementary Figure 2.1). Surprisingly, while CD24^{+}Sirp-α^{-} cDC development strictly requires *Irf8* in all sites, we find a variable requirement for *Batf3* that differs across anatomic locations. Specifically, we find that CD24^{+}Sirp-α^{-} cDCs are strongly *Batf3*-dependent in mesenteric lymph nodes (MLN) and spleen (SPL), partially *Batf3*-dependent in the thymus (THY), and nearly independent of *Batf3* in inguinal (skin-draining) lymph nodes (ILN) (Figure 2.5 **C,** Supplementary Figure 2.2). For example, the CD24^{+}Sirp-α^{-} cDCs comprise 44% of cDCs in MLN of WT mice, but only 3.4% in *Batf3*$^{-/-}$ mice (Figure 2.5 **C, D**), representing a 10-fold reduction. In SPL, THY, and Flt3L-treated BM cultures, we find a 2-3 fold reduction in CD24^{+} Sirp-α^{-} cDCs between WT and *Batf3*$^{-/-}$ mice (Figure 2.5 **C, D**). Finally, CD24^{+}Sirp-α^{-} cDCs represent 43% of cDCs in WT ILN, and 37% of cDCs in *Batf3*$^{-/-}$ mice (Figure 2.5 **C**). The same anatomic order of *Batf3*-dependence is seen on the 129SvEv strain, except for ILN which show a modest 3-fold reduction in CD24^{+}Sirp-α^{-} cDCs (Supplementary Figure 2.2). These data suggest that Irf8 and Batf3 play distinct roles in CD8α^{+} DC development, with Irf8 being strictly required for appearance of the early CD8α-committed, CD24^{+} Sirp-α^{-} population, and Batf3 acting later in its maturation. Second, the persistence of this CD24^{+} Sirp-α^{-} population may vary with anatomic location and genetic background.

2.3.6 *Batf3*-deficient CD24$^+$ SIRPα$^-$ DCs respond poorly to Flt3L and PAMP stimulation

Several studies have demonstrated that CD8α$^+$ DCs can develop independently of *Batf3*, *Id2*, or *Nfil3* in a high IL-12- or irradiation-induced setting[59,71]. This compensatory developmental pathway requires the paralogous factors *Batf* and *Batf2* [72]. Additionally, various pathogens are also known to regulate DC numbers positively and negatively. For example, pulmonary tuberculosis can lead to the expansion of the related lung CD103$^+$ DC, whereas systemic infection with plasmodium can enhance CD8α$^+$ DC numbers in the spleen [59,73]. Since DC numbers can vary dramatically in response to many disparate stimuli, we determined whether Batf3-deficient DCs could be rescued by other cytokines or PAMPs.

In response to Flt3L, all DC populations expand greatly with a preferential skewing toward the CD8α$^+$ DC lineage[29]. By contrast, intravenous administration of LPS is known to cause redistribution of CD11c$^+$ cells from the marginal zone to the T cell area of the spleen, whereupon the cells disappear after several days[74,75]. Intraperitoneal administration of recombinant Flt3L into Batf3-deficient mice resulted in poor expansion of splenic CD24$^+$SIRPα$^-$ DCs (Figure 2.6 **A)**. Moreover, CD24$^+$SIRPα$^-$ DCs expressed low levels of surface CD8α and CD205, but relatively high amounts of CD11b, a marker of the CD8α$^-$ DC lineage (Figure 2.6 **B**). Similarly, we observed a consistent reduction of CD24$^+$ DCs from either C57BL/6 or 129SvEv genetic backgrounds at both high and low doses of Flt3L *in vitro* (Supplementary Figure 2.3). These results suggest that Flt3L is involved in the maintenance rather than the terminal differentiation of DCs, especially with regard to the compensatory pathway. Next, we administered agonists for TLR3 (polyinosinic:polycytidylic acid, polyI:C), TLR4 (lipopolysaccharide, LPS), and TLR9 (CpG1826, type B) and analyzed DC compartment 24

hours later. We saw a consistent reduction of Batf3-deficient $CD24^+$ cells in response to inflammation (Figure 2.6 **C**). Lastly, we found this residual population of $CD24^+$ DCs poorly captured latex particles (Figure 2.6 **D**). Collectively, these data show *Batf3* deficiency results in an inability to respond to homeostatic cytokines, such as Flt3L, and inflammatory stimuli, indicating a terminal maturation defect.

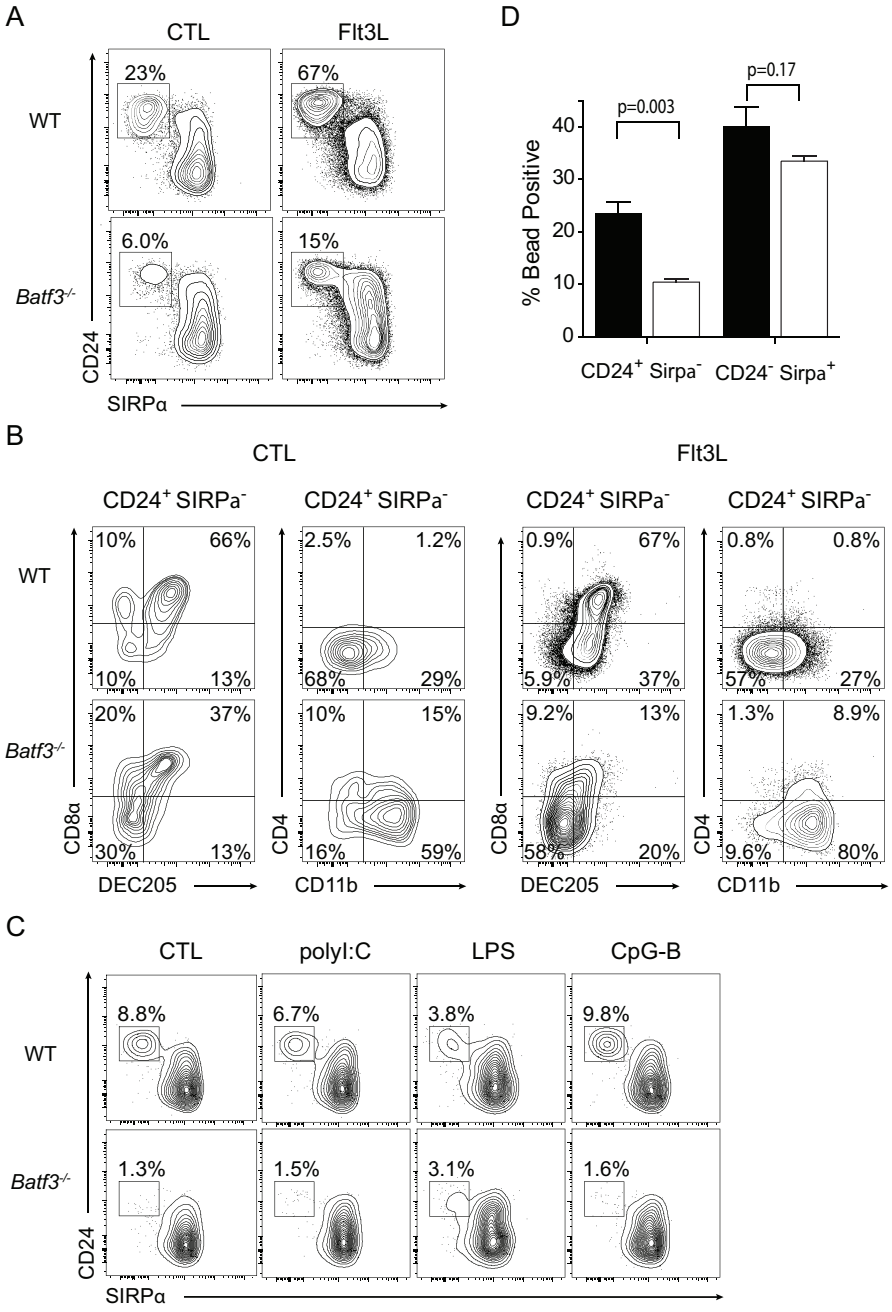

Figure 2.6: Exogenous Flt3 ligand and TLR stimulation fails to rescue Batf3$^{-/-}$

(A) Mice treated with 10 mg Flt3L (Flt3L) or PBS (CTL) and DCs analyzed on day 8. Data are representative of 3 mice per group. (B) DC evaluated by additional surface markers. (C) Mice treated with 50 mg of polyI:C, 20 mg of LPS, 5 nmol of CpG-B or PBS (CTL). Analysis at 42 hours. (D) Mice treated with 200 mL of 0.3% solution of Fluoresbrite Plain YG 1mm latex beads. DCs were analyzed for bead uptake after 1 hour. Shown are the percentage of cDCs positive for phagocytosis of latex beads as determined by fluorescence in FL1, with background determined by fluorescence of cells from mock injections.

2.3.7 *Batf3* is not required for development of the MDP, CDP or pre-cDC

To further establish the stage-specific actions of Irf8 and Batf3, we determined the expression pattern of various transcription factors in progenitor populations (Figure 2.7 **A**). *Irf8* expression increases significantly from the GMP or CMP to the CDP stage, after which it is maintained in BM pre-cDCs and CD8α$^+$ DCs, but extinguished from CD8α$^-$ DCs. In contrast, *Batf3* expression is low in progenitors, but high in mature CD8α$^+$ and CD8α$^-$ DCs. Conversely, other transcription factors important for DC development, such as *E2-2, Sfpi1,* or *Irf4*, are expressed as early as the CMP, CDP or pre-cDC, respectively. Interestingly, the expression of *RelB* and *Id2* is induced in mature DC subsets similarly to *Batf3*. The relatively late expression of *Batf3* in DC development lead us to hypothesize that defects seen in *Batf3*$^{-/-}$ mice are unlikely to be caused by cellular changes at the CDP or pre-cDC stage.

To test this hypothesis, we quantified DC progenitors from WT, *Batf3*$^{-/-}$, *Irf4*$^{-/-}$, and *Irf8*$^{-/-}$ mice (Fig. 2B, Fig. S3). *Ifr8*$^{-/-}$ mice and mice homozygous for the *Irf8*^{R294C} mutation [35] both show a 4-5 fold reduction in BM pre-cDCs (Figure 2.7 **B**), suggesting an early role in DC development [44]. In contrast, *Batf3*$^{-/-}$ and *Irf4*$^{-/-}$ mice have normal numbers of BM pre-cDCs (Figure 2.7 **B**), MDPs and CDPs (Supplementary Figure 2.4), and spleen-resident pre-cDCs (Figure 2.7 **C**). *Batf3*$^{-/-}$ pre-cDCs also showed normal competitive fitness in mixed chimeras generated from WT and *Batf3*$^{-/-}$ bone marrow (Figure 2.7 **D**). Finally, gene expression microarray analysis of CDPs and BM pre-cDCs from WT and *Batf3*$^{-/-}$ mice revealed few genes where expression changed in the absence of *Batf3* (Figure 2.7 **E, Table 1**). In summary, *Batf3* is

expressed late during cDC development and does not influence development or gene expression in the CDP or BM pre-cDC.

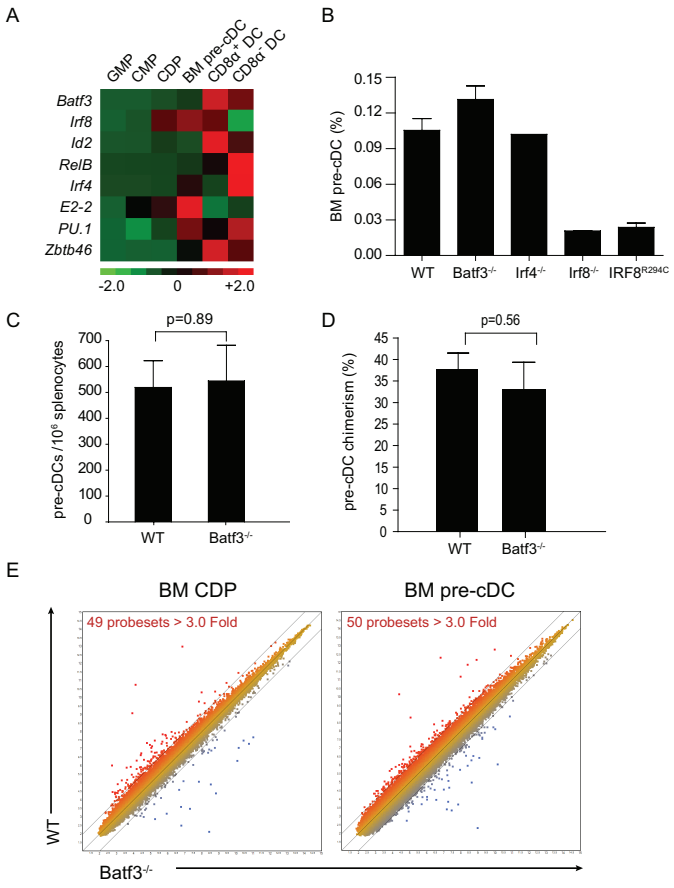

Figure 2.7: pre-cDC homeostasis is Irf8 dependent but Batf3 independent

(A) GMP, CMP, CDP, BM pre-cDC, and splenic CD8α$^+$ and CD8α$^-$ DCs were purified as shown in Fig. S3 and mRNA extracted. Microarray analysis performed as described in the Methods. Shown is a heat map for the relative expression levels of various transcription factors. (B) Shown are the numbers of pre-cDCs as a percentage of total BM cells from indicated mice. Error bars represent standard error of the mean for at least 5 mice per group. (C) Shown are the frequency of spleen-resident pre-cDCs. Error bars represent standard error of the mean, and p value for unpaired Student's t test for at least 5 mice. (D) Mixed BM chimeras were generated as described in Methods. After 8 to 12 weeks, chimerism for CD45.1 and CD45.2 was determined in splenic pre-DCs. Shown is the percentage of CD45.2 chimerism as a percentage of total splenic pre-cDCs. (E) Microarray analysis for CDP and BM pre-cDCs as indicated for WT and Batf3-/- mice. Shown are M-plots from WT and Batf3-/- microarrays. Indicated are probe sets expressed at least 3.0 fold higher (red) or lower (blue) in WT relative to Batf3-/- cells.

2.3.8 *Batf3*$^{-/-}$ CD24^{+} Sirp-α^{-} cDCs fail to develop into mature CD8α^{+} cDCs.

Given that *Irf8* expression is extinguished from the pre-cDC to the CD8α^{-} cDC, one explanation of a dual requirement for *Irf8* and *Batf3* in CD8α^{+} cDC development is that *Irf8* expression eventually becomes dependent on *Batf3*. In such a model, CD8α-committed DCs develop, but begin to lose *Irf8* expression in *Batf3*$^{-/-}$ mice, possibly explaining the complete absence of CD24^{+} Sirp-α^{-} cDCs in *Irf8*$^{-/-}$ mice but only a reduction in *Batf3*$^{-/-}$ mice. Alternatively, *Batf3* may act independently of lineage commitment to regulate the survival or maturation of CD24^{+} Sirp-α^{-} cDCs into functional CD8α^{+} cDCs.

To distinguish these possibilities, we first measured Irf8 expression by intracellular staining in CD8α^{+} and CD8α^{-} cDCs. In WT and *Batf3*$^{-/-}$ mice, Irf8 was normally expressed in CD8α^{+} cDCs, but not in CD8α^{-} cDCs, in all lymphoid tissues (Figure 2.8 **A,** Supplementary Figure 2.5 **A**). Furthermore, CD8α^{+} cDCs from WT and *Batf3*$^{-/-}$ mice expressed equivalent levels of *Irf8* mRNA (Figure 2.8 **B**). However, *Batf3*$^{-/-}$ CD8α^{+} cDCs expressed higher levels of CD11b and lower levels of CD103 than WT CD8α^{+} cDCs in both spleen (Figure 2.8 **C**) and lymph nodes (Supplementary Figure 2.5 **B**). In contrast, no alteration in CD11b or CD103 expression was observed in *Batf3*$^{-/-}$ CD8α^{-} cDCs (Figure 2.8 **C**, Supplementary Figure 2.5 **C**). Interestingly, *Batf3*$^{-/-}$ CD8α^{+} cDCs expressed slightly higher levels of *Irf4*, and failed to induce wild-type levels of key effector genes, such as *Clec9a*, *Xcr1* and *Tlr3* (Figure 2.8 **D**). These data suggest that Batf3 regulates the maturation of an Irf8-positive, CD24^{+} Sirp-α^{-} population into *bona fide* CD8α^{+} cDCs.

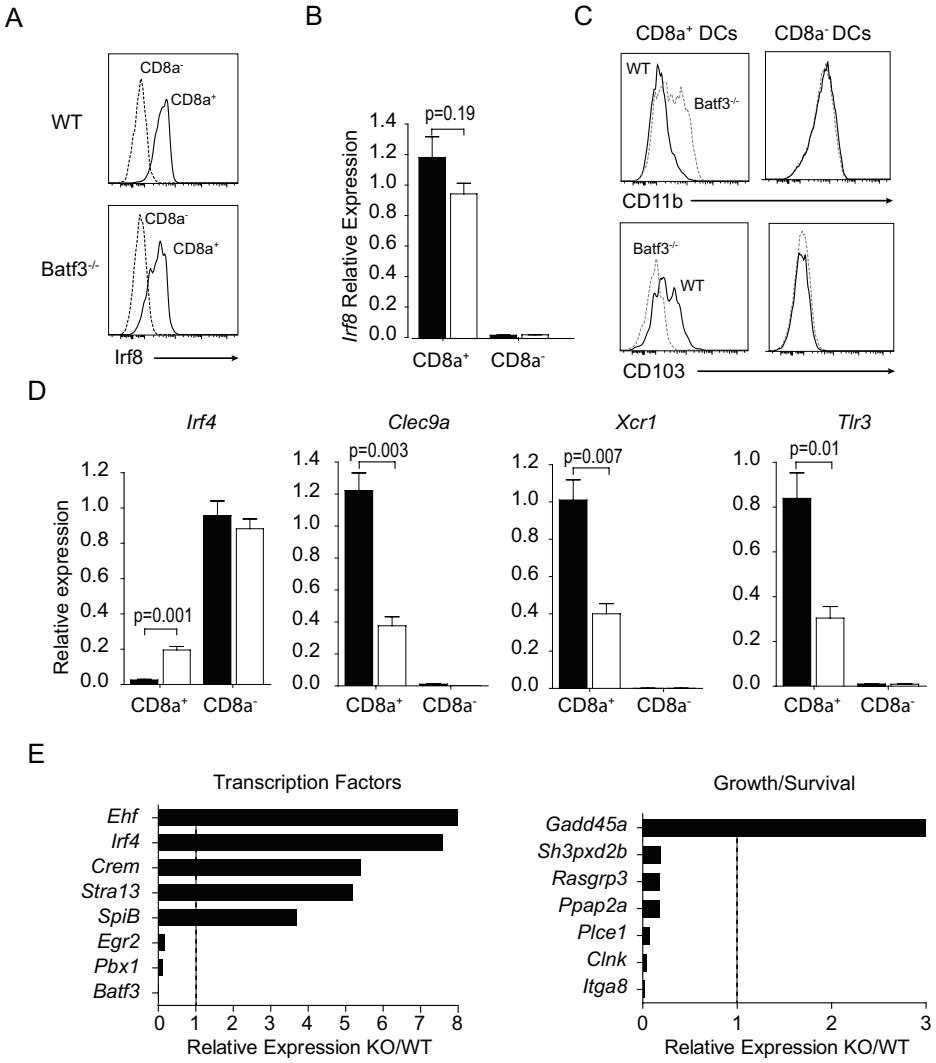

Figure 2.8: Batf3 regulates the terminal maturation of CD8α$^+$ DCs

(A) Splenic DCs analyzed for Irf8 protein levels. Shown are histograms for intracellular Irf8 levels. (B) DCs from spleen purified from WT (black bars) or Batf3$^{-/-}$ mice (open bars). mRNA was converted into cDNA, and Irf8 expression was measured by quantitative RT-PCR (qRT-PCR). Shown is the relative Irf8 expression normalized by HPRT expression as described in the Methods. (C) Shown are histograms for CD11b or CD103 expression for indicated DC subtypes. (D) DCs isolated from (B) were analyzed for expression of Irf4, Clec9a, Xcr1 and Tlr3 by qRT-PCR. Shown is the normalized expression of the indicated gene in WT (black bars) or Batf3$^{-/-}$ cDCs (open bars). (E) Microarray analysis of cells from (A). Expression of the indicated transcription factors (left panel) and growth/survival genes (right panel) is shown as a ratio of the value in Batf3$^{-/-}$ CD8α$^+$ DCs relative to WT controls. Bars represent standard error of the mean for 3 biological replicates and a p value from an unpaired Student's t test for (B) and (D).

Finally, gene expression microarray analysis of CD8α$^+$ cDCs from C57BL/6 WT and *Batf3*$^{-/-}$ mice identified a number of genes for which expression either increased or decreased by the loss of *Batf3* (Figure 2.8 **E**). Expression of the transcription factors *Ehf* and *Irf4*, which are normally restricted to CD8α$^-$ cDCs, increased by 7 to 8 fold in *Batf3*$^{-/-}$ CD8α$^+$ cDCs. Likewise, the factor *Pbx1*, normally restricted to CD8α$^+$ cDCs, was reduced several fold in *Batf3*$^{-/-}$ CD8α$^+$ cDCs. Several genes related to cell growth or survival were also decreased in *Batf3*$^{-/-}$ CD8α$^+$ cDCs (Figure 2.8 **E, right panel**), including *Rasgrp3* [76,77] and *Plce1* [78]. However, we find that CD8α$^+$ cDCs developed normally in both *Rasgrp3*$^{-/-}$ and *Plce1*$^{-/-}$ mice (Supplementary Figure 2.6 **E**), indicating that these *Batf3* target genes alone are dispensable for normal CD8α$^+$ cDC homeostasis.

2.3.9 BATF3 regulates the survival of CD8α-committed cDCs.

Our results indicate that Batf3 acts after an Irf8-dependent commitment step to promote functional maturation. Besides regulating CD8α$^+$ cDC-specific genes (*Clec9a, Tlr3, Xr1)*, Batf3 also regulates genes putatively involved in the proliferation or survival of the immature CD24$^+$ Sirp-α$^-$ progenitor cells. To test this idea, we assayed C57BL/6 WT and *Batf3*$^{-/-}$ mice for *in vivo* proliferation and turnover. Surprisingly, *Batf3*$^{-/-}$ CD24$^+$ Sirp-α$^-$ cDCs showed an increased fraction of non-quiescent cells relative to WT CD24$^+$ Sirp-α$^-$ cDCs as measured by Ki67 staining (Figure 2.9 **A, left panels, and 9 B**). In agreement, *Batf3*$^{-/-}$ CD24$^+$ Sirp-α$^-$ cDCs had a 2-fold increase of cells in S/G2/M phase of the cell cycle compared to WT counterparts (Figure 2.9 **A, middle panels**). Analysis of *in vivo* BrdU labeling also revealed a 2-fold increase in the rate of

incorporation at 4 hours by *Batf3*$^{-/-}$ CD24^{+} Sirp-α^{-} cDCs relative to WT CD24^{+} Sirp-α^{-} cDCs. Interestingly, BrdU incorporation was similar in WT and *Batf3*$^{-/-}$ CD24^{+} Sirp-α^{-} cDCs when the labeling pulse was extended to 24 hours (Figure 2.9 **C**). The increased BrdU incorporation in *Batf3*$^{-/-}$ CD24^{+} Sirp-α^{-} cDCs at 4 hours argues against a role for Batf3 in cellular proliferation *per se*. Combined with the normalization in BrdU incorporation by 24 hours, the results indirectly suggest a role for Batf3 in regulating survival.

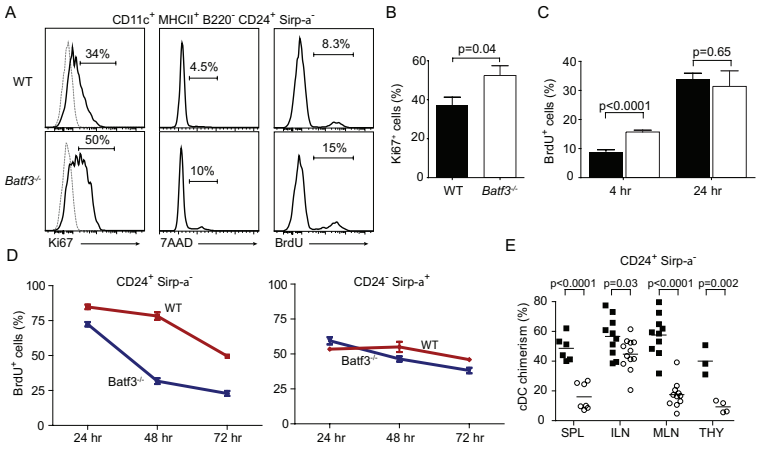

Figure 2.9: Batf3 regulates survival of CD8α^{+} DCs

(A) Proliferation of splenic pre-cDCs from wild type (WT) or Batf3$^{-/-}$. Shown are histograms of splenocytes for expression of Ki67 (solid lines), 7-Amino-actinomycin D (7AAD) staining, or BrdU incorporation (BrdU) as indicated and described in the Methods. Background staining for Ki67 expression was determined using an isotype control antibody (dashed lines). For BrdU incorporation, background was determined using cells from untreated mice. Numbers represent the percentage cells within the indicated gates. (B) Percentage of DCs positive for Ki67+ defined by gating in (A). Bars represent the standard error of the mean for groups of at least 5 mice, and p the value for an unpaired Student's t test. (C) Percentage of DCs that are BrdU+ defined by gating in (A) for WT (closed) or Batf3-/- (open bars) mice treated with BrdU for either 4 hr or 24 hr as indicated. Error bars represent SEM for groups of at least 5 mice, and p the value for an unpaired Student's t test. For 24 hr treatments, mice were housed with water supplemented with 0.8 mg/ml BrdU. (D) Mean BrdU incorporation as a percentage of BrdU+ cells for indicated populations from WT (red) and Batf3$^{-/-}$ mice (blue). (E) Mixed BM chimeras as described in Methods. After 8-12 weeks, the relative contribution by CD45.1 and CD45.2 cells to the indicated DC population was analyzed. Shown is CD45.2 chimerism as a percentage of total DCs.

To test survival directly, we performed a BrdU pulse-chase assay to compare the *in vivo* half-life of different DC populations between WT and *Batf3*$^{-/-}$ mice (Figure 2.9 **D**). The reported *in vivo* half-life of CD8α^{+} cDCs is approximately three days [79,80]. Consistent with this estimate, we find that WT CD24^{+} Sirp-α^{-} cDCs have a half-life of approximately three days (Figure 2.9 **D, left panel, red line**), while the half-life of *Batf3*$^{-/-}$ CD24^{+} Sirp-α^{-} cDCs was approximately 36 hours. This reduction in half-life was specific to CD24^{+} Sirp-α^{-} cDCs, as no difference in half-life of CD24^{-} Sirp-α^{+} cDCs between WT and *Batf3*$^{-/-}$ mice was observed (Figure 2.9 **D, right panel**).

We independently tested for a fitness defect using competitive mixed-BM chimeras. We observed that CD45.2^{+} *Batf3*$^{-/-}$ BM contributed to about 10-20% of the total CD24^{+} Sirp-α^{-} cDCs, whereas CD45.2^{+} WT BM consistently gave rise to about 50-60% of CD24^{+} Sirp-α^{-} cDCs in SPL, MLN, and THY (Figure 2.9 **E**). Notably, in the ILN, we observed a small but statistically significant difference in chimerism for CD24^{+} Sirp-α^{-} cDCs between WT and *Batf3*$^{-/-}$ BM (Figure 2.9 **E**). This reduction was specific for CD24^{+} Sirp-α^{-} cDCs, as no difference in chimerism for CD24^{-} Sirp-α^{+} cDCs between WT and *Batf3*$^{-/-}$ BM was observed in any lymphoid compartment (data not shown). These results support the idea that Batf3 regulates survival after an initial Irf8-dependent lineage commitment step.

2.4 Discussion

The major advance of this study is to draw a clear distinction between the roles of Irf8 and Batf3 in the development of CD8α^+ cDCs. We find that the CD24$^+$ Sirp-α^- cDC population fails to develop at all in the absence of Irf8. However, these committed progenitor cells develop in *Batf3*$^{-/-}$ mice, although at reduced frequency and with a shortened half-life, and they fail to induce genes characteristic of mature CD8α^+ cDCs. This distinction between the actions of these factors will be important in moving forward to define the molecular basis of their effects.

The decreased half-life and reduced population size of *Batf3*$^{-/-}$ CD24$^+$ Sirp-α^- cDCs is likely a consequence of the greatly reduced half-life of CD8α-commited cDCs. The increase in labeling of *Batf3*$^{-/-}$ CD24$^+$ Sirp-α^- cDCs by Ki67, 7AAD, and BrdU may at first seem paradoxical. Yet in light of the shorter half-life observed for *Batf3*$^{-/-}$ CD24$^+$ Sirp-α^- cDCs, we conclude that the absence of *Batf3* results in an *Irf8*-expressing, CD8α-committed population, which remains functionally immature and undergoes rapid proliferation and turnover. Consistent with this idea, we observe a significant reduction in the expression of CD8α^+ cDC-specific genes, such as *Clec9a*, *Xcr1*, and *Tlr3*, and genes involved in cell growth and survival. While these genes are candidates for Batf3-dependent transcription, the small size of cDC populations currently poses a technical challenge for identifying direct interactions of *Batf3* with loci by techniques such as chromatin immunoprecipitation.

In summary, we have distinguished the roles of Irf8 and Batf3 in CD8α^+ cDC development. Irf8 is strictly required for generation of immature CD24$^+$ Sirp-α^- cDCs, whereas Batf3 influences their survival and maturation into mature DCs. Identification of direct targets

of Batf3 transcriptional activity will be an important next step in understanding its mechanisms. It will also be important to understand how Batf3 promotes survival of CD8α+ cDCs but not CD8α- cDCs. Finally, it is intriguing that the Batf3-dependence of CD8α+ cDCs can vary with genetic background and anatomic site. Conceivably, an alternative Batf3-independent pathway of cell survival is operative within the skin-draining lymph nodes, which is absent in mesenteric lymph nodes where CD8α+ cDC development is strongly Batf3-dependent. Identification of such a Batf3-bypass pathway could provide insights to improve the effectiveness of CD8 T cell vaccines.

Table 2.1: *Batf3* is dispensable for DC progenitor gene expression

WT CDP / KO CDP		WT pre-cDC / KO pre-cDC	
Gene symbol	Fold change	Gene symbol	Fold change
Erdr1	71	Erdr1	46
Mid1	36	Mid1	14
1700112E06Rik	10	Hspa1b	11
Hmga2	6.0	Hspa1a	9.4
Dntt	5.1	Batf3	4.2
Ctla2a	4.9	Msn	4.0
Hmga2	4.8	Golph3	3.6
Batf3	4.7	Zwint	3.6
Cmah	4.5	Card11	3.4
Ets1	4.4	S100a9	3.3
Ctla2a	4.2	Acaa2	3.3
Gimap6	4.1	Ywhaz	3.1
Myl10	3.9	Syne2	3.1
Hmga2	3.7	Slc29a1	3.0
Gimap8	3.7	Wdfy1	0.3
Ctla2b	3.6	Klf9	0.3
Mn1	3.5	Igh-2, Igh-VJ558	0.3
Slc35d3	3.4	5830436I19Rik	0.3
Il7r	3.4	H2-gs10, H2-Q6	0.3
Angpt1	3.3	Ier3	0.3
Ptpn22	3.2	Per1	0.3
Hlf	3.1	Socs3	0.3
Hspa1b	3.0	Ptgs2	0.3
A030001D16Rik	3.0	Ddit4	0.2
Lcn2	0.3	Rasgrf2	0.2
Ddit4	0.3	Socs3	0.2
Per1	0.3	Fam84b	0.2
Pira2	0.3	Igk, Igk-C, Igk-J1, Igk-V28	0.2
Hmga2-ps1	0.3	Igh-2, Igh-VJ558	0.2
Igl, Igl-C1, Igl-V1	0.2	Igh-2, Igh-VJ558	0.1
Igl-V1	0.2	2010205A11Rik	0.1
Camp	0.1	Igk, Igk-C, Igk-J1, Igk-V28	0.1
S100a8	0.1	6030422H21Rik	0.1
S100a9	0.1	Ifi202b	0.1
Chi3l3	0.1		
Ngp	0.1		
Ifi202b	0.1		
Igk-V32	0.1		

CDP and BM pre-cDCs from WT and Batf3$^{-/-}$ mice (KO) mice were purified by cell sorting, total RNA prepared, and gene expression microarray analysis performed using Affymetrix Mouse Genome 430 2.0 arrays. Shown are the fold change for the indicated genes as a ration of the expression value in WT CDP to the expression value in KO CDP (WT CDP/ KO CDP) (left column), or WT pre-cDC to the expression value in KO pre-cDC (WT pre-cDC / KO pre-cDC).

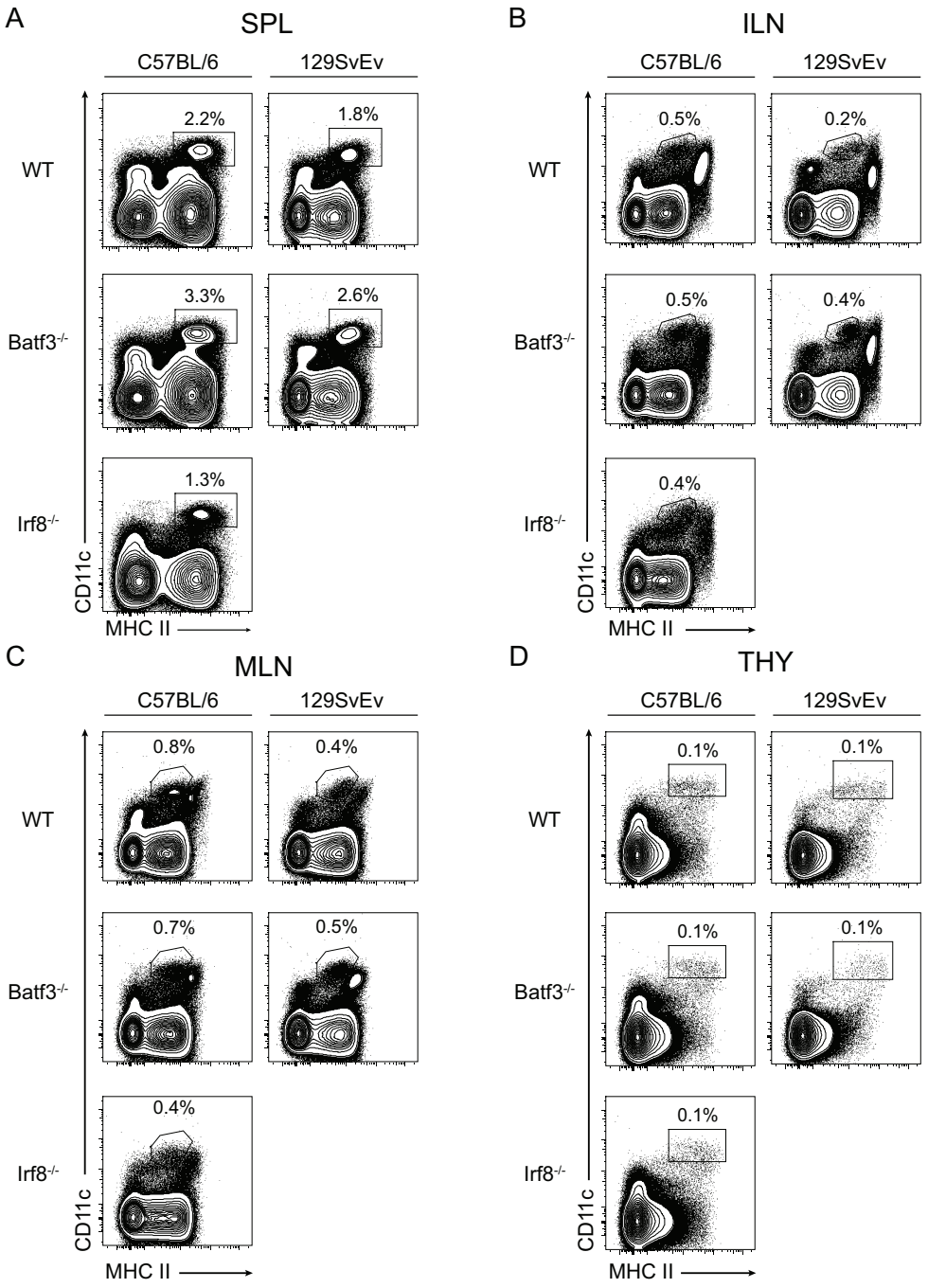

Supplementary Figure 2.1: Gating strategy for classical DCs

(A-D) Cells were harvested from spleen (SPL) (A), inguinal lymph nodes (ILN) (B), mesenteric lymph nodes (MLN) (C), or thymus (THY) from wild type, Batf3$^{-/-}$ or Irf8$^{-/-}$ C57BL/6 mice as indicated and analyzed by FACS as described in the Methods.

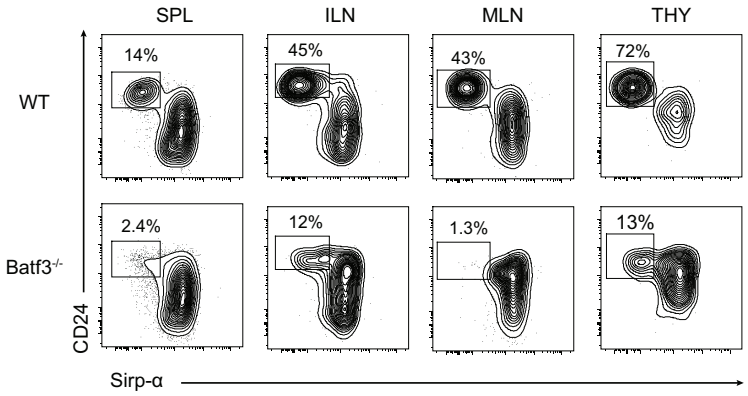

Supplementary Figure 2.2: Batf3$^{-/-}$ mice retain a residual populations of DCs that resemble CD8α^{+} DCs

Cells were harvested from SPL, ILN, MLN or THY as indicated from WT or Batf3$^{-/-}$ 129SvEV background mice. Shown are two parameter histograms.

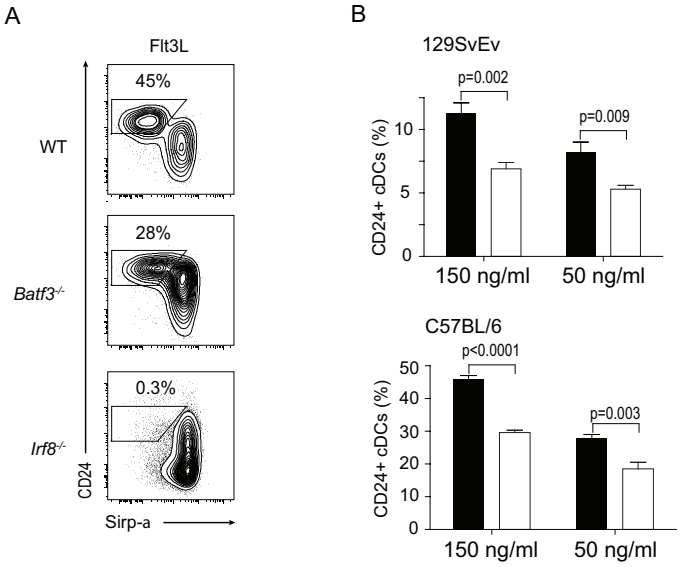

Supplementary Figure 2.3: Flt3 ligand stimulation fails to expand CD24^{+}SIRPα^{-} DCs in Batf3$^{-/-}$ mice

(A) BM cells from C57BL/6 and 129SvEv WT and Batf3-/- mice were harvested and cultured at the indicated concentrations of recombinant Flt3L for 10 days. Non-adherent cells were harvested and stained for DC analysis. BM cells from C57BL/6 Irf8-/- mice were also included. (B) Shown is the relative quantitation of CD24^{+}SIRPα^{-} DCs at the indicated concentrations of Flt3L. Numbers represent percent of cells in the cDC gate. Data are representative of three independent experiments.

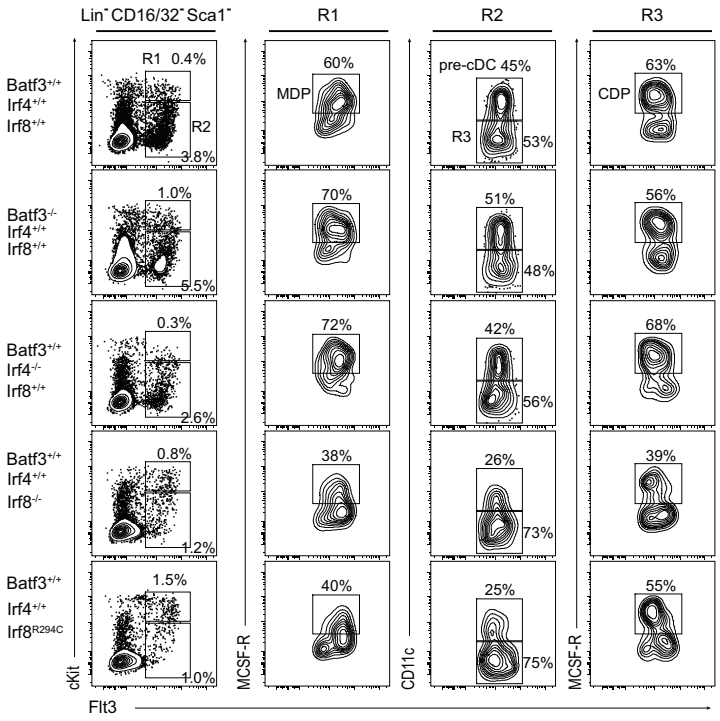

Supplementary Figure 2.4: Pre-cDC analysis in Irf8$^{-/-}$ and Batf3$^{-/-}$ mice

BM cells were gated as Lin-CD16/32-Sca-. MDPs (R1), pre-cDCs (R2), and CDPs (R3) are shown.

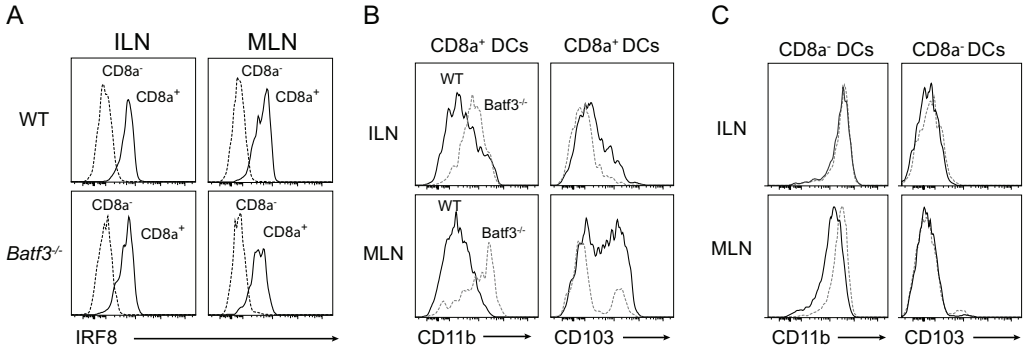

Supplementary Figure 2.5: Batf3$^{-/-}$ DCs induce Irf8 but fail to repress CD11b or induce CD103

(A) ILN and MLN were harvested from C57BL/6 WT or Batf3$^{-/-}$ mice and analyzed by FACS. Histograms for IRF8 levels in DCs gated either as CD24^{+}Sirpα^{-} Dec205^{+} CD8α^{+} DCs (CD8α^{+}, solid lines) or CD24^{-}Sirpα^{+} Dec205^{-}CD8α^{-} (CD8α^{-}, dashed lines). (B-C) Histograms for CD11b or CD103 expression for WT (solid lines) or Batf3$^{-/-}$ (dashed lines) mice.

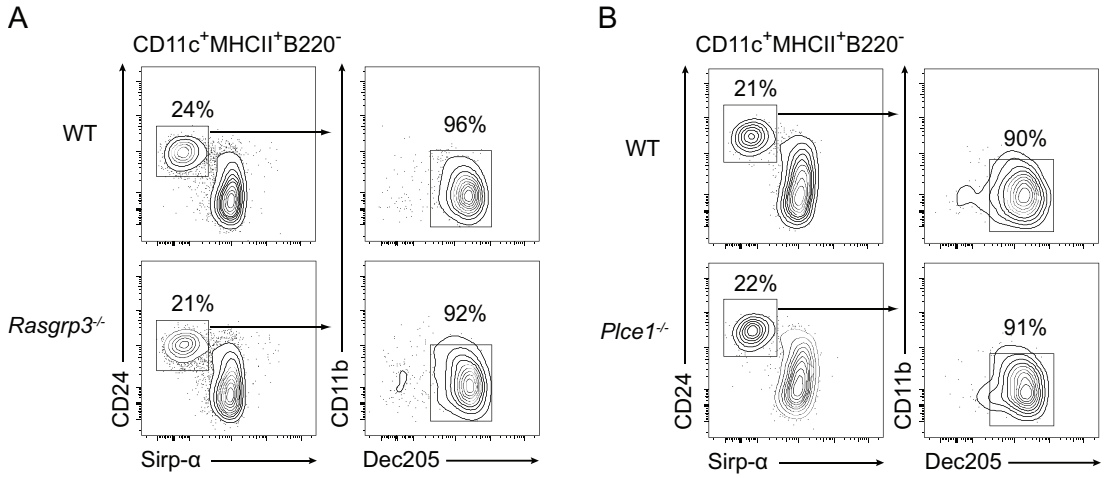

Supplementary Figure 2.6: *Rasgrp3* and *Plce1* are dispensable for CD8α$^+$ DC development

Splenocytes were harvested from C57BL/6 WT, Rasgrp3$^{-/-}$ (A) or Plce1$^{-/-}$ mice (B) and analyzed by FACS. Histograms for cells previously gated as CD11c$^+$MHCII$^+$B220$^-$ to identify DCs (left panels). Two color histograms for CD11b and Dec205 (right panels) are shown for cells in the CD24$^+$ Sirp-α$^-$ gate from the left panel. Numbers represent the percentage of cells in the indicated gate.

2.5 Materials and Methods

2.5.1 Mice

Wild-type 129S6/SvEv mice were purchased from Taconic. Wild-type C57BL/6 mice and the congenic strain B6.SJL were purchased from The Jackson Laboratory. *Batf3*$^{-/-}$ mice on either 129S6/SvEv or C57BL/6 backgrounds have been previously described [7,68]. *Irf8*$^{-/-}$ mice [40] were obtained from the European Mutant Mouse Archive and maintained in our animal facility. BXH2/TyJ mice carrying a point mutation in exon 7 of *Irf8* resulting in an Arg to Cys change at amino acid position 294 [39] were purchased from The Jackson Laboratory. The mice were then backcrossed to the C57BL/6 background for 10 generations and maintained as homozygous mutants. *Irf4* conditional (floxed) mutant mice [34] were purchased from The Jackson Laboratory and subsequently germline deletion was generated by crossing floxed mice to transgenic CMV-Cre mice (B6.C-Tg(CMV-Cre)1Cgn/J) (also purchased from The Jackson Laboratory). Generation of *Rasgrp3*$^{-/-}$ mice and *Plce1*$^{-/-}$ mice have been previously described [77,78]. Experiments were performed with sex- and age-matched mice at 6-20 weeks of age. Mice were bred and maintained in our specific pathogen-free animal facility according to institutional guidelines.

2.5.2 Antibodies and flow cytometry.

Staining was performed at 4°C in the presence of Fc block (clone 2.4G2, BD Biosciences) in FACS buffer (PBS, 0.5% BSA, 2 mm EDTA) The following antibodies were purchased from BD Biosciences: V450 and PerCP-Cy5.5 anti-NK1.1 (PK136), V450 anti-Ly6C/G (RB6-8C5), V450 anti-Ly6C (AL21), V500 anti-B220 (RA3-6B2), PE-Cy7 anti-CD8α

(53-6.7), PE-Cy7 anti-CD24 (M1/69), PerCP-Cy5.5 anti-Ly6G (1A8), FITC and APC anti-CD172a/Sirpα (P84), APC anti-CD4 (RM4-5). These antibodies were purchased from eBioscience: PE anti-NKp46 (29A1.4), PerCP-Cy5.5 anti-CD11b (M1/70), APCeFluor780 anti-CD11c (N418), PE anti-CD103 (2E7), APC anti-CD317/BST2 (eBio927), eFluor450 anti-MHCII (I-A/I-E) (M5/114.15.2), FITC and APC anti-CD45.2 (104), PE-Cy7 and PerCP-Cy5.5 anti-CD45.1 (A20), PerCP-Cy5.5 anti-CD16/32 (93), PE-Cy7 anti-cKit (2B8), eFluor450 anti-CD105 (MJ7/18), eFluor450 anti-Ter119, PE anti-CD135 (A2F10), Alexa700 anti-Sca1 (D7), FITC, APC and PerCP-eFluor710 anti-SiglecH (eBio440C), eFluor450 anti-Ter119 (Ter119), biotin anti-CD115 (AFS98). These antibodies were purchased from Miltenyi: PE anti-CD205/Dec205 (NLDC-145) and APC anti-CD205/Dec205 (NLDC-145). These antibodies were purchased from Invitrogen: APC anti-F4/80 (BM8), PE anti-B220 (RA3-6B2), FITC and APC anti-CD8α (5H10).

2.5.3 Intracellular Irf8 staining.

Cells were stained for surface markers, then fixed and permeabilized with Foxp3 Staining Buffer Set (eBioscience) according to manufacturer's instructions. Next, samples were incubated with unconjugated goat anti-Irf8 antibody (clone C-19, Santa Cruz Biotechnology) in 1X Permeabilization Buffer (Foxp3 Staining Buffer Set) for 30min at 4ºC. After washing, cells were incubated with FITC-conjugated donkey anti-goat F(ab')2 (Jackson ImmunoResearch Laboratories, Inc.) in 1X Permeabilization buffer for 30min at 4ºC, washed and analyzed by flow cytometry. Background staining was determined by the signal from *Irf8*$^{-/-}$ cells.

2.5.4 DC preparation.

Lymphoid organ dendritic cells were harvested and prepared as described [8,69]. Briefly, spleens, ILNs (inguinal), MLNs, and thymus were minced and digested in 5 ml Iscove's modified Dulbecco's media + 10% FCS (cIMDM) with 250 μg/ml collagenase B (Roche) and 30 U/ml DNase I (Sigma-Aldrich) for 30 min at 37°C with stirring. Red blood cells were lysed with ACK lysis buffer. Cells were counted on a Vi-CELL analyzer, and 5–10x10^6 cells were used per antibody staining reaction.

2.5.5 Bone marrow cultures.

Bone marrow cells from femurs and tibias were collected and red blood cells were lysed in ACK lysis buffer. Cells were cultured in cIMDM in six-well plates at 2×10^6 cells/ml containing either 150 ng/ml or 50 ng/ml murine Flt3L (Peprotech). Non-adherent cells were collected at day nine or ten for flow cytometry analysis.

2.5.6 Generation of mixed bone marrow chimeras.

BM cells from wild-type C57BL/6 mice (CD45.2), wild-type congenic B6.SJL (CD45.1), and C57BL/6 *Batf3*$^{-/-}$ mice (CD45.2) were collected from the femur and tibia. Cells were counted, and 5x10^6 cells from CD45.1 B6.SJL mice were mixed with either 5x10^6 cells from wild-type CD45.2 mice or 5x10^6 cells from *Batf3*$^{-/-}$ CD45.2 mice. A total of 10^7 BM cells were then transplanted by intravenous injection (tail vein) into B6.SJL (CD45.1) recipient mice that received 11 Gy whole body irradiation on the previous day. Chimeras were analyzed at eight to twelve weeks after transplant.

2.5.7 Cell proliferation assays.

For BrdU-incorporation studies, mice were injected intraperitoneally (i.p.) with 2mg BrdU (Sigma) in saline and then given 0.8mg/ml BrdU in sterile drinking water. Splenocytes were harvested at 4 hours and 24 hours following BrdU administration. For BrdU-chase studies, mice were kept on BrdU-containing drinking water (made fresh and changed daily) continuously for 10 days and then transferred to normal drinking water for either 24, 48, or 72 hours. BrdU staining was performed with FITC BrdU Flow Kit (BD Pharmingen) following cell-surface staining. In all BrdU studies, background was determined by cells from untreated mice. For detection of Ki67, cells were stained for surface markers, and then fixed and permeabilized with the FITC BrdU Flow Kit (BD Pharmingen) according to manufacturer's instructions. Cells were then stained with anti-Ki67 antibody (clone B56) or an isotype control from the FITC or PE Mouse Anti-Human Ki-67 Set (BD Pharmingen). To determine cell-cycle phase, dendritic cells were first enriched with CD11c MicroBeads (Miltenyi Biotec) and then surface markers were stained. Cells were then fixed and permeabilized with Foxp3 Staining Buffer Set (eBioscience) for 1hr at 4ºC. After washing, cells were incubated for 30min with 7AAD solution (BD Pharmingen) and then analyzed on a BD FACS CANTO II (BD Biosciences). During analysis, event rate was maintained at 300-400 events per second on the lowest flow rate to ensure doublet exclusion.

2.5.8 Statistical Analysis.

Differences between groups were analyzed by an unpaired, two-tailed Student's t-test, with *p* values less than or equal to 0.05 considered significant (GraphPad Prism, GraphPad Software, Inc.).

2.6 Author Contributions

W.K. and K.M. designed the entire study. W.K. performed all experiments with input from B.T.E, J.A., and A.S. X.W. performed principal component analysis and assisted with figure design. The text was written entirely by W.K.

2.7 References

1. Steinman,R.M. & Cohn,Z.A. Identification of a novel cell type in peripheral lymphoid organs of mice. I. Morphology, quantitation, tissue distribution. *J Exp. Med.* **137**, 1142-1162 (1973).

2. Shortman,K. & Naik,S.H. Steady-state and inflammatory dendritic-cell development. *Nat Rev Immunol* **7**, 19-30 (2007).

3. Steinman,R.M. Lasker Basic Medical Research Award. Dendritic cells: versatile controllers of the immune system. *Nat Med.* **13**, 1155-1159 (2007).

4. Naik,S.H. Demystifying the development of dendritic cell subtypes, a little. *Immunology and Cell Biology* **86**, 439-452 (2008).

5. Liu,K. & Nussenzweig,M.C. Origin and development of dendritic cells. *Immunological Reviews* **234**, 45-54 (2010).

6. Allan,R.S. *et al.* Epidermal viral immunity induced by CD8alpha+ dendritic cells but not by Langerhans cells. *Science* **301**, 1925-1928 (2003).

7. Hildner,K. *et al.* Batf3 deficiency reveals a critical role for CD8alpha+ dendritic cells in cytotoxic T cell immunity. *Science* **322**, 1097-1100 (2008).

8. Edelson,B.T. *et al.* Peripheral CD103+ dendritic cells form a unified subset developmentally related to CD8alpha+ conventional dendritic cells. *J. Exp. Med.* **207**, 823-836 (2010).

9. Bedoui,S. *et al.* Cross-presentation of viral and self antigens by skin-derived CD103(+) dendritic cells. *Nat.* **10**, 488-495 (2009).

10. Manz,M.G., Traver,D., Miyamoto,T., Weissman,I.L. & Akashi,K. Dendritic cell potentials of early lymphoid and myeloid progenitors. *Blood* **97**, 3333-3341 (2001).

11. Manz,M.G. *et al.* Dendritic cell development from common myeloid progenitors. *Ann. N. Y. Acad. Sci* **938**, 167-173 (2001).

12. Traver,D. *et al.* Development of CD8alpha-positive dendritic cells from a common myeloid progenitor. *Science* **290**, 2152-2154 (2000).

13. Kondo,M., Weissman,I.L. & Akashi,K. Identification of clonogenic common lymphoid progenitors in mouse bone marrow. *Cell* **91**, 661-672 (1997).

14. Akashi,K., Traver,D., Miyamoto,T. & Weissman,I.L. A clonogenic common myeloid progenitor that gives rise to all myeloid lineages. *Nature* **404**, 193-197 (2000).

15. Schlenner,S.M. *et al.* Fate mapping reveals separate origins of T cells and myeloid lineages in the thymus. *Immunity* **32**, 426-436 (2010).
16. Liu,K. *et al.* In vivo analysis of dendritic cell development and homeostasis. *Science* **324**, 392-397 (2009).

17. Fogg,D.K. *et al.* A clonogenic bone marrow progenitor specific for macrophages and dendritic cells. *Science* **311**, 83-87 (2006).

18. Onai,N. *et al.* Identification of clonogenic common Flt3(+) M-CSFR+ plasmacytoid and conventional dendritic cell progenitors in mouse bone marrow. *Nat.* **8**, 1207-1216 (2007).

19. Naik,S.H. *et al.* Development of plasmacytoid and conventional dendritic cell subtypes from single precursor cells derived in vitro and in vivo. *Nat Immunol* **8**, 1217-1226 (2007).

20. Cisse,B. *et al.* Transcription factor E2-2 is an essential and specific regulator of plasmacytoid dendritic cell development. *Cell* **135**, 37-48 (2008).

21. Naik,S.H. *et al.* Intrasplenic steady-state dendritic cell precursors that are distinct from monocytes. *Nat Immunol* **7**, 663-671 (2006).

22. Merad,M. & Manz,M.G. Dendritic cell homeostasis. *Blood* **113**, 3418-3427 (2009).

23. Satpathy,A.T., Murphy,K.M. & KC,W. Transcription factor networks in dendritic cell development. *Semin. Immunol.* **23**, 388-397 (2011).

24. Wu,L., Nichogiannopoulou,A., Shortman,K. & Georgopoulos,K. Cell-autonomous defects in dendritic cell populations of Ikaros mutant mice point to a developmental relationship with the lymphoid lineage. *Immunity* **7**, 483-492 (1997).

25. Allman,D. *et al.* Ikaros is required for plasmacytoid dendritic cell differentiation. *Blood* **108**, 4025-4034 (2006).

26. Carotta,S. *et al.* The transcription factor PU.1 controls dendritic cell development and Flt3 cytokine receptor expression in a dose-dependent manner. *Immunity* **32**, 628-641 (2010).

27. Zhang,D.E., Hetherington,C.J., Chen,H.M. & Tenen,D.G. The macrophage transcription factor PU.1 directs tissue-specific expression of the macrophage colony-stimulating factor receptor. *Mol Cell Biol* **14**, 373-381 (1994).

28. Hohaus,S. *et al.* PU.1 (Spi-1) and C/EBP alpha regulate expression of the granulocyte-macrophage colony-stimulating factor receptor alpha gene. *Mol Cell Biol* **15**, 5830-5845 (1995).

29. Maraskovsky,E. *et al.* Dramatic numerical increase of functionally mature dendritic cells in FLT3 ligand-treated mice. *Adv. Exp. Med. Biol* **417**, 33-40 (1997).

30. Rathinam,C. *et al.* The transcriptional repressor Gfi1 controls STAT3-dependent dendritic cell development and function. *Immunity* **22**, 717-728 (2005).

31. Tamura,T. *et al.* IFN regulatory factor-4 and -8 govern dendritic cell subset development and their functional diversity. *J Immunol* **174**, 2573-2581 (2005).

32. Suzuki,S. *et al.* Critical roles of interferon regulatory factor 4 in CD11bhighCD8alpha-dendritic cell development. *Proc. Natl. Acad. Sci U. S. A* **101**, 8981-8986 (2004).

33. Brustle,A. *et al.* The development of inflammatory T(H)-17 cells requires interferon-regulatory factor 4. *Nat Immunol* **8**, 958-966 (2007).

34. Klein,U. *et al.* Transcription factor IRF4 controls plasma cell differentiation and class-switch recombination. *Nat. Immunol.* **7**, 773-782 (2006).

35. Tailor,P., Tamura,T., Morse,H.C. & Ozato,K. The BXH2 mutation in IRF8 differentially impairs dendritic cell subset development in the mouse. *Blood* **111**, 1942-1945 (2008).

36. Aliberti,J. *et al.* Essential role for ICSBP in the in vivo development of murine CD8alpha + dendritic cells. *Blood* **101**, 305-310 (2003).

37. Tsujimura,H. *et al.* ICSBP/IRF-8 retrovirus transduction rescues dendritic cell development in vitro. *Blood* **101**, 961-969 (2003).

38. Gabriele,L. & Ozato,K. The role of the interferon regulatory factor (IRF) family in dendritic cell development and function. *Cytokine Growth Factor Rev* **18**, 503-510 (2007).

39. Turcotte,K. *et al.* A mutation in the Icsbp1 gene causes susceptibility to infection and a chronic myeloid leukemia-like syndrome in BXH-2 mice. *J. Exp. Med.* **201**, 881-890 (2005).

40. Holtschke,T. *et al.* Immunodeficiency and chronic myelogenous leukemia-like syndrome in mice with a targeted mutation of the ICSBP gene. *Cell* **87**, 307-317 (1996).

41. Schiavoni,G. *et al.* ICSBP is essential for the development of mouse type I interferon-producing cells and for the generation and activation of CD8alpha(+) dendritic cells. *J Exp. Med.* **196**, 1415-1425 (2002).

42. Satpathy,A.T., Wu,X., Albring,J.C. & Murphy,K.M. Re(de)fining the dendritic cell lineage. *Nat. Immunol.* **13**, 1145-1154 (2012).

43. Belz,G.T. & Nutt,S.L. Transcriptional programming of the dendritic cell network. *Nat. Rev. Immunol.* **12**, 101-113 (2012).

44. Becker,A.M. *et al.* IRF-8 extinguishes neutrophil production and promotes dendritic cell lineage commitment in both myeloid and lymphoid mouse progenitors. *Blood* **119**, 2003-2012 (2012).

45. Spits,H., Couwenberg,F., Bakker,A.Q., Weijer,K. & Uittenbogaart,C.H. Id2 and Id3 inhibit development of CD34(+) stem cells into predendritic cell (pre-DC)2 but not into pre-DC1. Evidence for a lymphoid origin of pre-DC2. *J Exp. Med.* **192**, 1775-1784 (2000).

46. Brasel,K., De Smedt,T., Smith,J.L. & Maliszewski,C.R. Generation of murine dendritic cells from flt3-ligand-supplemented bone marrow cultures. *Blood* **96**, 3029-3039 (2000).

47. Nakauchi,H., Sudo,K. & Ema,H. Quantitative assessment of the stem cell self-renewal capacity. *Ann. N. Y. Acad. Sci.* **938**, 18-24 (2001).

48. Shaulian,E. & Karin,M. AP-1 as a regulator of cell life and death. *Nat. Cell Biol.* **4**, E131-E136 (2002).

49. Lee,W., Mitchell,P. & Tjian,R. Purified transcription factor AP-1 interacts with TPA-inducible enhancer elements. *Cell* **49**, 741-752 (1987).

50. Wagner,E.F. & Eferl,R. Fos/AP-1 proteins in bone and the immune system. *Immunol Rev* **208**, 126-140 (2005).

51. Finn,R.D. *et al.* The Pfam protein families database. *Nucleic Acids Res.* **38**, D211-D222 (2010).

52. Landschulz,W.H., Johnson,P.F. & McKnight,S.L. The leucine zipper: a hypothetical structure common to a new class of DNA binding proteins. *Science* **240**, 1759-1764 (1988).

53. Turner,R. & Tjian,R. Leucine repeats and an adjacent DNA binding domain mediate the formation of functional cFos-cJun heterodimers. *Science* **243**, 1689-1694 (1989).

54. O'Shea,E.K., Rutkowski,R., Stafford,W.F., III & Kim,P.S. Preferential heterodimer formation by isolated leucine zippers from fos and jun. *Science* **245**, 646-648 (1989).

55. Schraml,B.U. *et al.* The AP-1 transcription factor Batf controls T(H)17 differentiation. *Nature* **460**, 405-409 (2009).

56. Iacobelli,M., Wachsman,W. & McGuire,K.L. Repression of IL-2 promoter activity by the novel basic leucine zipper p21(SNFT) protein. *J. Immunol.* **165**, 860-868 (2000).

57. Nakabeppu,Y. & Nathans,D. A naturally occurring truncated form of FosB that inhibits Fos/Jun transcriptional activity. *Cell* **64**, 751-759 (1991).

58. Chen,L., Glover,J.N., Hogan,P.G., Rao,A. & Harrison,S.C. Structure of the DNA-binding domains from NFAT, Fos and Jun bound specifically to DNA. *Nature* **392**, 42-48 (1998).

59. Tussiwand,R. *et al.* Compensatory dendritic cell development mediated by BATF-IRF interactions. *Nature* **490**, 502-507 (2012).

60. Glasmacher,E. *et al.* A Genomic Regulatory Element That Directs Assembly and Function of Immune-Specific AP-1-IRF Complexes. *Science* **338**, 975-980 (2012).

61. Li,P. *et al.* BATF-JUN is critical for IRF4-mediated transcription in T cells. *Nature* **490**, 543-546 (2012).

62. Dorner,B.G. *et al.* Selective expression of the chemokine receptor XCR1 on cross-presenting dendritic cells determines cooperation with CD8+ T cells. *Immunity* **31**, 823-833 (2009).

63. Schulz,O. *et al.* Toll-like receptor 3 promotes cross-priming to virus-infected cells. *Nature* **433**, 887-892 (2005).

64. Hettinger,J. *et al.* Origin of monocytes and macrophages in a committed progenitor. *Nat. Immunol.* **14**, 821-830 (2013).

65. Miller,J.C. *et al.* Deciphering the transcriptional network of the dendritic cell lineage. *Nat. Immunol.* **13**, 888-899 (2012).

66. Ginhoux,F. *et al.* Fate Mapping Analysis Reveals That Adult Microglia Derive from Primitive Macrophages. *Science* **330**, 841-845 (2010).

67. Ginhoux,F. & Merad,M. Ontogeny and homeostasis of Langerhans cells. *Immunol. Cell Biol.* **88**, 387-392 (2010).

68. Edelson,B.T. *et al.* Batf3-dependent CD11b(low/-) peripheral dendritic cells are GM-CSF-independent and are not required for Th cell priming after subcutaneous immunization. *PLoS One* **6**, e25660 (2011).

69. Edelson,B.T. *et al.* CD8a+ Dendritic Cells Are an Obligate Cellular Entry Point for Productive Infection by Listeria monocytogenes. *Immunity* **35**, 236-248 (2011).

70. Mashayekhi,M. *et al.* CD8a+ Dendritic Cells Are the Critical Source of Interleukin-12 that Controls Acute Infection by Toxoplasma gondii Tachyzoites. *Immunity* **35**, 249-259 (2011).

71. Seillet,C. *et al.* CD8alpha+ DCs can be induced in the absence of transcription factors Id2, Nfil3 and Batf3. *Blood* (2013).

72. Murphy,T.L., Tussiwand,R. & Murphy,K.M. Specificity through cooperation: BATF-IRF interactions control immune-regulatory networks. *Nat. Rev. Immunol.* **13**, 499-509 (2013).

73. Guermonprez,P. *et al.* Inflammatory Flt3l is essential to mobilize dendritic cells and for T cell responses during Plasmodium infection. *Nat. Med.* **19**, 730-738 (2013).

74. De Smedt,T. *et al.* Antigen-specific T lymphocytes regulate lipopolysaccharide-induced apoptosis of dendritic cells in vivo. *J. Immunol.* **161**, 4476-4479 (1998).

75. De Smedt,T. *et al.* Regulation of dendritic cell numbers and maturation by lipopolysaccharide in vivo. *J. Exp. Med.* **184**, 1413-1424 (1996).

76. Coughlin,J.J., Stang,S.L., Dower,N.A. & Stone,J.C. The role of RasGRPs in regulation of lymphocyte proliferation. *Immunol. Lett.* **105**, 77-82 (2006).

77. Coughlin,J.J., Stang,S.L., Dower,N.A. & Stone,J.C. RasGRP1 and RasGRP3 regulate B cell proliferation by facilitating B cell receptor-Ras signaling. *J. Immunol.* **175**, 7179-7184 (2005).

78. Zhang,L., Malik,S., Kelley,G.G., Kapiloff,M.S. & Smrcka,A.V. Phospholipase C epsilon scaffolds to muscle-specific A kinase anchoring protein (mAKAPbeta) and integrates multiple hypertrophic stimuli in cardiac myocytes. *J. Biol. Chem.* **286**, 23012-23021 (2011).

79. Kamath,A.T., Henri,S., Battye,F., Tough,D.F. & Shortman,K. Developmental kinetics and lifespan of dendritic cells in mouse lymphoid organs. *Blood* **100**, 1734-1741 (2002).

80. Waskow,C. *et al.* The receptor tyrosine kinase Flt3 is required for dendritic cell development in peripheral lymphoid tissues. *Nat Immunol* **9**, 676-683 (2008).

Chapter 3 BATF3-IRF8 complexes direct transcription of CD8α^{+} DC-specific genes

3.1 Abstract

Considerable progress has been made toward identifying homeostatic cytokines, defined lineage-restricted progenitors, and developmentally important transcription factors for the dendritic cell lineage. Yet the precise molecular mechanism underlying DC specification and functional specialization is still poorly understood, and most studies to date remain largely descriptive on these topics. Numerous studies across disparate cell lineages in eukaryotes have concluded that much of the active gene expression program is dominated by a small number of the many transcription factors expressed [1-4]. Similarly, CD8α^+ DC development and function is regulated by a small set of factors, namely *Irf8*, *Batf3*, *Nfil3*, and *Spi1* (PU.1)[5-7]. The molecular activities and possible cooperative interactions of among some of these factors remain poorly characterized, and studies focusing on these aspects of DC biology represent a major priority in the field.

The recent identification of a genomic regulatory element that is recognized by AP-1-IRF complexes[8-10], which can direct large components of lymphocyte gene expression, led us to hypothesize that a similar mechanism regulates lineage commitment and functional specialization of CD8α^+ DCs. Though evidence of AP-1-IRF interactions in DCs was presented, the studies focused on *in vitro* GM-CSF-derived DC subsets that poorly represent actual DC subtypes *in vivo* and have no reported phenotypes in the setting of *Batf3* deficiency[11-13]. Moreover, these examples provided few insights into the possible role of BATF3-IRF8 complexes in the regulation of *bona fide* CD8α^+ DC gene targets. By pairing genome-wide measurements of protein-DNA interactions with transcriptome profiling, we have determined that BATF3-IRF8 complexes occupy the proximal promoter regions and distal conserved non-

coding sequences (CNS) of a large number of CD8α$^+$ DC-specific genes. The loss of *Batf3* impaired the CD8α$^+$ DC-specific gene expression program, thereby suggesting that the role of AP-1-IRF complexes is to regulate the selective gene expression program of this lineage. Importantly, this indicates that the combination of PU.1 and IRF8 is insufficient for specifying the totality of CD8α$^+$ DC-specific gene expression program. This result is somewhat surprising because PU.1 is known to bind globally to enhancers and promoters. In addition, PU.1 and *Batf3* are expressed at equal levels between CD8α$^+$ DCs and CD11b$^+$ DCs, thereby being insufficient to regulate specific gene expression differences between the two populations. Instead, it is the combination of the three factors that appears to be necessary and sufficient to induce lineage specific expression module. The relatively high expression of PU.1 in DCs and near absence in CD4$^+$ T cells represents an important difference and warrants further investigation.

We characterized several direct targets of AP-1-IRF complex by analyzing knockout mice when available or performing overexpression rescue experiments on *in vitro* Flt3L cultures. Since no single gene target recapitulated the *Batf3*$^{-/-}$ developmental phenotype, we suggest that it is the combination of several genes involved in cell signaling, growth and survival that account for the observed deficits. Our previous work identified a compensatory developmental pathway for CD8α$^+$ DCs that required the paralogs *Batf* and *Batf2* during settings of type I immunity [8]. Though this pathway accounted for the reemergence of CD8α$^+$ DCs in the skin-draining lymph node, it failed to restore the development of peripheral tissue CD103$^+$ DCs. These data suggest that despite sharing many features (ontogeny, high cross-presentation capacity, requirement for similar cytokines and transcription factors), the CD103$^+$ DCs and CD8α$^+$ DCs have differential homeostatic requirements. We sought to account for this by identifying determinants that acted

differentially between these two related populations. Interestingly, we observed occupancy of BATF3-IRF8 complex at several well characterized microRNA clusters and found that miR-155 was important for the homeostasis of peripheral CD103$^+$ DCs but largely dispensable for splenic CD8α^+ DCs. miR-155 is a unique microRNA that functions primarily in the hematopoietic compartment in which it regulates many aspects of lymphocyte activation and development [14]. Although purported to affect DC function (at least *in vitro* derived DCs), miR155 has not been implicated in DC development until now. We hypothesize that miR155 may also play a role in CD8α^+ DCs following activation.

Lastly, *de novo* motif analysis revealed that both BATF3- and IRF8-enriched regions were near Ets (i.e., PU.1) elements, which is to be expected given that PU.1 is known to interact with both AP-1 and IRF proteins[15-17], and runt-related transcription factor 1 (*Runx1*) sites, which has not been reported. The proximity of AP-1 and IRF complexes to Runx sites suggests that the DC lineage is specified through the coordinated actions of AP-1, IRF, PU.1 and Runx proteins. We propose to investigate the potential role of Runx proteins in regulating DC development.

3.2 Introduction

Jacob and Monod initially defined features of gene regulation nearly half a century ago through pioneering studies of the *Escherichia coli* lac operon [18]. This early work and subsequent studies in higher organisms established the paradigm of DNA binding proteins (*trans*-factors) recognizing specific sequences at regulatory genomic regions (*cis*-elements) to modulate transcription. In higher organisms, the sequence-specific *trans*-factors recruit cofactors, chromatin remodeling proteins, and elements of the general transcription apparatus to alter the local architecture of the chromatin for productive transcription. Each step in the process is

subject to tight control with positive and negative feedback loops operating to enforce either activation or inhibition. In most cases, a combination of transcription factors bind to enhancer elements and then form physical contacts with the core promoter through a process that involves the looping of DNA [19]. In some instances, the proximal promoter can be bound directly by the very factors that also recognize enhancers [20]. Collectively, these actions give rise to a cell's transcriptome, which comprises housekeeping genes or cell-type specific genes. The expression of the latter set is largely regulated by a limited set of transcription factors, as evidenced by the conversion between cell states with a relatively few factors. Therefore, understanding the molecular basis of lineage specification in any developmental system requires the characterization of key lineage-defining transcription factors.

3.2.1 Interferon regulatory factor (IRF) family

The interferon regulatory factor (IRF) family of transcription factors comprises nine evolutionarily conserved members that play a critical role in host defense [21]. Though the family was initially identified in the context of type I interferon (IFN) signaling, it is now appreciated that specific members can also influence development of myeloid and lymphoid lineages[22,23]. All IRFs contain an N-terminal DNA binding domain, which forms a helix-turn-helix structure and recognizes the IFN-stimulated response elements (ISRE, NGAAANNGAAACT) [24]; and a C-terminal IRF association domain (IAD, except for IRF1 and 2) that mediates homo- and hetero-dimeric interactions with other transcription factors such as PU.1 and signal transducer and activator of transcription (STAT) [25]. IRF4 and IRF8 are more selectively expressed across immune lineages and are the two members of the family that play a role in development [26-29]. IRF4 is an important mediator of lymphocyte differentiation and function [30,31]. For example, it is

required for plasma cell differentiation and class switch recombination. It is also required for the development of helper $CD4^+$ lineages [30,32]. Although its activities are comparatively less well known in the myeloid lineages, IRF4 is known to influence the development of $CD11b^+$ DCs in lymphoid and peripheral tissues [33-35]. However, most studies on the actions of IRF4 in DCs have been largely descriptive. IRF8 also plays a role in B cell differentiation and may provide functional redundancy in the absence of IRF4 [22]. In the macrophages and DCs, IRF8 may function as either an activator or repressor depending on its association with interacting partner proteins [29,36]. IRF8 deficiency in both mouse and man results in widespread immunodeficiency and the absence of multiple dendritic cell lineages[37]. Both of these IRF proteins are known to bind the ISREs weakly and instead bind to DNA through cooperative interactions with partner proteins such as PU.1 on Ets-IRF composite elements (EICEs). However, the broad transcriptional activities of IRF4 and IRF8 cannot be simply explained by interactions with PU.1[9,10].

3.2.2 Activated protein 1 (AP-1) family

Basic leucine zipper transcription factor, ATF-like 3 (BATF3) is a member of the ATF subfamily of transcription factors, which also includes BATF, BATF2, JDP2, and ATF3 and is part of a larger class of basic leucine zipper (bZIP) transcription factors[38-40]. These proteins contain an N-terminal DNA binding region consisting of basic residues that form an α-helix and a C-terminal heptad repeat of leucines that form the leucine zipper motif [41-43]. The BATFs are obligate heterodimers that pair with JUN family members through extensive contacts in the leucine zipper. In addition, the leucine zipper has been proposed to mediate interactions with other transcription factor families to combinations of factors that can recognize additional DNA

elements. Interestingly, unlike the other bZIP proteins that dimerize with JUN (for example, FOS or ATF3), BATF3 and BATF contain only the basic region and leucine zipper. This parsimony in domain structure led to the idea that BATFs function by simply acting as dominant negative forms of FOS-like proteins.

Unlike other member of the bZIP family, *Batf3* and *Batf* expression is largely restricted to the immune system. *Batf* is an important regulator of B and T cell function. It is required for class switch recombination, follicular helper T cell development, induction of IL-17$^+$ CD4 T cells [44,45]. *Batf3* is required for the development of lymphoid-resident CD8α^+ DCs and peripheral tissue CD103$^+$ DCs. Early studies of these two factors made extensive use of overexpression and concluded that they function as inhibitors of AP-1 transcription. While the inhibitory actions may occur in certain contexts, much of its unique actions can now be explained by positive transcriptional regulation through interactions with IRF family members [46].

3.3 Results

3.3.1 BATF3 regulates the expression of CD8α^+ DC-specific genes

A recent large-scale transcriptome profiling of lymphoid-resident and peripheral tissue DCs led to the identification of signature transcription factors and cell surface markers for each DC subtype[47,48]. CD8α^- DCs or CD11b$^+$ DCs expressed high levels of the phagocytic receptor SIRPα, which was completely absent from CD8α^+ DCs or CD103$^+$ DCs. We used this marker in combination with other known CD8α^+ DCs or CD103$^+$ DCs (such as CD24 and CD205) to re-analyze Batf3-deficient mice *in vitro* and *in vivo*. Flt3L bone marrow cultures of Batf3-deficinet

cells from the C57BL/6 genetic background contained a population of CD24^{+}SRIPα^{-} DCs (Figure 3.1 **A,B**), which expressed significantly lower levels of CD103.

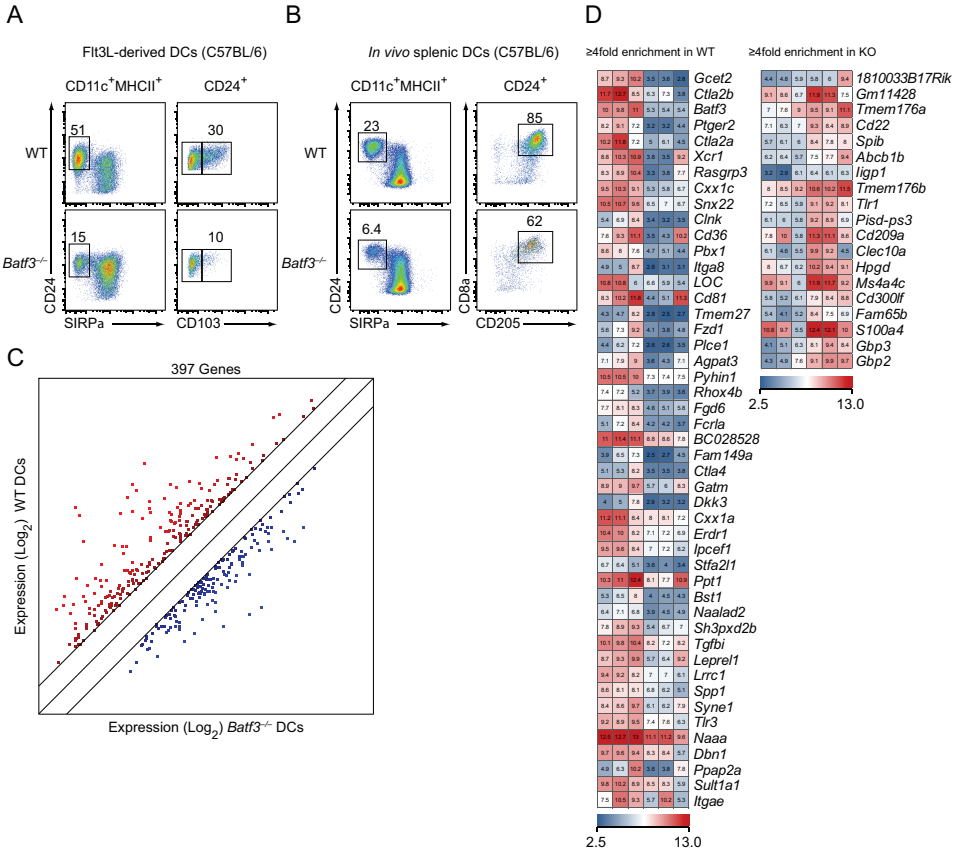

Figure 3.1: BATF3 regulates the expression of CD8α^{+} DC-specific genes

(A,B) Flt3L (A) and splenic-derived (B) DCs from WT and Batf3$^{-/-}$ mice. (C, D) Population gated in (A) and (B) were purified by cell sorting, RNA extracted and microarray analysis performed. After background correction and normalization with Robust Multi-array Average (RMA) method, probe sets with no known gene annotation and a linear expression value less than 16 were removed before differential gene expression analysis. Shown is an M-Plot (C) comparing the log 2 transformed expression values of genes different by at least 2-fold between WT (y axis, n = 3 biological replicates) and Batf3$^{-/-}$ (x axis, n = 3 biological replicates) CD8α^{+} DCs (mean expression values were averaged from in vivo and in vitro derived DCs). Show in (D) is a heat map generated with log2 transformed expression values for genes enriched by 4-fold in WT (LEFT) or KO (RIGHT).

Recently, several groups showed that surface CD103 expression can be induced by PAMPs or cytokines such as GM-CSF [11,49-51]; and the $CD103^+$ fraction of $CD24^+SRIP\alpha^-$ DCs represents a state that has higher cross-presentation capacity. Using slightly different markers for labeling $CD8\alpha^+$ DCs *in vivo*, we observed a small but measurable population of $CD24^+SIRPa^-$ DCs (Figure 3.1 **B**). We sorted all three populations from WT and *Batf3*$^{-/-}$ mice and carried out microarray analysis. We observed some 397 genes differentially expressed between WT and Batf3-deficient DCs. Notably, we saw significant reduction in key cell-type specific effector molecules, such as *Xcr1*, *Tlr3*, and *Itgae* (Figure 3.1 **C and D**). Also cell-signaling genes such as *Rasgrp3*, *Clnk*, and *Plce1* were significantly reduced. In summary, we conclude that BATF3 is necessary for the maximal expression of $CD8\alpha^+$ DC-specific effector genes, and that it regulates the survival of $CD8\alpha^+$ DCs by positively regulating survival promoting genes.

3.3.2 Generation of anti-BATF3 antibody

Chromatin immunoprecipitation followed by massively parallel sequencing (ChIP-Seq) is an important technique for describing genome-wide occupancy of DNA-binding factors. The unbiased nature of this approach and the high base-pair resolution can help identify previously unappreciated interactions among different transcription factors [52,53]. A major determinant in the accuracy and depth of ChIP-Seq profiles is the quality of antibody. Extensive characterization and validation are required before performing these experiments. We generated our own anti-BATF3 antibody and validated it for chromatin immunoprecipitation.

Batf3 was PCR amplified from a splenic CD11c-enriched cDNA library and cloned into the bacterial expression construct pET-28a(+). The resulting vector was transformed into expression competent *E. coli* and protein expression induced with low concentration IPTG at room temperature for 12 hours. Initial efforts to affinity purify recombinant full-length BATF3 was unsuccessful because of inclusion body formation. An alternative method using the detergents sarkosyl, Triton-X 100 and CHAPS has recently been described for solubilizing proteins from inclusion bodies [54]. We adapted this method and obtained relatively pure BATF3 (Figure 3.2 **A**). Rabbit anti-BATF3 serum was generated commercially (Harlan Labs) and anti-BATF3 antibody was affinity purified. The specificity of our antibody stock was confirmed by Western blot analysis of whole cell extracts of CD11c-enriched dendritic cells from wild type and Batf3-deficient mice (Figure 3.2 **B**).

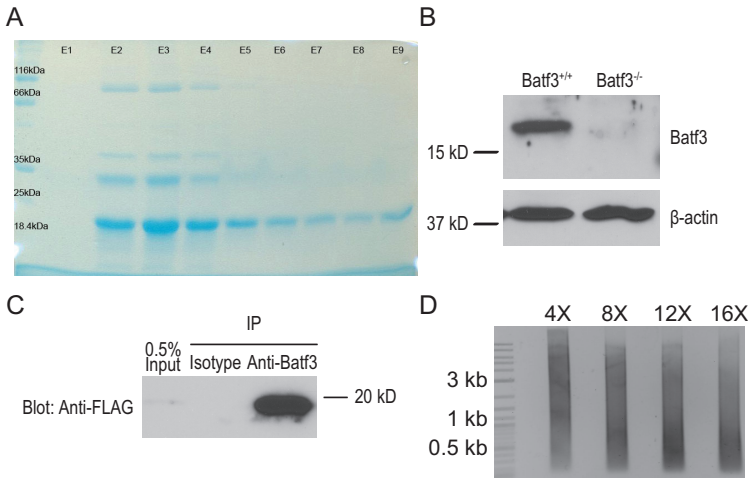

Figure 3.2: Generation of anti-BATF3 antibody

(A) SDS-PAGE of recombinant BATF3 purification. (B) Westernblot analysis of whole cell extracts from CD11c-enriched cells from WT and Batf3$^{-/-}$ mice. Top blot was probed with rabbit polyclonal anti-BATF3; bottom blot was probed with mouse anti-β-actin. (C) Westernblot of immunoprecipitated extracts from 3T3 fibroblasts stably expressing FLAG-tagged BATF3. Pull down was performed with polyclonal anti-BATF3. Blot was probed with anti-FLAG antibody. (D) Sonicated DNA on 2% agarose gel and stained with ethidium bromide. DNA was extracted from Flt3L-derived DCs after chromatin cross-linking was reversed.

Next, we evaluated the reactivity of our affinity-purified anti-BATF3 on cross-linked antigen, which is a necessary step in chromatin immunoprecipitation. We generated a line of murine 3T3 fibroblasts stably expressing FLAG-tagged BATF3. Chromatin immunoprecipitation was performed as previously described [55] with polyclonal anti-BATF3 antibody. Immunoblot analysis of the pulled-down product with a monoclonal anti-FLAG antibody confirmed the reactivity of the polyclonal antibody to cross-linked antigen (Figure 3.2 **C**). Lastly, we sonicated cross-linked DC extracts to determine the optimal shearing time for DC chromatin (Figure 3.2 **D**). In summary, we have generated a polyclonal BATF3 antibody with specific reactivity to native and cross-linked BATF3.

3.3.3 Genome-wide profiles of BATF3 and IRF8

We carried out chromatin immunoprecipitation with anti-BATF3 and anti-IRF8 antibodies on Flt3L-derived wild-type dendritic cell chromatin followed by sequencing. Control immunoprecipitation was performed on Batf3- and Irf8-deficient DC chromatin to serve as specificity controls for downstream data analyses. Raw sequencing data was aligned to the mouse genome assembly version 9 (mm9) with Novoalign, and duplicate or unmapped reads were removed for subsequent data processing steps. Model-based analysis of ChIP-Seq (MACS)[56] is a widely used computation tool for peak calling or discovery. We identified statistically significant BATF3 and IRF8-occupied regions or peaks – 12894 IRF8 peaks and 9471 BATF3 peaks (Figure 3.3 **A**). We then compared then compared the overlap between IRF8 and BATF3 peaks. This was done by first extending the summit of each peak or presumed binding point by the computationally determined average fragment length size. Next, we intersected the genomic coordinates for summit-extended reads and obtained 5523 peaks. In summary, a large fraction of IRF8 and BATF3 peaks are overlapping (Figure 3.3 **D**). Interestingly, when we analyzed the read density around a 4 kilobase window across promoters of all protein-encoding genes, the greatest coverage (and therefore supposed binding of each factor) appeared to be around the immediate transcription start site (Figure 3.3 **B and C**)

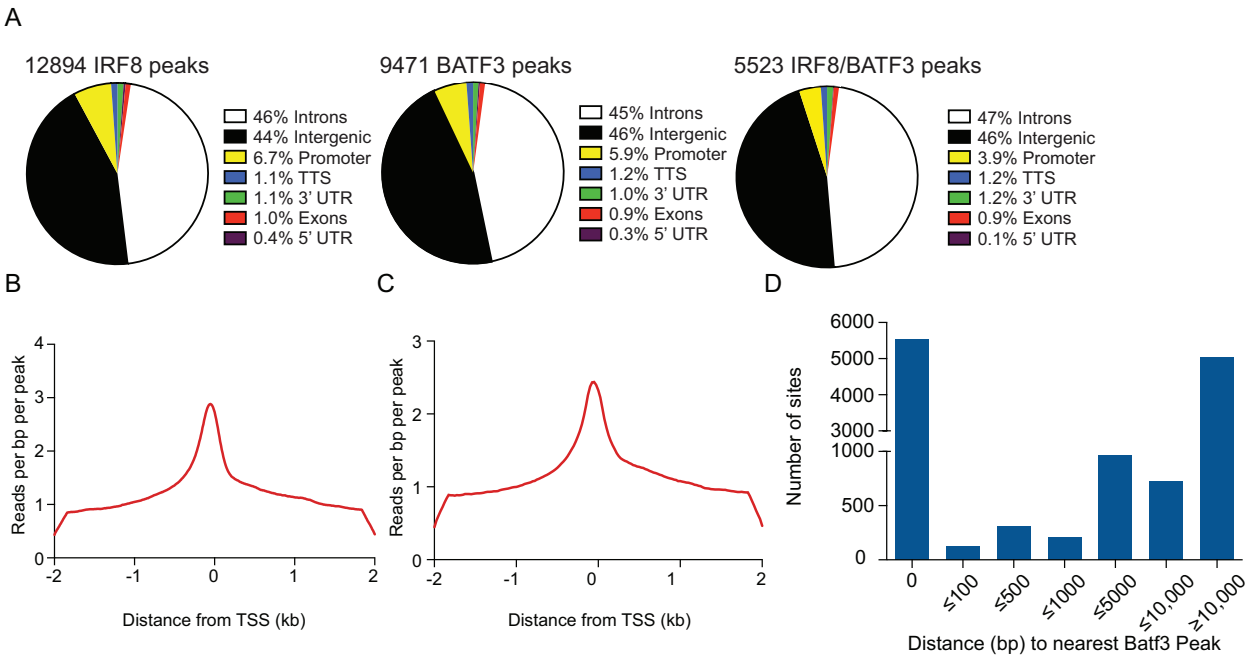

Figure 3.3: Genome-wide profiles of BATF3 and IRF8 binding

(A) Annotation (performed with HOMER software package) of IRF8 and BATF3 peaks, as determined by MACS. Also included is an annotation of peak regions common to both BATF3 and IRF8. (B,C) Coverage or read density over a 4 kilobase region centered on the transcription start site of all protein-coding genes. IRF8 (B) and BATF3 (C). (D) Average distance from an IRF8 peak to its nearest BATF3 peak. Peak distances have been grouped into 7 size ranges.

3.3.4 Composite Ets-IRF (EICE), composite AP-1-IRF (AICE) and Runx sites are enriched at regions occupied by IRF8 and BATF3

Although consensus recognition elements have been described for IRF8 and BATF3, the ISRE and AP-1 motifs, respectively, *de novo* motif discovery affords an opportunity to identify novel recognition sequences that may help characterize previously unappreciated interactions. We used the HOMER[57] software package to perform *de novo* motif discovery on the top 500 enriched peaks for BATF3 and IRF8 (executed 3 separate instances). As anticipated, analysis of IRF8 peaks identified EICE as the top motif. This analysis also found significant enrichment for

the recently described composite AP-1-IRF site (AICE). Notably, IRF8 peaks were enriched for AP-1 and Runx motifs (Figure 3.4 **A**). Interestingly, an almost identical list of motifs was generated from the analysis of BATF3 peaks (Figure 3.4 **B**). And yet there is no known interaction between Runx proteins and IRF or AP-1 factors. We therefore propose to extend the conclusions derived from the recent analyses on the interaction of IRF and AP-1 proteins by ChIP-Seq by suggesting that Runx may also be involved in the gene expression program of DCs.

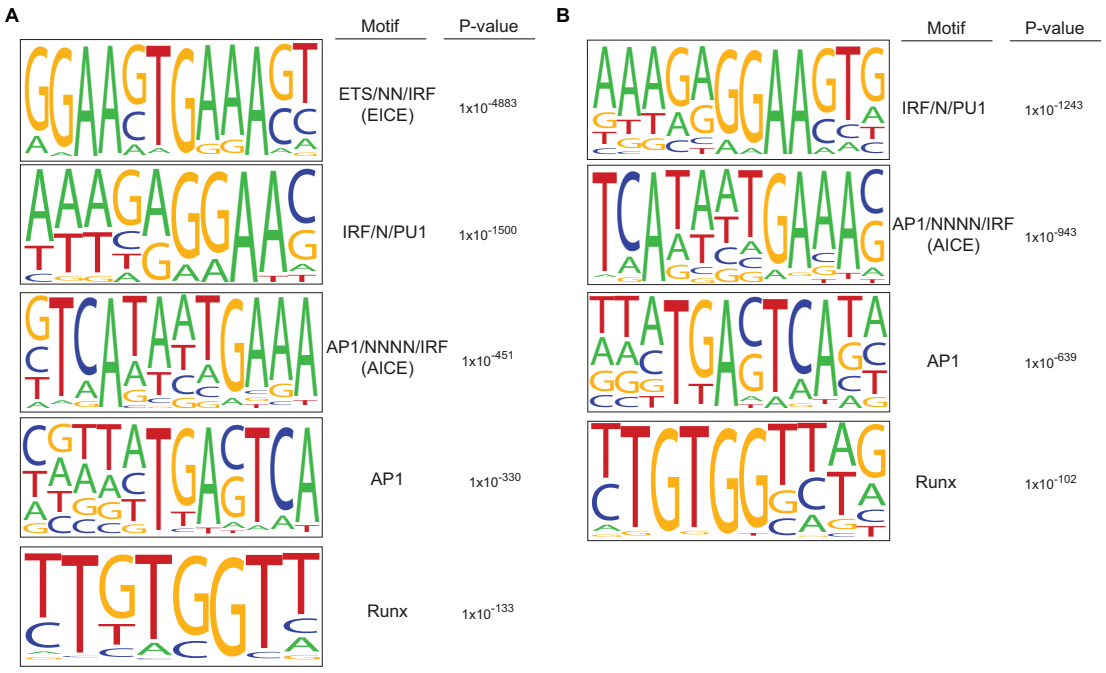

Figure 3.4: *de novo* motif analysis of BATF3 and IRF8 enriched peaks

(A, B) IRF8 (A) and BATF3 (B) peaks evaluated for *de novo* motif discovery with HOMER software package as described in the Methods. Top 4-6 DNA motifs empirically derived along with the closest known motif and the associated p-value from analysis.

3.3.5 IRF8 and BATF3 co-occupy the proximal promoter region of signature CD8α$^+$ DC genes

CD8a$^+$ DCs are the critical initiators of CD8 T cells responses to a diverse set of intracellular pathogens [58], but they can also mount responses to non-infectious threats such as tumors. This highly specialized function is in part due to the expression of unique viral and host sensors (such as *Tlr3* and *Clec9a*) and chemokine receptors (such as *Xcr1*). To date, little is known about the regulation of these important effector molecules. We identified an almost identical binding pattern of IRF8 and BATF3 at the proximal promoter of *Tlr3*, *Clec9a*, and *Xcr1* (Figure 3.5). The co-occupancy of IRF8 and BATF3 suggests that a cooperative interaction between these two factors drives the cell-type specific expression of *Tlr3*, *Clec9a*, and *Xcr1*. We also performed gene annotation analysis of IRF8 and BATF3 ChIP-Seq peaks with HOMER and discovered the presence of a BATF3-dependent IRF8 peak in the promoter region of microRNA 155 (miR155), which mediates broad actions throughout the hematopoietic compartment. We hypothesized miR155 plays a role in the homeostasis of DCs. In a preliminary analysis (data not shown), we observed a 50% reduction in lung CD103$^+$ DCs but no reduction in spleen-resident CD8a$^+$ DCs. Thus, miR-155 maybe differentially required between the closely related peripheral CD103$^+$ DCs and lymphoid-resident CD8a$^+$ DCs. These studies are still preliminary and require repeating with inclusion of additional tissues.

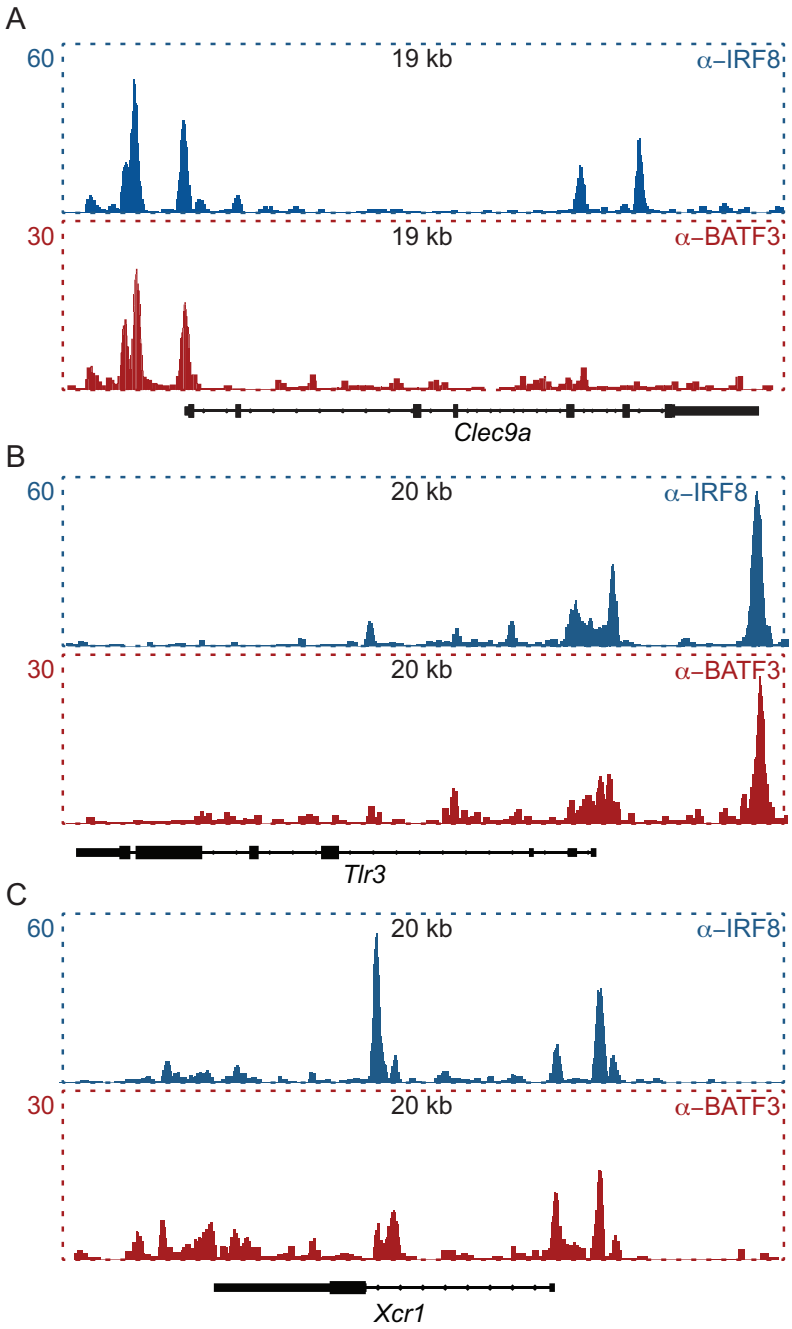

Figure 3.5: IRF8 and BATF3 co-occupy proximal promoter of CD8α$^+$ DC-specific genes

(A, B, C) Gene tracks for IRF8 (blue, top) and BATF3 (red, bottom) binding to the Clec9a (A), Tlr3 (B) and Xcr1 (C) genomic regions. Window size is indicated at the top of each track. The transcript configuration below each track is shown as depicted in the UCSC Browser. Numbers represent number of normalized reads.

3.4 Discussion

Genome-wide surveys of IRF4 and BATF binding revealed that a large number of functionally important genes in lymphocytes are directly regulated by the coordinated actions of these two factors[9,10]. While a similar transcriptional activity was proposed for the dendritic cell lineage, the use of inaccurate DC surrogates and the emphasis on IRF4 and BATF rather than IRF8 and BATF3 dramatically limited the conclusions of this study. We therefore carried out ChIP-Seq analysis of IRF8 and BATF3 binding in dendritic cells and discovered extensive overlap between the two factors. Moreover, signature CD8α^+ DC-specific genes showed identical binding patterns for IRF8 and BATF3 in the promoter proximal regions, confirming our hypothesis that these genes are directly controlled by IRF8 and BATF3 cooperativity. Lastly, *de novo* motif analysis revealed the presence of Runx-binding sites near both IRF8 and BATF3 peaks, which raises the interesting prospect of Runx interactions with either IRF or AP1 family members. This latter observation requires validation by analyzing the DC compartment of Runx knockout mice. We hypothesize that the residual transcription of *Tlr3*, *Xcr1*, and *Clec9a* in Batf3-deficient DCs is mediated by Runx-IRF activity.

3.5 Materials and Methods

3.5.1 Generation of a BATF3-specific rabbit polyclonal antibody and immunoblot analysis.

Murine full-length *Batf3* cDNA was PCR amplified from splenic CD8α^+ cDC cDNA library. The resulting PCR product was ligated into the expression vector pET-28a(+) (Novagen) downstream of the His-Tag and the final plasmid was transformed into the *Escherichia coli*

expression strain BL21-CodonPlus(DE3)-RIL (Stratagene). Recombinant BATF3 was expressed for 12 hours at room temperature and then affinity purified on Ni-NTA His·Bind® Resin (Novagen) according to manufacturer's instructions. Purified recombinant BATF3 was used to immunize New Zealand White Rabbits (Harlan Laboratories) according to a standard 112-day protocol. Finally, rabbit anti-mouse BATF3 sera were collected and BATF3 -specific antibody was affinity purified and tested by Western blot analysis.

For immunoblot analysis, either whole-cell extracts were prepared with RIPA lysis buffer containing protease inhibitors, or nuclei were obtained after cellular lysis with buffer containing 0.2% Nonidet P40 as described[59]. Extracts were denatured in Laemmli sample buffer at 95°C for 10 minutes, and $5x10^5$ to $1x10^6$ cell equivalent of denatured extract was loaded per well of a 7.5% precast mini polyacrylamide gel (Bio-Rad). Proteins were then transferred onto a nitrocellulose membrane using a Trans-Blot SD Semi-Dry Transfer Cell (Bio-Rad) according to manufacturer's instructions. Blots were blocked with a solution containing 5% non-fat milk and 0.05% Tween-20 for 1 hour at room temperature and then incubated with primary antibody overnight at 4ºC. After extensive washing, blots were incubated with a goat anti-rabbit IgG (H+L) conjugated to horseradish peroxidase (Jackson ImmunoResearch Laboratories, Inc.) for 1 hour at room temperature. Finally, blots were developed with ECL Western Blotting Substrate (Thermo Scientific) according to manufacturer's instructions.

3.5.2 Chromatin Immunoprecipitation (ChIP).

ChIP was carried out as previously described[55]. In summary, $30x10^6$ dendritic cells from a 10-day flt3-ligand culture of bone marrow from wild-type mice, $Irf8^{-/-}$ mice and $Batf3^{-/-}$ mice were harvested, washed twice with ice-cold 1x PBS, and re-suspended in 1x PBS. Cells were

cross-linked for 13 minutes at room temperature by the addition of one-tenth of the volume of 11% formaldehyde solution. Following the final wash, supernatant was discarded and cell pellets were flash frozen in liquid nitrogen for storage at -80°C. Thawed cell pellets were lysed with lysis buffer 1, washed with lysis buffer 2, and re-suspended in lysis buffer 3 for sonication. Chromatin was sonicated for 36 cycles of 15 seconds on and 20 seconds off per cycle with a Misonix Sonicator XL2020 outfitted with a Microtip and operated at a power setting between 2-3. Sheared DNA was run on a 2% agarose gel stained with ethidium bromide and imaged to determine the average size, which was between 200 and 300 bps. Sonicated lysates were incubated overnight at 4°C with magnetic beads bound to anti-Irf8 antibody to enrich for DNA fragments. Magnetic beads were prepared by blocking 50 microliter of Protein G Dynabeads (Invitrogen) with 0.5% BSA (w/v) in PBS, followed by an overnight incubation with 5 μg of goat anti-Irf8 (C-19, Santa Cruz) at 4°C. Beads containing DNA fragments were washed with RIPA buffer and TE + 50mM NaCl. Bound complexes were eluted in elution buffer at 65°C for 15 minutes with vortexing every 3 minutes. Crosslinks were reversed overnight at 65°C. RNA and protein were digested with RNase A and Proteinase K, respectively, and DNA was purified with phenol chloroform extraction followed by ethanol precipitation.

3.5.3 ChIP-Seq data processing and analysis.

ChIP-Seq data sets were aligned using Novoalign (Novocraft Technologies) to build version NCBI37/mm9 of the mouse genome. Alignments were carried out using the following parameter "-o SAM -r random -l 30 -e 100 -a AGATCGGAAGAGCGGTTCAGCAGGAATGCCGAG -H." Aligned and raw data can be found online under the following GEO Series ID GSE53311.

We used Model based analysis of ChIP-Seq (MACS v1.4.2)[56] peak finding algorithm to identify genomic regions enriched for IRF8 binding. A maximum of 1 duplicate tag and a p-value cutoff of $1x10^{-9}$ was used for all data sets. Background estimates were made using ChIP-Seq on *Irf8*$^{-/-}$ DCs as the control. Annotation (mm9) of the obtained peaks was performed using "annotatePeak.pl" function of the Homer software package[57]. Peaks were further analyzed for *de novo* motif discovery by using the "findMotifsGenome.pl" function of the Homer software package using default parameters except for "-size 50 -S 10."

3.6 Author Contributions

W.K. and K.M. designed the entire study. W.K. performed all experiments and informatics analyses with significant contributions from X.W. The text was written entire by W.K.

3.7 References

1. Ng,H.H. & Surani,M.A. The transcriptional and signalling networks of pluripotency. *Nat. Cell Biol.* **13**, 490-496 (2011).

2. Orkin,S.H. & Hochedlinger,K. Chromatin connections to pluripotency and cellular reprogramming. *Cell* **145**, 835-850 (2011).

3. Graf,T. Historical origins of transdifferentiation and reprogramming. *Cell Stem Cell* **9**, 504-516 (2011).

4. Lee,T.I. & Young,R.A. Transcriptional regulation and its misregulation in disease. *Cell* **152**, 1237-1251 (2013).

5. Belz,G.T. & Nutt,S.L. Transcriptional programming of the dendritic cell network. *Nat. Rev. Immunol.* **12**, 101-113 (2012).

6. Satpathy,A.T., Wu,X., Albring,J.C. & Murphy,K.M. Re(de)fining the dendritic cell lineage. *Nat. Immunol.* **13**, 1145-1154 (2012).

7. Geissmann,F. *et al.* Development of monocytes, macrophages, and dendritic cells. *Science* **327**, 656-661 (2010).

8. Tussiwand,R. *et al.* Compensatory dendritic cell development mediated by BATF-IRF interactions. *Nature* **490**, 502-507 (2012).

9. Li,P. *et al.* BATF-JUN is critical for IRF4-mediated transcription in T cells. *Nature* **490**, 543-546 (2012).

10. Glasmacher,E. *et al.* A Genomic Regulatory Element That Directs Assembly and Function of Immune-Specific AP-1-IRF Complexes. *Science* **338**, 975-980 (2012).

11. Edelson,B.T. *et al.* Batf3-dependent CD11b(low/-) peripheral dendritic cells are GM-CSF-independent and are not required for Th cell priming after subcutaneous immunization. *PLoS One* **6**, e25660 (2011).

12. Edelson,B.T. *et al.* Peripheral CD103+ dendritic cells form a unified subset developmentally related to CD8alpha+ conventional dendritic cells. *J. Exp. Med.* **207**, 823-836 (2010).

13. Hildner,K. *et al.* Batf3 deficiency reveals a critical role for CD8alpha+ dendritic cells in cytotoxic T cell immunity. *Science* **322**, 1097-1100 (2008).

14. Vigorito,E. *et al.* microRNA-155 regulates the generation of immunoglobulin class-switched plasma cells. *Immunity* **27**, 847-859 (2007).

15. Brass,A.L., Zhu,A.Q. & Singh,H. Assembly requirements of PU.1-Pip (IRF-4) activator complexes: inhibiting function in vivo using fused dimers. *EMBO J.* **18**, 977-991 (1999).

16. Brass,A.L., Kehrli,E., Eisenbeis,C.F., Storb,U. & Singh,H. Pip, a lymphoid-restricted IRF, contains a regulatory domain that is important for autoinhibition and ternary complex formation with the Ets factor PU.1. *Genes Dev.* **10**, 2335-2347 (1996).

17. Eisenbeis,C.F., Singh,H. & Storb,U. Pip, a novel IRF family member, is a lymphoid-specific, PU.1-dependent transcriptional activator. *Genes Dev.* **9**, 1377-1387 (1995).

18. JACOB,F. & MONOD,J. Genetic regulatory mechanisms in the synthesis of proteins. *J. Mol. Biol.* **3**, 318-356 (1961).

19. Krivega,I. & Dean,A. Enhancer and promoter interactions-long distance calls. *Curr. Opin. Genet. Dev.* **22**, 79-85 (2012).

20. Goodrich,J.A. & Tjian,R. Unexpected roles for core promoter recognition factors in cell-type-specific transcription and gene regulation. *Nat. Rev. Genet.* **11**, 549-558 (2010).

21. Tamura,T., Yanai,H., Savitsky,D. & Taniguchi,T. The IRF Family Transcription Factors in Immunity and Oncogenesis. *Annu. Rev Immunol* **26**, 535-584 (2008).

22. Wang,H. & Morse,H.C., III. IRF8 regulates myeloid and B lymphoid lineage diversification. *Immunol. Res.* **43**, 109-117 (2009).

23. Schiavoni,G. *et al.* ICSBP is essential for the development of mouse type I interferon-producing cells and for the generation and activation of CD8alpha(+) dendritic cells. *J Exp. Med.* **196**, 1415-1425 (2002).

24. Darnell,J.E.J., Kerr,I.M. & Stark,G.R. Jak-STAT pathways and transcriptional activation in response to IFNs and other extracellular signaling proteins. [Review] [97 refs]. *Science* **264**, 1415-1421 (1994).

25. Taniguchi,T., Ogasawara,K., Takaoka,A. & Tanaka,N. IRF family of transcription factors as regulators of host defense. *Annu. Rev. Immunol.* **19**, 623-655 (2001).

26. Sciammas,R. *et al.* Graded expression of interferon regulatory factor-4 coordinates isotype switching with plasma cell differentiation. *Immunity* **25**, 225-236 (2006).

27. Klein,U. *et al.* Transcription factor IRF4 controls plasma cell differentiation and class-switch recombination. *Nat. Immunol.* **7**, 773-782 (2006).

28. Aliberti,J. *et al.* Essential role for ICSBP in the in vivo development of murine CD8alpha + dendritic cells. *Blood* **101**, 305-310 (2003).

29. Tamura,T. & Ozato,K. ICSBP/IRF-8: its regulatory roles in the development of myeloid cells. *J Interferon Cytokine Res* **22**, 145-152 (2002).

30. Brustle,A. *et al.* The development of inflammatory T(H)-17 cells requires interferon-regulatory factor 4. *Nat. Immunol.* **8**, 958-966 (2007).

31. De Silva,N.S., Simonetti,G., Heise,N. & Klein,U. The diverse roles of IRF4 in late germinal center B-cell differentiation. *Immunol. Rev.* **247**, 73-92 (2012).

32. Bollig,N. *et al.* Transcription factor IRF4 determines germinal center formation through follicular T-helper cell differentiation. *Proc. Natl. Acad. Sci. U. S A* **109**, 8664-8669 (2012).

33. Schlitzer,A. *et al.* IRF4 Transcription Factor-Dependent CD11b(+) Dendritic Cells in Human and Mouse Control Mucosal IL-17 Cytokine Responses. *Immunity* **38**, 970-983 (2013).

34. Persson,E.K. *et al.* IRF4 Transcription-Factor-Dependent CD103(+)CD11b(+) Dendritic Cells Drive Mucosal T Helper 17 Cell Differentiation. *Immunity* **38**, 958-969 (2013).

35. Suzuki,S. *et al.* Critical roles of interferon regulatory factor 4 in CD11bhighCD8alpha-dendritic cell development. *Proc. Natl. Acad. Sci U. S. A* **101**, 8981-8986 (2004).

36. Kanno,Y., Levi,B.Z., Tamura,T. & Ozato,K. Immune cell-specific amplification of interferon signaling by the IRF-4/8-PU.1 complex. *J. Interferon Cytokine Res.* **25**, 770-779 (2005).

37. Hambleton,S. *et al.* IRF8 mutations and human dendritic-cell immunodeficiency. *N. Engl. J. Med.* **365**, 127-138 (2011).

38. Finn,R.D. *et al.* The Pfam protein families database. *Nucleic Acids Res.* **38**, D211-D222 (2010).

39. Landschulz,W.H., Johnson,P.F. & McKnight,S.L. The leucine zipper: a hypothetical structure common to a new class of DNA binding proteins. *Science* **240**, 1759-1764 (1988).

40. Lee,W., Mitchell,P. & Tjian,R. Purified transcription factor AP-1 interacts with TPA-inducible enhancer elements. *Cell* **49**, 741-752 (1987).

41. Chen,L., Glover,J.N., Hogan,P.G., Rao,A. & Harrison,S.C. Structure of the DNA-binding domains from NFAT, Fos and Jun bound specifically to DNA. *Nature* **392**, 42-48 (1998).

42. Vinson,C., Acharya,A. & Taparowsky,E.J. Deciphering B-ZIP transcription factor interactions in vitro and in vivo. *Biochim. Biophys. Acta* **1759**, 4-12 (2006).

43. Vinson,C. *et al.* Classification of human B-ZIP proteins based on dimerization properties. *Mol. Cell Biol.* **22**, 6321-6335 (2002).

44. Ise,W. *et al.* The transcription factor BATF controls the global regulators of class-switch recombination in both B cells and T cells. *Nat. Immunol.* **12**, 536-543 (2011).

45. Schraml,B.U. *et al.* The AP-1 transcription factor Batf controls T(H)17 differentiation. *Nature* **460**, 405-409 (2009).

46. Murphy,T.L., Tussiwand,R. & Murphy,K.M. Specificity through cooperation: BATF-IRF interactions control immune-regulatory networks. *Nat. Rev. Immunol.* **13**, 499-509 (2013).

47. Miller,J.C. *et al.* Deciphering the transcriptional network of the dendritic cell lineage. *Nat. Immunol.* **13**, 888-899 (2012).

48. Gautier,E.L. *et al.* Gene-expression profiles and transcriptional regulatory pathways that underlie the identity and diversity of mouse tissue macrophages. *Nat. Immunol.* **13**, 1118-1128 (2012).

49. de Brito,C. *et al.* CpG promotes cross-presentation of dead cell-associated antigens by pre-CD8alpha+ dendritic dells. *J Immunol* **186**, 1503-1511 (2011).

50. Sathe,P. *et al.* The acquisition of antigen cross-presentation function by newly formed dendritic cells. *J Immunol* **186**, 5184-5192 (2011).

51. King,I.L., Kroenke,M.A. & Segal,B.M. GM-CSF-dependent, CD103+ dermal dendritic cells play a critical role in Th effector cell differentiation after subcutaneous immunization. *J Exp. Med.* **207**, 953-961 (2010).

52. Landt,S.G. *et al.* ChIP-seq guidelines and practices of the ENCODE and modENCODE consortia. *Genome Res.* **22**, 1813-1831 (2012).

53. Kharchenko,P.V., Tolstorukov,M.Y. & Park,P.J. Design and analysis of ChIP-seq experiments for DNA-binding proteins. *Nat. Biotechnol.* **26**, 1351-1359 (2008).

54. Tao,H. *et al.* Purifying natively folded proteins from inclusion bodies using sarkosyl, Triton X-100, and CHAPS. *Biotechniques* **48**, 61-64 (2010).

55. Lee,T.I., Johnstone,S.E. & Young,R.A. Chromatin immunoprecipitation and microarray-based analysis of protein location. *Nat. Protoc.* **1**, 729-748 (2006).

56. Zhang,Y. *et al.* Model-based analysis of ChIP-Seq (MACS). *Genome Biol.* **9**, R137 (2008).

57. Heinz,S. *et al.* Simple combinations of lineage-determining transcription factors prime cis-regulatory elements required for macrophage and B cell identities. *Mol. Cell* **38**, 576-589 (2010).

58. Shortman,K. & Heath,W.R. The CD8+ dendritic cell subset. *Immunol Rev* **234**, 18-31 (2010).

59. Dignam,J.D., Lebovitz,R.M. & Roeder,R.G. Accurate transcription initiation by RNA polymerase II in a soluble extract from isolated mammalian nuclei. *Nucleic Acids Res.* **11**, 1475-1489 (1983).

Chapter 4 L-Myc is selectively expressed by dendritic cells and required for T-cell priming

The contents of this chapter have been previously published in *Nature*.
KC W, Satpathy AT, Rapaport A, Briseño CG, Wu X, Albring JC, Russler E, Kretzer NM, Persaud SP, Edelson BT, Loschko J, Cella M, Allen PM, Nussenzweig MC, Colonna M, Sleckman BP, Murphy TL, Murphy KM. L-Myc is selectively expressed by dendritic cells and required for T-cell priming during infections. *Nature*. 2014 Mar 13: 507(7491):243-7

4.1 Abstract

The proto-oncogenes *Myc* and *Mycn* encode transcription factors that regulate cellular growth in normal and pathologic settings[1,2], and their genetic ablation causes early embryonic lethality[3,4]. A third paralog, *Mycl1*, is dispensable for normal development[5] and its biological activity remains undefined[6]. We found that *Mycl1* was expressed selectively in the immune system by dendritic cells (DCs), which were in cell cycle but lacked expression of c-Myc and N-Myc. Using a newly targeted *Mycl1*^{gfp} allele, we found that L-Myc expression was controlled by IRF8 in multiple DC lineages and was initiated during development at the common DC progenitor (CDP) stage concurrent with loss of c-Myc expression. In mature DCs, L-Myc protein persisted in the presence of inflammatory signals, such as GM-CSF, and was necessary for normal proliferation and survival at steady state. L-Myc deficiency caused variable reductions in DC populations with the greatest effect on splenic CD8α^+ DCs and lung CD103$^+$ DCs, which revealed the differential homeostatic requirements for the DC lineage based on tissue site. Notably, L-Myc-deficient DCs were considerably smaller after *ex vivo* activation, which was caused in part by a significant reduction in the expression of eukaryotic translation initiation factor 1 (*eif1*) and the mitochondrial respiratory chain complex I subunit NADH dehydrogenase(ubiquinone) Fe-S protein 5 (*Ndufs*5).

In addition, loss of L-Myc modestly impaired expansion of CD8α^+ classical DCs (cDCs) after infection by *Listeria monocytogenes*[7,8] and significantly decreased *in vivo* T-cell priming to bacterial and viral infections by a T-cell extrinsic mechanism. Lastly, L-Myc-deficient mice were highly resistant to lethal *Listeria* challenge by intravenous route because of an impaired cell-intrinsic capacity of CD8α^+ DC to support viable growth of the bugs. However, ciritical

innate functions of DCs (such as IL-12 production in response to *Toxoplasma gondii* and IL-23 production to *Citrobacter rodentium*) were intact in L-Myc deficient mice. Thus, the switch from c-Myc to L-Myc in DCs may represent a strategy to preserve Myc activity in the setting of inflammation required for eliciting maximal T-cell responses[9]. Our study of the physiologic activities of L-Myc suggests that it functions comparably and affects similar cellular processes as c-Myc and N-Myc.

4.2 Introduction

4.2.1 Dendritic cells closely resemble other myeloid lineages in terms of anatomical location, surface phenotype, and cellular origin.

Distinguishing DCs from other myeloid and lymphoid lineages has been a constant problem in the field and has led to inaccurate conclusions about the specific activities of DC subsets [10-12]. This is due in part to the heavy reliance of sensitive but not specific surface markers, such as the CD11c (also known as αX integrin) and major histocompatibility complex, class II, (MHCII). Unlike T cells and B cells, DCs do not uniquely express a single receptor that is absolutely required for their development and can further be used for unequivocal identification. Although adequate genetic tools exist for tracking and deleting DCs, many of these mouse models manifest nonspecific or off target effects that greatly complicate any conclusions derived from their use. Until recently, most genetic tools to study DC populations exploited cell surface markers (*Cd11c*, *CD11b*, *Lysm*, *Csf1r*, and *Cx3cr1*)[13-15], which likely explains their lack of selectivity. Recently several large-scale transcriptome analyses of DCs and the closely related monocytes and macrophages have identified signature transcription factors for

each lineage, leading to a recommendation that transcription factors be used to carefully segregate DCs from macrophages[16,17]. As proof of concept, the BTB-ZF family member *Zbtb*46 was shown to specifically mark DCs in both lymphoid and peripheral tissues[18]. While *Zbtb46* represents an important tool, other mouse models are still needed to expand on this work and validate the conclusions made from these initial studies. Our own comparative microarray analysis has revealed the highly specific expression of *Mycl1* in the DC lineage.

4.2.2 Myc family of proto-oncogenes

The Myc family of proto-oncogenes (c-Myc, N-Myc, L-Myc) regulates many basic cellular processes such as proliferation, growth, metabolism, and death in both normal and pathologic settings[1,2,19]. Myc's capacity to affect broad cellular programs is a consequence of its occupancy of many genomic loci and subsequent activity in releasing paused RNA polymerase II complexes from proximal promoters[20]. This activity is quite distinct from most specific transcription factors, which function instead to regulate transcriptional initation rather than elongation. Thus, the Myc gene family is indispensable in all tissues undergoing rapid cellular growth and renewal. Moreover, the importance of this gene family is clearly evidenced by the frequent rate of mutations (insertions, translocations, amplifications) discovered among Myc family members in a diverse set of cancers; moreover, ablations of either c-Myc or N-Myc lead to early embryonic lethality (E9.5 or E10.5) because of multi-organ hypoplasia[3,4]. Surprisingly, the deletion of L-Myc revealed no gross abnormality or phenotype, which was presumed to be a consequence of compensation by the other Myc family members. Indeed, some investigators have even proposed that L-Myc represents an evolutionary dead-end among the Myc family members. However, the idea of L-Myc as a *bona fide* Myc factor has received renewed attention

with the demonstration that L-Myc reprograms fibroblasts into induced pluripotent stem cells more efficiently than c-Myc and L-Myc may play a role in β-cell dedifferentiation. In physiologic and malignant hematopoietic settings, FLT3 signaling leads to c-Myc induction via STAT-dependent pathways[21,22]. Therefore, the selective expression of L-Myc and concomitant absence of c-Myc in DCs is unexpected and requires further investigation.

4.2.3 Dendritic cells are short lived and require constant replenishment from bone marrow progenitors

A simple model of development posits that cellular intermediates or progenitors progressively lose the capacity to proliferate as undergo terminal differentiation. Yet this appears to be an oversimplification in the DC lineage, as a large fraction of DCs is actively dividing [23-25]. Almost all cDCs and pDCs turnover within 7-10 days; and the CD8α^+ DC has the shortest half-life of 3 days whereas pDCs are the longest lived. The relatively high capacity of DCs to proliferate *in situ* is one proposed mechanism by which homeostatic renewal is thought to occur. Although these early kinetic studies (i.e., BrdU labeling and parabiosis) provided descriptive insight into DC turnover, the downstream effector molecules controlling growth and survival were largely undefined. Elucidating the transcription factors affecting DC turnover will provide a more complete picture of the pathways controlling immune responses. For example, artificially extending the half-life of DCs leads to autoimmunity[26]. We therefore hypothesized that the rapid turnover and growth of DCs is in part controlled by some Myc factor.

4.3 Results

4.3.1 *Mycl1* is selectively expressed in cDCs, pDCs and committed DC progenitors

To identify DC-specific transcription factors (i.e., expressed in cDCs and pDCs), we purified several myeloid precursors (GMP and CMP/MDP) and the earliest committed DC-progenitor (CDP) (Figure 4.1 **A**), and performed microarray analysis in a manner similar to the approach previously used to identify the cDC-specific factor *Zbtb46* [18]. Using a pared down list of Pfam[27] annotated transcription factors with a linear expression of at least 100 in the CDP, we compared CDPs versus CMP/MDP and all DCs with an extensive panel of hematopoietic and non-hematopoietic cell types[28]. Interestingly, this approach identified several well-known DC transcriptional regulators such as *Irf8*, *Id2*, and *Klf4*[29-32] and a poorly characterized *Myc* paralog called *Mycl1*(Figure 4.1 **B**). To date, *Mycl1* expression has been reported in the central nervous system and small cell lung cancer[33-36]. We quantitated *Mycl1* expression by qPCR from splenic lymphoid and myeloid populations and observed detectable amounts in only DC subsets (Figure 4.1 **C**).

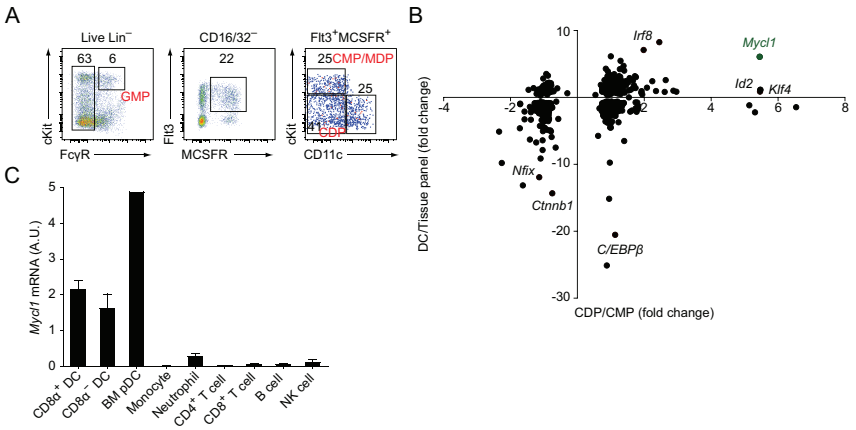

Figure 4.1: Mycl1 is selectively expressed in DCs

(A) WT BM cells stained with the indicated markers. (B) Microarray analysis of indicated populations. For each transcription factor, fold change was obtained and plotted based on the two comparisons indicated. Each dot indicates an individual probe set. (C) Relative amount of Mycl1 mRNA was determined by qPCR. Shown is a graph of Mycl1 values normalized to Hprt values (bar, SD; n=3 biological replicates per cell type).

4.3.2 c-Myc and N-Myc are not expressed in mature DC subsets

c-Myc and N-Myc are expressed in the hematopoietic compartment and play growth promoting roles in early progenitors and mature myeloid and lymphoid populations [37-42]. Laurenti and colleagues previously reported that *Mycl1*expression is absent in hematopoietic lineages; however, this study failed to include DC progenitors or DCs in the analysis. We therefore determined the expression pattern of all three Myc factors in progenitors and mature DC subsets. *Myc* was highly expressed by early hematopoietic progenitors but was significantly reduced in mature DCs (Figure 4.2 **A, left panel**). Like *Myc*, *Mycn* was highly expressed in hematopoietic stem cells (HSCs), multipotent progenitors (MPPs) and common lymphoid progenitors (CLPs), but was absent from DC progenitors and mature DCs (Figure 4.2 **A, middle**

panel). In contrast, we observed that *Mycl1* was expressed by CDPs, by committed precursors to cDCs[43,44] (pre-cDCs) and by mature splenic DCs (Figure 4.2 **A, right panel**). Interestingly, we observed a similarly conserved expression pattern of Myc factors in human hematopoietic lineages[45,46](Figure 4.2 **B, left panel**).

The absence of c-Myc from DCs caused us to evaluate the local proliferation of DCs[47] relative to other c-Myc-positive lineages. First, we used a 4-hour *in vivo* 5'-bromo-2'-deoxyuridine (BrdU) labeling assay to evaluate mature DC proliferation in relation to other myeloid and lymphoid populations (Figure 4.2 **C**). In contrast to B cells, monocytes and neutrophils, which showed ~1% BrdU uptake, splenic cDC subsets showed 4-8% BrdU uptake (Figure 4.2 **C**), in agreement with previous reports[25,47]. In addition, 4-7% of cDCs were in S/G2/M phase as determined by DAPI staining and between 17-34% of cDCs were in cell cycle as deteremined by Ki67 staining (Figure 4.2 **D**). Although splenic pDCs had little proliferative capacity (Figure 4.2 **B**), consistent with published findings[25], we observed a significant proportion of bone marrow (BM) pDCs in S/G2/M phase by DAPI staining (Figure 4.2 **E**), suggesting that tissue microenvironment can influence the proliferation state of DCs.

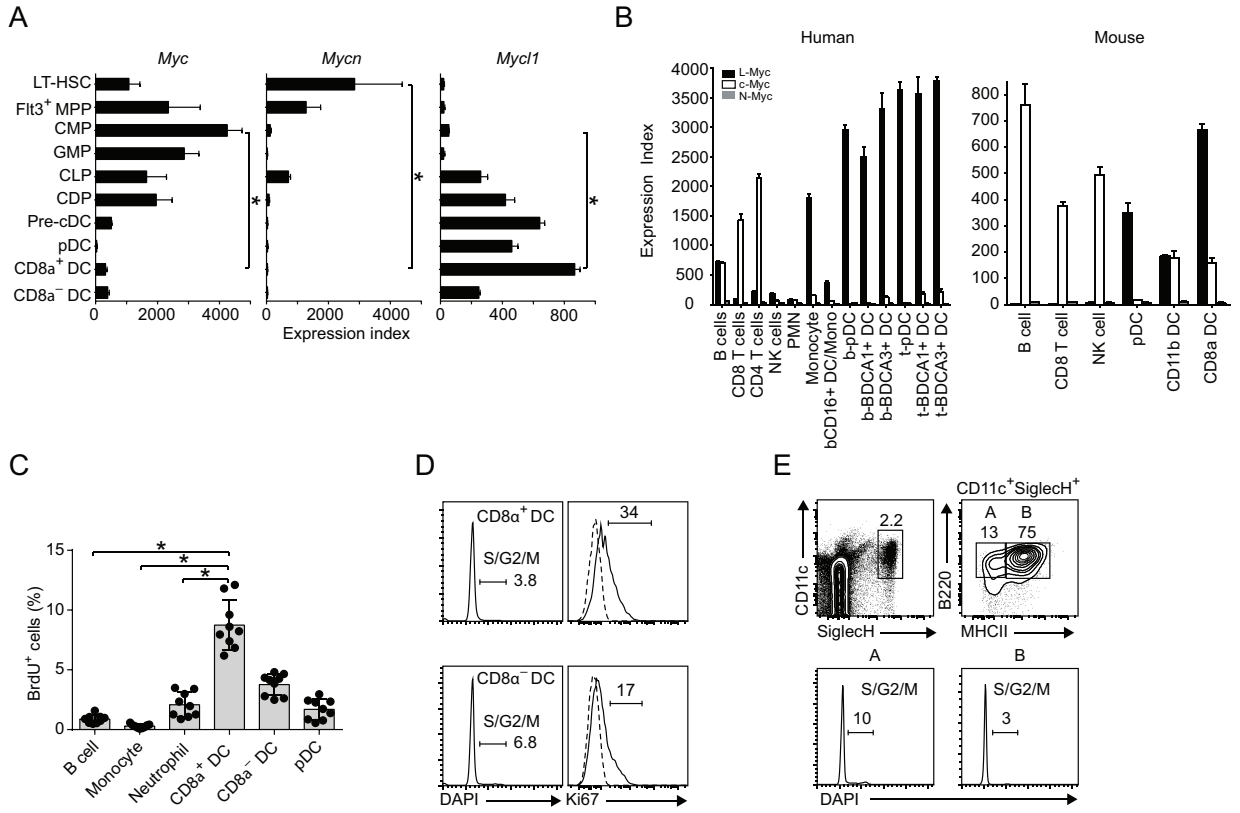

Figure 4.2: c-Myc and N-Myc are not expressed in mature DCs

(A) Shown are mean expression values for *Myc*, *Mycn*, and *Mycl1* for the indicated populations (bars, SD; n = 2-4 microarrays from biological replicates, one-way ANOVA Tukey's *post hoc* test). (B) Shown is the mean expression value of *Mycl1* mRNA in the indicated cell types purified from humans and mice. (C) The indicated lineages were stained for intracellular BrdU incorporation as described in Methods. Shown is the percent of $BrdU^+$ cells within each indicated lineage from individual mice. Data are from 2 independent experiments (bars, SD; n = 9 mice per group, one-way analysis of variance (ANOVA) Tukey's *post hoc* test). (D) DC populations stained for DNA content with DAPI and Ki67 expression. Dotted lines represent isotype control staining. Numbers represent percent of cells in the indicated gate. Data are representative of 3 independent experiments. (E) BM pDCs (gated as $CD11c^+SiglecH^+B220^+$) were separated into $MHCII^-$ (A) and $MHCII^+$ (B) fractions by cell sorting. Both A and B were then stained for DNA content with DAPI.

4.3.3 *Mycl1*^{gfp} expression is coincident with the loss of c-Myc transcript and protein

Mycl1 encodes 368 amino acids, and the protein contains an N-terminal *trans*-activating domain (TAD) and a C-terminal DNA binding domain (basic-helix-loop-helix structure). [35,48,49]. The genomic context comprises two exons (Supplementary Figure 4.1 **A**) with exon 1 encoding the 5' untranslated region (UTR) and 165 amino acids of the TAD. Our targeting strategy replaces the coding sequence immediately downstream of the 5' UTR with an enhanced GFP reporter cassette followed by a SV40 poly-adenylation sequence. The newly targeted genomic configuration, *Mycl1*^{gfp}, contains an inactive *Mycl1* but preserves promoter activity, allowing for detection of its expression (Supplementary Figure 4.1 **B-D**).

These above observations suggested that the induction of L-Myc expression was coincident with the loss of c-Myc and N-Myc (see previous section). To characterize the transition from c-Myc to L-Myc expression in the DC lineage with single-cell resolution, we examined mice carrying a *Myc*^{gfp} reporter allele encoding a GFP-c-Myc N-terminal fusion protein[50] and mice harboring our newly targeted *Mycl1*^{gfp} allele. We found that c-Myc protein was highly expressed in Flt3^{+} common myeloid progenitors[51] (CMPs), nearly extinguished in CDPs and pre-cDCs (Figure 4.3 **A and B**) and undetectable in mature splenic DCs (Figure 4.3 **C and D**). In contrast, *Mycl1*^{gfp} expression was absent in CMPs, became detectible in CDPs and increased in pre-cDCs (Figure 4.3 **A and B**). *Mycl1*^{gfp} was highly expressed in all mature splenic DC subsets (CD8α^{+} cDCs, CD8α^{-} cDCs, and pDCs) but was undetectable in neutrophils, monocytes, red pulp macrophages, NK cells and T and B cells (Figure 4.3 **C-E**), consistent with endogenous *Mycl1* mRNA measurements (Figure 4.1 **C**). All DC subsets developed in *Mycl1*$^{gfp/gfp}$ (L-Myc-deficient) mice without compensatory induction of *Myc* expression (Figure 4.3 **E,** Supplementary Figure 4.1 **E, right panel**). *In vitro*, *Mycl1*^{gfp} expression was observed in

Flt3 ligand (Flt3L)-treated BM cultures (Supplementary Figure 4.2 **A and B**). Overexpression of c-Myc in Flt3^{+} CMPs significantly reduced the proportion of cDCs and pDCs in Flt3-ligand (FLT3L) cultures, whereas overexpression of L-Myc produced no apparent defects (Supplementary Figure 4.2 **C and D**). These results suggest that L-Myc does not regulate the differentiation of mature DCs per se but may instead serve a non-redundant homeostatic role.

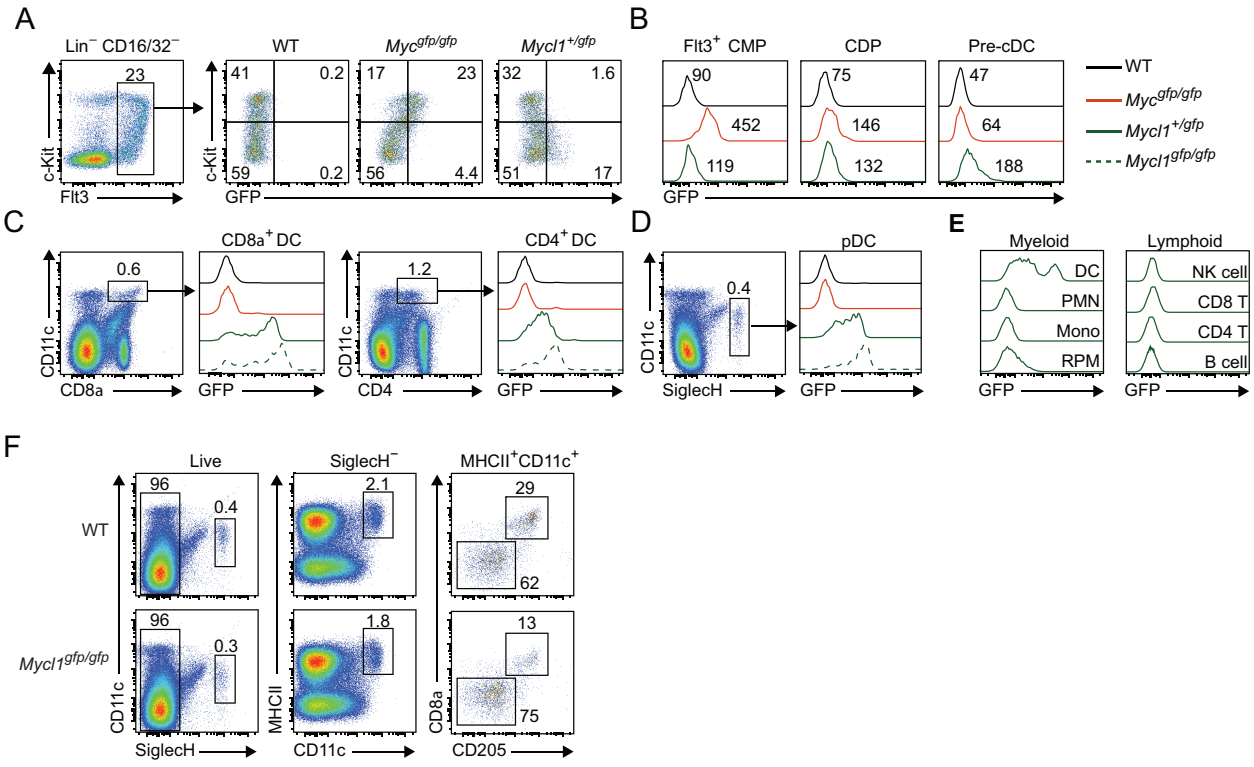

Figure 4.3: Mycl1 expression is coincident with loss of c-Myc expression

Histogram of GFP expression for Flt3^{+} progenitors from the indicated mice. Numbers represent percent of cells in the indicated gate. (B) CMP (left panel), CDP (middle panel), Pre-cDC (right panel). Numbers represent mean fluorescent intensities. (C-D) Cells from indicated mice were stained to identify CD8α^{+} DCs, CD4^{+} DCs, and pDCs. Histograms of GFP expression. (E) Mycl1$^{+/gfp}$ (solid green line) splenocytes were stained for myeloid (left panel) and lymphoid (right panel) populations. Histograms of GFP expression for DCs, neutrophils (PMN), monocytes (mono), red pulp macrophages (RPM), NK cells (NK cell), CD8 T cells (CD8 T), CD4 T cells (CD4 T) and B cells. (F) Histogram showing frequency of pDCs, CD8α^{+} DCs, and CD8α^{-} DCs. Data are representative of at least 5 independent experiments.

4.3.4 *Mycl1*^{gfp} expression marks the DC lineage in lymphoid and peripheral tissues

The tissue microenvironment and genetic background can be an important determinant of DC homeostasis[7,52,53]. Thus, we extended our comparison between *Myc*^{gfp} and *Mycl1*^{gfp} expression across numerous lymphoid and peripheral tissues. In tissues other than spleen, we observed a similar pattern of *Mycl1*^{gfp} expression even though DCs are known to incorporate BrdU at different rates[54]. In inguinal and mesenteric lymph nodes, *Mycl1*^{gfp}, but not *Myc*^{gfp}, was expressed by pDCs and by migratory and resident cDCs (Figure 4.4 **A,** Supplementary Figure 4.3 **A and B**). In the lung, liver, and dermis, *Mycl1*^{gfp} was expressed predominantly by CD11b^{-} cDCs, but, in the small intestine, *Mycl1*^{gfp} was expressed by CD11b^{+} and CD11b^{-} cDCs (Figure 4.4 **B**). *Mycl1*^{gfp} expression was absent in tissue macrophages, which can renew locally and proliferate in response to signals such as IL-4[55,56], suggesting that L-Myc expression can be used to distinguish DCs from closely related macrophage populations (Supplementary Figure 4.3 **C**).

To obtain a more complete profile of *Mycl*^{gfp} expression, we characterized the distribution and anatomical location of GFP-positive DCs in lymphoid and peripheral tissues. By histology, *Mycl1*^{gfp} was found in stellate cells within T-cell zones in spleen and lymph nodes and in scattered cells within B cell follicles and the splenic red pulp (Figure 4.4 **C**, Supplementary Figure 4.4**a-e**). *Mycl1*^{gfp}-expressing cells were sparsely present within the sub-capsular sinus of inguinal lymph nodes where *Zbtb46*$^{+}$ cDCs are known to reside[18] (Figure 4.4 **B,** Supplementary Figure 4.4 **B**). In addition, *Mycl1*^{gfp} was expressed by CD4^{-}B220^{-} cells in small intestinal lamina propria, inside villi and within Peyer's patches (Figure 4.4 **C,** Supplementary Figure 4.4 **D**). *Mycl1*^{gfp} expression was not apparent in stromal cells such as fibroblasts, and unlike *Zbtb46*, was undetected in vascular endothelium (Supplementary Figure 4.4 **E, F**). Thus, *Mycl*^{gfp} expression uniquely identifies DCs in both lymphoid and non-lymphoid peripheral tissues.

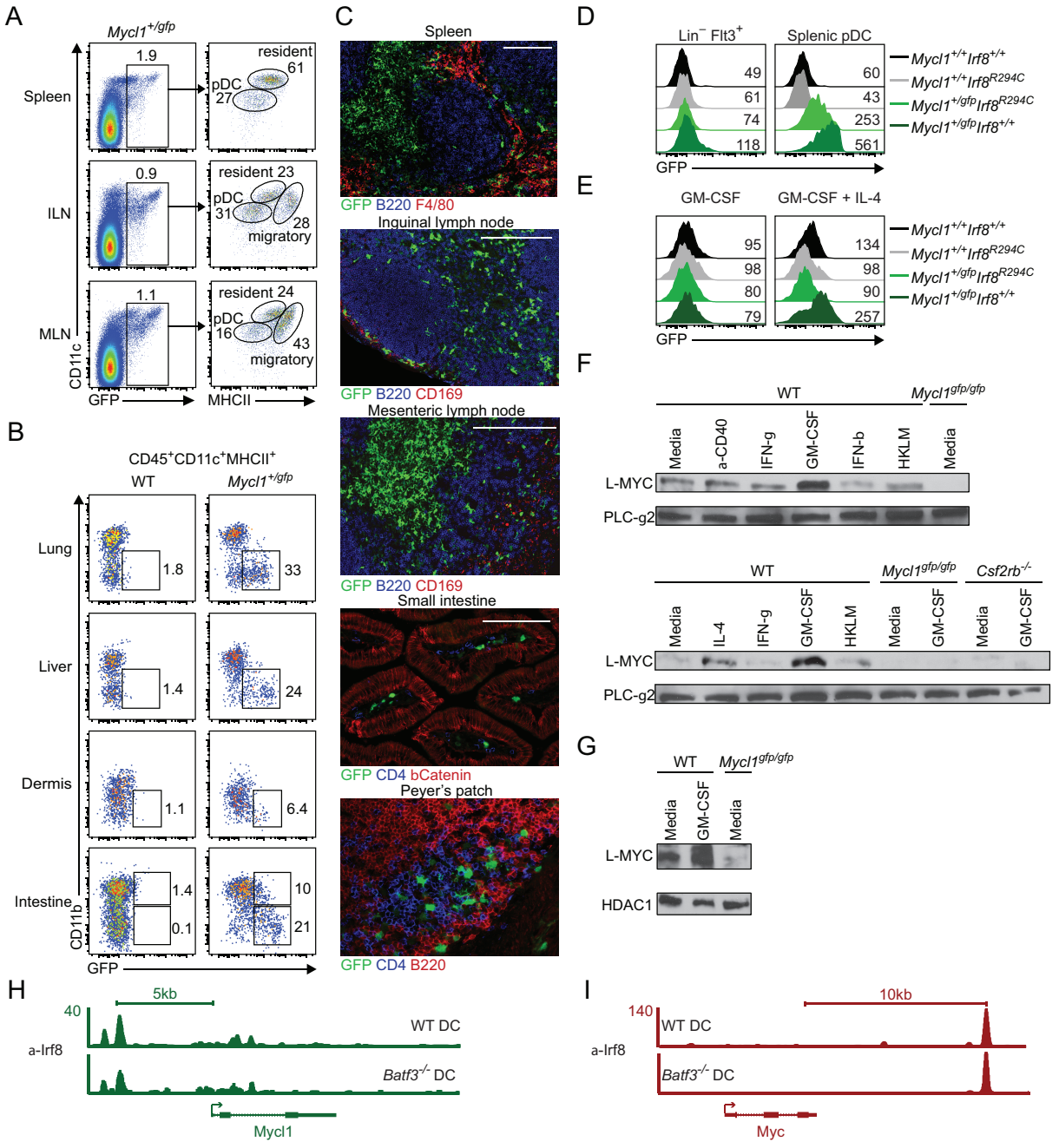

Figure 4.4: Mycl1 expression is restricted to DCs in lymphoid and peripheral tissues and is regulated by IRF8 and GM-CSF

(A) Spleen, inguinal lymph node (ILN), and mesenteric lymph node (MLN) cells of Mycl1$^{+/gfp}$ mice were stained for analysis. GFP^{+} cells are further gated as pDCs, resident DCs, or migratory DCs. Numbers represent percent of cells in the indicated gate. (B) Cells from lung, liver, dermis, and small intestine (intestine) of WT and Mycl1$^{+/gfp}$ mice were stained. Histograms of

CD11b and GFP expression for indicated cells is shown. (C) Tissue sections from Mycl1$^{+/gfp}$ mice were prepared for analysis by fluorescence microscopy. The stain for each tissue is indicated above the picture. (D) BM cells and splenocytes from indicated mice were stained for analysis. Histograms of GFP expression for lineage-negative Flt3^{+} progenitors and splenic pDCs. (E) BM monocytes were isolated from indicated mice and differentiated for 4 days with either GM-CSF (left panel) or GM-CSF and IL-4 (right panel). Histograms of GFP expression. (F) BM cells from indicated mice were cultured for 9 days in Flt3 ligand (Flt3L) and treated with media, anti-CD40 antibody (a-CD40), interferon gamma (IFN-g), granulocyte-macrophage colony-stimulating factor (GM-CSF), interferon beta (IFN-b), heat-killed Listeria monocytogenes EGD (HKLM), or interleukin 4 (IL-4) for 24 hours. Whole-cell extracts were prepared and Western blot analysis was performed. Shown are immunoblots for L-MYC (top) and PLC-g2 (bottom) from the indicated treatments. (G) BM cells from indicated mice were cultured for 9 days in Flt3L and treated with media or GM-CSF for 24 hours. Nuclear extracts were prepared and Western blot analysis was performed. Shown are immunoblots for L-MYC (top) and HDAC1 (bottom). (h-i) Gene tracks for IRF8 binding to the Mycl1(h) and Myc (i) genomic regions (20-kb window) in Flt3L-derived DCs from WT (top panel) or Batf3$^{-/-}$ (bottom panel) mice. The transcript configuration below each track is shown as depicted in the UCSC Browser. Numbers represent number of normalized reads. FACS data are representative of at least 5 independent experiments

4.3.5 IRF8 induces *Mycl1* expression in multiple DC subtypes and GM-CSF stabilizes L-Myc protein

In common myeloid progenitors (CMPs) and all-lymphoid progenitors (ALPs), which give rise to DCs, loss of the transcription factor IRF8 results in a decreased abundance of *Mycl1* transcript[57]. We found that *Mycl1*^{gfp} expression was absent in DC progenitors and significantly reduced in pDCs isolated from *Irf8*^{R294C} mice[58], which harbor a point mutation that abrogates IRF8 interactions with the transcription factor PU.1 (Figure 4.4 **D**, Supplementary Figure 4.5 **A**). Moreover, DCs differentiated from Ly6C^{hi} monocytes in the presence of IL-4 and GM-CSF[18,59,60] also induced *Mycl1*^{gfp} expression in WT cultures but not in *Irf8*^{R294C} cultures (Figure 4.4 **E**, Supplementary Figure 4.5 **B**). Using an L-Myc-specific antibody (Supplementary Figure 4.5 **C**), we found that L-Myc protein was maintained in cDCs under various inflammatory conditions, which included treatment with IFN-β or IFN-γ (Figure 4.4 **F**). In addition, L-Myc protein was increased by treatment with GM-CSF (Figure 4.4 **F and G**). ChIP-Seq analysis

identified several genomic regions enriched for IRF8 binding across the *Mycl1* and *Myc* loci. These binding occurrences did not require IRF8 interactions with the transcription factor BATF3 (Figure 4.4 **H and I**). Together, these results support a role for IRF8–PU.1 interactions, as opposed to IRF8–BATF3 interactions[61], in the direct regulation of *Mycl1* transcription; and indicate that L-Myc protein levels vary in response to activating signals, which is analogous to the regulation of c-Myc protein[62-64].

4.3.6 L-Myc regulates the growth and survival of CD8α$^+$ cDCs and pDCs

Next, we characterized the effect of L-Myc deficiency on DC homeostasis at steady state. In lymphoid and peripheral tissues, loss of L-Myc decreased the total number and relative frequency of DCs, and based on the analysis of competitive mixed BM chimeras, we found that these defects were due to cell-intrinsic mechanisms (Figure 4.5 **A-C,** Supplementary Figure 4.6**A-G**). The largest defect was observed in CD103$^+$CD11b$^-$ cDCs in the lung, an organ rich in GM-CSF[65]. A recent report concluded that GM-CSF is important for the survival of lung CD103$^+$ DCs [66]. In WT mice, CD103$^+$CD11b$^-$ cDCs in the lung showed higher expression of *Mycl1* and greater proliferative capacity as measured by Ki67 as compared to migratory CD103$^+$CD11b$^-$ cDCs from draining lymph nodes (Supplementary Figure 4.6 **H and I**). Using Gene Set Enrichment Analysis (GSEA)[67], a computational method for determining whether an *a priori* set of genes shows a statistically significant difference between two populations, we observed significant enrichment for cell-cycle–related transcripts in lung CD103$^+$CD11b$^-$ cDCs as compared to migratory CD103$^+$CD11b$^-$ cDCs from draining lymph nodes (Supplementary Figure 4.6 **J**). Thus, variations in the abundance of cell-extrinsic factors such as GM-CSF in the

local tissue microenvironment result in different homeostatic requirements for resident DCs that are revealed by the loss of L-Myc.

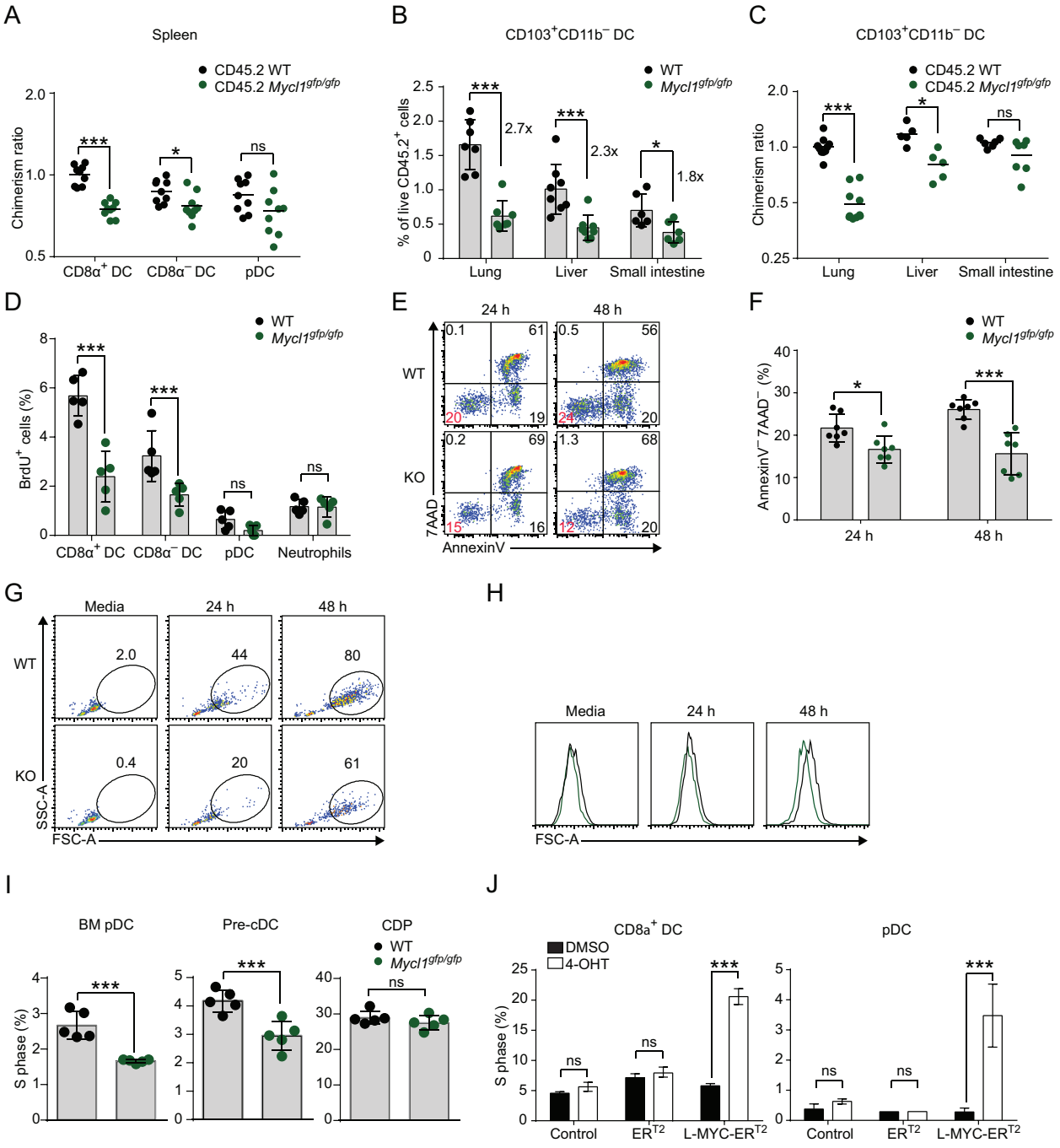

Figure 4.5: L-Myc regulates the growth and survival of DCs

(A) Mixed BM chimeras were generated as described in Methods. Splenocytes and peripheral blood cells were analyzed for relative donor contribution 8-10 weeks following lethal irradiation and transplant. Shown is the contribution of CD45.2$^+$ WT BM or CD45.2$^+$ Mycl1$^{gpf/gfp}$ BM to the indicated DC subset as a ratio of peripheral blood neutrophils (PMN) from the same animal (% CD45.2$^+$ contribution in DC / % CD45.2$^+$ in PMN). Data are representative of 3 independent experiments (bar, SD; n=9, Mann-Whitney U test). (B) CD103$^+$CD11b$^-$ DCs from lung, liver, and small intestine were quantitated as a percentage of live CD45.2$^+$ hematopoietic cells. Data are representative of 3-4 independent experiments (bar, SD; n=5-7, two-way ANOVA Holm-Sidak post hoc test). (C) Shown is the contribution of CD45.2$^+$ WT BM or CD45.2$^+$ Mycl1$^{gpf/gfp}$ BM to CD103$^+$CD11b$^-$ DCs in the indicated peripheral tissues as a ratio of peripheral blood neutrophils from the same animal. Data are representative of 3 independent experiments (bar, mean; n=5-9, Mann-Whitney U test). (D) Splenocytes were harvested 1 hour after BrdU injection. BrdU$^+$ cells within each indicated lineage from individual mice is shown. (bar, SD; n = 5 mice per group, Student's t-test). (E) Sorted pDCs were cultured in imiquimod for 24 hours (24 h, left panel) and 48 hours (48 h, right panel). Cells stained with 7AAD and AnnexinV to assess viability. Histograms depicting live cells (7AAD-AnnexinV-), early apoptotic cells (7AAD-AnnexinV+), and late apoptotic or necrotic cells (7AAD+AnnexinV+). (F) Quantitation of live pDCs from (E) (bar, SD; n = 7 biological replicates, Student's t-test). (G) Shown is a two-color histogram of side scatter (SSC-A) and forward scatter (FSC-A) for pre-gated live pDCs (7AAD-AnnexinV-) from media treated or imiquimod treated wells (24 h and 48 h). (H) Sorted CD8α^+ DCs were cultured in GM-CSF for the indicated time points. Histogram of FSC-A for live cells. (I) BM CDPs, pre-cDCs, MHCII- pDCs cultured in Flt3L for 24 h. Wells were pulsed with 10mM BrdU for the last 4 hours of culture. Shown is the percent of cells in S phase. Data are representative of 2-3 experiments (bar, SD; n = 5, Student's t-test). (J) BM cells from WT mice were cultured in Flt3L and infected on day 4 with a retrovirus expressing ERT2 or the L-MYC-ERT2 fusion protein and then cultured for an additional 6 days. Cells were harvested and purified into subsets as CD11c+ MHCII+ CD24+Sirp-a- (CD8a+ DC, left panel) or CD11cint SiglecH+ (pDC, right panel) by cell sorting. Infected and uninfected (control) cells were treated with vehicle (DMSO) or 100 nM 4-hydroxytamoxifen (4-OHT) for 24 hours in 100 ng/ml Flt3L, pulsed with BrdU for the last 4 hours and stained for intracellular BrdU incorporation. Shown is the percent of cells in S phase (bar, SD; n=4 independent retroviral transductions, two-way ANOVA Holm-Sidak post hoc test). *, $p<0.05$, **, $p<0.01$, ***, $p<0.001$, ns, $p>0.05$.

4.3.7 L-Myc regulates growth-related genes in CD8α^+ DCs and pDCs

Using gene expression microarrays, we found that L-Myc deficiency produced changes in gene expression that were distinct among pDCs, CD8α^+ cDCs, and CD8α^- cDCs (Supplementary Figure 4.7 **A and B**) at steady sate. In BM pDCs and splenic CD8α^+ cDCs, we observed target

genes associated with cellular proliferation and apoptosis (Supplementary Figure 4.7 **C**). Thus, we analyzed local DC proliferation *in vivo* and assayed survival after *ex vivo* activation of DCs. BrdU labeling *in vivo* showed a 50% decrease in local proliferation of splenic CD8α$^+$ cDCs in L-Myc-deficient mice relative to WT mice (Figure 4.5 **D**). Loss of L-Myc also decreased the size of splenic CD8α$^+$ cDCs and pDCs following GM-CSF treatment and toll-like receptor 7 (TLR7) activation, respectively (Figure 4.5 **E-H**). In the BM, L-Myc-deficient pDCs and pre-cDCs proliferated less in response to Flt3L than WT populations, as measured by the proportion of cells in S phase (Figure 4.5 **I**). However, L-Myc deficiency had no effect on CDP proliferation (Figure 4.5 **I**, Supplementary Figure 4.8 **A**). Using a tamoxifen-activated form of L-Myc (L-MYC-ER^{T2} fusion protein), we found that activation markedly and specifically increased the proliferation of CD8α$^+$ cDCs and pDCs expressing L-MYC-ER^{T2} (Figure 4.5 **J**, Supplementary Figure 4.8 **B and C**). Thus, in the absence of c-Myc or N-Myc, L-Myc can regulate DC proliferation and survival following activation.

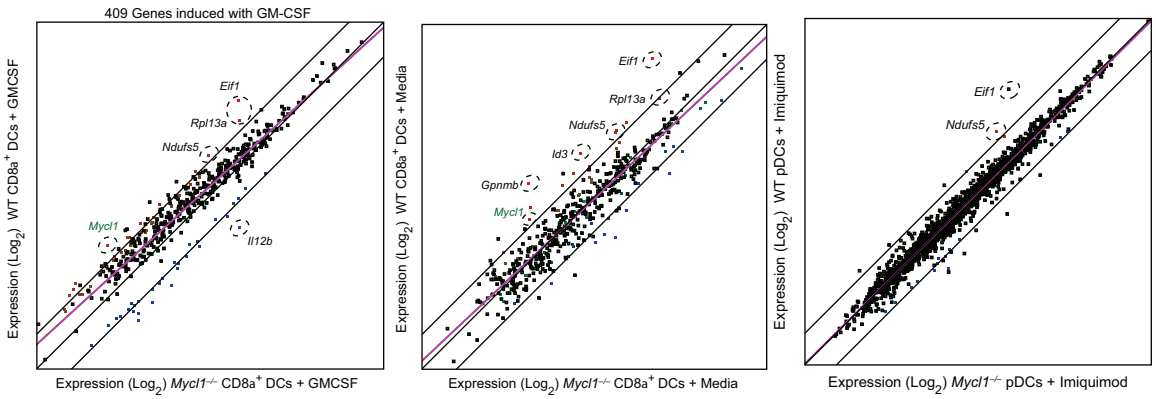

Figure 4.6: Gene expression analysis of L-Myc deficient CD8α$^+$ DCs and pDCs following activation

DCs were sorted from WT and Mycl1$^{-/-}$ mice treated with Flt3L and then cultured *in vitro*. RNA was purified and microarray analysis performed as described in Methods. M-Plots comparing the $\log_2$ transformed expression values of 409 GM-CSF inducible genes between WT (y axis, n = 3 biological replicates) and Mycl1$^{-/-}$ (x axis, n = 3 biological replicates) CD8α$^+$ DCs (left and

middle panels); and of all genes between WT (y axis, n = 3 biological replicates) and Mycl1$^{-/-}$ (x axis, n = 3 biological replicates) pDCs treated with imiquimod (right panel).

Recently, several reports have demonstrated that *Myc* influences the transcription of many genomic loci by mediating the release of paused RNA pol II complexes[68-70]. We asked whether the induction of 409 genes following GM-CSF was impaired in L-Myc deficient mice. We observed most inducible genes to be more highly enriched in WT vs KO, which was specific to treatment as this set showed no difference when compared with media treated DCs (Figure 4.6 **A and B**). Interestingly, some genes remained different between WT and KO despite showing no increase with GM-CSF. This list included *Eif1*, *Rpl13a*, and *Ndufs5*. Eukaryotic translation initiation factor 1 facilitates tRNA binding to the ribosome by stabilizing a conformation change in the small (40S) ribosomal subunit that opens the mRNA binding channel[71]. We also observed a similar reduction in *Eif1* and *Ndufs5* in pDCs activated with imiquimod; although in pDCs *Eif1* levels increased following treatment (Figure 4.6 **C)**. These data suggest that L-Myc can regulate the expression of many genomic loci and also modulate the expression of genes involved in controlling protein synthesis similar to c-Myc [72].

4.3.8 *Mycl1* is dispensable for the innate effector functions of DCs to *Toxoplasma gondii* and *Citrobacter rodentium*

Initially recognized for the superior capacity to prime adaptive immune responses, DCs are now known to mediate several key innate effector responses. For example, the CD8α^+ DC and the related CD103$^+$ DC sense infection by *Toxoplasma gondii* and are the critical source of IL-12 necessary for early host resistance[73]. Conversely, the Notch2-dependent intestinal CD11b$^+$ cDCs are the obligate source of IL-23 required for survival after infection with *C. rodentium,* a

model for attaching-and-effacing bacterial infections[74]. Interestingly, the only perihperal site where $CD11b^+$ DCs express detectible amounts of *Mycl1* is the small intestine lamina propria. We asked whether L-Myc played a role in these innate effector responses.

I.P. infection by tachyzoites of the type II avirulent Prugniaud (Pru) strain of *T. gondii* led to complete lethality of $Batf3^{-/-}$ mice relative to WT and $Mycl1^{-/-}$ mice (Figure 4.7 **A**). We also observed no difference in parasite burden at three different time points (Figure 4.7 **B**). These data confirm that L-Myc-deficient $CD8\alpha^+$ DCs sense and respond appropriately to *T. gondii* infection. Next, we infected mice with *C. rodentium* and monitored mice for weight loss and survival. As expected, conditional deletion of Notch2 led to rapid weight loss and complete lethality by 10 days. L-Myc-deficient mice displayed no weight loss and survived the infection for the duration of the experiment (Figure 4.7 **C and D**). These data suggest that L-Myc is dispensable for the innate effector functions of DCs.

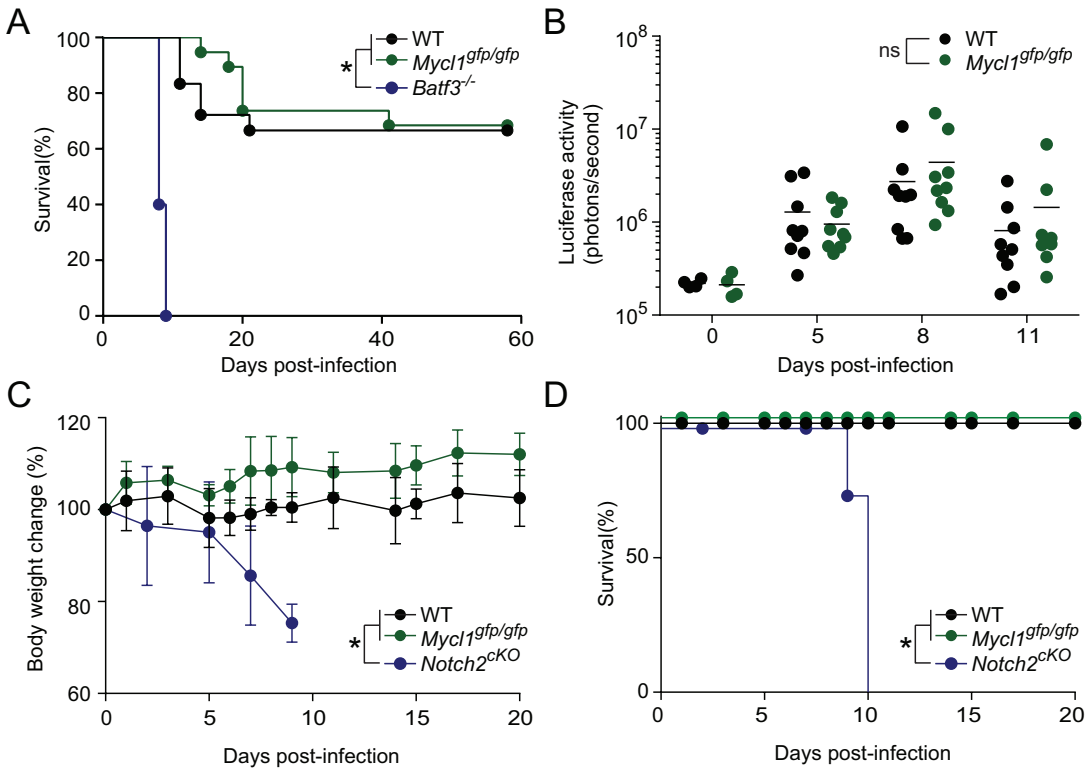

Figure 4.7: L-Myc is dispensable for the innate effector functions of DCs

(A) WT, Mycl1$^{-/-}$, and Batf3$^{-/-}$ mice were infected with an avirulent strain of Toxoplasma gondii as described in the Methods. (B) Infected mice underwent whole-body in vivo imaging throughout the course of infection to measure bioluminescence. Data shown are combined parasite burden from infected 129S6/SvEV mice from two independent experiments. (C) Weight loss (C) and survival (D) of the indicated mice given oral inoculation of C. rodentium (2 × 109 colony-forming units).

4.3.9 *Mycl1* is required for priming of CD8$^+$ T cells following bacterial and viral infection

Finally, we assessed whether L-Myc expression was required for T cell priming and other functions attributed to DCs[75,76]. In WT mice, CD8α$^+$ cDCs increased markedly from days 2 to 5 following infection with *L. monocytogenes*, consistent with previous reports [7]. However, CD8α$^+$ cDC expansion in L-Myc-deficient mice was significantly impaired relative to WT mice (Figure 4.8 **A**, Supplementary Figure 4.8 **D**). We then measured antigen-specific CD8 and CD4 T cell responses after infection with *L. monocytogenes* expressing soluble ovalbumin (LM-OVA).

Loss of L-Myc significantly decreased the total number and relative frequency of IFN-γ-producing OVA-specific CD8 and CD4 T cells (Figure 4.8 **B and C,** Supplementary Figure 4.9**a-d**). To demonstrate that these effects were not the result of a requirement for L-Myc in T cells, we adoptively transferred congenically marked L-Myc-sufficient OT-I CD8 T cells into WT and L-Myc-deficient mice. After infection with LM-OVA, OT-I CD8 T cell expansion was dramatically reduced in L-Myc-deficient mice as compared to WT mice (Figure 4.8 **D and E**, Supplementary Figure 4.9 **E and F**). Likewise, after infection with LM-OVA, congenically marked L-Myc-sufficient listeriolysin O (LLO)-specific CD4 T cells (LLO118) adoptive transferred into L-Myc-deficient mice were decreased in frequency as compared to WT mice (**Supplementary Figure 9 G**). L-Myc-deficient mice also showed impaired CD8 T cell priming after infection with vesicular stomatitis virus expressing ovalbumin (VSV-OVA) (Figure 4.8 **F,** Supplementary Figure 4.9 **H**).

These priming defects were attributable to the action of L-Myc in $CD8\alpha^+$ cDCs, as depletion of pDCs[77] or Notch2-dependent $CD11b^+$ cDCs[78] had no impact on CD8 T cell priming after infection with LM-OVA (Supplementary Figure 4.10 **A-C**). We found no cell-intrinsic defect in the antigen processing and presentation capacity of any subset of L-Myc-deficient DCs (Supplementary Figure 4.9 **D and E**) *in vitro*. In addition, L-Myc deficient DCs cross-presented and cross-primed T cells *in vivo* to syngeneic tumor grafts, which requires the actions of the $CD8\alpha^+$ DC[76,79]. These data suggest that L-Myc deficiency in the $CD8\alpha^+$ DC is the cause of impaired priming, but the mechanism probably does not entail antigen processing or presentation per se. Supporting this conclusion is a large body of literature describing the critical role this cell

type plays in capturing and spreading the initial *Listeria* infection as well as performing the initial presentation of antigen to T cells [80-83].

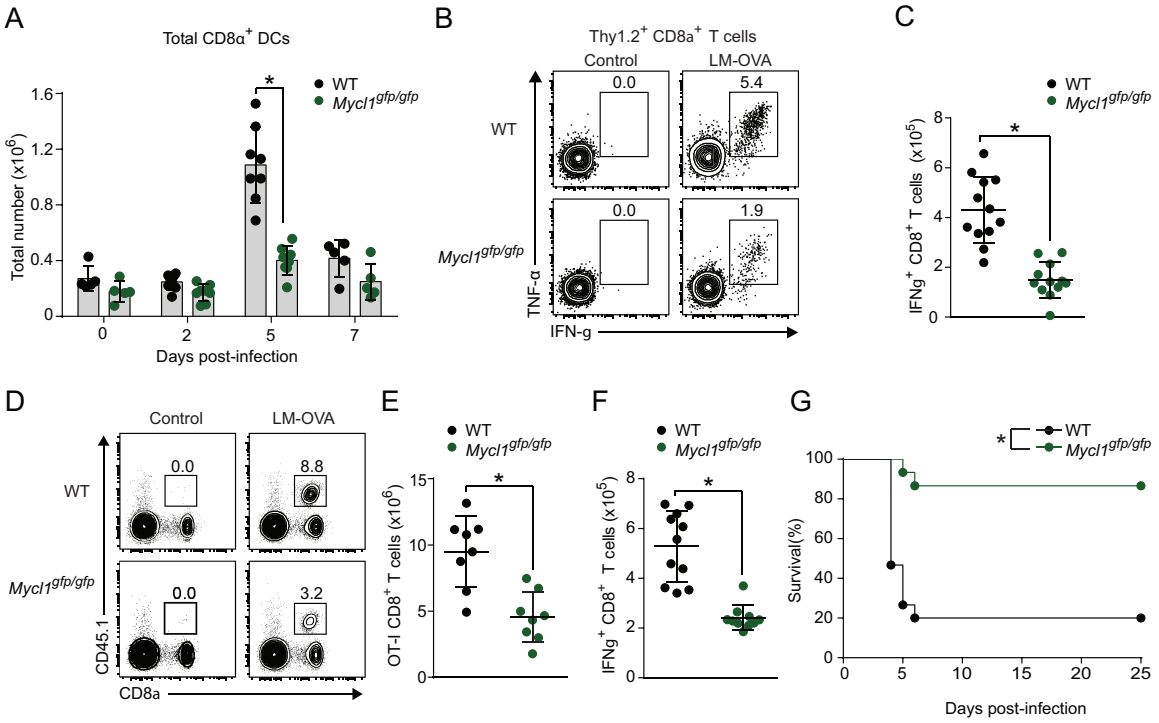

Figure 4.8: L-Myc deficiency results in abnormal T cell priming and resistance to *Listeria monocytogenes*

(A) Splenocytes from mice infected with LM-OVA were harvested at the indicated time points and stained for analysis. Total number of CD8α$^+$ DCs was determined for each indicated day following infection. Data are from 2 independent experiments (bar, SD; n=8 biological replicates, two-way ANOVA Holm-Sidak post hoc test). (B) Splenocytes were harvested 7 days after infection with LM-OVA, re-stimulated with SIINFEKL peptide *in vitro* for 5 hours and stained for analysis. Histogram of TNF-a and IFN-g expression for cells pre-gated gated as Thy1.2$^+$CD8α$^+$. Numbers represent the percent of cells in the indicated gate. Data are from 2 independent experiments. (C) Shown is the total number of SIINFEKL-specific CD8$^+$ T cells determined for infections described in (B). Data are from 2 independent experiments (bar, SD; n=12 infected biological replicates, Student's t-test). (D) Expansion of transferred WT OT-I CD8$^+$ T cells was determined 7 days after infection. Numbers represent the percent of donor OT-I CD8$^+$ T cells. (E) Shown is the total number of OT-I CD8$^+$ T cells determined for the infection described in (D). Data are from 2 independent experiments (bar, SD; n=8 infected biological replicates, Student's t-test). (F) WT (black dots) or Mycl1$^{gfp/gfp}$ (green dots) mice were infected intravenously with 5x10^6 PFU VSV-OVA. Splenocytes were harvested 7 days after infection and re-stimulated as in (B). Shown is the total number of SIINFEKL-specific CD8+ T cells. Data are from 2 independent experiments (bar, SD; n=11 biological replicates, Student's t-test). (G) WT (black dots) and Mycl1$^{gfp/gfp}$ (green dots) mice were infected intravenously with 100,000

Listeria monocytogenes (wild-type strain EGD) and followed daily for survival. Data are from 3 independent experiments (n=15 mice per group, Log-rank Mantel-Cox test). *, $p<0.001$, ns, $p>0.05$

We also assessed the capacity of CD8α$^+$ cDCs to capture and promote infection by *L. monocytogenes* in the absence of L-Myc. CD8α$^+$ cDCs are the initial cellular target for intracellular *L. monocytogenes* infection[82], and *Batf3*$^{-/-}$ mice, which lack CD8α$^+$ cDCs, are resistant to lethal infection by *L. monocytogenes*[80]. We observed that L-Myc-deficient mice were also resistant to infection by *L. monocytogenes* as compared to WT mice (Figure 4.8 **G**). Since the CD8α$^+$ DCs are modestly reduced in the spleen of L-Myc-deficient mice, we hypothesized that the resistance phenotype was caused by either impaired bug capture or poor initial spreading and proliferation of bugs within this DC compartment[82]. Although previously thought to infect predominantly splenic macrophages [84,85], Busch and colleagues showed that the initial viable burden is heaviest among CD8α$^+$ DCs, and any impairment of bug growth and spreading in these cells dramatically attenuates overall infection and T cell priming.

We performed similar sorting experiments on different splenic populations from WT mice and confirmed the selective presence of viable *L. monocytogenes* within CD8α$^+$ DCs for 24 hours following infection(data not shown). The initial capture of *L. monocytogenes* by L-Myc deficient CD8α$^+$ DCs was equal to WT DCs (Figure 4.9 **A, right panel**)and comparable to published values[81,82]. However, we observed a significant reduction in viable *L. monocytogenes* within L-Myc deficient CD8α$^+$ DCs as compared to WT (Figure 4.9 **A, left panel**) by 24 hours. This defect was cell-intrinsic as sorted L-Myc deficient CD8α$^+$ DCs poorly supported *L. monocytogenes* growth. Consequently, the reported spread to other myeloid lineages, including

CD8α$^-$ DCs, was greatly diminished in L-Myc-deficient mice. Lastly, the decreased pathogen burden seen in *Mycl1*$^{-/-}$ mice was reflected in substantially reduced histological lesions in spleen and liver compared to WT mice. The WT mice had characteristically large lesions in the PALS, which represent apoptotic death of lymphocytes[86], but L-Myc-deficient mice had a large number of unaffected PALS (Figure 4.9**D**). In summary, L-Myc-deficient CD8α$^+$ DCs inefficiently support the initial *L. monocytogenes* infection, thereby limiting pathogen spread but also attenuating T cell responses.

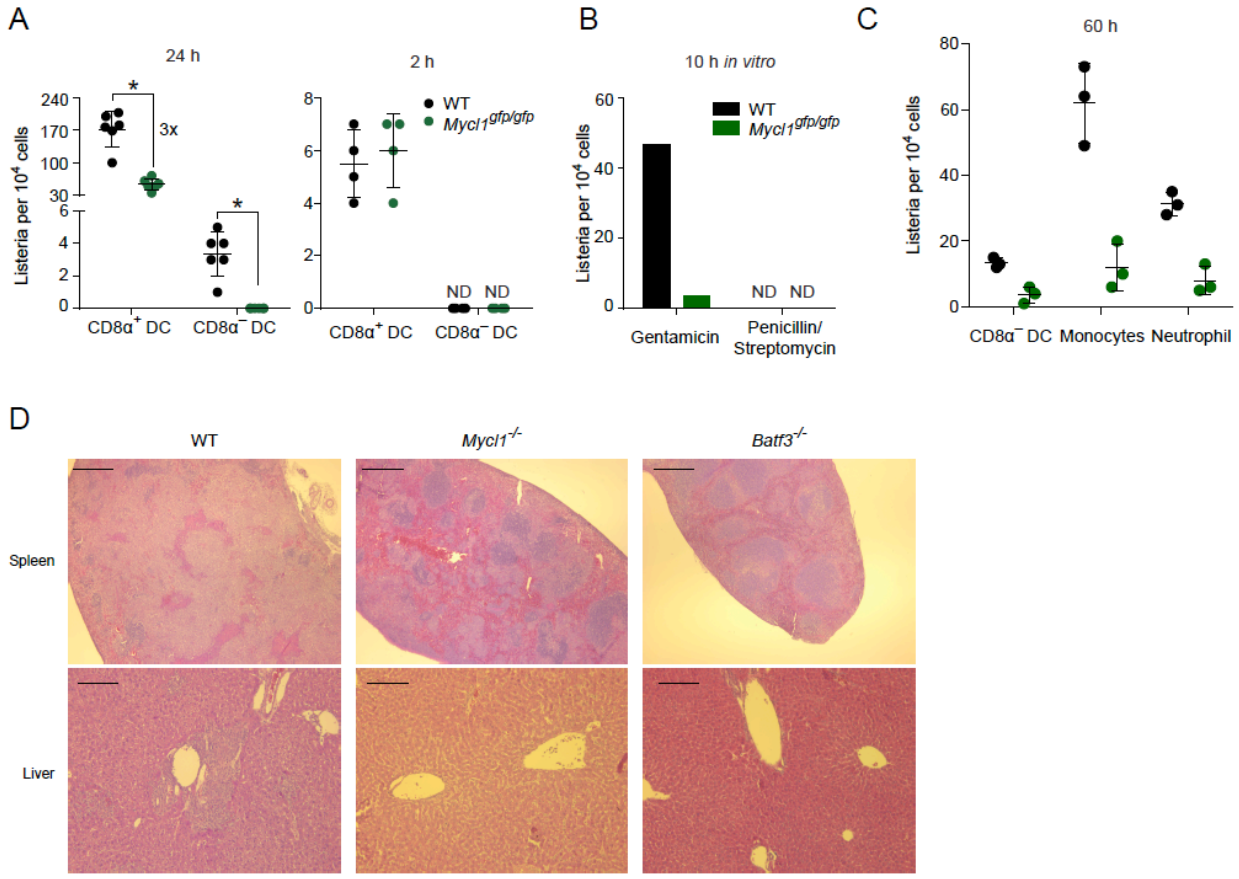

Figure 4.9: L-Myc-deficient CD8α$^+$ DCs capture but do not support growth of *L. monocytogenes*

(A) Mice were infected with LM-EGD and the indicated DC subsets were sorted after either 2 hours (2 h) or 24 hours (24 h) according to the Methods. CFU burden for DC subsets was determined as described in Methods. (B) Mice were infected with

$50x10^6$ CFU LM-EGD and DCs were isolated 2 h post-infection. Sorted $CD8\alpha^+$ DCs were cultured in the presence of the indicated antibiotics. Cells were harvested after 10 hours of growth at 37ºC and bug burden was determined as in (A). (C) Mice were infected as in (A) and the indicated myeloid populations were purified after 60 hours and bug burden determined. (D) Mice were infected with 10^5 CFU LM-EGD and histopathology (H&E) of spleen (top panels) and liver (bottom panels) was carried out. Scale bars for spleen represent 400 μm; bars for liver represent 160 μm.

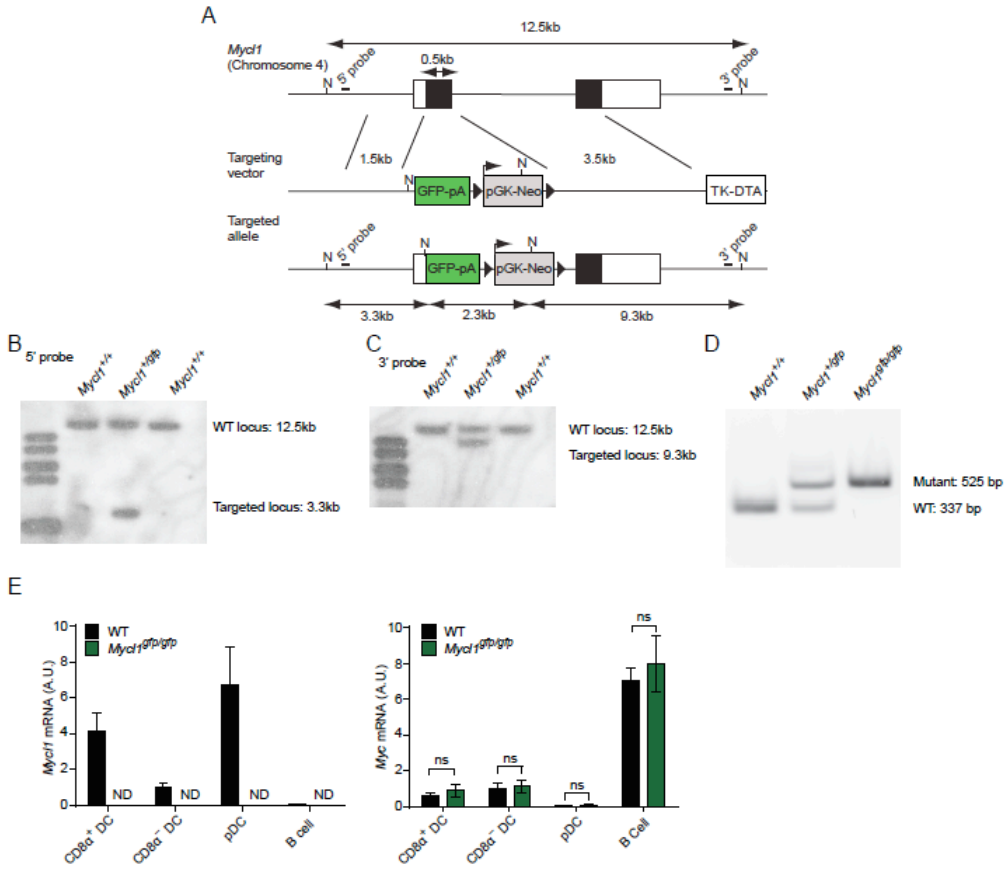

Supplementary Figure 4.1: Generation of Mycl1$^{gfp/gfp}$ mice by homologous recombination

(A) Genomic context of *Mycl1*, the targeting vector, and targeted allele are shown. Restriction enzyme digestion with NcoI of the wild-type locus generates a 12.5 kb fragment detectable by either 5' or 3' probes. NcoI digestion of the targeted locus generates a 3.3 kb fragment (detected by 5' probe), a 2.3 kb fragment containing most of the GFP-Neo cassette, and a 9.3kb fragment (detected by 3' probe). (B) Southern blot analysis of NcoI-digested total DNA with the 5' probe. (C) Southern blot analysis of NcoI-digested genomic DNA with the 3' probe. (D) Genotyping PCR of indicated mice. The wild-type genomic allele yields a 337 bp band and the mutant allele yields a 525 bp band. (E) The relative amount of *Mycl1* and *Myc* mRNA was determined by qPCR for indicated genotypes. Shown is a graph of *Mycl1*and *Myc* values normalized to *Hprt* values (bar, SD; n=3 biological replicates per cell type).

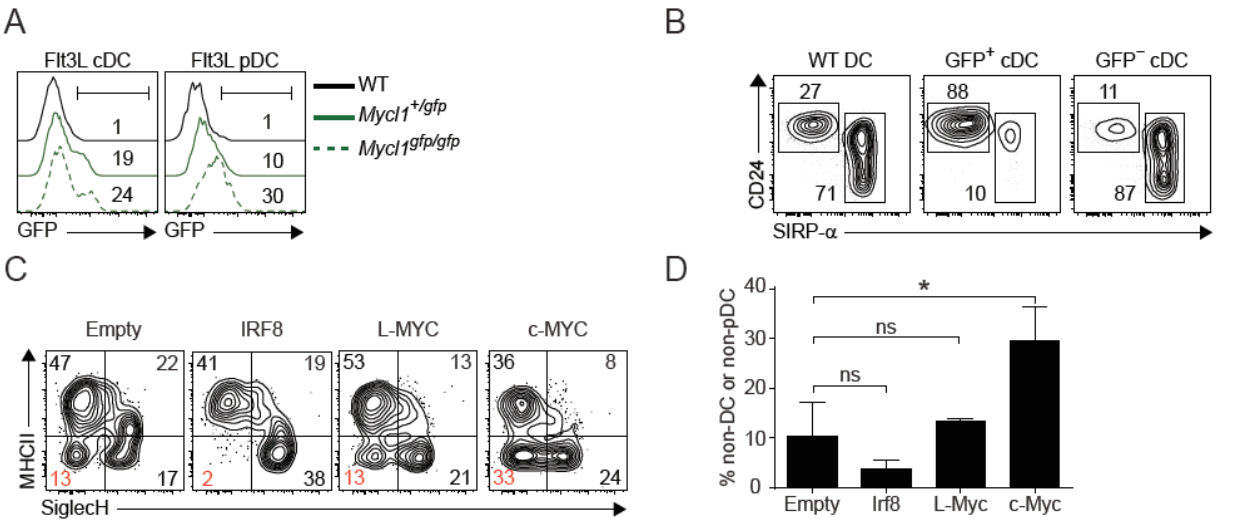

Supplementary Figure 4.2: *In vitro* derived DCs express Mycl1

(A) Histograms of GFP expression for the indicated cells derived from WT, *Mycl1*$^{+/gfp}$, and *Mycl1*$^{gfp/gfp}$ BM cultured in Flt3L for 10 days. Numbers represent GFP^{+} cells as a percent of live cells. Data are representative of 3 independent experiments. (B) Histograms of CD24 and SIRP-α expression for Flt3L DCs as described in (**A**). Flt3L DCs from BM of *Mycl1*$^{+/gfp}$ mice were pre-gated either as GFP^{+} or GFP^{-}. (C) BM cells from WT mice were harvested and Flt3^{+} CMPs were purified by cell sorting. CMPs were cultured in Flt3L for 12 hours before being transduced with control (Empty), *Irf8*, *Mycl1*, or *Myc* expressing retrovirus. Cells were cultured an additional 5 days and then stained for analysis. Numbers represent the percent of cells in the quadrant gate. (D) Shown is the quantitation of undifferentiated (non-DC or non-pDC) cells from (**c**). Data are from 4 independent transductions per retrovirus (bar, SD; n=4, one-way ANOVA Tukey's *post hoc* test). *, $p<0.01$; ns, $p>0.05$.

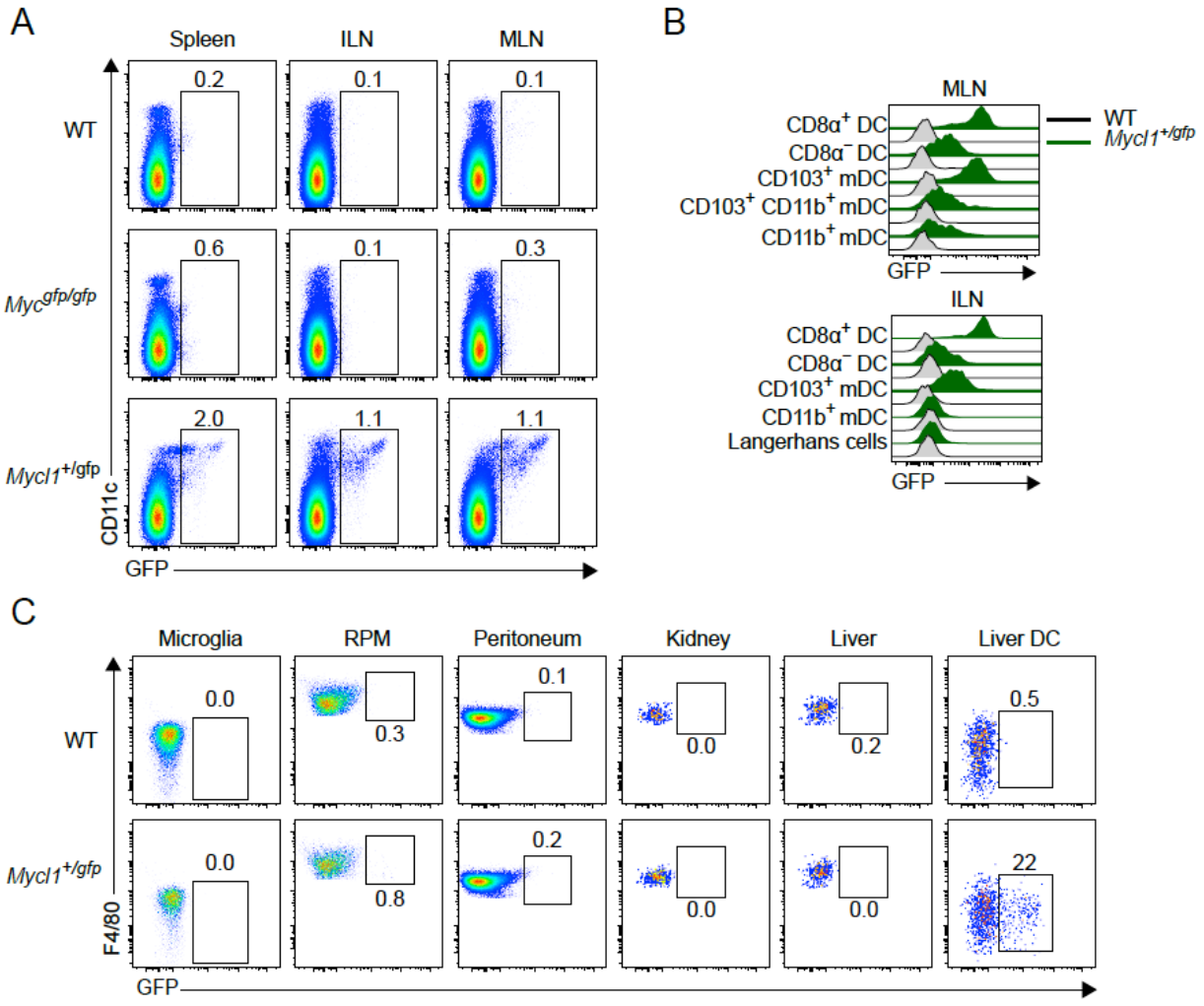

Supplementary Figure 4.3: Mycl1 expression is restricted to DCs in secondary lymphoid tissues

(A) Spleen (left panel), inguinal lymph node (ILN, middle panel), and mesenteric lymph node (MLN, right panel) stained for analysis. Histograms of auto-fluorescent negative cells. Numbers represent percent of cells in the indicated gate. Data are representative of at least 5 independent experiments. (B) Historgrams of GFP expression for resident DCs and migratory DCs from MLN and ILN of WT (grey lines) and *Mycl1*$^{+/gfp}$ mice (green lines). (C) Cells from the brain, spleen, peritoneum, kidney, and liver stained for analysis. Histograms of F4/80 and GFP expression for microglia (CD45^{int}CD11b^{+}), splenic red pulp macrophages (F4/80^{+}autofluorescent^{high}, RPM), peritoneum macrophages (F4/80^{+}CD11b^{+}, Peritoneum), liver and kidney macrophages (F4/80^{+}CD11b^{int}, liver, kidney), and liver DCs (CD11c^{+}MHCII^{+}). Live hematopoietic cells were pre-gated in all non-lymphoid tissues as CD45$^{+/int}$7AAD^{-}. Numbers represent percent of cells in the indicated gate. Data are representative of 2-3 independent experiments.

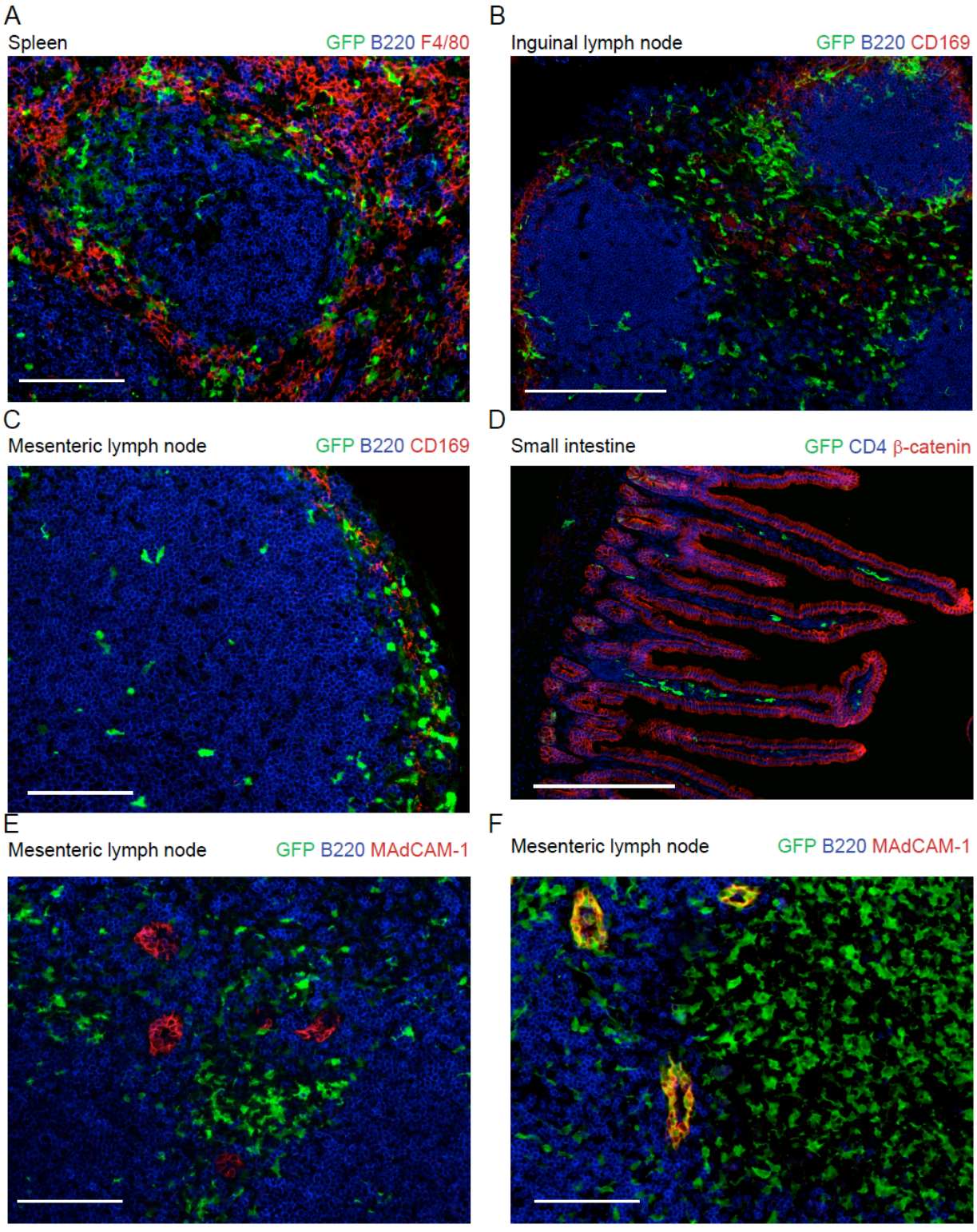

Supplementary Figure 4.4: Mycl1 expression is restricted to DCs by microscopy

(A) Sections of spleen from *Mycl1*$^{+/gfp}$ mice were analyzed by fluorescence microscopy for B220 (blue), F4/80 (red) and GFP (green). (B) Inguinal lymph node from *Mycl1*$^{+/gfp}$ mice was analyzed by fluorescence microscopy for B220 (blue), CD169 (red) and GFP (green). (C) Mesenteric lymph node from *Mycl1*$^{+/gfp}$ mice was analyzed by fluorescence microscopy for B220 (blue), CD169 (red) and GFP (green). (D) Sections of small intestine from *Mycl1*$^{+/gfp}$ mice were analyzed by fluorescence microscopy for CD4 (blue), β-catenin (red) and GFP (green). (E) Mesenteric lymph node from *Mycl1*$^{+/gfp}$ mice was analyzed by fluorescence microscopy for B220 (blue), MAdCAM-1 (red) and GFP (green). (F) Mesenteric lymph node from *Zbtb46*$^{+/gfp}$ mice was analyzed by fluorescence microscopy for B220 (blue), MAdCAM-1 (red) and GFP (green). Scale bars, 200 μM (Inguinal lymph node, small intestine), 100 μM (Spleen, Mesenteric lymph node).

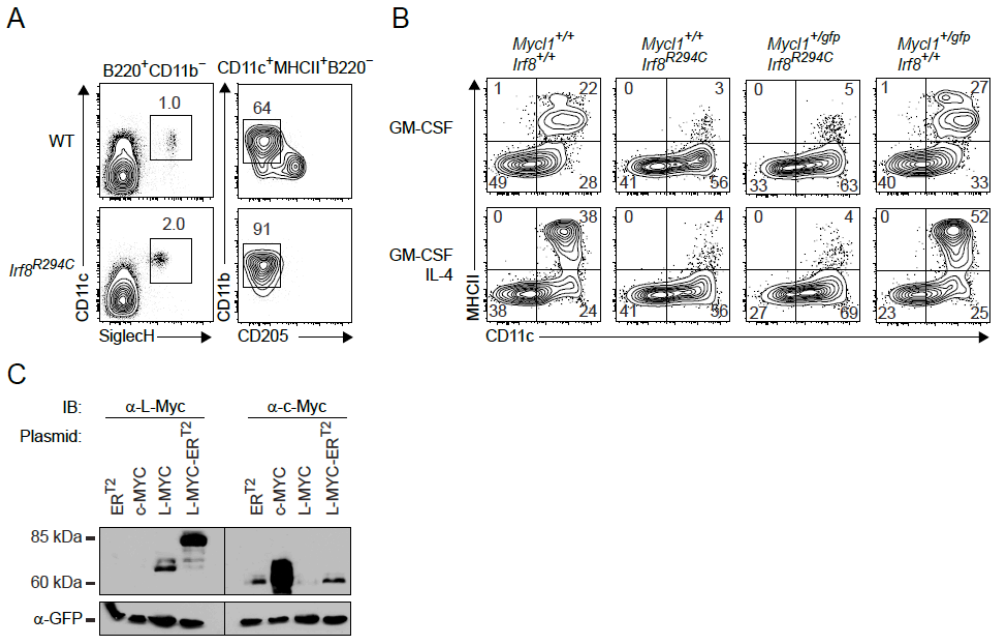

Supplementary Figure 4.5: IRF8 regulates Mycl1 expression

(A) Splenocytes indicated mice were stained for analysis. Histograms of CD11c and SiglecH expression (left panels), and CD11b and CD205 expression (right panels). Numbers represent the percent of cells in the indicated gates. Data are representative of 2 independent experiments. **b,** BM Ly6C^{+} monocytes were purified by cell sorting. Monocytes were cultured in either GM-CSF or GM-CSF and IL-4 for 4 days and stained for analysis. Histograms of MHCII and CD11c expression for differentiated monocytes. **c,** Phoenix E cells were transfected with Murine Stem Cell Virus (MSCV) retroviral plasmids expressing the mutant human estrogen receptor (ER^{T2}), murine *Myc* (c-MYC), murine *Mycl1* (L-MYC), and a fusion between *Mycl1* and the mutant human estrogen receptor (L-MYC-ER^{T2}). Whole-cell extracts were prepared 2 days after transfection and Western blot analysis was performed. Shown are immunoblots for L-MYC (left) and c-MYC (right) on the indicated transfections. Blots were stripped and re-probed for GFP (bottom).

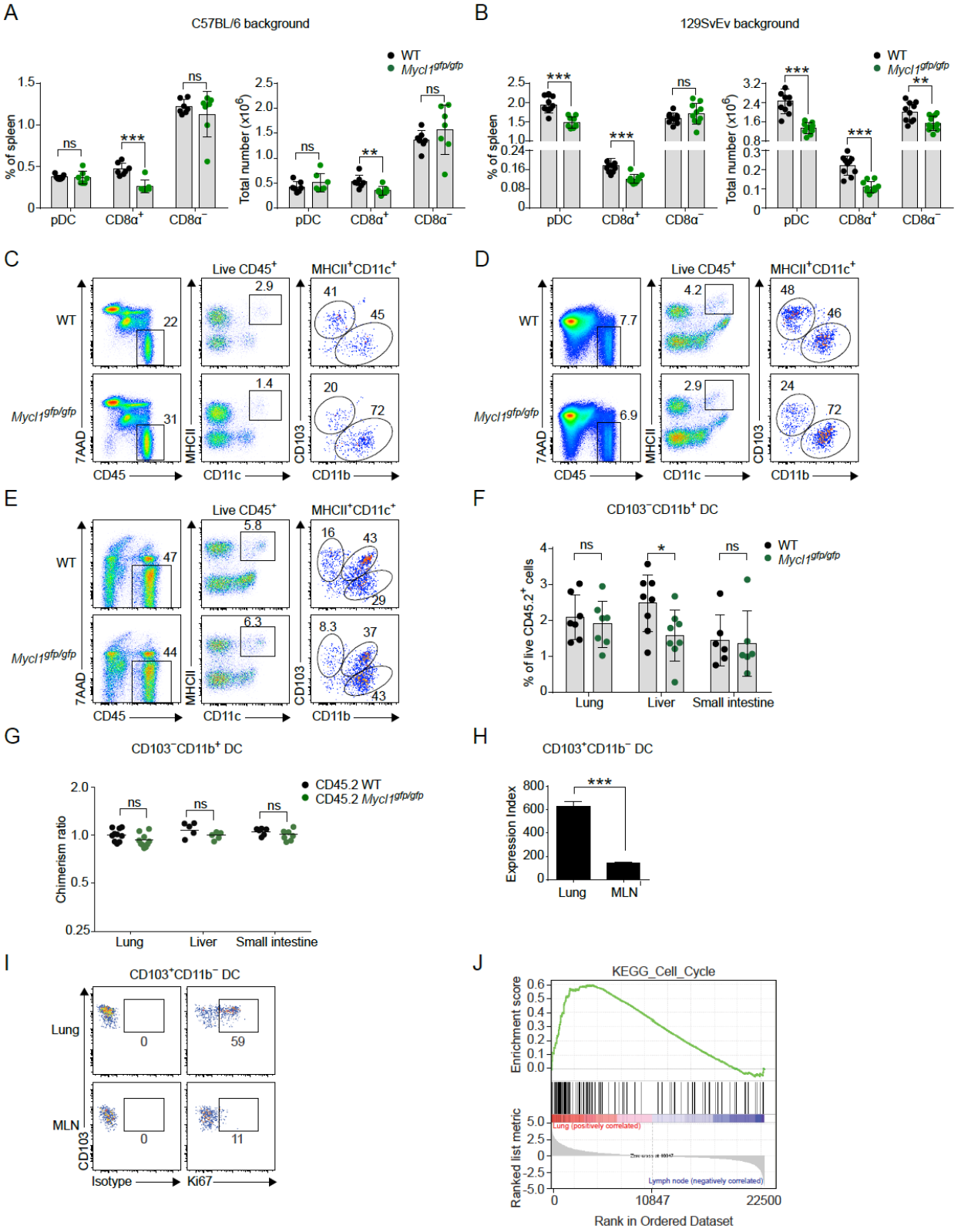

Supplementary Figure 4.6: L-Myc regulates DC homeostasis

(A) Shown is the quantitation of splenic DC subsets as gated in (**Figure 3 F**) from WT (black dots) and *Mycl1*$^{gfp/gfp}$ (green dots) mice on the C57BL/6 (**A**) and 129SvEv (**B**) genetic backgrounds. Total number of the indicated DC subset per spleen (right panels) and DC subset as a percent of all splenocytes (left panels) was determined for each genetic background. Data are from 3 independent experiments (bar, SD: n=7 biological replicates for C57BL/6 background and 10 biological replicates for 129SvEv background, Student's *t*-test). (C-E) Cells were harvested from liver (**C**), lung (**D**), and small intestine (**E**) of WT and *Mycl1*$^{gfp/gfp}$ mice on the C57BL/6 genetic background and stained for analysis. Shown are two-color histograms for indicated markers. (F) Shown is the quantitation of CD103^{-}CD11b^{+} DCs from the lung, liver and small intestine as gated in (**C-E**) as a percent of all live hematopoietic cells. Data are from 3-4 independent experiments (bar, SD, n=6-7 biological replicates, two-way ANOVA Holm-Sidak *post hoc* test). (G) Cells were harvested from the lung, liver and small intestine of the mixed BM chimeras described in (**Figure 5 A,C**) and analyzed for relative donor contribution. Shown is the contribution of CD45.2^{+} WT BM or CD45.2^{+} *Mycl1*$^{gpf/gfp}$ BM to CD103^{-}CD11b^{+} DCs in the indicated peripheral tissues as a ratio of peripheral blood neutrophils from the same animal. Data are representative of 3 independent experiments (bar, SD; n=5-10, Mann-Whitney U test). (H) Shown is the relative expression of *Mycl1* from gene expression microarrays of lung-resident CD103^{+}CD11b^{-} DCs and migratory CD103^{+}CD11b^{-} DCs from mediastinal lymph nodes (MLN) (bar, SD; n=3 biological replicate arrays, Student's *t*-test). (I) Cells were harvested from lung and MLN of WT mice and stained for analysis. Shown is a two-color histogram of CD103 and isotype expression, or CD103 and Ki67 expression for pre-gated CD103^{+}CD11b^{-} DCs from the lung and MLN. (J) Shown is Gene Set Enrichment Analysis (GSEA) plot comparing gene expression microarrays from lung-resident CD103^{+}CD11b^{-} DCs (Lung, red) and migratory CD103^{+}CD11b^{-} DCs (Lymph node, blue) using "KEGG_Cell_Cycle" list of genes (Signal-to-noise calculation , n=3 biological replicate arrays per group). *, $p<0.05$; **, $p<0.01$, ***, $p<0.001$; ns, $p>0.05$;

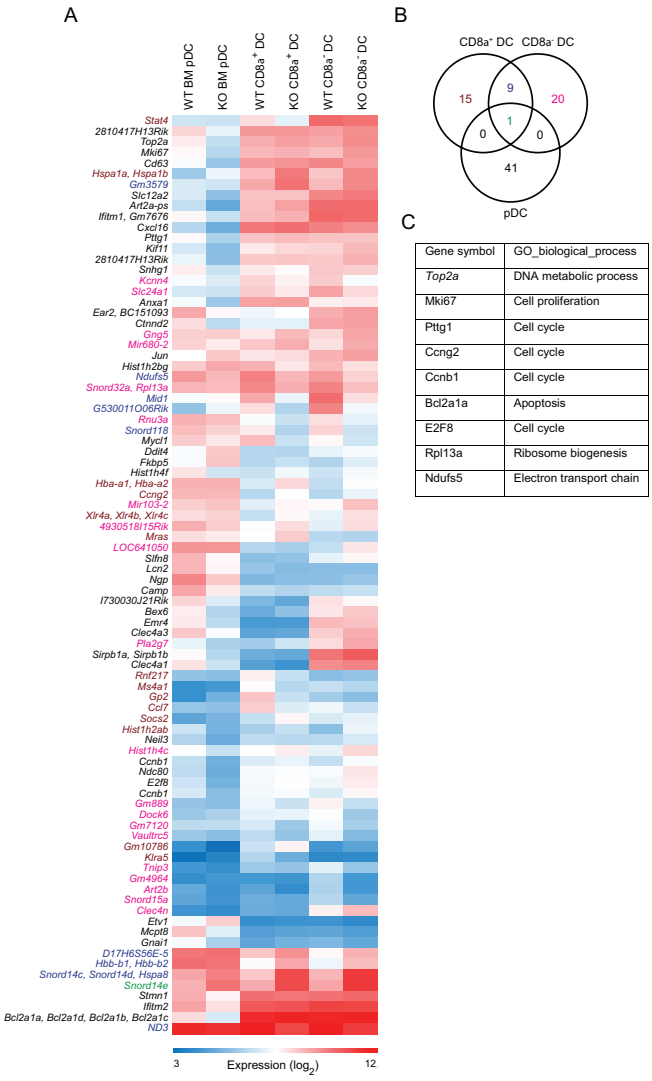

Gene symbol	GO_biological_process
Top2a	DNA metabolic process
Mki67	Cell proliferation
Pttg1	Cell cycle
Ccng2	Cell cycle
Ccnb1	Cell cycle
Bcl2a1a	Apoptosis
E2F8	Cell cycle
Rpl13a	Ribosome biogenesis
Ndufs5	Electron transport chain

Supplementary Figure 4.7: Gene expression analysis of L-Myc deficient DCs

(A) Indicated DC subsets were sorted and microarray analysis performed. A 2-fold difference in linear expression value between WT and KO DCs was used as the threshold for further analysis. Shown is a heat map of $\log_2$-transformed linear expression values for genes determined to be differentially expressed. Representative genes were distributed based on hierarchical clustering of gene expression data from the indicated WT and KO DCs. Gene names have been color coded according to their distribution within the Venn diagram described in (**B**). (B) Shown is a Venn diagram of genes satisfying a 2-fold cutoff for all three indicated DC populations. The total number of genes unique to a particular DC subset or common to any two or all three DC subsets is indicated within the respective zones of the diagram. **c,** Shown is a table containing growth-related genes from the heat map in (**A**). The gene symbol as well as the putative "GO_biological_process" has been noted.

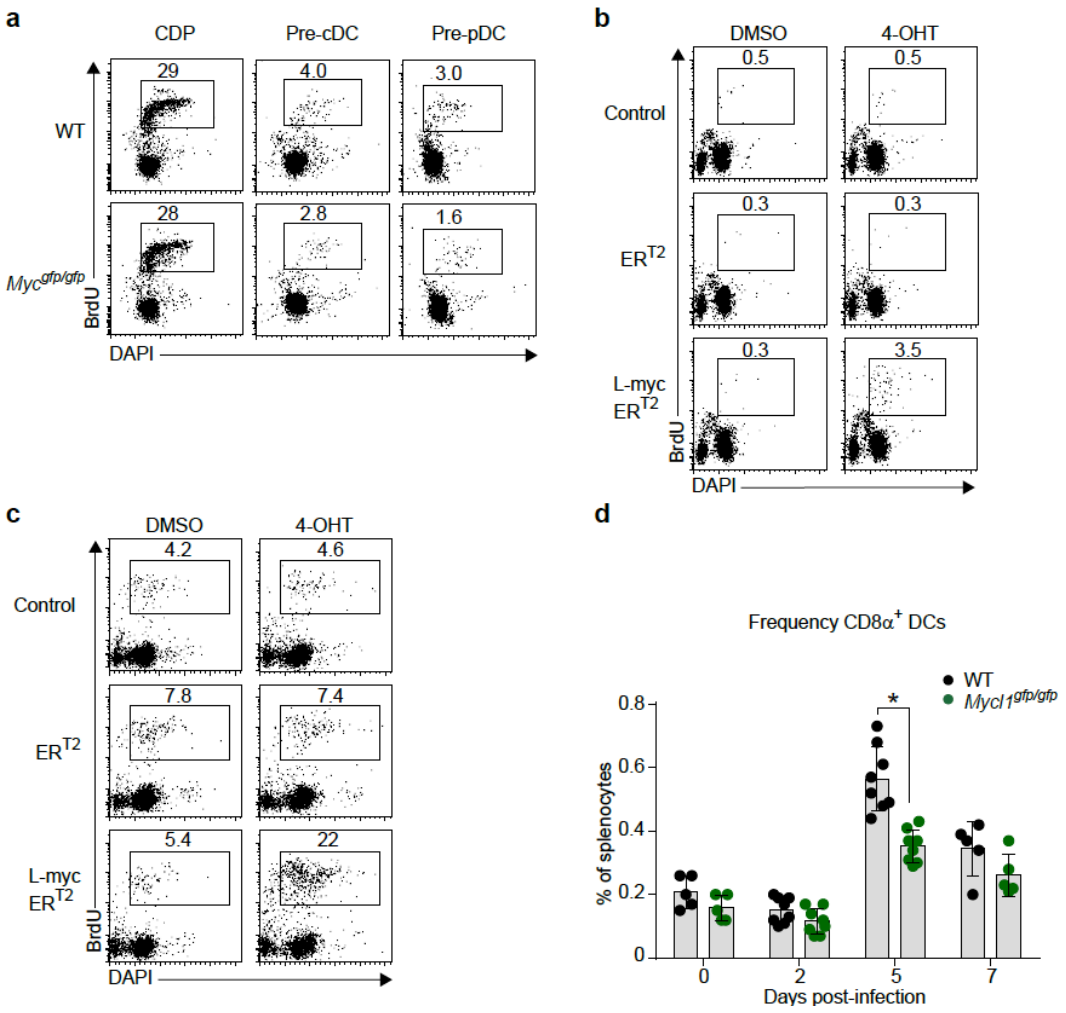

Supplementary Figure 4.8: L-Myc regulates DC proliferation

(A) BM CDPs, pre-cDCs, and pDCs were cultured in Flt3L for 24 h. Wells were pulsed with 10μM BrdU for the last 4 h of culture. Histogram of BrdU and DAPI for the indicated pre-gated cells. Data are representative of 2-3 experiments. (B,C) BM cells from WT mice were cultured in Flt3L and infected on day 4 with a retrovirus expressing ER^{T2} or the L-MYC-ER^{T2} fusion protein and then cultured for an additional 6 days. Cells were harvested and purified into subsets as $CD11c^{int}$ $SiglecH^{+}$ (pDC, **B**) or $CD11c^{+}$ $MHCII^{+}$ $CD24^{+}Sirp\text{-}\alpha^{-}$ ($CD8\alpha^{+}$ DC, **C**) by cell sorting. Infected cells and uninfected control cells were treated with vehicle (DMSO) or 4-hydroxytamoxifen (4-OHT) for 24 h in 100 ng/ml Flt3L, pulsed with 10 μM BrdU for the last 4 h and stained for BrdU incorporation. Shown is the percent of cells in S phase. (D) WT (black dots) or *Mycl1*$^{gfp/gfp}$ (green dots) mice were infected intravenously with $3x10^{3}$ *Listeria monocytogenes* expressing ovalbumin (LM-OVA). Splenocytes were harvested at the indicated time points and stained for analysis. Percent of $CD8\alpha^{+}$ DCs was determined for each indicated day following infection. Data are from 2 independent experiments (bar, SD; n=8 biological replicates, two-way ANOVA Holm-Sidak *post hoc* test). *, $p<0.001$; ns $p>0.05$.

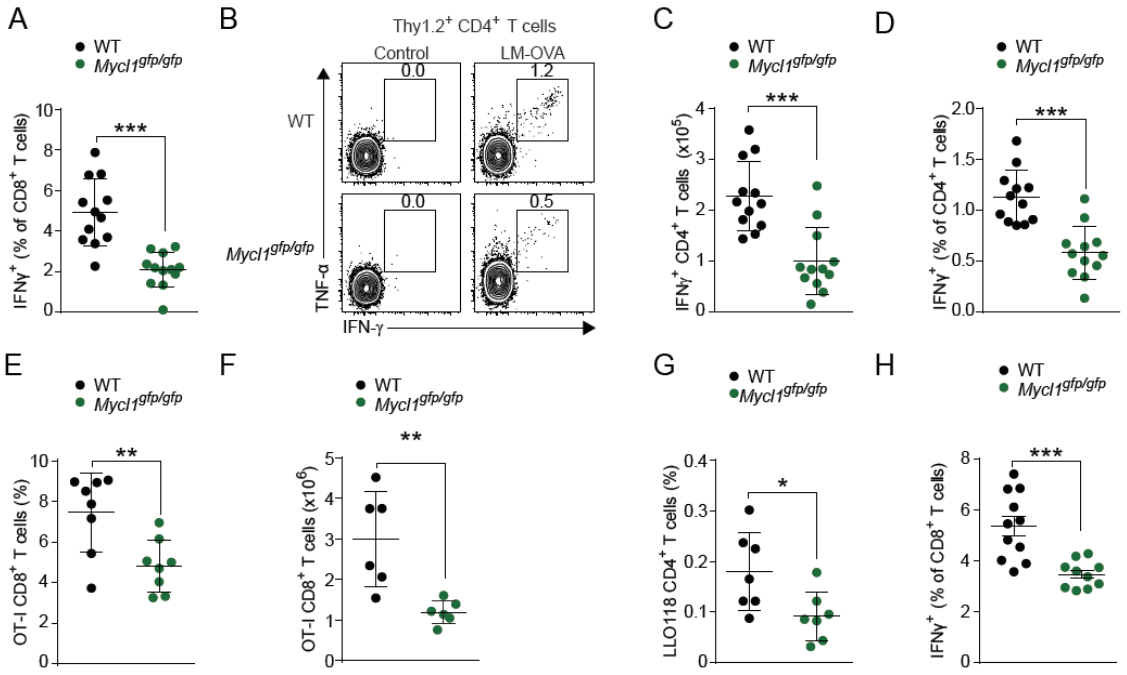

Supplementary Figure 4.9: Mycl1 is necessary for optimal T cell priming by DCs

(A-D) WT (black dots) and *Mycl1*$^{gfp/gfp}$ (green dots) mice infected with 3x10^3 LM-OVA were analyzed 7 days later by re-stimulation with SIINFEKL(**A**) or LLO$_{190-210}$ (**B-D**) peptide *in vitro*. Shown is the quantitation of IFN-γ$^+$ cells. Data are from 2 independent experiments (bar, SD; n=12 biological replicates, Student's *t*-test). (E) Shown is the frequency of OT-I CD8$^+$ T cells (gated as CD45.1$^+$CD8α$^+$) as a percent of all splenocytes for the experiment described in (**Figure 8 D**). Data are from 2 independent experiments (bar, SD; n=8 biological replicates, Student's *t*-test). (F) Shown is the absolute number of donor OT-I CD8$^+$ T cells from mice infected with 300 LM-OVA and analyzed as in (**Figure 8 D**). Data are from 2 independent experiments (bar, SD; n=6 biological replicates, Student's *t*-test). (G) 1000 CD45.1$^+$ LLO118 CD4$^+$ T cells were transferred intravenously into CD45.2$^+$ WT or CD45.2$^+$ *Mycl1*$^{gfp/gfp}$ recipients 1 day before infection with LM-OVA. Expansion of donor LLO118 CD4$^+$ T cells was determined 7 days after infection. Shown is the frequency of LLO118 CD4$^+$ T cells (gated as CD45.1$^+$CD4$^+$) as a percent of all splenocytes. Data are from 2 independent experiments (bar, SD; n=7 biological replicates, Student's *t*-test). (H) WT (top panels) or *Mycl1*$^{gfp/gfp}$ (bottom panels) mice were infected intravenously with 5x10^6 PFU VSV-OVA. T cell restimulation was performed as in (**A**). Shown is a two-color histogram of TNF-α and IFN-γ expression for cells pre-gated gated as Thy1.2$^+$CD8α$^+$. Numbers represent the percent of cells in the indicated gate. Data are representative of 2 independent experiments. (I) Shown is the quantitation of IFN-γ$^+$ cells as a percent of CD8$^+$ T cells (gated as Thy1.2$^+$ CD8α$^+$). Data are from 2 independent experiments (bar, SD; n=11 biological replicates, Student's *t*-test). **i**, *, p<0.05; **, p<0.01; ***, p<0.001; ns, p>0.05.

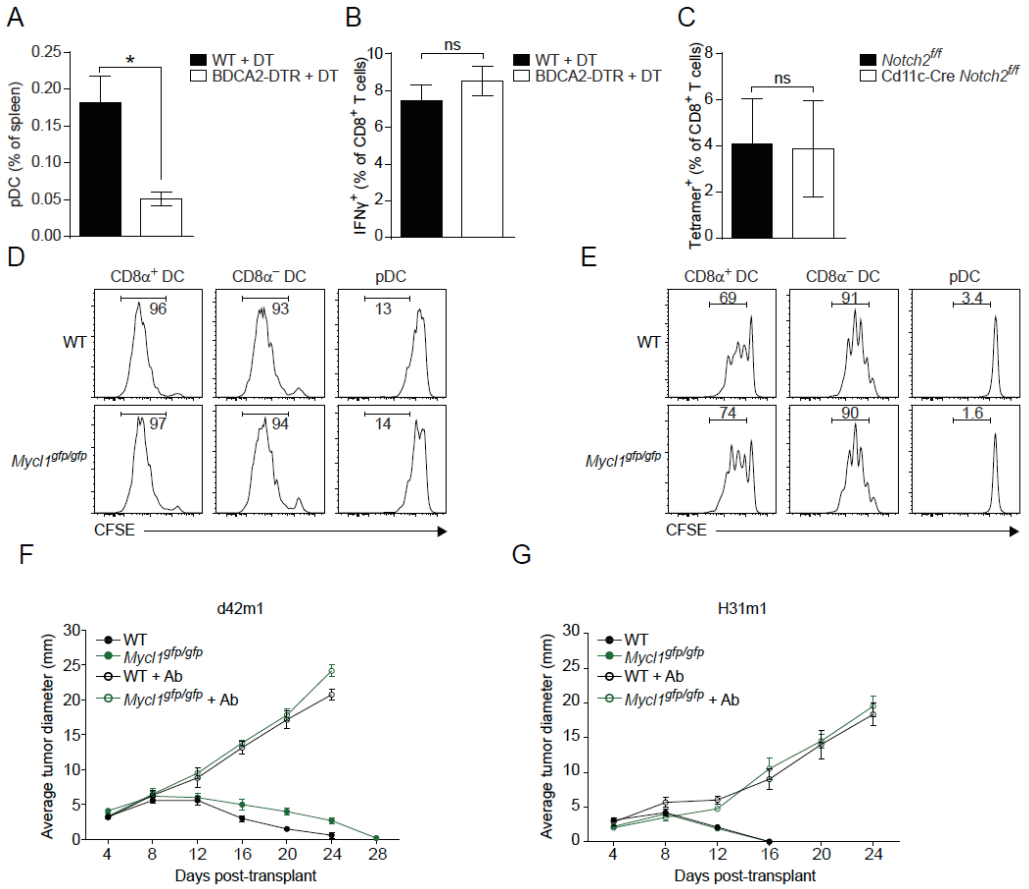

Supplementary Figure 4.10: pDCs and Notch2-dependent CD11b$^+$ DCs are dispensable for T cell priming

(A) WT and BDCA2-DTR transgenic mice were treated with 125 ng diphtheria toxin (DT) per mouse one day before infection with LM-OVA. Shown is the quantitation of pDCs as a percent of all splenocytes to confirm efficiency of deletion (bar, SD; n=4 biological replicates per group, Student's *t*-test). (B) Shown is the quantitation of IFN-γ$^+$ cells as a percent of CD8$^+$ T cells following re-stimulation of infection from (**A**) (gated as Thy1.2$^+$ CD8α$^+$). (bar, SD; n=4 biological replicates, Student's *t*-test). (C) Peripheral blood CD8$^+$ T cells from indicated mice were stained with H-2K^b-SIINFEKL tetramer on day 7 of infection with LM-OVA. Shown is the frequency of tetramer$^+$ cells as a percent of CD8$^+$ T cells. (bar, SD; n=4 biological replicates, Student's *t*-test). (D,E) DCs, OT-I CD8$^+$ T cells, and OT-II CD4$^+$ T cells were isolated by cell sorting and T cells labeled with CFSE. DCs were pulsed with whole ovalbumin protein (Ova) for 2 h at 37ºC and then washed extensively before either OT-I CD8$^+$ T cells (**D**) or OT-II CD4$^+$ T cells (**E**) were plated. Cells were collected 3 days later and stained for analysis. Shown are single-color histograms of CFSE levles for pre-gated T cells. (F,G) d42m1 or H31m1 fibrosarcoma cells were injected subcutaneously and tumor diameter (± SD) (n=10) was measured. Mice were treated with antibodies to deplete CD8 T cells, CD4 T cells and IFN-γ.

4.4 Discussion

In the hematopoietic compartment, c-Myc and N-Myc act in many cell types and regulate broad cellular processes, including B cell proliferation, T cell metabolism, and maintenance of progenitor populations[37,38,42,87]. Distinct thresholds of c-Myc expression result in cellular proliferation or apoptosis, suggesting that the cellular abundance of this protein is stringently regulated[88]. Recent findings indicate that c-Myc acts as a global amplifier of transcription by direct interactions with RNA polymerases I, II and III[20,68-70,89], thus providing a mechanism that accounts for its regulation of disparate and context-dependent target loci across cell types[90]. For L-Myc, a third Myc family member, a direct role in proliferation and apoptosis has been questioned because of its weaker ability to promote cellular growth, apoptosis or transformation as compared to c-Myc or N-Myc[91,92]. Although L-Myc reprograms fibroblasts into induced pluripotent stem cells more efficiently than c-Myc[93], a unique physiologic function *in vivo* for L-Myc has not yet been established[5].

Among hematopoietic lineages, DCs are uniquely specialized in priming antigen-specific immune responses based on their ability to process and to present antigens to T cells[94]. Mature DC populations show a significant rate of proliferation *in vivo*[25,47], and the receptor FMS-like tyrosine kinase 3 (FLT3) regulates cDC homeostasis by promoting the division of these cells *in situ*[24]. In other physiologic and malignant settings, FLT3 signaling leads to c-Myc induction via STAT-dependent pathways[21,22]. However, in DCs, proliferation and expansion[7,8] occurs in the presence of inflammatory cytokines such as type I interferons (IFN) that suppress *Myc* transcription through STAT1 interactions at GAS elements in the promoter region[95-97]. To further examine the homeostatic mechanisms that regulate the frequency of DCs at steady state and during inflammation, we studied the expression of c-Myc and its paralogs and investigated

whether L-Myc plays a non-redundant role in supporting continued proliferation and expansion in these cells. We determined that L-Myc regulates many of the same cellular processes as c-Myc or N-Myc. For example, cell size and growth were dramatically affected by L-Myc deficiency, suggesting possible functional equivalence in certain contexts. Moreover, L-Myc also regulated many inducible genes following activation. Through our cellular studies of L-Myc deficient mice, we characterized a critical cell-intrinsic role for CD8α^+ DCs in supporting the initial growth of *L. monocytogenes*, which is also necessary for establishing optimal priming of CD8 and CD4 T cell responses. This latter observation may help explain why early antibiotic treatment of mice dramatically blunts antigen-specific responses[98-100].

Although L-Myc is a functional member of the Myc family[34,101], its function and relationship to other Myc factors has remained uncertain[5,6]. L-Myc is selectively expressed in DCs, maintained in the presence of inflammation, and regulates proliferation and survival required for normal DC-mediated T cell priming to bacterial and viral infections. Since c-Myc is repressed by interferons[95-97], the switch from c-Myc to L-Myc expression in DCs may be a strategy to maintain DC function in the setting of inflammation required for driving optimal T-cell responses. L-Myc may therefore represent a therapeutic target for selective inhibition or augmentation of immune responses during autoimmunity or vaccination.

4.5 Materials and Methods

4.5.1 Mice.

Wild-type (WT) 129S6/SvEv mice were purchased from Taconic. WT C57BL/6 mice, *Csf2rb*$^{-/-}$ mice and the congenic strain B6.SJL-*Ptprc*^{a} *Pepc*^{b}/BoyJ (B6.SJL) were purchased from The

Jackson Laboratory. Mice were bred and maintained in our specific pathogen-free animal facility according to institutional guidelines. The generation of GFP-c-Myc (*c-Myc*$^{gfp/gfp}$), *Zbtb46*$^{DTR/DTR}$, and BXH2 (*Irf8*^{R294C}) mice has been described previously[50,58,102]. *Irf8*^{R294C} mice were backcrossed to the C57BL/6 background for 11 generations. Experiments were performed with sex- and age-matched mice at 6-16 weeks of age. All pathogen infections were performed on mice of the 129S6/SvEv genetic background unless otherwise indicated.

4.5.2 Generation of *Mycl1*^{gfp} mice.

The *Mycl1*-gfp targeting construct was assembled using MultiSite Gateway Technology (Invitrogen). The pENTR-lox-GFP.Neo plasmid was constructed as published[18]. The 5′ homology arm (1584 bp) was amplified by PCR from EDJ22 ESC genomic DNA (129S6/SvEvTac background) using the following oligonucleotides, which contain attB4 and attB1 sites: 5′- GGGGACAACTTTGTATAGAAAAGTTGGTAGCCTGTTTATGATAACACA -3′ and 5′-GGGGACTGCTTTTTTGTACAAACTTGGTCCGCTCCCTGCGGGAGGG-3′. The BP recombination reaction between the attB4 and attB1-flanked PCR product and pDONR P4-P1R (Invitrogen) resulted in the pENTR-Mycl1-5HA plasmid. The 3′ homology arm (3497 bp) was amplified by PCR from EDJ22 ESC genomic DNA using the following oligonucleotides, which contain attB2 and attB3 sites: 5′-GGGGACAGCTTTCTTGTACAAAGTGGGTAAGGACCACCCGGGGGCT-3′ and 5′-GGGGACAACTTTGTATAATAAAGTTGTTAGTAGCCACTGAGGTACG-3′. The BP recombination reaction between the attB2 and attB3-flanked PCR product and pDONR P2R-P3 (Invitrogen) resulted in the pENTR-Mycl1-3HA plasmid. A LR recombination reaction was performed using pENTR-Mycl1-5HA, pENTR-lox-GFP.Neo, pENTR-Mycl1-3HA, and pDEST

DTA-MLS[103] to generate the final targeting construct. The SwaI linearized vector was electroporated into EDJ22 embryonic stem cells (129SvEv background), and targeted clones were identified by Southern blot analysis. Probes were amplified from genomic DNA using the following primers: Mycl1_ProbeA_Fwd, TGCATGCCTGACAACAAGAC; Mycl1_ProbeA_Rev, CCAATTCATCTAGAATCCTACA; Mycl1_ProbeB_Fwd, ATGCTATTCTGAGGCCATTTG; and Mycl1_ProbeB_Rev, GCCCCTTGATGTGTGCATAC. Blastocyst injections were performed and resulting male chimeras were bred to female 129S6/SvEvTac mice. Genotyping was conducted by PCR to confirm germline transmission and to determine the genotype of progeny mice using primers Mycl15UTR_Fwd (TGAACTCGCTCCCCTCAG), Mycl1Exon1_Rev (GCACCAGCTCGAATTTCTTC), and Mycl1GFP_Rev (AAGTCGTGCTGCTTCATGTG) which resulted in WT band of 337 bp and KO band of 525 bp. For indicated experiments *Mycl1*^{gfp} mice were backcrossed to C57BL/6J for at least seven generations. The loxP-flanked neo resistance cassette was removed from the germline by crossing to B6.C-Tg(CMV-cre)1Cgn/J (The Jackson Laboratory) at F4 and loss of the CMV-cre transgene in subsequent generations was confirmed by PCR.

4.5.3 Generation of L-MYC-specific rabbit polyclonal antibody and immunoblot analysis.

Murine full-length *Mycl1* cDNA was PCR amplified from splenic CD8α^+ cDC cDNA library. The resulting PCR product was ligated into the expression vector pET-28a(+) (Novagen) downstream of the His-Tag and the final plasmid was transformed into the *Escherichia coli* expression strain BL21-CodonPlus(DE3)-RIL (Stratagene). Recombinant L-MYC was expressed for 12 hours at room temperature and then affinity purified on Ni-NTA His·Bind® Resin (Novagen) according to manufacturer's instructions. Purified recombinant L-MYC was used to

immunize New Zealand White Rabbits (Harlan Laboratories) according to a standard 112-day protocol. Finally, rabbit anti-mouse L-MYC sera were collected and L-MYC-specific antibody was affinity purified and tested by Western blot analysis.

For immunoblot analysis, either whole-cell extracts were prepared with RIPA lysis buffer containing protease inhibitors, or nuclei were obtained after cellular lysis with buffer containing 0.2% Nonidet P40 as described[104]. Extracts were denatured in Laemmli sample buffer at 95°C for 10 minutes, and $5x10^5$ to $1x10^6$ cell equivalent of denatured extract was loaded per well of a 7.5% precast mini polyacrylamide gel (Bio-Rad). Proteins were then transferred onto a nitrocellulose membrane using a Trans-Blot SD Semi-Dry Transfer Cell (Bio-Rad) according to manufacturer's instructions. Blots were blocked with a solution containing 5% non-fat milk and 0.05% Tween-20 for 1 hour at room temperature and then incubated with primary antibody overnight at 4ºC. After extensive washing, blots were incubated with a goat anti-rabbit IgG (H+L) conjugated to horseradish peroxidase (Jackson ImmunoResearch Laboratories, Inc.) for 1 hour at room temperature. Finally, blots were developed with ECL Western Blotting Substrate (Thermo Scientific) according to manufacturer's instructions.

c-MYC Western blot analysis was performed similarly to the abovementioned protocol except a commercial rabbit anti-c-Myc antibody (Y69) was used (Abcam). Rabbit anti-GFP antibody (sc-8334, Santa Cruz Biotechnology, Inc.) and Rabbit anti-HDAC1 (Abcam) were used to determine equivalent loading across blots.

4.5.4 BrdU incorporation and cell-cycle analysis.

For *in vivo* BrdU-incorporation studies, mice of the C57BL/6 genetic background were injected intraperitoneally (i.p.) with 2 mg BrdU (Sigma) or intravenously (i.v.) with 1 mg BrdU in pyrogen-free saline. Splenocytes were harvested after 4 hours for i.p. injected and 1 hour for i.v. injected mice. Intracellular BrdU staining was performed with APC BrdU Flow Kit (BD Pharmingen) according to manufacturer's instructions following cell-surface staining. I*n vitro* BrdU-incorporation studies to determine the frequency of cells in S phase of cell cycle were performed on sorted populations, which were then cultured for 24 hours in 100 ng/ml Flt3 ligand (Flt3L). To detect cells in S phase of cell cycle, 10 μM BrdU was added for the last 4 hours of culture, after which cells were fixed, permeablized, and stained according to APC BrdU Flow Kit instructions. Analysis was performed on a BD FACS CANTO II (BD Biosciences) and the event rate was maintained below 300 events per second on the lowest flow rate to ensure doublet exclusion. Total frequency of cells in S/G2/M phase of cell cycle was determined by DAPI staining of isolated populations as described previously[105].

4.5.5 Pathogen infections.

Listeria monocytogenes expressing a secreted form of OVA (LM-OVA[106]) was a gift from Dr. H. Shen (University of Pennsylvania School of Medicine, Philadelphia, PA). LM-OVA was stored as glycerol stocks at −80ºC and diluted into pyrogen-free saline for i.v. injection into mice. Mice were infected with $3x10^3$ LM-OVA and sacrificed 7 days later for T cell analysis unless otherwise indicated. Vesicular stomatitis virus encoding full-length ovalbumin (VSV-OVA) was a gift from Dr. L. Lefrancois (University of Connecticut Health Center, Farmington, CT)[107]. VSV-OVA stocks were stored in PBS at -80ºC and diluted into pyrogen-free PBS prior to

injections into mice. Mice were infected i.v. with $5x10^6$ PFU of virus and sacrificed 7 days later for T cell analysis unless otherwise indicated.

For lethal infectious challenge, the wild-type *L. monocytogenes* strain EGD was used in this study[80]. *Listeria* was stored as glycerol stocks at -80°C and diluted into pyrogen-free saline for i.v. injection into mice. A dose of 100,000 CFU diluted from concentrated frozen stocks was determined to be 80-90% lethal for 8-week-old wild-type male mice on the C57BL/6 genetic background. *Mycl1*$^{gpf/gfp}$ mice on the 129SvEv genetic background were backcrossed for 10 generations with mice on the C57BL/6 genetic background to establish *Mycl1*$^{gfp/gfp}$ mice on C57BL/6 background for lethal *Listeria* challenge.

Toxoplasma gondii: The type II Prugniaud strain of T. gondii expressing a firefly luciferase and GFP transgene (PRU-FLuc-GFP) (provided by J. Boothroyd, Stanford University, Palo Alto, CA) was used in all tachyzoite experiments. The parasites were grown in culture in human foreskin fibroblasts as previously described[108]. For infections, freshly egressed parasites were filtered, counted, and injected intraperitoneally into mice. C57BL/6, 129S6/SvEv, and BALB/c mice were infected with 100, 200, and 1,000 tachyzoites, respectively, for most experiments. BALB/c mice used for tetramer studies were infected with 5,000 tachyzoites. BALB/c bone marrow chimeras and controls were infected with 100 tachyzoites.

*Citrobacter rodentium***:** Mice were infected by intraoral inoculation of 2 × 109 colony-forming units of C. rodentium, strain DBS100 (American Type Culture Collection) as described[109]. Survival and weight loss were monitored for 30–45 d. Survival studies were done in accordance with institutional guidelines and with protocols approved by the Animal Studies Committee at Washington University in St. Louis.

4.5.6 Sorting of pathogen infected tissue.

Mice were infected with $5x10^5$ CFU LM-EGD (2 hour time point), $1x10^5$ CFU LM-EGD (24 hour time point), or $8x10^4$ CFU LM-EGD (60 hour time point) as previously described[82]. Single cell suspensions were prepared with collagenase B and DNAse I in the presence of 5 μg/ml gentamicin. After ACK lysis of red blood cells, splenocytes were switched to MACS buffer for enrichment of CD11c-expressing cells (following manufacturers guidelines). Samples were then stained and sorted on an ARIA II directly into MACS buffer. Samples were then spun down at 400xg for 5min, buffer was removed and cell lysed in PBS + 0.05% Triton-X 100. Lysates were plated on BHI agar plates and colon forming units were quantitated 24 hours later.

4.5.7 *In vitro* T cell restimulation after LM-OVA or VSV-OVA infection.

7 days after infection, spleens were mechanically disrupted, red blood cells were lysed with ACK lysis buffer, and single cell suspensions were counted on a Vi-CELL (Beckman Coulter). 2×10^6 splenocytes were restimulated for 5 hours in the presence of 1 μg/mL Brefeldin A and 5μM of either OVA peptide (257-264) or LLO peptide (190-201) (Anaspec) to activate either CD8 T cells or CD4 T cells, respectively. After restimulation, splenocytes were surface stained with antibodies to identify T cell populations, fixed in paraformaldehyde and stained for intracellular IFN-γ and TNF-α in a saponin-based buffer. Dead cells were excluded with LIVE/DEAD® Fixable Aqua Dead Cell Stain Kit (Invitrogen) according to manufacturer's instructions and analysis was performed on a BD FACS CANTO II.

4.5.8 Quantitative RT-PCR.

Wild-type myeloid and lymphoid cells from spleens of C57BL/6 mice were sorted to greater than 95% purity on a BD FACSAria II (BD Biosciences). DNase-treated total RNA was prepared with RNeasy Micro Kit (Qiagen) and first-strand cDNA synthesis was performed with SuperScript III Reverse Transcriptase (Invitrogen) using Oligo(dT)20 Primer (Invitrogen). Relative quantitation of gene expression was performed on a StepOnePlus Real-Time PCR System (Applied Biosystems) according to the Relative Standard Curve method and using HotStart-IT SYBR Green qPCR Master Mix (Affymetrix/USB). PCR conditions were 10 min at 95°C, followed by 40 two-step cycles consisting of 15 sec at 95°C and 1 min at 60°C. Primers used for L-Myc (*Mycl1*) and *Hprt* expression were as follows: *Mycl1*_qPCR_ Fwd, CCCCAGCGATTCTGAAGGT; *Mycl1*_qPCR_ Rev, TGTCCAGAGATCGCCTCTTCTC; *Hprt*-F, TCAGTCAACGGGGGACATAAA; and *Hprt*-R, GGGGCTGTACTGCTTAACCAG.

4.5.9 Expression microarray analysis.

Bone marrow (BM) pDCs (gated as $CD11c^{+}SiglecH^{+}B220^{+}MHCII^{+}$) from wild type (WT) and *Mycl1*$^{gfp/gfp}$ mice of the 129SvEv genetic background were sorted to greater than 95% purity on a BD FACSAria II (BD Biosciences). Splenic $CD8\alpha^{+}$ cDC (gated as $CD11c^{+}MHCII^{+}CD205^{+}CD8\alpha^{+}CD11b^{-}B220^{-}$) and $CD8\alpha^{-}$ cDC (gated as $CD11c^{+}MHCII^{+}CD11b^{+}$ $CD205^{-}CD8\alpha^{-}B220^{-}$) from WT and *Mycl1*$^{gfp/gfp}$ mice of the C57BL/6 genetic background were similarly sorted. DNase-treated total RNA was isolated from cells using the Ambion RNAqueous-Micro Kit. For Mouse Gene 1.0 ST Arrays, RNA was amplified with the Ovation Pico WTA System (NuGEN), and then fragmentation and labeling was performed with Encore Biotin Module (NuGEN). Background-corrected expression values were

normalized using RMA quantile normalization and expression values were modeled using ArrayStar software (DNASTAR). All original microarray data have been deposited in NCBI's Gene Expression Omnibus (GEO) and are accessible through GEO: Myc family expression values were determined from the following published microarray datasets: hematopoietic progenitors (GSE14833, GSE20244), dendritic cell (DC) progenitors (GSE37030), mature DC subsets (GSE9810). Gene Set Enrichment Analysis (GSEA)[67] tool (Broad Institute, MIT) was used to compare lung and lymph node dendritic cell gene expression profiles. We used the "KEGG_Cell_Cycle" list under C2 (curated gene sets). Since 3 biological replicates were available per tissue, enrichment was assessed through the use of gene-set permutations (x1000) and $\log_2$ ratio of classes as metric for ranking genes. Lung and mediastinal lymph node $CD103^+$ DC microarrays were obtained from the Immunological Genome Project dataset (GSE15907). Microarray data of wild-type and L-Myc-deficient dendritic cells have been deposited in GEO as GSE53312.

4.5.10 Immunofluorescence microscopy.

Spleens and lymph nodes were fixed in 2% methanol-free paraformaldehyde (Electron Microscopy Sciences) for 12 hours followed by incubation in 30% sucrose/H_2O overnight, embedded in OCT compound, and cryosectioned at 7 microns. Staining of sections, image acquisition and processing were performed as published[18]. Briefly, sections were blocked/stained in CAS Block (Invitrogen) supplemented with 0.2% TritonX-100 and mounted with ProLong Gold Antifade reagent containing DAPI (Invitrogen). Monochrome images were acquired with either 10X or 20X objective and exported into ImageJ software for subsequent color balancing and overlaying.

4.5.11 Dendritic cell and macrophage preparation.

Dendritic cells from lymphoid organs and non-lymphoid organs were harvested and prepared as described[110]. Briefly, spleens and lymph nodes were minced and digested in 5 ml Iscove's modified Dulbecco's media + 10% FCS (cIMDM) with 250 μg/ml collagenase B (Roche) and 30 U/ml DNase I (Sigma-Aldrich) for 30 min at 37°C with stirring. Cells were passed through a 70-μm strainer before red blood cell (RBC) lysis. Cells were then counted on a Vi-CELL analyzer, and 5–10 × 10^6 cells were used per antibody staining reaction. Lung, liver, and kidney cell suspensions were prepared after perfusion with 10 ml Dulbeccos PBS. Dissected and minced tissues were digested in 5ml cIMDM with 4mg/ml collagenase D (Roche) for 1 h at 37°C with stirring. Digested tissues were filtered and RBCs lysed as above. Cells from the peritoneal cavity were collected by flushing with 10 ml PBS+5%FCS and 2mM EDTA. Epidermal and dermal cell suspensions were prepared as described previously[111]. Microglia were isolated as described previously [105]. Lastly, small intestine lamina propria cells were isolated as described previously[112].

4.5.12 *In vitro* BM-derived dendritic cells.

Femurs and tibias were manually flushed to collect BM cells, and then RBCs were lysed in ACK lysis buffer. To obtain Flt3-ligand derived pDC and cDC equivalents, BM cells were cultured in complete IMDM at a density of 2×10^6 cells/ml containing 150 ng/ml murine Flt3L (Peprotech) for 9 or 10 days. Alternatively, GM-CSF DCs were obtained by culturing BM cells in complete IMDM at a density of 6x10^5 cells/ml containing 20ng/ml murine GM-CSF (Peprotech) for 8 days. Non-adherent cells were collected for FACS analysis or sorting. Sorted progenitors were cultured at a density of 50x10^4 cells/ml for either 24 hours or 4 days in 100 ng/ml Flt3L.

4.5.13 Plasmids and retroviral infection of DCs.

cDNA for *Mycl1* was generated by PCR from cDNA of CD8α$^+$ DCs. We used the previously described method for generating a functional Myc-ER fusion protein[88], which placed a segment of the estrogen receptor (ER) at the C-terminus of the Myc protein. Specifically, the cDNA for ER^{T2} was obtained by PCR from the p-Cre-ER^{T2} vector (a gift from Dr. T. Egawa, Washington University School of Medicine, St. Louis, MO) and cloned into the retroviral plasmid MSCV-IRES-GFP, creating the construct ER^{T2}-MSCV-IRES-GFP. After removing the stop codon, *Mycl1* cDNA was cloned upstream of the ER^{T2} sequence derived from Cre-ER^{T2} (ref [113,114]), creating the plasmid L-Myc-ER^{T2}-MSCV-IRES-GFP. Retroviral plasmids were transfected into Phoenix E packaging cells as described previously[115], and Flt3-ligand cultures were infected as described previously[7] except infections were performed on day 4. cDNA for murine *Irf8* and *Myc* were generated by PCR from cDNA of splenocytes of C57BL/6 mice, sequenced to confirm identity, and cloned into the MSCV-IRES-GFP retroviral plasmid.

For transduction of macrophage-dendritic cell progenitors (MDP), we isolated MDPs from the bone marrow (BM) of 6-week-old C57BL/6 mice and cultured them for 12 h in Flt3-ligand before transduction. Transduced MDPs were allowed to differentiate for an additional 5 days before analysis.

4.5.14 Antibodies and flow cytometry.

Staining was performed at 4°C in the presence of Fc block (clone 2.4G2, BD Biosciences) in FACS buffer (PBS, 0.5% BSA, 2 mm EDTA). The following antibodies were purchased from BD Biosciences: V450 and PerCP-Cy5.5 anti-NK1.1 (PK136), V450 anti-Ly6C/G (RB6-8C5), V450 anti-Ly6C (AL21), V500 anti-B220 (RA3-6B2), PE and PE-Cy7 anti-CD8α (53-6.7), PE-

Cy7 and APC anti-CD4 (RM4-5), PE-Cy7 anti-CD24 (M1/69), PerCP-Cy5.5 anti-Ly6G (1A8), FITC and APC anti-CD172a/Sirpα (P84). These antibodies were purchased from eBioscience: PE anti-NKp46 (29A1.4), PerCP-Cy5.5 and AlexaFluor700 anti-CD11b (M1/70), APCeFluor780 anti-CD11c (N418), PE anti-CD103 (2E7), APC anti-CD317/BST2 (eBio927), eFluor450 anti-MHCII (I-A/I-E) (M5/114.15.2), FITC and APC anti-CD45.2 (104), PE-Cy7 and PerCP-Cy5.5 anti-CD45.1 (A20), PerCP-Cy5.5 anti-CD16/32 (93), PE-Cy7 anti-cKit (2B8), eFluor450 anti-CD105 (MJ7/18), eFluor450 and Biotin anti-Ter119, PE anti-CD135 (A2F10), AlexaFluor700 and PerCP-Cy5.5 anti-Sca1 (D7), FITC, APC and PerCP-eFluor710 anti-SiglecH (eBio440C), Biotin and APC anti-CD115 (AFS98). These antibodies were purchased from Miltenyi: PE anti-CD205/Dec205 (NLDC-145) and APC anti-CD205/Dec205 (NLDC-145). These antibodies were purchased from Invitrogen: APC anti-F4/80 (BM8), PE anti-B220 (RA3-6B2), FITC and APC anti-CD8α (5H10). These antibodies were purchased from Biolegend: PE and APC anti-SiglecH (551), Biotin anti-Ly6G (1A8), Biotin anti-MHCII (M5/114.15.2).

4.5.15 Luciferase Imaging

Imaging was done as previously described [116]. In brief, mice were given intraperitoneal injections of D-Luciferin (Biosynth AG, Switzerland) at 150 mg/kg and allowed to remain active for 5 min. Animals were then anesthetized with 2% isoflurane for 5 min and then imaged with a Xenogen IVIS 200 machine (Caliper Life Sciences). Data were analyzed with the Living Image software (Caliper Life Sciences).

4.5.16 Statistical analysis.

Analysis of all data was done with Prism 6 (GraphPad Software, Inc.). *P* values were calculated with Student's *t* test, Mann-Whitney test, or analysis of variance (ANOVA) with appropriate *post hoc* test as specified in figure legends. Statistical analysis of mouse survival was determined using log-rank test. *P* values less than 0.05 were considered significant.

4.6 Author Contributions

W.K. and K.M. designed the study. W.K. performed all experiments and analysis of *Mycl1*^{gfp} mice with contributions from individual co-authors. W.K. generated *Mycl1*^{gfp} mice with gene-targeting assistance from J.A. and A.S. A.S. contributed to generating DC progenitor microarrays (with guidance from D.B.), monocyte culture experiments and immunofluorescence experiments. B.E., X.W., C.B., N.K. contributed to experiments related to *L. monocytogenes* infection. A.R. performed VSV infections. X.W. provided assistance with the manuscript.

4.7 References

1. Dang,C.V. MYC on the path to cancer. *Cell* **149**, 22-35 (2012).

2. Eilers,M. & Eisenman,R.N. Myc's broad reach. *Genes Dev.* **22**, 2755-2766 (2008).

3. Charron,J. *et al.* Embryonic lethality in mice homozygous for a targeted disruption of the N-myc gene. *Genes Dev.* **6**, 2248-2257 (1992).

4. Davis,A.C., Wims,M., Spotts,G.D., Hann,S.R. & Bradley,A. A null c-myc mutation causes lethality before 10.5 days of gestation in homozygotes and reduced fertility in heterozygous female mice. *Genes Dev.* **7**, 671-682 (1993).

5. Hatton,K.S. *et al.* Expression and activity of L-Myc in normal mouse development. *Mol. Cell Biol.* **16**, 1794-1804 (1996).

6. Pirity,M., Blanck,J.K. & Schreiber-Agus,N. Lessons learned from Myc/Max/Mad knockout mice. *Curr. Top. Microbiol. Immunol.* **302**, 205-234 (2006).

7. Tussiwand,R. *et al.* Compensatory dendritic cell development mediated by BATF-IRF interactions. *Nature* **490**, 502-507 (2012).

8. Guermonprez,P. *et al.* Inflammatory Flt3l is essential to mobilize dendritic cells and for T cell responses during Plasmodium infection. *Nat. Med.* **19**, 730-738 (2013).

9. Lauvau,G. *et al.* Priming of memory but not effector CD8 T cells by a killed bacterial vaccine. *Science* **294**, 1735-1739 (2001).

10. Satpathy,A.T., Wu,X., Albring,J.C. & Murphy,K.M. Re(de)fining the dendritic cell lineage. *Nat. Immunol.* **13**, 1145-1154 (2012).

11. Murphy,K.M. Comment on "Activation of beta-catenin in dendritic cells regulates immunity versus tolerance in the intestine". *Science* **333**, 405 (2011).

12. Geissmann,F., Gordon,S., Hume,D.A., Mowat,A.M. & Randolph,G.J. Unravelling mononuclear phagocyte heterogeneity. *Nat Rev Immunol* **10**, 453-460 (2010).

13. Hume,D.A. Applications of myeloid-specific promoters in transgenic mice support in vivo imaging and functional genomics but do not support the concept of distinct macrophage and dendritic cell lineages or roles in immunity. *J. Leukoc. Biol.* **89**, 525-538 (2011).

14. Bar-On,L. & Jung,S. Defining in vivo dendritic cell functions using CD11c-DTR transgenic mice. *Methods Mol Biol* **595**, 429-442 (2010).

15. Bennett,C.L. & Clausen,B.E. DC ablation in mice: promises, pitfalls, and challenges. *Trends Immunol* **28**, 525-531 (2007).

16. Miller,J.C. *et al.* Deciphering the transcriptional network of the dendritic cell lineage. *Nat. Immunol.* **13**, 888-899 (2012).

17. Gautier,E.L. *et al.* Gene-expression profiles and transcriptional regulatory pathways that underlie the identity and diversity of mouse tissue macrophages. *Nat. Immunol.* **13**, 1118-1128 (2012).

18. Satpathy,A.T. *et al.* Zbtb46 expression distinguishes classical dendritic cells and their committed progenitors from other immune lineages. *J. Exp. Med.* **209**, 1135-1152 (2012).

19. Meyer,N. & Penn,L.Z. Reflecting on 25 years with MYC. *Nat. Rev. Cancer* **8**, 976-990 (2008).

20. Rahl,P.B. *et al.* c-Myc regulates transcriptional pause release. *Cell* **141**, 432-445 (2010).

21. Kim,K.T. *et al.* Constitutive Fms-like tyrosine kinase 3 activation results in specific changes in gene expression in myeloid leukaemic cells. *Br. J. Haematol.* **138**, 603-615 (2007).

22. Takahashi,S. Downstream molecular pathways of FLT3 in the pathogenesis of acute myeloid leukemia: biology and therapeutic implications. *J. Hematol. Oncol.* **4**, 13 (2011).

23. Kamath,A.T. *et al.* The development, maturation, and turnover rate of mouse spleen dendritic cell populations. *J. Immunol.* **165**, 6762-6770 (2000).

24. Waskow,C. *et al.* The receptor tyrosine kinase Flt3 is required for dendritic cell development in peripheral lymphoid tissues. *Nat Immunol* **9**, 676-683 (2008).

25. Liu,K. *et al.* Origin of dendritic cells in peripheral lymphoid organs of mice. *Nat Immunol* **8**, 578-583 (2007).

26. Chen,M. *et al.* Dendritic cell apoptosis in the maintenance of immune tolerance. *Science* **311**, 1160-1164 (2006).

27. Finn,R.D. *et al.* The Pfam protein families database. *Nucleic Acids Res.* **38**, D211-D222 (2010).

28. Lattin,J.E. *et al.* Expression analysis of G Protein-Coupled Receptors in mouse macrophages.*Immunome. Res* **4**, 5 (2008).

29. Schiavoni,G. *et al.* ICSBP is essential for the development of mouse type I interferon-producing cells and for the generation and activation of CD8alpha(+) dendritic cells. *J Exp. Med.* **196**, 1415-1425 (2002).

30. Park,C.S. *et al.* Kruppel-like factor 4 (KLF4) promotes the survival of natural killer cells and maintains the number of conventional dendritic cells in the spleen. *J. Leukoc. Biol.* **91**, 739-750 (2012).

31. Feinberg,M.W. *et al.* The Kruppel-like factor KLF4 is a critical regulator of monocyte differentiation. *EMBO J.* **26**, 4138-4148 (2007).

32. Hacker,C. *et al.* Transcriptional profiling identifies Id2 function in dendritic cell development. *Nat Immunol* **4**, 380-386 (2003).

33. De Greve,J. *et al.* The human L-myc gene encodes multiple nuclear phosphoproteins from alternatively processed mRNAs. *Mol. Cell Biol.* **8**, 4381-4388 (1988).

34. DePinho,R.A., Hatton,K.S., Tesfaye,A., Yancopoulos,G.D. & Alt,F.W. The human myc gene family: structure and activity of L-myc and an L-myc pseudogene. *Genes Dev.* **1**, 1311-1326 (1987).

35. Legouy,E. *et al.* Structure and expression of the murine L-myc gene. *EMBO J.* **6**, 3359-3366 (1987).

36. Rudin,C.M. *et al.* Comprehensive genomic analysis identifies SOX2 as a frequently amplified gene in small-cell lung cancer. *Nat. Genet.* **44**, 1111-1116 (2012).

37. Laurenti,E. *et al.* Hematopoietic stem cell function and survival depend on c-Myc and N-Myc activity. *Cell Stem Cell* **3**, 611-624 (2008).

38. de Alboran,I.M. *et al.* Analysis of C-MYC function in normal cells via conditional gene-targeted mutation. *Immunity* **14**, 45-55 (2001).

39. Malynn,B.A. *et al.* N-myc can functionally replace c-myc in murine development, cellular growth, and differentiation. *Genes Dev.* **14**, 1390-1399 (2000).

40. Calado,D.P. *et al.* The cell-cycle regulator c-Myc is essential for the formation and maintenance of germinal centers. *Nat. Immunol.* **13**, 1092-1100 (2012).

41. Reavie,L. *et al.* Regulation of hematopoietic stem cell differentiation by a single ubiquitin ligase-substrate complex. *Nat. Immunol.* **11**, 207-215 (2010).

42. Wang,R. *et al.* The transcription factor Myc controls metabolic reprogramming upon T lymphocyte activation. *Immunity* **35**, 871-882 (2011).

43. Onai,N. *et al.* Identification of clonogenic common Flt3(+) M-CSFR+ plasmacytoid and conventional dendritic cell progenitors in mouse bone marrow. *Nat.* **8**, 1207-1216 (2007).

44. Liu,K. *et al.* In vivo analysis of dendritic cell development and homeostasis. *Science* **324**, 392-397 (2009).

45. Du,X. *et al.* Genomic profiles for human peripheral blood T cells, B cells, natural killer cells, monocytes, and polymorphonuclear cells: comparisons to ischemic stroke, migraine, and Tourette syndrome. *Genomics* **87**, 693-703 (2006).

46. Lindstedt,M., Lundberg,K. & Borrebaeck,C.A. Gene family clustering identifies functionally associated subsets of human in vivo blood and tonsillar dendritic cells. *J. Immunol.* **175**, 4839-4846 (2005).

47. Kabashima,K. *et al.* Intrinsic lymphotoxin-beta receptor requirement for homeostasis of lymphoid tissue dendritic cells. *Immunity* **22**, 439-450 (2005).

48. Ma,A. *et al.* DNA binding by N- and L-Myc proteins. *Oncogene* **8**, 1093-1098 (1993).

49. Barrett,J., Birrer,M.J., Kato,G.J., Dosaka-Akita,H. & Dang,C.V. Activation domains of L-Myc and c-Myc determine their transforming potencies in rat embryo cells. *Mol. Cell Biol.* **12**, 3130-3137 (1992).

50. Huang,C.Y., Bredemeyer,A.L., Walker,L.M., Bassing,C.H. & Sleckman,B.P. Dynamic regulation of c-Myc proto-oncogene expression during lymphocyte development revealed by a GFP-c-Myc knock-in mouse. *Eur. J. Immunol.* **38**, 342-349 (2008).

51. Karsunky,H., Merad,M., Cozzio,A., Weissman,I.L. & Manz,M.G. Flt3 ligand regulates dendritic cell development from Flt3+ lymphoid and myeloid-committed progenitors to Flt3+ dendritic cells in vivo. *J. Exp. Med.* **198**, 305-313 (2003).

52. Bogunovic,M. *et al.* Origin of the lamina propria dendritic cell network. *Immunity* **31**, 513-525 (2009).

53. Varol,C. *et al.* Intestinal lamina propria dendritic cell subsets have different origin and functions. *Immunity* **31**, 502-512 (2009).

54. Kamath,A.T., Henri,S., Battye,F., Tough,D.F. & Shortman,K. Developmental kinetics and lifespan of dendritic cells in mouse lymphoid organs. *Blood* **100**, 1734-1741 (2002).

55. Jenkins,S.J. *et al.* Local macrophage proliferation, rather than recruitment from the blood, is a signature of TH2 inflammation. *Science* **332**, 1284-1288 (2011).

56. Schulz,C. *et al.* A lineage of myeloid cells independent of Myb and hematopoietic stem cells. *Science* **336**, 86-90 (2012).

57. Becker,A.M. *et al.* IRF-8 extinguishes neutrophil production and promotes dendritic cell lineage commitment in both myeloid and lymphoid mouse progenitors. *Blood* **119**, 2003-2012 (2012).

58. Tailor,P., Tamura,T., Morse,H.C. & Ozato,K. The BXH2 mutation in IRF8 differentially impairs dendritic cell subset development in the mouse. *Blood* **111**, 1942-1945 (2008).

59. Inaba,K. *et al.* Generation of large numbers of dendritic cells from mouse bone marrow cultures supplemented with granulocyte/macrophage colony-stimulating factor. *J Exp. Med.* **176**, 1693-1702 (1992).

60. Sallusto,F. & Lanzavecchia,A. Efficient presentation of soluble antigen by cultured human dendritic cells is maintained by granulocyte/macrophage colony-stimulating factor plus interleukin 4 and downregulated by tumor necrosis factor alpha. *J Exp. Med.* **179**, 1109-1118 (1994).

61. Glasmacher,E. *et al.* A Genomic Regulatory Element That Directs Assembly and Function of Immune-Specific AP-1-IRF Complexes. *Science* **338**, 975-980 (2012).

62. Sears,R. *et al.* Multiple Ras-dependent phosphorylation pathways regulate Myc protein stability. *Genes Dev.* **14**, 2501-2514 (2000).

63. Lutterbach,B. & Hann,S.R. Hierarchical phosphorylation at N-terminal transformation-sensitive sites in c-Myc protein is regulated by mitogens and in mitosis. *Mol. Cell Biol.* **14**, 5510-5522 (1994).

64. Popov,N., Schulein,C., Jaenicke,L.A. & Eilers,M. Ubiquitylation of the amino terminus of Myc by SCF(beta-TrCP) antagonizes SCF(Fbw7)-mediated turnover. *Nat. Cell Biol.* **12**, 973-981 (2010).

65. Scott,C.L. *et al.* Functional analysis of mature hematopoietic cells from mice lacking the beta c chain of the granulocyte-macrophage colony-stimulating factor receptor. *Blood* **92**, 4119-4127 (1998).

66. Greter,M. *et al.* GM-CSF Controls Nonlymphoid Tissue Dendritic Cell Homeostasis but Is Dispensable for the Differentiation of Inflammatory Dendritic Cells. Immunity 36(6), 1031-1046. 2012. Ref Type: Generic

67. Subramanian,A. *et al.* Gene set enrichment analysis: a knowledge-based approach for interpreting genome-wide expression profiles. *Proc. Natl. Acad. Sci. U. S A* **102**, 15545-15550 (2005).

68. Loven,J. *et al.* Revisiting global gene expression analysis. *Cell* **151**, 476-482 (2012).

69. Nie,Z. *et al.* c-Myc is a universal amplifier of expressed genes in lymphocytes and embryonic stem cells. *Cell* **151**, 68-79 (2012).

70. Lin,C.Y. *et al.* Transcriptional amplification in tumor cells with elevated c-Myc. *Cell* **151**, 56-67 (2012).

71. Passmore,L.A. *et al.* The eukaryotic translation initiation factors eIF1 and eIF1A induce an open conformation of the 40S ribosome. *Mol. Cell* **26**, 41-50 (2007).

72. van Riggelen,J., Yetil,A. & Felsher,D.W. MYC as a regulator of ribosome biogenesis and protein synthesis. *Nat. Rev. Cancer* **10**, 301-309 (2010).

73. Mashayekhi,M. *et al.* CD8a+ Dendritic Cells Are the Critical Source of Interleukin-12 that Controls Acute Infection by Toxoplasma gondii Tachyzoites. *Immunity* **35**, 249-259 (2011).

74. Satpathy,A.T. *et al.* Notch2-dependent classical dendritic cells orchestrate intestinal immunity to attaching-and-effacing bacterial pathogens. *Nat. Immunol.* (2013).

75. Shortman,K. & Heath,W.R. The CD8+ dendritic cell subset. *Immunol Rev* **234**, 18-31 (2010).

76. Hildner,K. *et al.* Batf3 deficiency reveals a critical role for CD8alpha+ dendritic cells in cytotoxic T cell immunity. *Science* **322**, 1097-1100 (2008).

77. Swiecki,M., Gilfillan,S., Vermi,W., Wang,Y. & Colonna,M. Plasmacytoid dendritic cell ablation impacts early interferon responses and antiviral NK and CD8(+) T cell accrual. *Immunity* **33**, 955-966 (2010).

78. Lewis,K.L. *et al.* Notch2 receptor signaling controls functional differentiation of dendritic cells in the spleen and intestine. *Immunity* **35**, 780-791 (2011).

79. Diamond,M.S. *et al.* Type I interferon is selectively required by dendritic cells for immune rejection of tumors. *J. Exp. Med.* **208**, 1989-2003 (2011).

80. Edelson,B.T. *et al.* CD8a+ Dendritic Cells Are an Obligate Cellular Entry Point for Productive Infection by Listeria monocytogenes. *Immunity* **35**, 236-248 (2011).

81. Verschoor,A. *et al.* A platelet-mediated system for shuttling blood-borne bacteria to CD8alpha+ dendritic cells depends on glycoprotein GPIb and complement C3. *Nat. Immunol.* **12**, 1194-1201 (2011).

82. Neuenhahn,M. *et al.* CD8alpha+ dendritic cells are required for efficient entry of Listeria monocytogenes into the spleen. *Immunity* **25**, 619-630 (2006).

83. Belz,G.T., Shortman,K., Bevan,M.J. & Heath,W.R. CD8alpha+ dendritic cells selectively present MHC class I-restricted noncytolytic viral and intracellular bacterial antigens in vivo. *J Immunol* **175**, 196-200 (2005).

84. Muraille,E. *et al.* Distinct in vivo dendritic cell activation by live versus killed Listeria monocytogenes. *Eur. J Immunol* **35**, 1463-1471 (2005).

85. Aichele,P. *et al.* Macrophages of the splenic marginal zone are essential for trapping of blood-borne particulate antigen but dispensable for induction of specific T cell responses. *J. Immunol.* **171**, 1148-1155 (2003).

86. Carrero,J.A., Calderon,B. & Unanue,E.R. Lymphocytes are detrimental during the early innate immune response against Listeria monocytogenes. *J Exp. Med.* **203**, 933-940 (2006).

87. Trumpp,A. *et al.* c-Myc regulates mammalian body size by controlling cell number but not cell size. *Nature* **414**, 768-773 (2001).

88. Murphy,D.J. *et al.* Distinct thresholds govern Myc's biological output in vivo. *Cancer Cell* **14**, 447-457 (2008).

89. Gomez-Roman,N., Grandori,C., Eisenman,R.N. & White,R.J. Direct activation of RNA polymerase III transcription by c-Myc. *Nature* **421**, 290-294 (2003).

90. Chandriani,S. *et al.* A core MYC gene expression signature is prominent in basal-like breast cancer but only partially overlaps the core serum response. *PLoS One* **4**, e6693 (2009).

91. Oster,S.K., Mao,D.Y., Kennedy,J. & Penn,L.Z. Functional analysis of the N-terminal domain of the Myc oncoprotein. *Oncogene* **22**, 1998-2010 (2003).

92. Wasylishen,A.R. *et al.* New model systems provide insights into Myc-induced transformation. *Oncogene* **30**, 3727-3734 (2011).

93. Nakagawa,M., Takizawa,N., Narita,M., Ichisaka,T. & Yamanaka,S. Promotion of direct reprogramming by transformation-deficient Myc. *Proc. Natl. Acad. Sci. U. S A* **107**, 14152-14157 (2010).

94. Banchereau,J. & Steinman,R.M. Dendritic cells and the control of immunity. *Nature* **392**, 245-252 (1998).

95. Resnitzky,D. & Kimchi,A. Deregulated c-myc expression abrogates the interferon- and interleukin 6-mediated G0/G1 cell cycle arrest but not other inhibitory responses in M1 myeloblastic cells. *Cell Growth Differ.* **2**, 33-41 (1991).

96. Melamed,D., Tiefenbrun,N., Yarden,A. & Kimchi,A. Interferons and interleukin-6 suppress the DNA-binding activity of E2F in growth-sensitive hematopoietic cells. *Mol. Cell Biol.* **13**, 5255-5265 (1993).

97. Ramana,C.V. *et al.* Stat1-independent regulation of gene expression in response to IFN-gamma. *Proc. Natl. Acad. Sci. U. S. A* **98**, 6674-6679 (2001).

98. Pamer,E.G. Immune responses to Listeria monocytogenes. *Nat Rev Immunol* **4**, 812-823 (2004).

99. Mercado,R. *et al.* Early programming of T cell populations responding to bacterial infection. *J. Immunol.* **165**, 6833-6839 (2000).

100. Badovinac,V.P., Porter,B.B. & Harty,J.T. Programmed contraction of CD8(+) T cells after infection. *Nat Immunol* **3**, 619-626 (2002).

101. Moroy,T. *et al.* High frequency of myelomonocytic tumors in aging E mu L-myc transgenic mice. *J. Exp. Med.* **175**, 313-322 (1992).

102. Meredith,M.M. *et al.* Expression of the zinc finger transcription factor zDC (Zbtb46, Btbd4) defines the classical dendritic cell lineage. *J. Exp. Med.* **209**, 1153-1165 (2012).

103. Iiizumi,S. *et al.* Simple one-week method to construct gene-targeting vectors: application to production of human knockout cell lines. *Biotechniques* **41**, 311-316 (2006).

104. Dignam,J.D., Lebovitz,R.M. & Roeder,R.G. Accurate transcription initiation by RNA polymerase II in a soluble extract from isolated mammalian nuclei. *Nucleic Acids Res.* **11**, 1475-1489 (1983).

105. Ginhoux,F. *et al.* Fate Mapping Analysis Reveals That Adult Microglia Derive from Primitive Macrophages. *Science* **330**, 841-845 (2010).

106. Pope,C. *et al.* Organ-specific regulation of the CD8 T cell response to Listeria monocytogenes infection. *J Immunol* **166**, 3402-3409 (2001).

107. Kim,S.K. *et al.* Generation of mucosal cytotoxic T cells against soluble protein by tissue-specific environmental and costimulatory signals. *Proc. Natl. Acad. Sci. U. S A* **95**, 10814-10819 (1998).

108. Robben,P.M. *et al.* Production of IL-12 by macrophages infected with Toxoplasma gondii depends on the parasite genotype. *J Immunol* **172**, 3686-3694 (2004).

109. Zheng,Y. *et al.* Interleukin-22 mediates early host defense against attaching and effacing bacterial pathogens. *Nat. Med.* **14**, 282-289 (2008).

110. Edelson,B.T. *et al.* Peripheral CD103+ dendritic cells form a unified subset developmentally related to CD8alpha+ conventional dendritic cells. *J. Exp. Med.* **207**, 823-836 (2010).

111. Ginhoux,F. *et al.* Blood-derived dermal langerin+ dendritic cells survey the skin in the steady state. *J Exp. Med.* **204**, 3133-3146 (2007).

112. Lefrancois,L. & Lycke,N. Isolation of mouse small intestinal intraepithelial lymphocytes, Peyer's patch, and lamina propria cells. *Curr. Protoc. Immunol.* **Chapter 3**, Unit (2001).

113. Feil,R., Wagner,J., Metzger,D. & Chambon,P. Regulation of Cre recombinase activity by mutated estrogen receptor ligand-binding domains. *Biochem. Biophys. Res. Commun.* **237**, 752-757 (1997).

114. Mahfoudi,A., Roulet,E., Dauvois,S., Parker,M.G. & Wahli,W. Specific mutations in the estrogen receptor change the properties of antiestrogens to full agonists. *Proc. Natl. Acad. Sci. U. S A* **92**, 4206-4210 (1995).

115. Sedy,J.R. *et al.* B and T lymphocyte attenuator regulates T cell activation through interaction with herpesvirus entry mediator. *Nat. Immunol.* **6**, 90-98 (2005).

116. Saeij,J.P., Boyle,J.P., Grigg,M.E., Arrizabalaga,G. & Boothroyd,J.C. Bioluminescence imaging of Toxoplasma gondii infection in living mice reveals dramatic differences between strains. *Infect. Immun.* **73**, 695-702 (2005).

Chapter 5 *Bcl11a* controls Flt3 expression in early hematopoietic progenitors and is required for pDC development *in vivo*

The contents of this chapter have been previously published in *PLoS One.*
Wu X, Satpathy AT, KC W, Liu P, Murphy TL, Murphy KM. Bcl11a controls Flt3 expression in early hematopoietic progenitors and is required for pDC development in vivo. PLoS One. 2013 May 31;8(5)

5.1 Abstract

Bcl11a is a transcription factor known to regulate lymphoid and erythroid development. Recent bioinformatic analysis of global gene expression patterns has suggested a role for Bcl11a in the development of dendritic cell (DC) lineages. We tested this hypothesis by analyzing the development of DC and other lineages in *Bcl11a*$^{-/-}$ mice. We found that Bcl11a was required for expression of IL-7 receptor (IL-7R) and Flt3 in early hematopoietic progenitor cells. In addition, we found severely decreased numbers of plasmacytoid dendritic cells (pDCs) in *Bcl11a*$^{-/-}$ fetal livers and in the bone marrow of *Bcl11a*$^{-/-}$ fetal liver chimeras. Moreover, *Bcl11a*$^{-/-}$ cells showed severely impaired *in vitro* development of Flt3L-derived pDCs and classical DCs (cDCs). In contrast, we found normal *in vitro* development of DCs from *Bcl11a*$^{-/-}$ fetal liver cells treated with GM-CSF. These results suggest that the persistent cDC development observed in *Bcl11a*$^{-/-}$ fetal liver chimeras reflects derivation from a Bcl11a- and Flt3-independent pathway *in vivo*.

5.2 Introduction

Dendritic cells (DCs), comprising classical DCs (cDCs) and plasmacytoid DCs (pDCs), develop from a common DC progenitor (CDP) residing in the bone marrow (BM); unlike myeloid progenitors at earlier stages of development, CDPs have excluded monocyte and macrophage potential but give rise to all DC subsets at the clonal level [1-4]. Several transcription factors that act broadly in hematopoiesis are known to regulate the development of all DCs, including Ikaros [5,6], PU.1 [7,8], and Gfi1 [9]. Transcription factors that regulate specific subsets of DCs have also been reported. For example, E2-2 is required for development of pDCs [10], Batf3

for $CD8^+$ cDCs [11], Irf8 for pDCs and $CD8^+$ cDCs [12,13], and the NF-κB family member RelB for $CD4^+$ cDCs [5,14,15].

A bioinformatic analysis of global gene expression patterns has identified groups of transcription factors that may be involved in fate decisions along the DC lineage [16]. Among genes that increase in expression from the macrophage–DC progenitor (MDP) to the CDP, those that do not increase in expression from the MDP to the monocyte were labeled in that analysis as possible promoters of DC commitment. Transcription factors identified by these criteria include some previously associated only with pDC development, including E2-2 and Spi-B [17,18], and some previously associated only with cDCs, including Zbtb46 [19,20]. Other factors identified in this analysis include Irf8, Bcl11a, and Runx2. Recently, it has been demonstrated in the setting of competitive BM reconstitution that Irf8 promotes the development of all DC subsets [21], even though *Irf8*$^{-/-}$ mice in other settings do not show defects in $CD4^+$ cDC development [12,13]. We wondered, therefore, whether a similar early role in DC development could be identified for another factor such as Bcl11a.

Bcl11a was first described as a gene located at a common proviral integration site in BXH2 myeloid leukemias, and its human ortholog was found to be a recurrent target of translocations in B cell malignancies [22,23]. This gene encodes a Krüppel-like zinc finger transcription factor expressed in neural and lymphoid tissues that is essential for the development of B cells and for thymocyte maturation [24]. In the erythroid lineage, BCL11A acts *in trans* to silence the fetal hemoglobin locus in cooperation with the transcription factor SOX6 [25,26]. Indeed, differences in stage-specific expression between human BCL11A and mouse Bcl11a account at least in part for interspecies differences in fetal hemoglobin expression patterns [25].

Although *Bcl11a* has been recognized as a useful marker of pDCs [27,28], its actual role in DC development remains unreported. Thus, we sought to examine DC development in the setting of Bcl11a deficiency *in vivo* and *in vitro*. We found that Bcl11a was required for normal expression of IL-7 receptor (IL-7R) as well as Flt3 in early hematopoietic progenitors. In addition, we observed a strict requirement for Bcl11a in pDC development and found evidence for a Bcl11a-independent pathway of cDC development *in vivo*.

5.3 Results

5.3.1 Bcl11a is required for development of CLPs and CDPs

During hematopoiesis, *Bcl11a* is expressed at similar levels in the hematopoietic stem cell (HSC), multipotent progenitor (MPP), common lymphoid progenitor (CLP), common myeloid progenitor (CMP), and megakaryocyte–erythroid progenitor (MEP) [16]. To study the function of Bcl11a in hematopoietic progenitors, we used mice targeted for deletion of the first exon of *Bcl11a* [24]. Since *Bcl11a*$^{-/-}$ mice die *in utero* or perinatally, we compared hematopoietic progenitor populations present in wild type (WT) and *Bcl11a*$^{-/-}$ fetal livers at embryonic day 14.5. First, we analyzed development of Lin^{-}Sca-1^{+}c-Kit^{+} (LSK), CLP, granulocyte-macrophage progenitor (GMP), MEP, and CDP populations (Figure 5.1). WT and *Bcl11a*$^{-/-}$ fetal livers showed comparable frequencies of GMPs and MEPs. However, *Bcl11a*$^{-/-}$ fetal livers showed a greater than twofold decrease in the frequency of LSK cells and more marked decreases in frequencies of IL-7R^{+} CLPs and Flt3^{+} CDPs relative to WT fetal livers (Figure 5.1**A, B**); within the LSK fraction, *Bcl11a*$^{-/-}$ fetal livers showed defects in both CD150 (Slamf1)$^{+}$ and CD150^{-} populations (Figure 5.1**C**). One study has demonstrated that a Sca-1^{lo}c-Kit^{+}Flt3^{+}CD150^{-}

population with granulocyte and macrophage potential (SL-GMP) can be identified which excludes mast cell potential [29]; GMPs in the *Bcl11a*$^{-/-}$ fetal liver, however, lacked Flt3 expression (data not shown) and no SL-GMP population could be identified (Figure 5.1**D**). Next, we analyzed hematopoietic development in chimeras produced by transferring WT or *Bcl11a*$^{-/-}$ fetal liver cells into lethally irradiated congenic recipient mice (Figure 5.2). Four to six weeks after transfer, donor-derived *Bcl11a*$^{-/-}$ BM showed decreased frequencies of LSK cells, CLPs, and CDPs but comparable frequencies of GMPs and MEPs relative to donor-derived WT BM (Figure 5.2**A, B**); within the LSK fraction, donor-derived *Bcl11a*$^{-/-}$ BM showed a greater proportion of CD150^{+} cells than did donor-derived WT BM, corresponding to a decrease in the overall frequency of the more differentiated CD150^{-} population (Figure 5.2**C**). As in *Bcl11a*$^{-/-}$ fetal livers, no SL-GMP population could be identified in donor-derived *Bcl11a*$^{-/-}$ BM (Figure 5.2**D**). In summary, the loss of Bcl11a in hematopoietic progenitors resulted in impaired development of LSK cells as well as a selective loss of CLPs and CDPs; these effects were observed both in the fetal stage and in the adult chimera, demonstrating that this factor is required in fetal and adult hematopoiesis.

Conceivably, the absence of IL-7R^{+} CLPs and Flt3^{+} CDPs in *Bcl11a*$^{-/-}$ fetal livers and BM could result from a requirement for Bcl11a in the development of the CLP and CDP or from a more restricted requirement for Bcl11a in the expression of IL-7R and Flt3, the surface markers that identify these populations. In either case, however, the loss of Bcl11a should result in DC defects because Flt3 ligand (Flt3L) signaling is essential for DC development in the steady state [30-32].

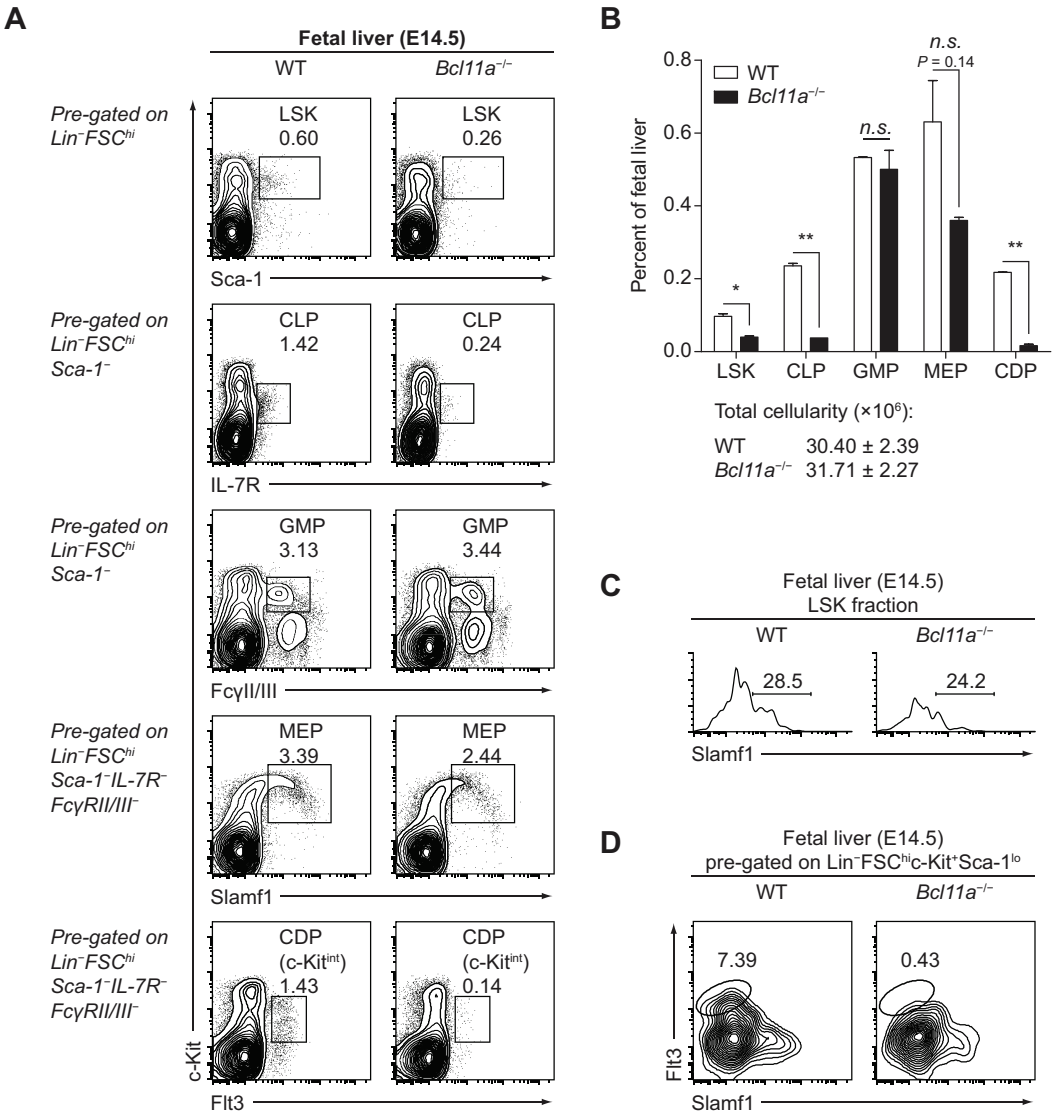

Figure 5.1:Bcl11a is required for development of lymphoid and DC progenitors in the fetus

(A) Flow cytometry analysis of progenitor populations in WT and *Bcl11a*$^{-/-}$ fetal livers dissected at embryonic day 14.5 (E14.5). Populations are gated as indicated; numbers represent the percentage of cells within the histogram that lie in the indicated gate. Data are representative of two mice per group. (B) Progenitor populations in WT and *Bcl11a*$^{-/-}$ fetal livers at E14.5, analyzed by flow cytometry as in (A) and presented as a percentage of total fetal liver cells. Bars represent the mean (± SEM) of two mice per group. (C) CD150 (Slamf1) expression within the LSK fraction in WT and *Bcl11a*$^{-/-}$ fetal livers at E14.5. (D) SL-GMPs in WT and *Bcl11a*$^{-/-}$ fetal livers at E14.5

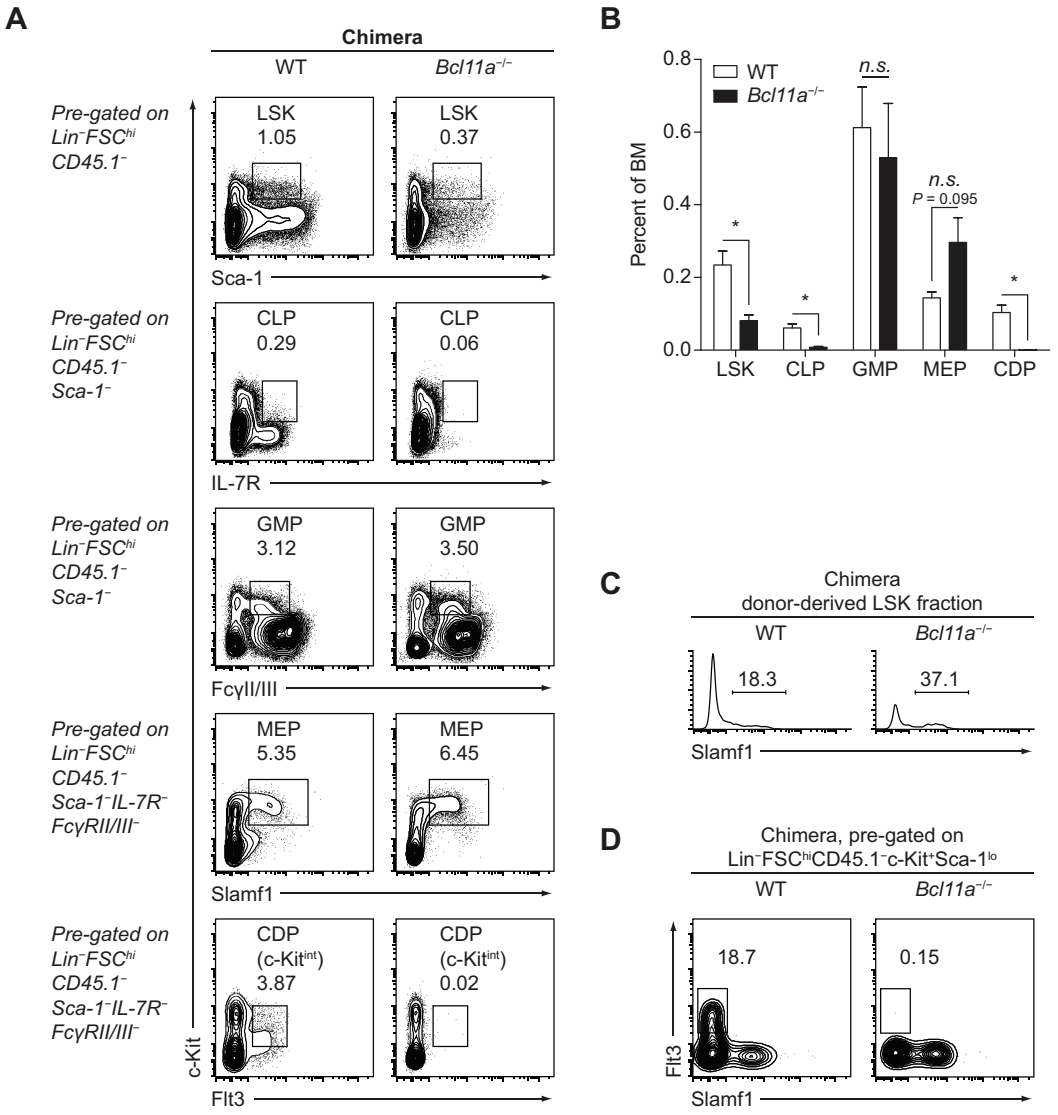

Figure 5.2: Bcl11a is required for development of lymphoid and DC progenitors in the adult

(A) Flow cytometry analysis of progenitor populations in lethally irradiated congenic mice reconstituted with WT or *Bcl11a*$^{-/-}$ fetal liver cells, analyzed four weeks after transplant. Data are representative of three mice per group. (B) Progenitor populations in WT and *Bcl11a*$^{-/-}$ fetal liver chimeras at four weeks after transplant, analyzed by flow cytometry as in (A) and presented as a percentage of total BM cells. Bars represent the mean (± SEM) of three mice per group. (C) CD150 (Slamf1) expression within the donor-derived LSK fraction in WT and *Bcl11a*$^{-/-}$ fetal liver chimeras at four weeks after transplant. (D) SL-GMPs in WT and *Bcl11a*$^{-/-}$ fetal liver chimeras at four weeks after transplant.

5.3.2 Bcl11a regulates expression of *Il7r* and *Flt3*

To identify Bcl11a target genes that explain its role in hematopoietic progenitors, we compared global gene expression by microarray for donor-derived WT and *Bcl11a*$^{-/-}$ populations isolated from chimeric BM (Figure 5.3). Since we observed that IL-7R- and Flt3-expressing populations were affected by the loss of Bcl11a, we avoided the use of these surface markers in order to allow for comparison of equivalent populations across genotypes. Thus, we isolated multipotent progenitors (MPPs) as identified by the lack of CD150 expression within the LSK fraction [33-35]. We also isolated GMPs from the same BM, since the size of this population was unaffected by loss of Bcl11a.

We found that WT and *Bcl11a*$^{-/-}$ GMPs were more similar to each other in gene expression than WT and *Bcl11a*$^{-/-}$ MPPs were to each other (Figure 5.3**A**). One hundred and thirty-four probe sets showed a greater than twofold change in expression between WT and *Bcl11a*$^{-/-}$ GMPs. In contrast, 1020 probe sets showed a greater than twofold change in expression between WT and *Bcl11a*$^{-/-}$ MPPs; of these, only 38 also show a greater than twofold change between WT and *Bcl11a*$^{-/-}$ GMPs (Figure 5.3**B**). These data suggest that GMP population size is unaffected by loss of Bcl11a because this transcription factor regulates relatively few genes in GMPs.

Since the loss of Bcl11a impaired development of CDPs but not GMPs, we examined Bcl11a target genes which showed expression patterns that distinguish DCs from monocytes and macrophages. Thus, we compared the ratio of gene expression in CDPs relative to monocytes

against the ratio of gene expression in *Bcl11a*$^{-/-}$ MPPs relative to WT MPPs (Figure 5.3**C**). Of genes most highly expressed in CDPs relative to monocytes, those most affected by loss of Bcl11a included *Flt3*, *Cnn3* (encoding calponin 3), *Dntt* (encoding the template-independent DNA polymerase TdT), *Il7r*, and *Blnk* (encoding B-cell linker protein, which links components of B-cell receptor signaling). We also compared changes in gene expression between WT and *Bcl11a*$^{-/-}$ MPPs for members of the core cDC transcriptional signature identified in a published bioinformatic analysis [16] (Figure 5.3**D**). Within this core signature, we found only three genes—*Ass1*, *Amica1*, and *Flt3*—that showed a greater than twofold decrease in expression in *Bcl11a*$^{-/-}$ MPPs relative to WT MPPs. Taken together, the decreased expression of *Flt3* and *Il7r* in *Bcl11a*$^{-/-}$ MPPs suggests that Bcl11a may be specifically required for the expression of these genes.

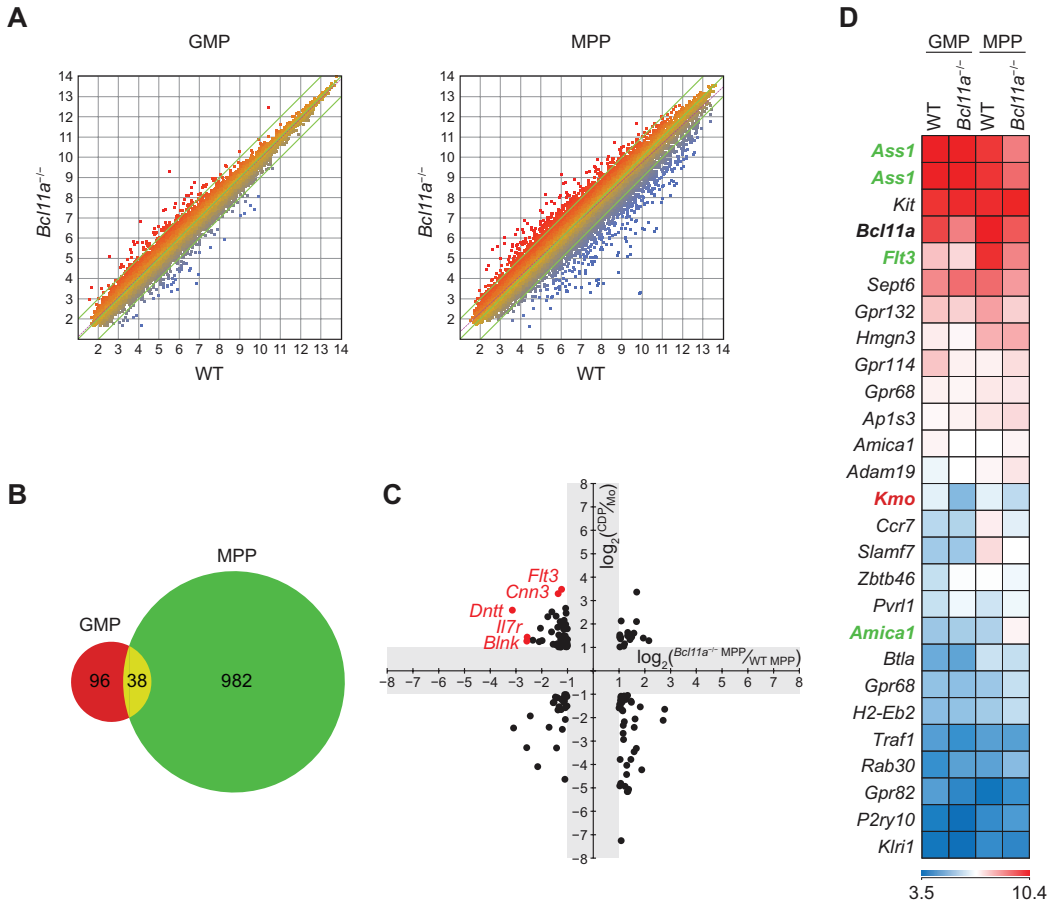

Figure 5.3: Bcl11a regulates the expression of *Flt3* and *Il7r*

(A) Microarray analysis of sorted GMPs (left) and MPPs (right) from WT and *Bcl11a*$^{-/-}$ fetal liver chimeras. (B) Shown is a Venn diagram of probe sets (excluding normalization controls) with a greater than twofold change in expression between WT and *Bcl11a*$^{-/-}$ MPPs. (C) Shown are $\log_2$-transformed ratios of gene expression in *Bcl11a*$^{-/-}$ MPPs relative to WT MPPs (*x*-axis) plotted against $\log_2$-transformed ratios of gene expression in WT CDPs relative to WT monocytes (ImmGen; *y*-axis). For clarity, probe sets with less than twofold changes in expression ($\log_2$-transformed ratios between −1 and 1) along either dimension are omitted (gray). (D) Shown is a heat map of $\log_2$-transformed gene expression in WT and *Bcl11a*$^{-/-}$ GMPs and MPPs for probe sets that constitute an ImmGen core cDC signature. Highlighted are genes that show a greater than twofold change in expression between WT and *Bcl11a*$^{-/-}$ GMPs (red) or between WT and *Bcl11a*$^{-/-}$ MPPs (green).

5.3.3 Bcl11a is required for pDC but not cDC development *in vivo*

Next, we examined the development of mature hematopoietic subsets in WT and *Bcl11a*$^{-/-}$ fetal liver chimeras (Figure 5.4). In accordance with previous reports [24], we observed atrophic thymi in *Bcl11a*$^{-/-}$ chimeras (data not shown). In the BM, the size of the donor-derived compartment was comparable in WT and *Bcl11a*$^{-/-}$ chimeras; in the spleen and skin-draining lymph nodes, *Bcl11a*$^{-/-}$ cells were somewhat impaired in their competition against the residual host population (Figure 5.4**A**). Within the donor-derived compartment of the spleen, a profound defect in pDC development was apparent in *Bcl11a*$^{-/-}$ chimeras relative to WT chimeras (Figure 5.4**B**). In contrast, donor-derived cDCs were present in *Bcl11a*$^{-/-}$ chimeras with no significant decrease relative to WT chimeras (Figure 5.4**C**).

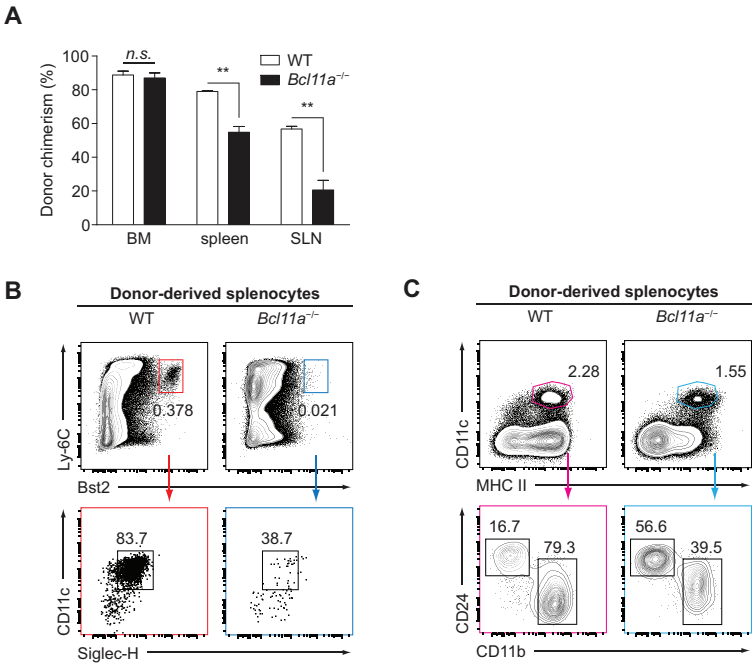

Figure 5.4: Bcl11a is required *in vivo* for development of pDCs but not cDCs

(A) Donor-derived ($CD45.2^+$) chimerism in the BM, spleen, and skin-draining lymph node (SLN) of WT and $Bcl11a^{-/-}$ fetal liver chimeras. Bars represent the mean (± SEM) of three mice per group. (B) Flow cytometry analysis of donor-derived pDCs in the spleen. Data are representative of three mice per group. (C) Flow cytometry analysis of donor-derived cDCs in the spleen. Data are representative of three mice per group.

Among lymphoid subsets, donor-derived B cells, CD4 T cells, CD8 T cells, and γδ T cells were decreased in frequency by at least tenfold in the spleens of $Bcl11a^{-/-}$ chimeras as compared to WT chimeras, consistent with previous reports [24], while NK cells were decreased by slightly more than threefold (Figure 5.5**A**). Among myeloid subsets other than pDCs, donor-derived $CD8^-$ cDCs showed a modest threefold decrease in the spleens of $Bcl11a^{-/-}$ chimeras as compared to WT chimeras; other myeloid populations examined, including $CD8^+$ cDCs, were

not decreased in frequency (Figure 5.5**B**). Thus, Bcl11a was strictly required for the development of pDCs but not cDCs *in vivo*.

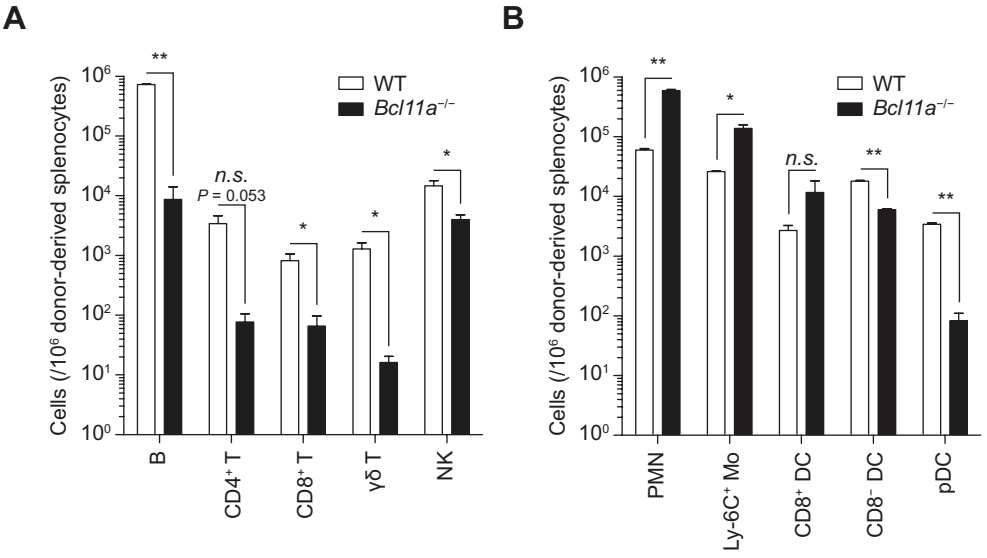

Figure 5.5: Bcl11a deficiency *in vivo* impairs development of lymphoid and myeloid populations

(A) Donor-derived lymphoid populations in the spleen of WT and *Bcl11a*$^{-/-}$ fetal liver chimeras, analyzed by flow cytometry. Bars represent the mean (± SEM) of three mice per group. (B) Donor-derived myeloid populations in the spleen of WT and *Bcl11a*$^{-/-}$ fetal liver chimeras, analyzed by flow cytometry as in Fig. 4. Bars represent the mean (± SEM) of three mice per group.

5.3.4 Flt3-dependent, but not GM-CSF–dependent, DC development requires Bcl11a *in vitro*

We compared the development of WT and *Bcl11a*$^{-/-}$ cells *in vitro* in response to treatment with Flt3L or granulocyte macrophage colony-stimulating factor (GM-CSF) (Figure 5.6). The observation that *Flt3*$^{-/-}$ mice retain DC development [36] suggests an alternative receptor

for Flt3L or a Flt3L-independent pathway for DC development. Thus, we supplied excess Flt3L or GM-CSF to distinguish between these possibilities in the context of Bcl11a deficiency. As expected, pDCs developed from WT fetal liver cells (Figure 5.6**A**) and from the donor-derived BM cells of WT chimeras (Figure 5.6**B**) in response to Flt3L treatment. In contrast, pDCs developed in markedly decreased numbers from *Bcl11a*$^{-/-}$ fetal liver cells and completely failed to develop from the donor-derived BM cells of *Bcl11a*$^{-/-}$ chimeras under these conditions (Figure 5.6**A, B**), demonstrating that Bcl11a is required for pDC development in response to Flt3L both *in vivo* and *in vitro*. We also examined cDC development from WT and *Bcl11a*$^{-/-}$ fetal liver cells *in vitro* in response to treatment with Flt3L or GM-CSF. Flt3L-derived cDCs were markedly reduced in cultures of *Bcl11a*$^{-/-}$ fetal liver cells relative to cultures of WT fetal liver cells (Figure 5.6**C, E**). However, GM-CSF–derived DCs developed in normal numbers from cultures of *Bcl11a*$^{-/-}$ fetal liver cells relative to cultures of WT fetal liver cells (Figure 5.6**D, F**). These results suggest that Flt3L cannot signal through an alternative receptor to rescue cDC development in *Bcl11a*$^{-/-}$ cells, but that an alternative pathway of DC development may be mediated by GM-CSF.

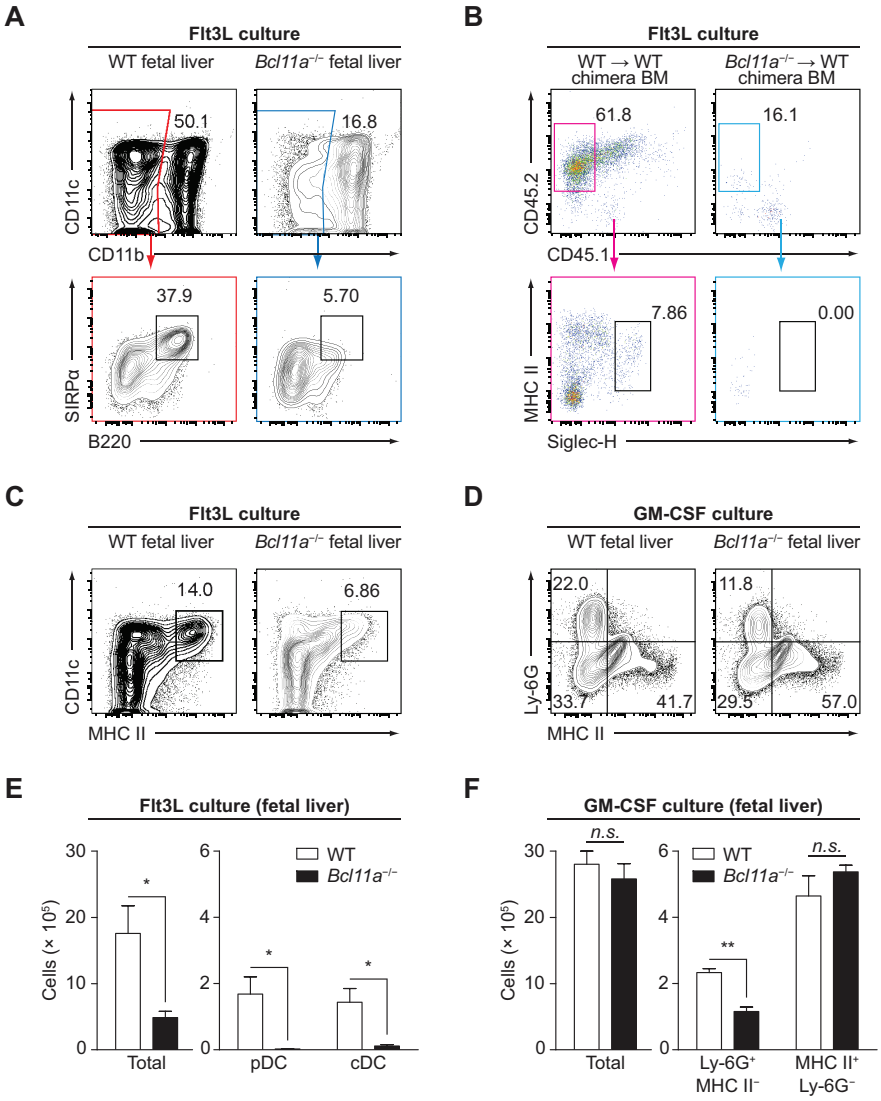

Figure 5.6: Bcl11a is required in vitro for development of Flt3L-derived pDCs and cDCs but not GM-CSF-derived cDCs

(A) Flow cytometry analysis of pDCs in Flt3L cultures of fetal liver cells. Data are representative of three to four replicates over two experiments. (B) Flow cytometry analysis of pDCs in Flt3L cultures of BM cells derived from fetal liver chimeras. Data are representative of three replicates. (C, D) Flow cytometry analysis of Flt3L-derived cDCs (C) or GM-CSF-derived DCs (D) in cultures of fetal liver cells. Data are representative of three to four replicates over two experiments. (E, F) Counts of total cells and indicated subsets in Flt3L cultures (E) or GM-CSF cultures (F) of fetal liver cells, analyzed by flow cytometry as in (C) or (D), respectively. Bars represent the mean (± SEM) of three to four replicates per group pooled from two experiments.

5.3.5 Loss of Flt3L results in lineage-specific defects in pDC development

Next, we examined the development of splenic pDCs in the context of IL-7R or Flt3L deficiency. A previous study has demonstrated that splenic pDCs in *Il7r*$^{-/-}$ mice or *Il7*$^{-/-}$ mice are decreased in absolute number when compared to WT controls [37]. We found that splenic pDCs in *Il7r*$^{-/-}$ mice were not decreased in proportion to total splenocytes when compared to WT controls matched for strain, age, and sex (Figure 5.7**A**). This result suggests that the hematopoietic defects in these mice may have relatively few lineage-specific consequences for pDC development.

Previously, it has been found that *Flt3*$^{-/-}$ mice and *Flt3l*$^{-/-}$ mice show defects in the development of pDCs [36,38]. Accordingly, and in contrast to our observations in *Il7r*$^{-/-}$ mice, we found that *Flt3l*$^{-/-}$ mice showed a greater than fourfold reduction in splenic pDC frequency as compared to WT littermate controls (Figure 5.7**B**), in addition to reductions in absolute spleen size (data not shown).

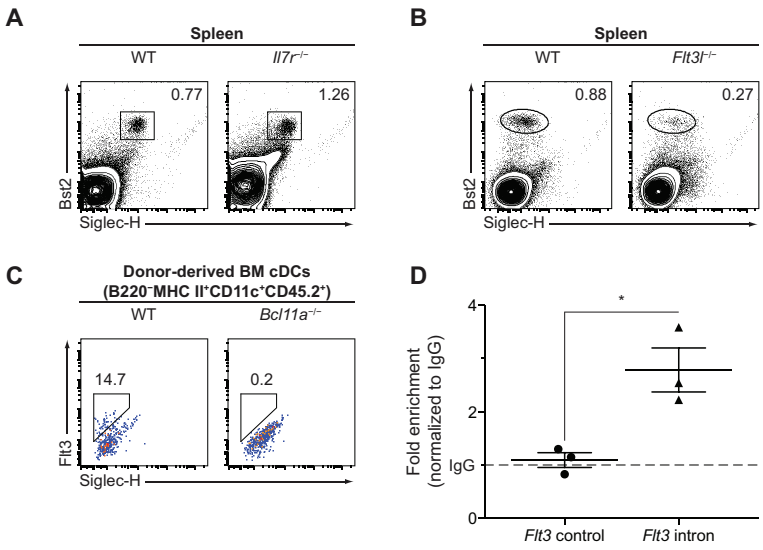

Figure 5.7: Cytokine signaling in DC development and regulation by Bcl11a

(A) Flow cytometry analysis of pDCs in WT and *Il7r*$^{-/-}$ spleens. Data are representative of four mice per group over two experiments. (B) Flow cytometry analysis of pDCs in WT and *Flt3l*$^{-/-}$ spleens. Data are representative of three mice per group over two experiments. (C) Flow cytometry analysis of donor-derived cDCs in the spleen of WT and *Bcl11a*$^{-/-}$ fetal liver chimeras, analyzed by flow cytometry as in Fig. 4. Data are representative of three mice per group. (D) Bcl11a binding in the *Flt3* genomic locus assayed by ChIP-qPCR. Data are represented as fold enrichment as compared to isotype control.

5.3.6 Bcl11a is required for Flt3 expression in cDCs and binds the *Flt3* genomic locus

Because we observed cDC development in *Bcl11a*$^{-/-}$ chimeras, we assessed whether these cells might express Flt3 in a Bcl11a-independent manner; however, unlike WT cDCs in the BM, *Bcl11a*$^{-/-}$ cDCs in the same compartment showed no discernible Flt3 expression by flow cytometry (Figure 5.7**C**), again suggesting that a Flt3-independent pathway is instead responsible for their development. Finally, to assay Bcl11a binding at the *Flt3* locus, we performed chromatin immunoprecipitation (ChIP) using mouse pro-B cells. By quantitative real-time

polymerase chain reaction (qPCR), we detected an approximately threefold enrichment at a region in the first intron of the *Flt3* locus in DNA precipitated using anti-Bcl11a antibody as compared to isotype control (Figure 5.7**D**).

In summary, our results document a strict requirement for Bcl11a in pDC development both *in vivo* and *in vitro*; further, the requirement for Bcl11a in cDC development may differ based on the cytokine stimulus to which progenitors are exposed. The actions of Bcl11a include regulation of Flt3 expression by direct binding to the *Flt3* locus, and Bcl11a is required for Flt3 expression in DCs and their progenitors.

5.4 Discussion

This study extends the known actions of *Bcl11a* in immune lineage development and provides a mechanism for its effects. Although *Bcl11a* has been recognized as a factor required for normal lymphoid development [24], the basis for this requirement has been unclear. It has been shown that Bcl11a acts upstream of the B cell factors Ebf1 and Pax5 and that *Il7r* mRNA is not expressed in *Bcl11a*$^{-/-}$ fetal livers [24]. Lack of IL-7Rα or the cytokine receptor common γ chain (γ_c, encoded by *Il2rg*) severely impairs T and B cell development [39-43]. In T cell development, IL-7R signaling is thought to promote thymocyte survival, since Bcl-2 rescues impaired T cell development in *Il7r*$^{-/-}$ or *Il2rg*$^{-/-}$ mice [44-48]. In B cell development, Bcl-2 does not rescue development in the absence of IL-7R or γ_c [44-47,49], and IL-7R signaling is thought to induce expression of the transcription factor Ebf in the CLP [50-52].

Here, we demonstrate that Bcl11a is required for normal expression of IL-7R as early as the CLP and we add the novel observation that Bcl11a promotes the development of Flt3-

dependent lineages. Together, these actions provide a more complete account for previously observed defects in lymphocyte development in *Bcl11a*$^{-/-}$ mice, since T cell potential is preserved in IL-7–deficient CLPs in a Flt3L-dependent manner [53,54]. The mechanisms by which Bcl11a deficiency impairs T and B cell development, however, still remain incompletely explored. Consistent with a previous report [24], we confirmed the presence of residual T and B cells in the spleen of chimeras reconstituted with *Bcl11a*$^{-/-}$ fetal liver cells. By contrast, tamoxifen-induced deletion of *Bcl11a* in chimeras that have been reconstituted with *Rosa26-CreERT2*;*Bcl11a*$^{flox/flox}$ BM cells results in a more profound loss of T and B cells [55]. Thus, synchronous deletion of *Bcl11a* within a previously intact hematopoietic compartment produces a different outcome than does sustained deficiency throughout hematopoiesis. These results may point to a crucial lymphopoietic role for cells in which Bcl11a is dispensable for survival but necessary for development or maturation, or vice versa; these cells could include HSCs, mature T and B cells, or even residual CLPs undetectable due to a lack of IL-7R and Flt3 expression.

In line with a previous finding that E2-2 regulates *Bcl11a* expression [18], we also document a strict requirement for Bcl11a in the development of pDCs. The development of pDCs *in vivo* was lost in *Bcl11a*$^{-/-}$ fetal liver chimeras. In agreement, Flt3L cultures of BM derived from these *Bcl11a*$^{-/-}$ chimeras showed a complete loss of pDC development *in vitro*. Because mature pDCs are short-lived, non-proliferative, and continuously replenished from progenitor populations [56,57], the nearly complete loss of this population is most attributable to a developmental defect and not merely to cell survival defects in mature pDCs. This interpretation would be consistent with a finding that rescue of Bcl11a-deficient progenitors from increased apoptosis by p53 deficiency is unable to restore lymphoid potential [55].

Notably, however, *in vitro* development of cDCs was eliminated in Flt3L cultures of *Bcl11a*$^{-/-}$ fetal liver cells but was maintained in GM-CSF cultures of *Bcl11a*$^{-/-}$ fetal liver cells. Flt3L and GM-CSF have distinct, non-redundant actions in supporting cDC development [58,59]. The combined loss of Flt3L and GM-CSF causes a more severe cDC deficiency than loss of Flt3L alone; indeed, Flt3L-deficient mice retain an appreciable population of Flt3-expressing progenitors [38]. The maintenance of cDCs in *Bcl11a*$^{-/-}$ fetal liver chimeras suggests that these cells may rely on a Bcl11a- and Flt3-independent pathway for their development, survival, or expansion. Conditional knockout models would clarify which of these alternatives underlie the observed phenotype in *Bcl11a*$^{-/-}$ mice. Since DCs developed normally *in vitro* from *Bcl11a*$^{-/-}$ progenitors treated with GM-CSF, it is possible that *Bcl11a*$^{-/-}$ cDCs *in vivo* indeed represent development from GM-CSF–dependent progenitors, related perhaps to monocyte-derived dendritic cell lineages [60].

5.5 Materials and Methods

5.5.1 Mice.

C57BL/6, B6.SJL, *Il7*$^{-/-}$, and *Il7r*$^{-/-}$ mice were purchased from The Jackson Laboratory. *Flt3l*$^{-/-}$ and *Rag2*$^{-/-}$ mice were purchased from Taconic Farms. *Flt3l*$^{-/-}$ mice were subsequently crossed to *Zbtb46*$^{gfp/gfp}$ mice generated previously [19]; F2 offspring were studied in the present experiments, with *Zbtb46*$^{+/gfp}$;*Flt3l*$^{+/+}$ or *Zbtb46*$^{gfp/gfp}$;*Flt3l*$^{+/+}$ mice used as WT littermate controls. *Bcl11a*$^{-/-}$ mice were obtained from Dr. Pentao Liu [24]. Mice were bred and maintained in our specific pathogen free animal facility at Washington University in St. Louis. Mice were sacrificed by CO_2 overdose followed by cervical dislocation.

5.5.2 Single-cell suspensions of fetal liver.

At embryonic day 14.5, fetal livers were mechanically dissociated with a syringe plunger and sterile 70-μm cell strainer (Fisher) into IMDM + 10% (v/v) FCS (I10F). For subsequent cell culture or flow cytometry, red blood cells were lysed in ACK lysing buffer before counting by Vi-CELL (Beckman Coulter).

5.5.3 Antibodies.

The following antibodies were purchased from BD Biosciences: FITC anti-CD3e (145-2C11), APC anti-CD4 (RM4-5), V450 anti-CD4 (RM4-5), PerCP-Cy5.5 anti-CD8a (53-6.7), PerCP-Cy5.5 anti-CD11b (M1/70), APC anti-CD11c (HL3), APC anti-CD19 (1D3), PE-Cy7 anti-CD24 (M1/69), APC anti-CD25 (PC61), FITC anti-CD45 (30-F11), APC anti-CD45.2 (104), APC-Cy7 anti-CD45.2 (104), PE anti-CD135 (A2F10.1), APC anti-CD172a (P84), FITC anti-B220 (RA3-6B2), V500 anti-B220 (RA3-6B2), PE anti-Gr-1 (RB6-8C5), V450 anti-Gr-1 (RB6-8C5), PerCP-Cy5.5 anti-IgM (R6-60.2), PE-Cy7 anti-Ly-6A/E (Sca-1) (D7), FITC anti-Ly-6C (AL-21), V450 anti-Ly-6C (AL-21), PE anti-Ly-6G (1A8), PE anti-MHC II (I-A/I-E) (M5/114.15.2), PE anti-TCRγδ (GL3). The following antibodies were purchased from eBioscience: APC-eFluor 780 anti-CD11c (N418), eFluor 450 anti-CD11c (N418), PerCP-Cy5.5 anti-CD16/32 (93), APC-eFluor 780 anti-CD44 (IM7), biotin anti-CD45.1 (A20), PerCP-Cy5.5 anti-CD45.1 (A20), Alexa Fluor 700 anti-CD45.2 (104), PE-Cy7 anti-CD49b (DX5), PE anti-CD103 (2E7), APC-eFluor 780 anti-CD117 (ACK2), PE-Cy7 anti-CD117 (2B8), FITC anti-CD127 (A7R34), APC anti-CD150 (mShad150), eFluor 450 anti-B220 (RA3-6B2), PE-Cy7 anti-B220 (RA3-6B2), APC anti-BST2 (eBio927), eFluor 450 anti-BST2 (eBio927), FITC anti-F4/80 (BM8), PE anti-IgD (41239), eFluor 450 anti-MHC II (I-A/I-E) (M5/114.15.2), eFluor 450 anti-

NKp46 (29A1.4), FITC anti-Siglec-H (eBio440C). The following antibodies were purchased from Caltag: FITC anti-CD8a (5H10), PE anti-B220 (RA3-6B2). Qdot 605 streptavidin was purchased from Invitrogen and V500 streptavidin was purchased from BD Biosciences.

5.5.4 Flow cytometry and sorting.

Staining was performed at 4°C in the presence of Fc block (clone 2.4G2, BD Biosciences or BioXCell) in FACS buffer (DPBS + 0.5% BSA + 2 mM EDTA). Cells were analyzed using a FACSCanto II (BD Biosciences) or sorted using a FACSAria (BD Biosciences); data were visualized using FlowJo software (TreeStar).

5.5.5 Cell cultures.

Cells were diluted to 2×10^6 cells/ml in I10F + 20 ng/ml Flt3L or GM-CSF, cultured in 12-well plates for 10 d (Flt3L) or 7 d (GM-CSF), then analyzed by flow cytometry.

5.5.6 Chimeras.

B6.SJL mice were lethally irradiated (1200 rad) and injected intraorbitally with 4×10^6 fetal liver cells isolated from WT or *Bcl11a*$^{-/-}$ fetuses. After 4 or 6 weeks, BM was isolated by grinding and Histopaque-1119 (Sigma-Aldrich) centrifugation and either sorted by flow cytometry or cultured. From these mice, thymi were minced and digested in 250 µg/ml collagenase B (Roche) and 30 U/ml DNase I (Sigma-Aldrich) and analyzed by flow cytometry.

5.5.7 Microarray analysis.

MPP and GMP populations were sorted from fetal liver chimeras and pooled by donor genotype. RNA was isolated using an RNAqueous-Micro Kit (Ambion) and submitted for

amplification, labeling and hybridization. Expression values were analyzed after RMA quantile normalization using ArrayStar software (DNASTAR). Data were deposited in the Gene Expression Omnibus (GEO) repository under accession no. GSE46270.

5.5.8 ChIP-qPCR.

Pro-B cell cultures were established using *Rag2*$^{-/-}$ BM isolated by flushing and resuspended in I10F + 5 ng/ml IL-7. Chromatin was prepared from 1×10^7 cultured pro-B cells sonicated using a Bioruptor (Diagenode), immunoprecipitation was performed with a rabbit polyclonal anti-Bcl11a antibody (NB600-261, Novus Biologicals) or control rabbit IgG, and qPCR analysis was carried out using SYBR Green-based detection and the following previously published primers [61]: *Flt3* control forward, 5′-TTTGCACTCGTAGCAAATGG-3′; *Flt3* control reverse, 5′-GTTCAGCTGCCAAAGAGAGG-3′; *Flt3* promoter forward, 5′-GTTCAGCTGCCAAAGAGAGG-3′; *Flt3* promoter reverse, 5′-CGTCACTGACCACAGATTCC-3′; *Flt3* intron forward, 5′-AAAAGAGGAACTATTGGTATTTCG-3′; *Flt3* intron reverse, 5′-TGACAGTAGTGAAAACACACACACA-3′.

5.5.9 Statistics.

Statistical differences were identified using Prism 6 (GraphPad) by multiple unpaired Student's *t* tests, controlling the false discovery rate (Q) by the method of Benjamini and Hochberg. *, Q = 0.05; **, Q = 0.01.

5.6 Author contributions

A.S., W.K. and K.M. designed the study. A.S. and W.K. performed all *Bcl11a*$^{-/-}$ experiments and generated microarray datasets. X.W. analyzed microarray data. P.L. provided *Bcl11a*$^{-/-}$ mice. X.W. and K.M. wrote the manuscript with contributions from A.S. and W.K.

5.7 References

1. Naik,S.H. *et al.* Intrasplenic steady-state dendritic cell precursors that are distinct from monocytes. *Nat Immunol* **7**, 663-671 (2006).

2. Onai,N. *et al.* Identification of clonogenic common Flt3(+) M-CSFR+ plasmacytoid and conventional dendritic cell progenitors in mouse bone marrow. *Nat.* **8**, 1207-1216 (2007).

3. Naik,S.H. *et al.* Development of plasmacytoid and conventional dendritic cell subtypes from single precursor cells derived in vitro and in vivo. *Nat Immunol* **8**, 1217-1226 (2007).

4. Liu,K. *et al.* In vivo analysis of dendritic cell development and homeostasis. *Science* **324**, 392-397 (2009).

5. Wu,L., Nichogiannopoulou,A., Shortman,K. & Georgopoulos,K. Cell-autonomous defects in dendritic cell populations of Ikaros mutant mice point to a developmental relationship with the lymphoid lineage. *Immunity* **7**, 483-492 (1997).

6. Allman,D. *et al.* Ikaros is required for plasmacytoid dendritic cell differentiation. *Blood* **108**, 4025-4034 (2006).

7. Guerriero,A., Langmuir,P.B., Spain,L.M. & Scott,E.W. PU.1 is required for myeloid-derived but not lymphoid-derived dendritic cells. *Blood* **95**, 879-885 (2000).

8. Anderson,K.L. *et al.* Transcription factor PU.1 is necessary for development of thymic and myeloid progenitor-derived dendritic cells. *J Immunol* **164**, 1855-1861 (2000).

9. Rathinam,C. *et al.* The transcriptional repressor Gfi1 controls STAT3-dependent dendritic cell development and function. *Immunity* **22**, 717-728 (2005).

10. Cisse,B. *et al.* Transcription factor E2-2 is an essential and specific regulator of plasmacytoid dendritic cell development. *Cell* **135**, 37-48 (2008).

11. Hildner,K. *et al.* Batf3 deficiency reveals a critical role for CD8alpha+ dendritic cells in cytotoxic T cell immunity. *Science* **322**, 1097-1100 (2008).

12. Tsujimura,H., Tamura,T. & Ozato,K. Cutting edge: IFN consensus sequence binding protein/IFN regulatory factor 8 drives the development of type I IFN-producing plasmacytoid dendritic cells. *J Immunol* **170**, 1131-1135 (2003).

13. Tamura,T. *et al.* IFN regulatory factor-4 and -8 govern dendritic cell subset development and their functional diversity. *J Immunol* **174**, 2573-2581 (2005).

14. Burkly,L. *et al.* Expression of relB is required for the development of thymic medulla and dendritic cells. *Nature* **373**, 531-536 (1995).

15. Wu,L. *et al.* RelB is essential for the development of myeloid-related CD8alpha- dendritic cells but not of lymphoid-related CD8alpha+ dendritic cells. *Immunity.* **9**, 839-847 (1998).

16. Miller,J.C. *et al.* Deciphering the transcriptional network of the dendritic cell lineage. *Nat. Immunol.* **13**, 888-899 (2012).

17. Schotte,R., Nagasawa,M., Weijer,K., Spits,H. & Blom,B. The ETS transcription factor Spi-B is required for human plasmacytoid dendritic cell development. *J. Exp. Med.* **200**, 1503-1509 (2004).

18. Ghosh,H.S., Cisse,B., Bunin,A., Lewis,K.L. & Reizis,B. Continuous expression of the transcription factor e2-2 maintains the cell fate of mature plasmacytoid dendritic cells. *Immunity* **33**, 905-916 (2010).

19. Satpathy,A.T. *et al.* Zbtb46 expression distinguishes classical dendritic cells and their committed progenitors from other immune lineages. *J. Exp. Med.* **209**, 1135-1152 (2012).

20. Meredith,M.M. *et al.* Expression of the zinc finger transcription factor zDC (Zbtb46, Btbd4) defines the classical dendritic cell lineage. *J. Exp. Med.* **209**, 1153-1165 (2012).

21. Becker,A.M. *et al.* IRF-8 extinguishes neutrophil production and promotes dendritic cell lineage commitment in both myeloid and lymphoid mouse progenitors. *Blood* **119**, 2003-2012 (2012).

22. Nakamura,T. *et al.* Evi9 encodes a novel zinc finger protein that physically interacts with BCL6, a known human B-cell proto-oncogene product. *Mol. Cell Biol.* **20**, 3178-3186 (2000).

23. Satterwhite,E. *et al.* The BCL11 gene family: involvement of BCL11A in lymphoid malignancies. *Blood* **98**, 3413-3420 (2001).

24. Liu,P. *et al.* Bcl11a is essential for normal lymphoid development. *Nat. Immunol.* **4**, 525-532 (2003).

25. Sankaran,V.G. *et al.* Developmental and species-divergent globin switching are driven by BCL11A. *Nature* **460**, 1093-1097 (2009).

26. Xu,J. *et al.* Transcriptional silencing of {gamma}-globin by BCL11A involves long-range interactions and cooperation with SOX6. *Genes Dev.* **24**, 783-798 (2010).

27. Pelayo,R. *et al.* Derivation of 2 categories of plasmacytoid dendritic cells in murine bone marrow. *Blood* **105**, 4407-4415 (2005).

28. Pulford,K. *et al.* The BCL11AXL transcription factor: its distribution in normal and malignant tissues and use as a marker for plasmacytoid dendritic cells. *Leukemia* **20**, 1439-1441 (2006).

29. Franco,C.B., Chen,C.C., Drukker,M., Weissman,I.L. & Galli,S.J. Distinguishing mast cell and granulocyte differentiation at the single-cell level. *Cell Stem Cell* **6**, 361-368 (2010).

30. McKenna,H.J. *et al.* Mice lacking flt3 ligand have deficient hematopoiesis affecting hematopoietic progenitor cells, dendritic cells, and natural killer cells. *Blood* **95**, 3489-3497 (2000).

31. Laouar,Y., Welte,T., Fu,X.Y. & Flavell,R.A. STAT3 is required for Flt3L-dependent dendritic cell differentiation. *Immunity* **19**, 903-912 (2003).

32. Onai,N., Obata-Onai,A., Tussiwand,R., Lanzavecchia,A. & Manz,M.G. Activation of the Flt3 signal transduction cascade rescues and enhances type I interferon-producing and dendritic cell development. *J Exp. Med.* **203**, 227-238 (2006).

33. Spangrude,G.J., Heimfeld,S. & Weissman,I.L. Purification and characterization of mouse hematopoietic stem cells. *Science* **241**, 58-62 (1988).

34. Ogawa,M. *et al.* Expression and function of c-kit in hemopoietic progenitor cells. *J. Exp. Med.* **174**, 63-71 (1991).

35. Kiel,M.J. *et al.* SLAM family receptors distinguish hematopoietic stem and progenitor cells and reveal endothelial niches for stem cells. *Cell* **121**, 1109-1121 (2005).

36. Waskow,C. *et al.* The receptor tyrosine kinase Flt3 is required for dendritic cell development in peripheral lymphoid tissues. *Nat Immunol* **9**, 676-683 (2008).

37. Vogt,T.K., Link,A., Perrin,J., Finke,D. & Luther,S.A. Novel function for interleukin-7 in dendritic cell development. *Blood* **113**, 3961-3968 (2009).

38. Kingston,D. *et al.* The concerted action of GM-CSF and Flt3-ligand on in vivo dendritic cell homeostasis. *Blood* **114**, 835-843 (2009).

39. Peschon,J.J. *et al.* Early lymphocyte expansion is severely impaired in interleukin 7 receptor-deficient mice. *J. Exp. Med.* **180**, 1955-1960 (1994).

40. Cao,X. *et al.* Defective lymphoid development in mice lacking expression of the common cytokine receptor gamma chain. *Immunity* **2**, 223-238 (1995).

41. DiSanto,J.P., Muller,W., Guy-Grand,D., Fischer,A. & Rajewsky,K. Lymphoid development in mice with a targeted deletion of the interleukin 2 receptor gamma chain. *Proc. Natl. Acad. Sci. U. S A* **92**, 377-381 (1995).

42. Ohbo,K. *et al.* Modulation of hematopoiesis in mice with a truncated mutant of the interleukin-2 receptor gamma chain. *Blood* **87**, 956-967 (1996).

43. Sugamura,K. *et al.* The interleukin-2 receptor gamma chain: its role in the multiple cytokine receptor complexes and T cell development in XSCID. *Annu. Rev. Immunol.* **14**, 179-205 (1996).

44. Maraskovsky,E. *et al.* Bcl-2 can rescue T lymphocyte development in interleukin-7 receptor-deficient mice but not in mutant rag-1-/- mice. *Cell* **89**, 1011-1019 (1997).

45. Kondo,M., Weissman,I.L. & Akashi,K. Identification of clonogenic common lymphoid progenitors in mouse bone marrow. *Cell* **91**, 661-672 (1997).

46. Akashi,K., Kondo,M., Freeden-Jeffry,U., Murray,R. & Weissman,I.L. Bcl-2 rescues T lymphopoiesis in interleukin-7 receptor-deficient mice. *Cell* **89**, 1033-1041 (1997).

47. Kondo,M., Akashi,K., Domen,J., Sugamura,K. & Weissman,I.L. Bcl-2 rescues T lymphopoiesis, but not B or NK cell development, in common gamma chain-deficient mice. *Immunity* **7**, 155-162 (1997).

48. Freeden-Jeffry,U., Solvason,N., Howard,M. & Murray,R. The earliest T lineage-committed cells depend on IL-7 for Bcl-2 expression and normal cell cycle progression. *Immunity* **7**, 147-154 (1997).

49. Maraskovsky,E., Peschon,J.J., McKenna,H., Teepe,M. & Strasser,A. Overexpression of Bcl-2 does not rescue impaired B lymphopoiesis in IL-7 receptor-deficient mice but can enhance survival of mature B cells. *Int. Immunol.* **10**, 1367-1375 (1998).

50. Kikuchi,K., Lai,A.Y., Hsu,C.L. & Kondo,M. IL-7 receptor signaling is necessary for stage transition in adult B cell development through up-regulation of EBF. *J. Exp. Med.* **201**, 1197-1203 (2005).

51. Dias,S., Silva,H., Jr., Cumano,A. & Vieira,P. Interleukin-7 is necessary to maintain the B cell potential in common lymphoid progenitors. *J. Exp. Med.* **201**, 971-979 (2005).

52. Kikuchi,K., Kasai,H., Watanabe,A., Lai,A.Y. & Kondo,M. IL-7 specifies B cell fate at the common lymphoid progenitor to pre-proB transition stage by maintaining early B cell factor expression. *J. Immunol.* **181**, 383-392 (2008).

53. Moore,T.A., Freeden-Jeffry,U., Murray,R. & Zlotnik,A. Inhibition of gamma delta T cell development and early thymocyte maturation in IL-7 -/- mice. *J. Immunol.* **157**, 2366-2373 (1996).

54. Sitnicka,E. *et al.* Critical role of FLT3 ligand in IL-7 receptor independent T lymphopoiesis and regulation of lymphoid-primed multipotent progenitors. *Blood* **110**, 2955-2964 (2007).

55. Yu,Y. *et al.* Bcl11a is essential for lymphoid development and negatively regulates p53. *J. Exp. Med.* **209**, 2467-2483 (2012).

56. Liu,K. *et al.* Origin of dendritic cells in peripheral lymphoid organs of mice. *Nat Immunol* **8**, 578-583 (2007).

57. Merad,M. & Manz,M.G. Dendritic cell homeostasis. *Blood* **113**, 3418-3427 (2009).

58. Edelson,B.T. *et al.* Batf3-dependent CD11b(low/-) peripheral dendritic cells are GM-CSF-independent and are not required for Th cell priming after subcutaneous immunization. *PLoS One* **6**, e25660 (2011).

59. Greter,M. *et al.* GM-CSF Controls Nonlymphoid Tissue Dendritic Cell Homeostasis but Is Dispensable for the Differentiation of Inflammatory Dendritic Cells. Immunity 36(6), 1031-1046. 2012.

60. Satpathy,A.T., Murphy,K.M. & KC,W. Transcription factor networks in dendritic cell development. *Semin. Immunol.* **23**, 388-397 (2011).

61. Carotta,S. *et al.* The transcription factor PU.1 controls dendritic cell development and Flt3 cytokine receptor expression in a dose-dependent manner. *Immunity* **32**, 628-641 (2010).

Curriculum Vitae

Department of Pathology and Immunology
School of Medicine
Washington University in St. Louis
660 South Euclid Ave, 7766 Clinical Science Research Building
St. Louis, MO 63110

Tel: 314-362-2004
Email: kcw@wusm.wustl.edu

Current Position

MD/PhD Student
Laboratory of Dr. Kenneth M. Murphy

Education

8/06 – 5/15 Washington University in St. Louis, Medicine, M.D./Ph.D.
Medical Scientist Training Program

8/02 – 5/06 University of Colorado at Boulder, Biochemistry, B.A.

Academic positions

8/08 – 10/13 Washington University in St. Louis, Graduate Student, Immunology
Principal Investigator: Dr. Kenneth M. Murphy

8/03 – 5/06 University of Colorado at Boulder, Research Assistant, Department of Chemistry and Biochemistry. Principal Investigator: Dr. Ray Fall

Academic and Professional Honors

2014 David M. Kipnis Award in Biomedical Sciences (top honors for dissertation work), Washington University
2006 B.A. with Honors, University of Colorado
2004-2006 Alumni Association Scholarship, University of Colorado
2003 Merck Index Award (top honors in chemistry), University of Colorado

Teaching

9/08 – 6/09 Washington University in St. Louis, Graduate Teaching Assistant, Cell and Organ Systems, Advisor: Dr. Robert Wilkinson

8/05 – 12/05 University of Colorado at Boulder, Teaching Assistant, Chemistry

Publications

Peer Reviewed Articles

KC W, Satpathy AT, Rapaport A, Briseño CG, Wu X, Albring JC, Russler E, Kretzer NM, Persaud SP, Edelson BT, Loschko J, Cella M, Allen PM, Nussenzweig MC, Colonna M, Sleckman BP, Murphy TL, Murphy KM. L-Myc is selectively expressed by dendritic cells and required for T-cell priming during infections. *Nature*. 2014 Mar 13: 507(7491):243-7

Haldar M, Kohyama M, So AY, **KC W**, Wu X, Briseño CG, Satpathy AT, Kretzer NM, Arase H, Rajasekaran NS, Wang L, Egawa T, Igarashi K, Baltimore D, Murphy TL, Murphy KM. Heme-Mediated SPI-C Induction Promotes Monocyte Differentiation into Iron-Recycling Macrophages. *Cell*. 2014 Mar 13;156(6):1223-34.

KC W, Satpathy AT, Albring JC, Edelson BT, Wu X, Dower NA, Stone JC, Smrcka AV, Bhattacharya D, Murphy TL, Murphy KM. Batf3 controls survival and maturation subsequent to Irf8-dependent lineage-commitment in development of $CD8\alpha^{+}$ dendritic cells. *Manuscript in preparation*

Satpathy AT, Briseño CG, Lee JS, Ng D, Manieri NA, **KC W**, Wu X, Thomas SR, Lee WL, Turkoz M, McDonald KG, Meredith MM, Song C, Guidos CJ, Newberry RD, Ouyang W, Murphy TL, Stappenbeck TS, Gommerman JL, Nussenzweig MC, Colonna M, Kopan R, Murphy KM. Notch2-dependent classical dendritic cells orchestrate intestinal immunity to attaching-and-effacing bacterial pathogens. *Nat Immunol*. 2013 Sep;14(9):937-48. (cover article)

Wu X, Satpathy AT, **KC W**, Liu P, Murphy TL, Murphy KM. Bcl11a controls Flt3 expression in early hematopoietic progenitors and is required for pDC development in vivo. *PLoS One*. 2013 May 31;8(5). e64800

Tussiwand R, Lee WL, Murphy TL, Mashayekhi M, **KC W**, Albring JC, Satpathy AT, Rotondo JA, Edelson BT, Kretzer NM, Wu X, Weiss LA, Glasmacher E, Li P, Liao W, Behnke M, Lam SS, Aurthur CT, Leonard WJ, Singh H, Stallings CL, Sibley LD, Schreiber RD, Murphy KM. Compensatory dendritic cell development mediated by BATF-IRF interactions. *Nature.* 2012 Oct 25;490(7421):502-7.

Cai M, Langer EM, Gill JG, Satpathy AT, Albring JC, **KC W**, Murphy TL, Murphy KM. Dual actions of Meis1 inhibit erythroid progenitor development and sustain general hematopoietic cell proliferation. *Blood*. 2012 July 12; 120(2):335-46.

Satpathy AT, **KC W**, Albring JC, Edelson BT, Kretzer NM, Bhattacharya D, Murphy TL, Murphy KM. Zbtb46 expression distinguishes classical dendritic cells and their committed progenitors from other immune lineages. *J Exp Med.* 2012 June 4; 209(6):1135-52. (cover article)

Edelson BT, Bradstreet TR, **KC W**, Hildner K, Herzog JW, Sim J, Russell JH, Murphy TL, Unanue ER, Murphy KM. Batf3-dependent CD11b(low/-) peripheral dendritic cells are GM-CSF-independent and are not required for Th cell priming after subcutaneous immunization. *PLoS One.* 2011 Oct 17; 6(10): e25660.

Edelson BT, Bradstreet TR, Hildner K, Carrero JA, Frederick KE, **KC W**, Belizaire R, Aoshi T, Schreiber RD, Miller MJ, Murphy TL, Unanue ER, Murphy KM. CD8a(+) dendritic cells are an obligate cellular entry point for productive infection by Listeria monocytogenes. *Immunity*. 2011 Aug 26; 35(2): 236-48.

Satpathy AT, Murphy KM, **KC W**. Transcription factor networks in dendritic cell development. *Semin Immunol.* 2011 Oct; 23(5): 388-97.

Edelson BT, **KC W**, Juang R, Kohyama M, Benoit LA, Klekotka PA, Moon C, Albring JC, Ise W, Michael DG, Bhattacharya D, Stappenbeck TS, Holtzman MJ, Sung SS, Murphy TL, Hildner K, Murphy KM. Peripheral CD103+ dendritic cells form a unified subset developmentally related to CD8alpha+ conventional denritic cells. *J Exp Med.* 2010 Apr 12; 207(4): 823-36.

Cadwell K, Liu JY, Brown SL, Miyoshi H, Loh J, Lennerz JK, Kishi C, **KC W**, Carrero JA, Hunt S, Stone CD, Brunt EM, Xavier RJ, Sleckman BP, Li E, Mizushima N, Stappenbeck TS, Virgin HW 4th. A key role for autophagy and the autophagy gene Atg16l1 in mouse and human intestinal Paneth cells. *Nature*. 2008 Nov 13; 456(7219): 259-63.

Selected Talks

KC W, Murphy KM. Transcription factor L-Myc is selectively expressed in cDCs and pDCs. Washington University Immunology Seminar, Petosi, MO, September 2012.

KC W, Murphy KM. Batf3 control the survival and terminal maturation of $CD8\alpha^+$ cDCs. Washington University MSTP Seminar, St. Louis, MO, November 2011.

Selected Poster Presentations

KC W, Satpathy AT, Albring JC, Edelson BT, Murphy KM. Batf3 controls survival and maturation subsequent to Irf8-dependent lineage-commitment in development of $CD8\alpha^+$ dendritic cells. 12^{th} International Symposium on Dendritic Cells DC2012. Daegu, Korea, October 2012

KC W, Satpathy AT, Murphy KM. Identifying transcription factor selectively expressed by the dendritic cell lineage. Washington University Immunology Seminar, Petosi, MO, September 2010.

Research Support

American Heart Association Research Programs Predoctoral Fellowship. "Determining the role of dendritic cell subsets in atherosclerosis." 12PRE12050419. 07/01/12-06/30/13. Role: Principal Investigator

Howard Hughes Medical Institute (HHMI) funding, 08/08-06/12

Washington University in St. Louis School of Medicine, Medical Scientist Training Program Internal Funding, 2006-2008.

Undergraduate Research Opportunities Program. "Characterizing the enzymatic requirements for the biosynthesis of isoprene from *Populus deltoides*." 08/04 – 12/05. Role: Principal Investigator.

Profession and Community Activities

2006 – 2007 Volunteer, Saturday Neighborhood Health Clinic, Washington University in St. Louis